Disparidad e Integración en el cráneo de Archosauria:

Aplicaciones de la Morfología Teórica y la Morfometría Geométrica en Macroevolución.

Tesis Doctoral

Jesús Marugán Lobón

Memoria presentada para la obtención del titulo de Doctor en Ciencias con la Mención de Doctor Europeus

Dirigida por la Dra.

Ángela D. Buscalioni

Departamento de Biología
Unidad de Paleontología

UNIVERSIDAD AUTÓNOMA DE MADRID

Madrid, Febrero 2007

Disparity and Integration of the skull in Archosauria:

Applications of Theoretical Morphology & Geometric Morphometrics in Macroevolution

Doctoral Thesis

Jesús Marugán Lobón

Dissertation presented for the PhD degree in Sciences
with the Doctor Europeus Mention

Supervised by Dr.

Ángela D. Buscalioni

Departamento de Biología
Unidad de Paleontología

UNIVERSIDAD AUTÓNOMA DE MADRID

Madrid, February 2007

A tres personas admirables…

Marta (mi *Madre*), Maite (mi *Mujer*) y Ángela (mi *Mentora*)

… y en memoria de Borja Terán, mi amigo y hermano por siempre….

shine on you crazy Diamond

Contenidos/*Contents*

BOXES

APPENDIX

i. Agradecimientos/Aknowledgements

Desde los primeros esbozos de este trabajo y hasta ahora nunca he dejado de aprender y de disfrutar aprendiendo, y esto se lo debo a mucha gente. A Ángela Buscalioni, mi profesora y mentora, porque confió en mí para desarrollarlo y siempre ha estado, y está ahí, para explicármelo todo. Mi madre, Marta, quién me ha enseñado a ser, a aprender escuchando, y a ver siempre las cosas en positivo (mil gracias Madre!). Y Maite, mi pareja, maestra en querer, en escuchar y comprender. Juntos construimos el día a día…te quiero Techu.

En la UAM, siempre aprendo; en la Unidad de Paleo, Montse y Ana (con quién he crecido), el Gran Oscar (eres un máquina, amigo), Joaquín, Javi Barbadillo, Fran, Diego, Pepelu, Bea, Joannis, Hugo y Patxi (que me enseño a preparar los fósiles de Las Hoyas). También comparto el espacio de la UAM con tres grandes personas; Luis Rios, Enrique Turiegano (Turi) y Miguel Pita.

En otras instituciones de Madrid, también; en el Museo de Ciencias Naturales, con Jorge Morales (un padre paleontológico), Javier Lobón (Tío ecológico, científico hasta la médula, y de astuta ironía…mil gracias Javierito), Isra Sánchez y Manolo Salesa (amigos de grandes momentos), y Vicki, Isra García, Iñigo y Cristina, Susana, Manuel Hernández, Pablo Peláez, Lauro, Beni, Quique, Manolo Nieto y Antonio Rosas. Allí también mora Markus Bastir, gran amigo fuera y dentro de la ciencia.

En la complu están Marian Fregenal y Nieves López. Sabias. En el Instituto de Investigaciones Biomédicas "Alberto Sols", Miguel Manzanares y su equipo, quienes me han prestado su tiempo y me han escuchado.

De otras instituciones españolas, siempre; de Valencia (Instituto Cavanilles y UV) Sole y Carlos, con quién alucino desde que nos conocimos en el EJIP. De Valladolid, Paco Pastor, cuyo tesón ha dado fruto a una colección magnífica de vertebrados en la facultad de medicina, que además nos ha dejado estudiar (¡gracias!).

De Europa, en Portugal (Museo de Ciencias Naturales de Lisboa), Luís Rodríguez (ACBDO, con quién he aprendido y me he perdido en distintos lugares del mundo…juntos conquistamos el AMNH y su fotocopiadora!), y Vanda Dosantos (con quién también nos perdimos los dos en Oklahoma!). En Alemania, he aprendido y disfrutado a raudales; en el Museum für Natürkunde de Berlín, con D. Unwin, quién me acogió en su despacho unos meses y me enseño el mundo de los pterosaurios, que me fascinan (thanks Dave!). Silke Franhert, de cuya mano vino la colección Hess del museo casi como por arte de magia, y permitió su estudio con una beca Synthesys (danke!). Dirk Fuschs y sus "kalamar" fueron grandes aliados en Choriner Strasse, igual que Sandra. En Munich está Matthias Starck, que me acogió en la universidad y en su casa, me invitó a dar una charla, y siempre me enseña. Kai Schmidt, que me cuidó en su cálido hogar. También conocí a Ulf Bauchinger, una gran Persona. En Inglaterra están Rob Asher (ahora en Cambridge, pero un ciudadano del mundo), Susan Evans (que escuchó con interés en Jena y se leyó nuestro primer trabajo), y Paul O'higgins,

que en los últimos momentos de la tesis me ha dado todo su apoyo. En Holanda, al principio Jan, y luego Albert y Joke, me salvaron del frío, me alimentaron y compartimos unos buenos momentos mientras exploraba las maravillas de la colección Hubrecht de la mano de Jenny Narraway, la Gran Jenny! (saviour of the jewel).

En Estados Unidos; en SUNY Stony Brook el profesor J. Rohlf me enseñó los entresijos de la morfometría geométrica en su "morphometrics lab" simulando puntos en el espacio multidimensional; le debo mucho (thanks indeed Jim). Y a Waleed Garaibeh también, que en el labo me explicó qué eran esos entresijos y esos puntos, y con quién he compartido, junto a Kerry Brown, mucho dentro y fuera del campus (y más allá de Stony Brook). En el departamento también está Winsord Aguirre, con quién charlé mucho. En antropología estaba Callum Ross (ahora en Chicago) que me invitó a dar una charla y elaborándola me di cuenta de lo que estaba haciendo (cheers Callum!). También tuve el placer de conocer allí a Kathy Foster, y a los "Justins", Sipla y Georgy, con quién compartir ideas es un placer y seguro que colaboraremos pronto. El Museo de Historia Natural de Nueva York es una institución increíble y allí, M. Norell me enseñó y dejó entera libertad para estudiar los fósiles más alucinantes del mundo, y me dejó soñar en las bibliotecas…. (thanks so much Mark!). Carl Mehlin me hizo la vida mucho más fácil en el laberinto (thank you doc!), y Mike Ellison me dejó su escáner y su super cámara para digitalizar muchas cosas. Ana Balcarcel me sacó del cotolengo donde vivía y me dio cobijo (gracias!). Eric Delson y Will Harcourt-Smith dejaron que tuviera mi primer contacto con un microscribe, y con Mark Siddall y Julia Clarke charlé mientras fumábamos clandestinamente. En especial, quiero agradecer desde aquí a Paul Sweet y Shannon Kenney, de ornitología, su ayuda sin la que no habría podido estudiar la colección de aves actuales. En Los Ángeles está Luis Chiappe, con quién aprendo la evolución de las aves desde el fósil, y me ha cuidado en su ciudad, L.A., en Beijing, y en los confines de la Argentina, allá por el Lanín. Un beso enorme para Megan, y…para el pequeño Luca!

En la vida fuera de la paleo está mi familia, ti@s y prim@s, mi familia Aguado-Molina, y la pequeña Miga, todos siempre un apoyo incondicional. Y como no, mis amig@s, Juan Carlos y Laura, Cuti, David (Padi), Chico y Marimar, Pablo, Miguel y Bea, Juan (Burgues) y Maria, Juan (Twity) y Cristina, Raul, Julio, Chirlo, Nacho, Juan y Maria, Juanki y Ana, y Chona ¡Nada de esto habría sido posible sin vosotros!

Hay mucha más gente más, tanta que haría que estas líneas excedieran en magnitudes la amplitud de la propia tesis. Extiendo desde aquí a todos, ellas y ellos, mi más sincera y enorme gratitud.

El desarrollo de todo el trabajo se realizó con la ayuda de una beca FPU del Ministerio de Educación, de las Ayudas para el estudio de Colecciones del AMNH (Collection Study Grants), el proyecto Synthesys de la EU, y de la Jurassic Foundation. Así mismo, el proyecto se ha realizado bajo el auspicio del proyecto de investigación DGCYT "".

ii. Objetivos y esquema de trabajo

El cráneo arcosauriano se ha utilizado como unidad de estudio en un contexto comparativo. Capturando aspectos de su geometría mediante de dos metodologías analíticas distintas, la morfología teórica y la morfometría geométrica, el objetivo es dilucidar aspectos sobre su evolución morfológica que permitan desvelar algunos procesos causales que subyacen a su transformación. Así, se espera que la utilización de estas dos técnicas contribuya al un conocimiento más detallado del cráneo y de su evolución, así como para mostrar las posibilidades que ofrece utilizar éstas técnicas para tal efecto. Del mismo modo, se pretende evaluar la aplicabilidad y utilidad de estas técnicas en el campo de la teoría macroevolutiva.

En particular, estudiando la geometría craneal arcosauriana perseguimos desvelar patrones de su disparidad como un fenómeno asociado a su *variación* morhológica. El objetivo es obtener claves desde las que deducir un modelo que explique la organización fenotípica del cráneo. Así mismo, el objetivo es explorar si la integración morfológica juega algún papel evolutivo en dicha organización morfológica del cráneo, fenómeno que exploraremos en términos de *covariación*. El desarrollo de ambos objetivos pasa por identificar qué posibles unidades fundamentales, o módulos, pueden subyacer a la identidad formal del cráneo arcosauriano.

El estudio de la geometría craneal se realizará explorando distintos criterios de subdivisión de las partes del cráneo entre los que destacan criterios funcionales (complejo facial, órbita y caja craneana), y criterios embriológicos (el condrocráneo y el dermatocráneo, o los conceptos de parte cordal y parte precordal). Adicionalmente se estudiarán determinados aspectos de la evolución fenotípica del sistema nervioso central en asociación con la organización fenotípica craneal, aunque en especial, dentro del contexto neontológico de las aves modernas.

La agenda de trabajo para desarrollar estos objetivos generales se ha desglosado en seis aproximaciones distintas que conforman la **Tercera Parte** del volumen:

El **Capítulo 1** (*Disparity and Geometry of the Skull in Archosauria (Reptilia: Diapsida*), es un articulo publicado en el Biological Journal of the Linnean Society, y en el se estudian cráneos de gran parte del clado desde la perspectiva de la Morfología Teórica y un morfoespacio basado en una métrica proporcional (variación de forma unidimensional de partes craneales a un estándar de longitud total). Desde este modelo se explora la disparidad geométrica craneal externa atendiendo a una subdivisión funcional del cráneo (la relación entre el rostro, la órbita ocular, y la caja craneal), y se espera encontrar una geometría craneal propia del linaje.

El **Capitulo 2**.(*Insights on avian skull shape macroevolution on the basis of Geometric Morphometric procedures*) explora la disparidad y la integración morfológica en aves modernas desde la operatividad de la morfometría geométrica. Un objetivo adicional es mostrar el funcionamiento de la técnica, su capacidad resolutiva y sus posibles limitaciones a una escala macroevolutiva. Se utilizan técnicas estadísticas

multivariantes para el estudio de la alometría evolutiva del cráneo, deformaciones de mallas basadas en el Thin Plate Spline, morfoespacios empíricos, y el uso de nuevas técnicas de visualización del cambio de forma (*image unwarping*) y de visualizar la covarición entre variables (*contour plots*). Se plantea la subdivisión del cráneo atendiendo a criterios funcionales y embriológicos.

El **Capítulo 3** (*Avian skull morphological evolution: exploring exo- and endocranial covariation with Two-block Partial Least Squares*), es un articulo publicado en Zoology y representa la primera aproximación cuantitativa a la integración morfológica en arcosaurios (aves) desde herramientas estadístico geométricas de la morfometría programadas para este fin (Mínimos Cuadrados Parciales en Dos-bloques). Se combinan dos tipos de métricas; ángulos endocraneales obtenidos de la literatura clásica (y que incluyen aspectos de variación exo- y endocraneal), y variables de forma obtenidas desde la superposición de landmarks descritos sobre estructuras visibles desde el exterior del cráneo aviano.

El **Capítulo 4** (*Braincase shape disparity and evolutionary allometry in modern birds (Neornithes: Archosauria)*) explora la organización fenotípica de la caja craneana en aves desde el plano medial-sagital (endocranealmente). En él se utilizan herramientas estadísticas exploratorias, morfoespacios empíricos, y se examina la alometría evolutiva desde la estadística multivariante. Se re-evalúan las hipótesis planteadas en los trabajos anteriores, y se comprueba la posibilidad de plantear un modelo que analice la integración fenotípica del cráneo desde su desglose en unidades, o módulos, atendiendo a criterios de origen celular embriológico (partes cordal y precordal).

El **Capítulo 5** (*Avian braincase and central nervous system shape evolution and their association with ontogenetic strategies*) explora, en la misma muestra que el capitulo anterior, la posible asociación entre la evolución de la ontogenia y la forma de la caja craneana (e indirectamente, sobre la evolución fenotípica del sistema nervioso central). Se estudia la probabilidad de pertenencia a un grupo de desarrollo determinado (tipo de desarrollo; altricial-Precocial), desde la morfología del cráneo utilizando métodos de análisis discriminantes multivariantes (análisis Canónicos), así como Análisis de Pendientes Separadas (Modelos Lineares Generales), para comprobar la posibilidad de encontrar diferencias alométricas entre grupos de estrategia reproductiva.

El **Capítulo 6** (*Morphological integration of the avian Central Nervous System and the braincase*) es una exploración estadístico-geométrica en la que se explora la posible integración morfológica entre el sistema nervioso central y el cráneo en aves utilizando la técnica de Mínimos Cuadrados Parciales en Dos-bloques. En el modelo se integra información relativa a las proporciones de peso entre partes del cerebro obtenida de la literatura y se conjugan con información geométrica del plano medial-sagital de la caja craneana. En este modelo se explora la integración de dos sistemas diferentes (neural y osteológico).

iii. Objetives and work schedule

We have used the Archosaurian skull as a unit of study in a comparative framework. Capturing aspects of its geometry by means of two different methodologies, Theoretical Morphology and Geometric Morphometrics, with the objective of unveiling aspects of its morphological evolution. While this approach might allow deciphering processes underlying its transformation, we also aim that the application of these two different methodologies serve as a way for learning more details about archosaurian skull morphology. At the same time, we aim showing the utility of these techniques in the field of macroevolutionary theory.

In particular, we pursue unveling patterns of the geometric disparity of the archosaurian skull as a phenomenon of morphological *variation*. The objective is to obtain keys from which to elucidate a model that explains the phenotypic organization of the skull. Likewise, the scope is to explore if morphological integration plays a role on the organization of the skull in this evolutionary context. We will explore this phenomenon in terms of *covariation*.

The development of these two principal objectives passes by identifying which possible fundamental units, or modules, might underlie the formal identity of the archosaurian skull. The study of cranial geometry will be carried out exploring different criteria for the subdivision of the skull, such as functional (facial complex, orbits, and braincase), or embryological (chondrocranium and dermatocranium, or chordal and prechordal parts). Additionally, particular aspects of the phenotypic evolution of the central nervous system will be studied yet in association with braincase phenotypic organization, all within the context of modern birds.

The work schedule to fulfil these general objectives has been sequenced in six different works, all of which configure the **Third Part** of the thesis:

Chapter 1 (*Disparity and Geometry of the Skull in Archosauria (Reptilia: Diapsida)*), is a paper published in the Biological Journal of the Linnean Society, in which we studied skulls from most groups of the archosaurian lineage from the perspective of Theoretical Morphology and a morphospace based on proportional metrics (unidimensional form variation of cranial parts with respect to a standard of total length). We explore the geometric disparity of the skull from this model attending to a functional subdivision of the parts (rostrum, orbit, and braincase), expecting to find a particular skull geometric characteristic of the lineage.

Chapter 2 (*Insights on avian skull shape macroevolution on the basis of Geometric Morphometric procedures*) explores the disparity and morphological integration of the avian skull by means of geometric morphometrics procedures. One additional aim is to show the application of the techniques, its resolutive capabilities, and its possible constraints at macroevolutionary scales. Multivariate statistical techniques are used for the study of evolutionary allometry of the skull, plus deformation grids based on

the Thin Plate Spline, empirical morphospaces, and new visualization techniques for shape change (image unwarpping) and the visualization of covariation between variables (contour plots). The subdivision of skull parts is proposed following both functional and embryological criteria.

Chapter 3 (*Avian skull morphological evolution: exploring exo- and endocranial covariation with Two-block Partial Least Squares*), is a paper published in Zoology, and represents the first quantitative approximation to the morphological integration of the skull in archosaurs (birds) using geometric-statistical techniques programmed fro this sake (i.e. Two-block Partial Least Squares). Two types of metrics are combined; angles obtained from classic literature, and containing information both of exo- and endocranial aspects of variation, and shape variables obtained from the superimposition of landmarks capturing externally visible aspects of the avian skull.

Chapter 4 (*Braincase shape disparity and evolutionary allometry in modern birds (Neornithes: Archosauria)*) explores the phenotypic organization of the braincase in birds in the mid-sagittaly plane (i.e. endocranially). In this study statistical-exploratory techniques are used, empirical morphospaces, and evolutionary allometry is tested using multivariate regressions. There is a re-evaluation of the previously proposed hypotheses, and a model of braincase modularity is tested on the basis of embryological criteria used for distinguishing between its parts (the chordal and the prechordal parts).

Chapter 5 (*Avian braincase and central nervous system shape evolution and their association with ontogenetic strategies*) explores in the same sample as in the previous chapter the probability of association between ontogenetic evolution and braincase architecture (and, indirectly, its relation with central nervous system organization). We therein study the probability of pertinence to developmental group (altricial-precocial) with a specific braincase shape by means of Canonical Variates Analyses. Likewise, multivariate Separate Slopes models are used to test if birds of each developmental group follow different allometric trajectories.

Chapter 6 (*Morphological integration of the avian Central Nervous System and the braincase*) is a geometric-statistic exploration in which we explore the possible integration between the central nervous system and the braincase using Two-block Partial Least Squares. proportional weights of the central nervous system parts are incorporated in the analysis as one block of variables, which are tested agians shape information obtained after the superimposition of landmark configurations placed onto the mid-sagittal plane of the braincase. The model explores the possible evolutionary integration

between two different systems (neural and osteological).

La memoria de la tesis doctoral que a continuación exponemos se desarrolla en tres partes. La **Primera parte** es un epítome sobre la motivación que ha promovido todo el estudio. En ella también se recapitula sobre el contexto conceptual en el que se enmarca el estudio, y finalmente, se desglosan los objetivos perseguidos. La **Segunda parte** de la memoria es un sumario que reúne los materiales y los métodos aplicados. Comienza con una revisión general del la morfología craneal del clado Archosauria, pasando después a resumir los aspectos más importantes de las metodologías utilizadas. La **Tercera parte** contiene todos los resultados obtenidos divididos en seis capítulos distintos. Cada uno de estos capítulos expone sus objetivos particulares y la estrategia analítica aplicada para alcanzarlos. A cada exposición introductoria le siguen los resultados obtenidos y su discusión. El final de la tercera parte contiene las conclusiones y las consideraciones finales del proyecto realizado. Al texto le acompañan cinco recuadros (denominados como *Boxes*) con información adicional.

-Any tendency for production of species at larger or smaller than ancestral size also implies a cascade of sequelae, some by new adaptation in response to Galileo's old surface/volume principle (and therefore conventionally explainable), but others by inherited developmental correlation with this most pervasive and potent of all factors (these may be interpreted as legacies of past adaptations, but many must be spandrels…).

S. J. Gould; Speciation and sorting as the source of evolutionary trends, or 'things are seldom what they seem' (1990)

PRIMERA
PARTE

1.1. Descripción y motivación de la investigación

El proyecto de tesis doctoral que hemos desarrollado rinde esta memoria. En ella desbrozamos todos los aspectos estudiados sobre la disparidad y la integración morfológica craneal del grupo natural de los reptiles arcosaurios. La aproximación a estos dos fenómenos morfológicos se ha llevado a cabo desde de dos metodologías distintas; la Morfología Teórica y su herramienta fundamental, el morfoespacio, y la Morfometría Geométrica junto con sus herramientas de estadística multivariante para el análisis de configuraciones de coordenadas (landmarks).

El estudio representa una comparación de los cráneos de arcosaurios persiguiendo caracterizar sus variaciones. Puesto que la exploración de la variación evolutiva se basa en el método comparado, el estudio parte del establecimiento de una hipótesis de homología sólida, la cual se fundamenta principalmente en la naturaleza monofilética del grupo. Enmarcado en un contexto macroevolutivo, el estudio se ha desarrollado utilizando herramientas métricas, y desde esta perspectiva, los caracteres homólogos han pasado a ser variables que capturan exclusivamente la variación geométrica como un atributo de la morfología craneal. Así pues, los caracteres homólogos en los que se basan los datos son estructuras anatómicamente identificables que, no obstante, pasan a parametrizárse en forma de ángulos y/o proporciones, cuando se trabaja desde una métrica tradicional, o como configuraciones de coordenadas (landmarks), cuando trabajamos desde la morfometría geométrica. En definitiva, el uso de un código métrico permite utilizar un conjunto de herramientas analíticas como el morfoespacio (en morfología teórica), o la estadística multivariante cuando se trabaje desde la superposición de landmarks (morfometría geométrica).

Caracterizar la forma biológica (en nuestro caso, la forma del cráneo) desde una simbología cuantitativa puede parecer una desventaja en cuanto a la pérdida de otros aspectos descriptivos inherentes a la morfología tan importantes como pueden ser, por ejemplo, el color, la textura, o el número de elementos entre otros. Sin embargo, permite capturar con una objetividad analítica los aspectos más importantes de la geometría del cráneo en el conjunto de organismos del clado Archosauria. La perspectiva analítica de la geometría desacopla la ambigüedad de la descriptiva cualitativa, pues permite una discusión explícita relativa exclusivamente a las limitaciones y/o a la capacidad explicativa de la técnica que se escoja para realizar la investigación. En efecto, este hecho ha motivado durante décadas la propuesta de que la manera más objetiva para aproximarse al estudio de la integración morfológica y a la disparidad resida en el análisis cuantitativo (Olson y Miller, 1958; Foote,

1997).

Históricamente, sin embargo, todos los razonamientos que han perseguido explicar la forma biológica y su transformación evolutiva tienen unas raíces muy profundas. Estos razonamientos, además, suelen ir acompañados de cierta complejidad ya que su lógica seguramente residirá en más de una escala de la jerarquía biológica. Intentaremos no obstante resumir los aspectos sobre la historia, la lógica y los factores implicados en el estudio paleobiológico y morfológico del cráneo, en un esfuerzo por esbozar las cuestiones más importantes que incumben al contexto ontológico, epistemológico y práctico del trabajo que se resume en esta memoria. Suplementamos el compromiso de tener que limitarnos a escribir un sumario resaltando las fuentes más importantes que contengan información más extensa respecto a cada uno de los aspectos sobre la materia que desarrollamos a continuación.

1.2. Macroevolución

El estudio de la macroevolución ha ocupado casi siempre una posición secundaria, e incluso opuesta, a las corrientes principales de investigación evolutiva desde la mitad del siglo pasado. Sin embargo, la estrategia del método comparado a este nivel "transespecifico" ha sido siempre una *raison d'ètre* extendida en el estudio morfológico (Russel, 1916; Rensch, 1959), y ha contribuido sin duda a forjar la simiente de la Teoría Evolutiva.

La teoría macroevolutiva se enmarca en escalas taxonómicas por encima del nivel de especie (Cracraft y Eldredge, 1979; Stanley, 1979); siempre al menos desde la unidad de Familia taxonómica para Simpson; 1953), mientras que la microevolución es el marco operativo desde el que se estudia la variabilidad orgánica a niveles intraespecíficas e inter- o intrapoblacionales. Se considera que los patrones y procesos macroevolutivos son propios de esta escala de comparación, y por tanto, que los fenómenos que se observan son claramente distinguibles de aquellos procesos propios de la microevolución (ver p. ej. Gould, 2002).

La propuesta actual, no obstante, es una visión quizá más relajada de la problemática, tendiendo por tanto a omitir las tensiones que históricamente han separado ambas aproximaciones, para así incorporar y relacionar la información que es capaz de aportar cada una de ellas en un contexto evolutivo universal. Así, la distinción entre ambas escalas operativas se ve cada vez más desde este contexto unificador (aunque haya grupos que todavía se resistan a ello), y la estrategia pasa por declarar que ambas aproximaciones al estudio de la evolución se desacoplan tanto por las diferencias en respuestas que persiguen, como por los protocolos metodológicos que cada una aplica a sus pesquisas.

Efectivamente, es necesario asumir que la macroevolución y la microevolución son empírica y teóricamente distintas por la dimensión a la que cada una tiene lugar, así como por los procesos que emergen y pueden observarse al operar en desde cada punto de vista. Sin embargo, es importante también asumir que el desacoplamiento total entre ambas puede resultar ilógico puesto que en definitiva, las preguntas que se realizan siempre hacen alusión a los mismos organismos independientemente de la escala desde la que se opere (Eble, 2004).

La forma es el recurso informativo clave con el que cuenta la paleontología, ya que es la información que preserva el registro fósil. Desde aqui pretendemos hacer un énfasis especial en la importancia que tiene comparar formas para aproximarse a la variación morfológica desde escalas comparativas que, en la jerarquía biológica, impliquen situarse por encima del nivel de especies. Consideramos que este marco puede facilitar una resolución capaz de desvelar aspectos claves de la evolución vistos desde la morfología.

Box 1

El clado*Archosauria*

Las relaciones entre grupos reptilianos han sido siempre dificultosas, aunque los cocodrilos, dinosaurios, los reptiles voladores (pterosaurios) y otras formas más basales como los tecodontes, han sido unificados siempre y expeditivamente bajo la misma subclase taxonómica *Archosauria* (Romer, 1966; Fig. 3.1).

El nombre Archosauria deriva de la conjunción entre *sauros* del griego 'lagarto', y el prefijo *arkhos*, también del griego, 'gobernante' o 'dominante'. La biodiversidad de los arcosaurios es solo inferior a la de los insectos, la de las plantas y, en el universo vertebrado, la de algunos grupos de peces. Al mismo tiempo, la cantidad de medios que los arcosaurios han sido capaces de colonizar a lo largo de su historia sobre el planeta refleja su elevada disparidad de formas. Hay formas de arcosaurios asociadas a medios acuáticos, tanto continentales como marinos, a medios terrestres, y al medio aéreo, siendo éste un mundo explorado por primera vez por los pterosaurios, sólo conocidos desde el registro fósil, y ahora dominado por las aves modernas.

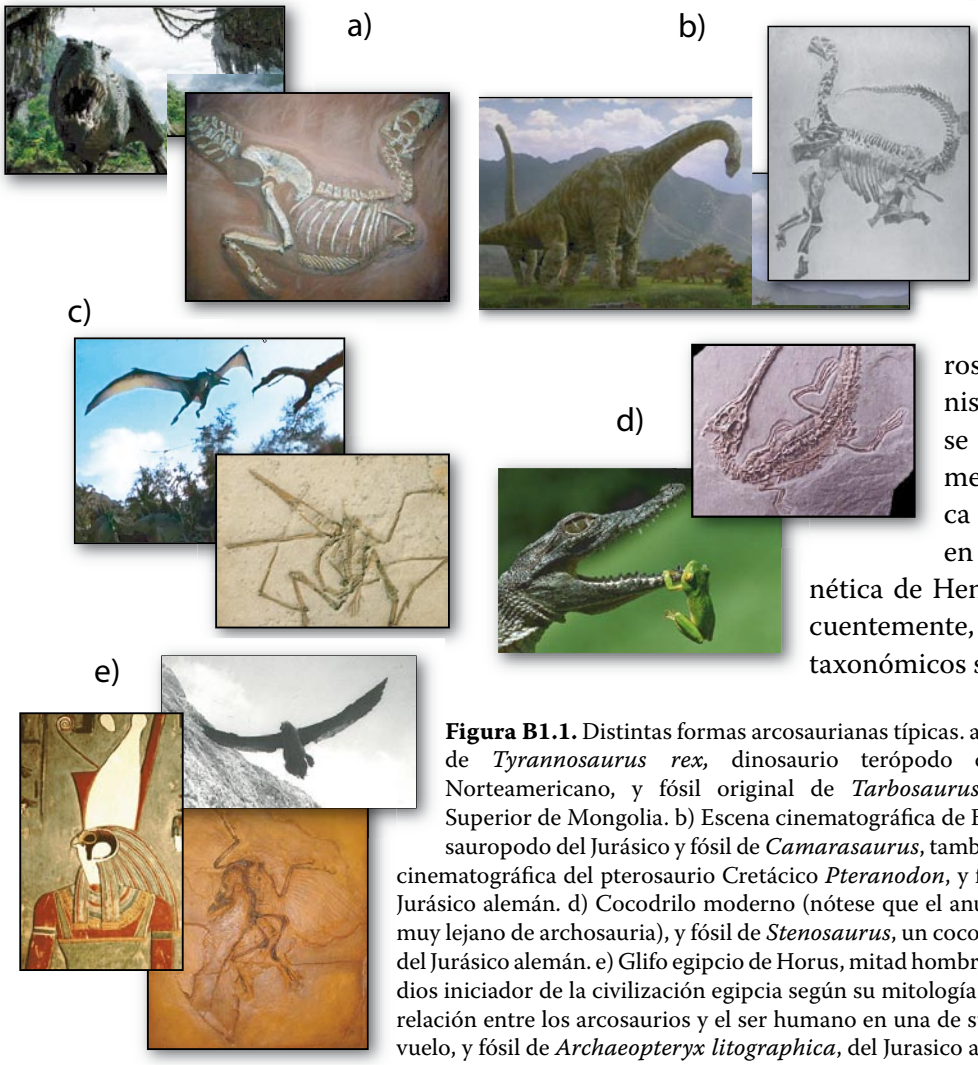

Figura B1.1. Distintas formas arcosaurianas típicas. a) Escena cinematográfica de *Tyrannosaurus rex,* dinosaurio terópodo del Cretácico Superior Norteamericano, y fósil original de *Tarbosaurus bataar*, del Cretácico Superior de Mongolia. b) Escena cinematográfica de Brachiosaurus, dinosaurio sauropodo del Jurásico y fósil de *Camarasaurus*, también del Jurásico. c) Escena cinematográfica del pterosaurio Cretácico *Pteranodon*, y fósil de *Pterodactylus* del Jurásico alemán. d) Cocodrilo moderno (nótese que el anuro representa a un linaje muy lejano de archosauria), y fósil de *Stenosaurus*, un cocodrilo marino (Neosuchia) del Jurásico alemán. e) Glifo egipcio de Horus, mitad hombre mitad halcón (Neoaves), dios iniciador de la civilización egipcia según su mitología mostrado para resaltar la relación entre los arcosaurios y el ser humano en una de sus vertientes. Albatros en vuelo, y fósil de *Archaeopteryx litographica*, del Jurasico alemán.

Los arcosaurios son de los primeros grupos de organismos sobre los que se estableció una nomenclatura taxonómica filogenética basado en la teoría fiologenética de Hennig (1968). Consecuentemente, como los nombres taxonómicos se fundamentarán a partir del uso de la cladística en la relación antecesor-descendiente, el taxón Archosauria pasó a convertirse en una Subclase parafilética. En su definición actual, *Archosauria* deja de contener a varios de los grupos que contenían las señas de identidad de la subclase (p. ej. los dientes tecodontos o la fenestra anteorbitaria; Romer, 1966). Así pues, el nombre *Archosauria* alude a un clado, un grupo natural monofilético que contiene al ancestro común de las aves y cocodrilos y todos sus descendientes (Gauthier y Padian, 1985; *fide* Brochu, 2001). 'Archosauria', que incluye a los tecodontos, y es un término que se acepta por su carácter histórico, pero en práctica se sustituye en por el término Archosauriformes, clado que incluye a Archosauria, Proterosuchidae, Proterochampsidae, *Euparkeria* y Erythrosuchidae.

Los arcosaurios (*s.s.*) evolucionan de formas ancestrales dentro de Archosauriformes del Triásico temprano, y el clado se dicotomiza en dos grandes grupos, Ornihodira y Crurotarsi. Los grupos divergieron muy probablemente en la base del Triásico, y la diferencia entre ambos se establece atendiendo a la estructura de los huesos del tarso. En la etapa más tardía del Triásico empezarán a surgir formas más basales de dinosaurios y pterosaurios. Crurotarsi, por el contrario, tiene una mayor representación anterior (Rauisuchia, Phytosauria, Aetosauria, y otras formas ancestrales de cocodrilos).

Con la extinción Triásico-Jurásica desaparecen muchos grupos de Crurotarsi, sobreviviendo formas de dinosaurios y pterosaurios dentro de Ornithodira (Benton, *op. cit.*), y Sphenosuchia y Protosuchia y descendientes cocodrilianos de Crurotarsi.

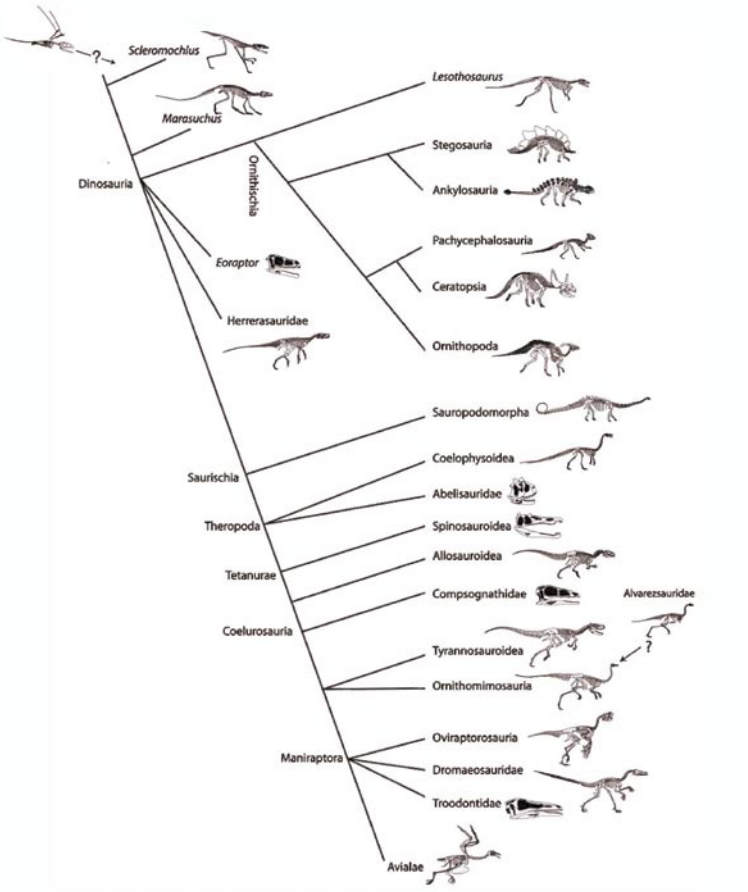

Figura B1.2. Relaciones filogenéticas en Ornithodira. Nótese la posición dudosa de Alvarezsauridae. Original de Brochu (2001).

Así pues, la "dominación" de estos saurios se extiende por la práctica totalidad del Mesozoico, aunque solo llegan al hasta nuestros días en las formas actuales de cocodrilos (Crurotarsi) y aves (Ornithodira). Las relaciones filogenéticas entre cocodrilos actuales son menos controvertidas que las de las aves. Como se señalará posteriormente en este mismo capitulo de materiales, por motivos prácticos el estudio realizado se ha focalizado más particularmente en formas pertenecientes al clado Ornithodira (dinosaurios y, más particularmente, aves actuales), por lo que desarrollaremos más extensamente sus relaciones filogenéticas.

Dentro de Ornithodira la condición monofilética del clado Dinosauria tiene soporte completo en la práctica totalidad de los análisis de Archosauria, y del mismo modo, existen pocas dudas en la literatura sobre el origen dinosauriano de las aves (Padian y Chiappe, 1998). El registro más antiguo sitúa la primera dicotomía del clado Dinosauria en el Triásico en la forma de herrerasauridos (p. ej. *Herrerasaurus ischigualastensis*) y *Eoraptor lunensis*, del Tríasico Argentino (Holtz, 2000; B1.2).

El desenterramiento constante de nuevo material fósil de terópodos nutre, no obstante, un cladograma que entre dromeosaurios (Coelurosauria) está todavía por resolver (Turner et al., 2006). Los Alvarezsauridos, por ejemplo, son un grupo complejo que sigue siendo motivo de controversia; tras su hallazgo fueron diagnosticados como aves no voladoras modificadas, pero ahora se les considera más probablemente emparentados con el clado Avialae, aunque fuera del clado (Holtz, op. cit.; Fig. B1.2).

Entre las formas de aves modernas también existen incongruencias entre las distintas hipótesis propuestas. Debido a las incongruencias entre datos moleculares y morfológicos es difícil resolver la identidad (y nombre) del grupo corona (*crown-group*) de las aves, que puede nominarse como Aves o Neornithes (Cracraft, 2001). Utilizaremos Neornithes como clado consenso que incluye al último ancestro común de paleognatas y neognatas (los dos linajes de aves actuales) y todos sus descendientes (ver también; Cracraft y Clarke, 2001; Van Tuinen, 2002), por ser un clado en el que estudios moleculares y morfológicos parecen aceptar sin controversias. Avialae es el clado que incluye a Neorni-

thes (Fig. B1.3), todos los dinosaurios terópodos cercanos y el dromeosaurio *Deinonychus* (Padian et al., 1999). Como curiosidad, nótese que desde cualquiera de las propuestas es difícil definir qué es un "pájaro", lo que convierte a un término tan al uso en un concepto biológico relativamente ambiguo).

El número de aves mesozoicas fósiles se ha disparado en los últimos quince años, casi todos han sido incluidos en el clado Enantiornithes (Walker, 1981; Sanz et al., 1995; Chiappe, 1995; Zhang y Zhou, 2000), aunque nuevos hallazgos hacen que algunos autores pongan en duda su identidad monofilética (*Apsaravis ukhaana*; Clarke y Norell, 2002). De lo que no cabe ninguna duda es que las aves ya habían diversificado, y que estaban ampliamente diseminadas geográficamente en el cretácico superior. Esto hace que el impacto de la extinción K-T sea todavía materia de debate.

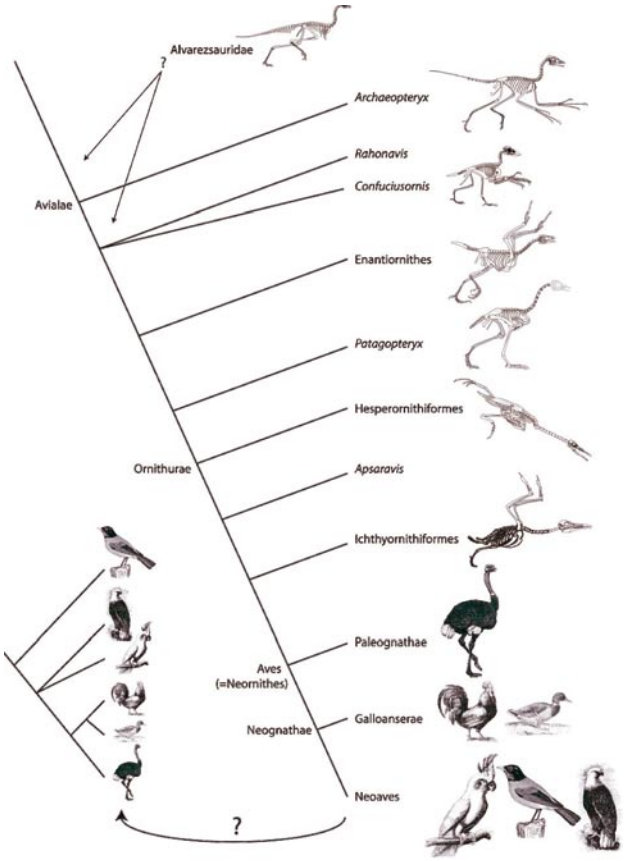

Figura B1.3. Relaciones filogenéticas en Avialae. Nótese la incertidumbre en el nodo Neovaves. Original de Brochu (2001).

Dentro de Neornithes, la división clásica entre aves Palegnatas y Neognatas basándose en la estructura de la región palatal parece tener actualmente un soporte filogenético (molecular y filogenético), posicionando a las anteriores como un clado basal (Paleognathae). Del nodo hermano, *Neognathae*, se separan *Galloanseres* como grupo monofilético (Galliformes y Anseriformes, ambos *sensu lato*). Solo algunos estudios moleculares encuentran incongruencias entre taxa dentro del clado. Es en la siguiente dicotomía, *Neoaves*, donde todavía no existe un consenso estricto entre todos los resultados obtenidos hasta la fecha. La filogenia más resuelta y más extendida es la de Sibley y Alquist (1993). No obstante, es una filogenia de la que se duda desde hace casi ya una década debido a la desconfianza en las técnicas de hibridación de ADN utilizadas. Otras filogenias mucho más completas (incorporando datos moleculares y morfológicos de diversa índole) están todavía en preparación (Livezey y Zusi, 2000; Van Tuinen, 2002).

Todavía existen controversias en cuanto a sus relaciones con el clado Archosauria. Los pterorsaurios son los primeros vertebrados voladores conocidos, aparecen por primera vez en el registro del Triásico superior de Italia (*Eudimorphodon*),y su registro fósil es más pobre que el de cualquiera de los clados que hemos citado anteriormente (Kellner, 2003; Unwin, 2003).

Casi todos los análisis filogenéticos sitúan a los pterosaurios dentro de arcosauria (Fig. B1.2), y más cercanos a las aves que a los cocodrilos, aún cuando está universalmente aceptado que no comparten un ancestro común con las aves como se propuso inicialmente. La controversia más extendida se centra en si los pterosaurios se relacionan con un pequeño arcosaurio más antiguo (del Carniense de Inglaterra; *Scleromochlus taylori*; Fig. B1.2) o no, lo que hace que en realidad, las diferencias topológicas que se propone en los distintos escenarios dentro de Archosauria sean bastante sutiles (Brochu, 2001). Es por ello que asumimos su pertenencia a Archosauria por ser esta la hipótesis más generalizada hasta el momento.

1.3. Disparidad e integración en macroevolución

En teoría macroevolutiva, la idea de que el espacio potencial de formas producidas por la naturaleza a lo largo del tiempo pueda ser teóricamente infinito, se enfrenta con la posibilidad de que la ocupación de ese espacio sea limitada. Se postula que un sesgo en la variación morfológica a escala macroevolutiva se deba a la existencia de factores condicionantes, factores que pueden venir impuestos por el medio, o por las propiedades del propio sistema del desarrollo (ver p. ej.; Alberch, 1989; Maynard-Smith et al., 1985). En términos biológicos estos factores condicionantes se aúnan en el término *constraints*, un vocablo adaptado del inglés cuyo significado es "restricciones".

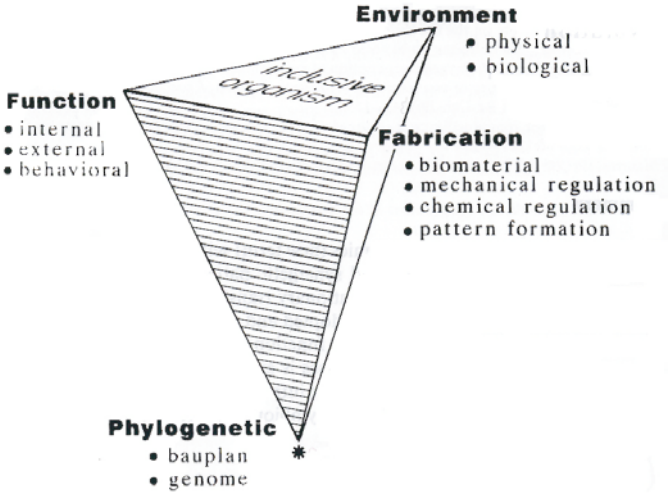

Figura 1.1. Marco conceptual de constraints (factores limitantes o restrictivos) sobre la variación de la forma según Seilacher (1970; superficie rayada). El modelo expuesto es una ampliación actualizada del mismo autor, extendiendo el Triángulo primigenio a una Pirámide tras la adición de una dimensión adicional; el factor ambiental. Nótese que el vértice filogenético puede ser, según el autor, equivalente al ontogenético. Modificado de Seilacher (1991).

En biología evolutiva la palabra inglesa *constraint* tiene un uso generalizado pues cuenta con una definición propia; *la existencia de factores restrictivos sobre la producción de variantes fenotípicas* (Maynard-Smith et al., op. cit.). En un contexto macroevolutivo se considera que la morfología y su transformación puede estar sujeta a factores condicionantes, o constraints, de naturaleza histórica (filogenéticos), estructurales (biomecánicos), del desarrollo (ontogenéticos), y ambientales (el medio)(Seilacher, 1970, 1991; Fig. 1.1). Tanto la disparidad como la integración morfológica son fenómenos macroevolutivos intrínsecos a la morfología; ambos emergen como fenómenos de la organización fenotípica en el tiempo y están ligados a la existencia de constraints.

1.3.1. Disparidad

En textos especializados se utiliza comúnmente "diversidad o diversificación morfológica", "variedad morfológica", o "rango anatómico" entre los más comunes, para referirse a la variación y las diferencias de forma entre los organismos. La propuesta de utilizar *disparidad* como un término distintivo fue propuesto por Janusson y por Runnegar (casi simultáneamente en los años ochenta, *fide* Raff, 1996) para unificar todas las acepciones en un solo término.

El término de disparidad en paleobiología se propone como independiente del número de especies argumentando que, a diferencia de la diversidad, su significado alude únicamente a la forma de los organismos, siempre enfatizando sus diferencias. Así, en términos macroevolutivos la disparidad es un fenómeno que surge de la comparación entre organismos, y será un término que alude explícitamente a las diferencias que observamos en la organización morfológica de los organismos (Buscalioni, 1999).

Mientras que la diversidad biológica es una estimación de riqueza taxonómica, ésta lleva implícita una cualidad de diferencia, pero no la expresa. Por ejemplo, podemos imaginar que un determinado número de especies se encuentra en una zona o un estrato, implica que hay formas distintas. Sin embargo, el dato no nos dice ni en que ni cuanto de distintas son esas especies. La disparidad, por el contrario, es una valoración directa de la diferencia morfológica (Foote, 1997). Concretamente la disparidad es la expresión cuantificada de las diferencias morfológicas que separan a los organismos en un morfoespacio (Gould, 1999; Raff, 1996; Foote, 1997).

La disparidad puede adquirir un valor escalar el cual se extrae desde la distribución de las formas en un morfoespacio determinado. La obtención de un valor para la disparidad es, por tanto, dependiente de la relación entre un conjunto de variables desde las que se abstraiga la morfología (p. ej. la geometría), es decir, será dependiente de los escalares de las variables desde las que se construye el morfoespacio. Esto a su vez permite que la disparidad pueda estudiarse estadísticamente, por ejemplo, en términos de varianza (desde la media muestral obtenida a partir del conjunto de variables con las que se construye el morfoespacio), o en términos de distancias espaciales entre los taxones representados dentro de esa misma distribución en el morfoespacio (p. ej., distancias entre medias, o la distancia Procrustes en el espacio de forma de la morfometría geométrica; Wills, 1998; Zelditch et al., 2004).

La cuestión que más se ha estudiado sobre la disparidad es su dinámica en el tiempo. Muchos

estudios paleobiologicos han revisado los patrones de disparidad de determinados linajes (principalmente en invertebrados), y estos se han comparado con los patrones estimados para la diversidad de los mismos linajes. Los resultados generalmente permiten concluir que la diversidad y la disparidad son distintas, aunque lo más llamativo es que muestran que el diseño estructural y la riqueza taxonómica no ocurren de manera sincrónica en el tiempo geológico. Muchos de estos estudios han demostrado que en determinados linajes el aumento de disparidad ocurre antes del aumento diversidad (Foote, op. cit.), es decir, que a una escala macroevolutiva parece que en la génesis de clados, primero se conforman determinados diseños estructurales (*baupläne*, o planes morfológicos) desde la emergencia de novedades evolutivas, y que éstas se mantienen y son la base para la diversificación taxonómica. La clave fundamental que se despeja de esta observación es que una vez establecido un patrón estructural, este permanece relativamente estable a lo largo del tiempo, es decir, todas las especies que permiten enumerar la diversidad mantienen la misma organización. En definitiva, el mantenimiento de un plan estructural (*bauplan*, en singular) apunta a la existencia de constraints.

Un ejemplo, ya clásico, lo representa la fauna de calizas laminadas de Burguess Shale, del Cámbrico canadiense, cuyo registro muestra una disparidad de organismos (un número de Filos) mayor de la que existe actualmente. El registro de Burguess Shale nos sugiere, según Gould (1999), que la diversidad puede haber aumentado (aunque la realidad de su *modo* todavía gira entorno a un intenso debate; Benton, 2001), sin embargo el número de Filos ha descendido a lo largo del tiempo hasta la actualidad (ver también un modelo teórico estructuralista desde la ocupación del morfoespacio en Thomas et al., 1999).

El programa de investigación de la disparidad pretende desvelar la incógnita sobre qué factores intervienen y/o condicionan estos patrones tan característicos. El estudio que desarrollamos en este ámbito persigue caracterizar la disparidad craneal en arcosaurios para, después, desvelar factores que expliquen el patrón encontrado sobre el morfoespacio. En particular, desbrozando la organización fenotípica del cráneo pretendemos desvelar qué factores pueden estar asociados a ella en una escala macroevolutiva.

1.3.2. Integración morfológica

La integración morfológica es el epítome de la herencia *correlacionada* a la que se hacía alusión desde el párrafo que abre la memoria de la tesis (Gould, 1990). La idea de integración es fruto del acervo investigador que se remonta a más de dos siglos atrás.

Entre los autores que forjaron la simiente podríamos enmarcar a Cuvier o Saint-Hillaire ya en el s. XVIII y principios de XIX, y entre los autores que posteriormente defendiesen la integridad organísmica resalta la figura de D'Arcy Thompson (1860-1948).

La fenomenología de la integración también ha sido siempre una cuestión latente en biología evolutiva y, sobre todo, en paleobiología. La integración morfológica implica una concepción holística del organismo, y es un fenómeno que se reconoce como la variación coordinada entre las partes de un todo en un contexto dinámico que incorpora el *tiempo*. El fenómeno implica la existencia de una coherencia estructural y funcional resultante de la variación coordinada de los elementos, las partes, o las unidades que constituyen el organismo. Incorporar la variable tiempo implica que la covariación es dinámica, bien en la ontogenia o bien, en un sentido evolutivo.

La identidad taxonómica de cada organismo, del "todo", es un compromiso holístico de unidad. La posibilidad de reconocer cada taxón depende directamente de su estatus organizado, y por ende, de su integración. La acepción holística de -una estructura aislada, un organismo (el todo)-, tiene su raíz en el principio morfológico de la "correlación de caracteres" propuesto hace más de dos siglos por el anatomista y morfólogo Georges Cuvier (1769-1832).

La integración morfológica desde este punto de vista permite asumir que la identidad de un organismo puede subrogarse a alguna de sus partes, práctica que, por otra parte, es común (quizá también, una necesidad) en paleontología. Atendiendo a este principio, el compromiso que podemos asumir en el presente trabajo es que la organización fenotípica del cráneo contendrá la suficiente información como para aproximarse a comprender una parte importante de la evolución morfológica del clado Archosauria.

La formalización del estudio de la integración morfológica como programa de investigación paleobiológico, sin embargo, parte de la propuesta escrita por los paleontólogos Olson y Miller (1958) a mediados del s. XX en su libro con el título homónimo de "Morphological Integration". La síntesis que elaboraron en el giraba siempre en torno a la noción de covariación entre estructuras morfológicas debidas al desarrollo o la función. En su formalización Olson y Miller (1958) razonan que la explicación al fenómeno reside en la asociación funcional (biomecánica) entre las partes de un "todo", pero también en gran medida, de las reglas de construcción de la morfología del organismo (el desarrollo y la morfogénesis).

La idea general de integración ha apuntado siempre a una concepción organísmica u

holista frente a las tendencias reduccionistas que surgían en la década de los cincuenta (atomismo, *sensu*; Gould, 1977). En efecto, la integración morfológica como un programa de investigación necesario es la piedra angular de la objeción a un paradigma; el que la evolución morfológica sea un producto de la variabilidad de un conjunto inconexo de caracteres independientes (la clave de un mosaico de caracteres; ver Mayr, 2000 como resumen actualizado de los postulados generales desde la perspectiva Neodarwinista Sintética). Olson y Miller (1958) cimentarán su argumento dictando que:

-Not only should the interrelationships of changing characters be a primary of interest, but the nature and intensity of the relationships should remain evident all stages of [their] study.

Estudiando la integración la morfología se desliga del binomio gen-carácter y el azar necesario, núcleo conceptual de la propuesta del "mosaico de caracteres", pasando incorporar a un modelo morfológico dependiente de las propiedades emergentes y la cohesión entre elementos, donde genes y rutas de señalización, células y poblaciones celulares, se enmarcan en un contexto de procesos epigenéticos de interacción en la génesis morfológica.

Desde su formalización, el estudio de la integración ha recorrido un largo camino aunque siempre en paralelo a las corrientes principales del estudio en evolución. La palabra "integración" alude a un aspecto organizativo del fenotipo, y por tanto, atiende a su faceta más compleja y difícil de aprehender. Así, la situación del programa de investigación en integración morfológica ha corrido siempre en paralelo, no sólo por la llegada de la biología molecular y de su acopio de la actividad investigadora, sino por ciertos problemas conceptuales y técnicos que acarreaba su práctica en el momento de proponerla como un fenómeno a tratar.

Hasta su resurgimiento en la década de los noventa, los obstáculos a los que se ha enfrentado la investigación de la integración morfológica eran carecer de una enunciación coherente del fenómeno (*viz.* una definición *única* de integración; Pligliucci y Preston, 2004). También era difícil plantear un contexto teórico (explicativo) y práctico (experimental) en el que apoyarse sin evidencias experimentales procedentes del desarrollo. Igualmente, la formalización remitía a la abstracción matemática del fenotipo y a su análisis desde la estadística. Desde ese momento, otra constante frente a la propuesta sería el rechazo a su

praxis. En palabras de Olson y Miller (1958, p. 7):

- The fact that statistical studies require quantification has given rise to a feeling of uneasiness and suspicion among many morphologists about results of statistical tests. The form and beauty of a fine dissection or a careful preparation are likely to be lost as an animal is reduced to a set of numbers….The aesthetic value of an elegant bit of mathematical manipulation can hardly substitute for the loss and is more likely to engender than to assuage suspicion.

Justificar la aplicación de nociones y técnicas estadísticas complejas era para los autores una condición *sine qua non* no existiría la posibilidad de sondear aspectos de la integración morfológica. Así se podría mantener, primero, la posibilidad de repetir el experimento por cualquier observador, y segundo, conservar la objetividad en el tratamiento metodológico de los datos (ver también; Bookstein et al., 1985; Chernoff y Magwene, 1999; Roth y Mercer, 2000).

Para Olson y Miller (op. cit.) los caracteres (*traits*) serán variables que representan medidas (longitudes, ángulos, etc.), y un conjunto de medidas servirá como compromiso para abstraer una serie de atributos inherentes al organismo. La idea se fundamenta en las premisas del método comparado, donde la homología contextualice y dé sentido a la comparación en un sentido biológico y evolutivo. El criterio de homología es clave para las medidas, pero lo es también para la elección de los landmarks que caracterizan la forma en una configuración de coordenadas si se trabaja desde la morfometría geométrica. Sin este criterio sería imposible describir qué se está comparando (ver Segunda Parte del volumen).

En la década de los noventa comienzan a solventarse estas dudas y el estudio de la integración morfológica comienza a resurgir como un enfoque multidisciplinar en biología evolutiva. Por un lado, la ambigüedad que caracterizaba su interpretación mecanística reside ahora en bases empíricas probadas por la biología del desarrollo. Igualmente, la estadística ha evolucionado y la aversión a su aplicación ha disminuido drásticamente. El advenimiento de computadoras potentes, económicamente más asequibles y de fácil manejo permite extender el aprendizaje y el uso de la estadística multivariante. Más importante aún, el desarrollo de las computadoras facilitó el nacimiento y una rápida evolución de la morfología teórica y de la morfometría geométrica, herramientas fundamentales para el estudio de la integración morfológica.

El razonamiento macroevolutivo que relaciona la disparidad con la integración fenotípica es que ambos fenómenos se reflejan en la ocupación del morfoespacio. La disparidad se ve desde la distribución en el morfoespacio, y la integración se presenta como un fenómeno asociado al sesgo en la distribución (y la variación), y por ende, ambos fenómenos se abordan atendiendo a la existencia de *constraints*. La premisa estratégica es desentramar la identidad de los factores implicados en el sesgo. La tendencia más generalizada apunta a asociar la fenomenología de la integración con su papel limitante sobre la evolución morfológica, siempre desde la herencia de las reglas condicionales del programa del desarrollo (Magwene, 2001).

Para aproximarse al estudio de la disparidad y la integración morfológica (*variación* y *covariación* en términos estadísticos), puede utilizarse la morfología teórica y el morfoespacio (en su vertiente cuantitativa; Raup y Michelson, 1965; McGhee, 1999; Chapman y Rasskin-Gutman, 2001), y la morfometría geométrica con sus herramientas asociadas a la estadística multivariante (Benson et al., 1982; Bookstein, 1991; Rohlf y Marcus, 1993; Adams et al., 2004).

La morfología teórica permite investigar la existencia de principios geométricos comunes subyacentes a la disparidad y a la distribución de formas en el morfoespacio. Estos principios se interpretarán como un reflejo directo de la existencia de restricciones morfogenéticas. En el morfoespacio se puede explorar el patrón de distribución de la disparidad para comprender qué factores condicionan que unas formas se den (habrá unas regiones ocupadas por la distribución) y otras no (otras regiones quedarán vacías). La morfometría geométrica, igualmente, permite desvelar las pautas que siguen la variación morfológica y la disparidad desde la construcción de morfoespacios empíricos (más concretamente, espacios de configuraciones, del inglés –*shape spaces*). También, la morfometría permite comprender el cambio de forma en términos de su covariación con otros factores (p. ej. el tamaño; Bookstein, 1998; Roth y Mercer, 2000).

Olson y Miller dedicaron parte de su libro a desglosar la posibilidad de argumentar sobre los procesos que subyacían a los patrones de correlación encontrados. Sin embargo, y como apuntábamos al principio del epígrafe, no es hasta la actualidad y gracias a la biología del desarrollo contemporánea, cuando referirse a estos procesos ha dejado de parecer mera especulación, aún cuando todavía siguen siendo bastante elusivos.

En secciones posteriores mostraremos algunos ejemplos de causas desde las que plantear una explicación a la integración. De hecho, hasta aquí hemos hablado del significado de

integración como un fenómeno de covariación entre estructuras, pero no hemos evaluado cómo definir una o unas partes, ni qué criterio establecer para establecer una delimitación entre las partes que suponemos que estarán integradas en el cráneo de un arcosaurio.

1.3.3 Integración morfológica y modularidad

Para entender la organización fenotípica de un sistema es indispensable identificar qué partes pueden ser diferenciadas y delimitadas, y para ello hay que establecer un criterio de subdivisión (*parcelación* del sistema según, Wagner, 1996). En términos más generales donde mejor se realiza esta posibilidad de parcelación es entre las partes del esqueleto.

El aspecto más importante que se desprende del concepto de parcelación es el la modularidad. La noción de que los organismos puedan estar organizados modularmente ha sido reconocida por la morfología hace tiempo (p. ej. Bateson, 1894, fide Carroll et al., 2004). Una de las ideas fundamentales que subyacen a entender la organización fenotípica del organismo como modular es que permite una flexibilidad de cambio; cambio en una o unas partes sin que afecte al resto (la clave conceptual deriva del trabajo seminal de *The genetic basis of evolutionary change*; Lewontin, 1974). Así se añade a la agenda investigadora en integración la condición de evolvabilidad, donde la premisa es que un módulo puede cambiar y variar implica que, en definitiva, un módulo o módulos serán el sustrato base del proceso evolutivo (Winther, 2001).

También, concebir la organización fenotípica desde la modularidad permite explicar la amalgama de distintos niveles de organización de un organismo bajo un mismo contexto explicativo. La modularidad se entiende como un fenómeno que abarca la organización estructural en partes ordenadas jerárquicamente a partir de distintos niveles de organización biológicos (ver la epistemología en Riedl, 1978; ver también Callebaut y Rasskin-Gutman, 2005). Así, la organización modular puede ser genética, celular, así como estructural o funcional. De hecho, una dificultad que lleva consigo la concepción de una definición explícita de modularidad es que, en realidad, es muy adaptable al contexto desde el que se aplique (Bolker, 2003). En principio, la integración y la modularidad desde un punto de vista morfológico representan el compromiso entre el todo y las partes.

Desde el punto de vista de la integración, un módulo será una unidad que, aún estando integrada, actuará de manera relativamente más autónoma frente al resto. La idea general es que un organismo es una entidad altamente integrada y organizada desde su desarrollo, pero también es relativamente flexible al cambio (evolución). Del mismo modo, hay

una considerable capacidad de cambio de partes específicas mientras que la robustez del plan morfológico general permanece prácticamente inalterable (idea de invariantes fenotípicas). Un módulo será una parte o unidad que es coherente internamente por muchas interacciones de sus elementos, y será relativamente autónomo de otras unidades con las que está conectado también (integrado), pero en menor proporción o más débilmente (Simon, 1969; Klingenberg, 2004; Fig. 1.2).

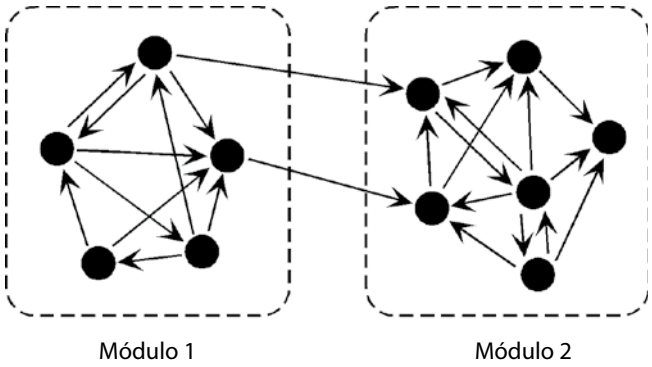

Figura 1.2. Esquema descriptivo de la definición de dos módulos relacionados por interacciones del desarrollo. Los componentes del módulo están interconectados por muchas interacciones (flechas), mientras que hay pocas interacciones entre módulos. Modificado de Klingenberg (2004).

Box 2

Restricciones sobre la variación morfológica y el sesgo de variantes fenotípicas en macroevolución

La existencia de distintos factores condicionantes sobre la morfología y su patrón evolutivo se resume, según Gould (1977), en una de las etarnas metáforas en paleontología; la intervención de factores externos o internos, o lo que es lo mismo, la intervención de factores ecológicos o del desarrollo. Gould (1983) también los llamará *funcionalismo* y *estructuralismo* respectivamente y, posteriormente, Alberch (1989) formalizará la dicotomía en los conceptos de *externalismo* e *internalismo*.

En ambas visiones se aboga por la autenticidad del sesgo de formas que observamos en la naturaleza y su efecto como un fenómeno emergente tanto en las tendencias macroevolutivas como en la distribución de formas sobre el morfoespacio. Sin embargo, este sesgo se ve desde dos perspectivas distintas, una de ellas asociada a la operatividad de la selección natural (el medio externo), y otra a la selección interna (el programa del desarrollo). La hipótesis del equilibrio puntuado de Eldredge y Gould (1972) involucraba la existencia de dos factores; el *estasis* morfológico en los linajes, y la existencia de saltos entre linajes antecesor y descendiente, en el sentido más *drevresiano* o saltacionista del concepto (ver también, Gould, 2002).

Así, se introducirían dos nociones fundamentales en el discurso de la biología evolutiva contemporánea –estabilidad y discontinuidad, (De Renzi et al., 1999). La existencia de factores condicionantes en el desarrollo implica la existencia de un conjunto limitado de fenotipos posibles, cada uno de ellos teniendo una determinada probabilidad de producción determinada por las posibilidades que ofrezca el desarrollo. El desarrollo, por otra parte, puede ser descrito como un sistema no lineal, y por tanto, la existencia de parámetros de inequiprobabilidad, de bifurcación y de umbral, típicas de estos sistemas, serán aspectos fundamentales de su dinámica (Alberch, 1980; 1982; Oster y Alberch, 1982; ver también De Renzi et al., 1999). La existencia de estos parámetros retaba la visión gradualista de la evolución, dibujando las discontinuidades fenotípicas como resultantes del desarrollo y no por la selección natural. Desde esta perspectiva, de hecho, el desarrollo es el causante de la estabilidad estructural (covariación) y la convergencia, así como de las discontinuidades tácitamente expresadas desde el modelo macroevolutivo puntuacionista.

La evolución morfológica está ligada a los cambios que tengan lugar en el programa del desarrollo (Waddington, 1963). Alberch (1989) simuló una manera intuitiva de mostrar la capacidad de las restricciones en sesgar la cantidad de variantes fenotípicas en la naturaleza (disparidad). Para ello propuso una abstracción teórica de la distribución de una serie de formas sobre un espacio fenotípico. Abstrayendo la forma (el fenotipo) a un conjunto de parámetros (variables), se puede representar la distribución de formas como puntos en un espacio fenotípico multidimensional (o morfoespacio) atendiendo a los valores específicos de cada uno de los taxa estudiados.

Desde el punto de vista taxonómico podemos definir tipos morfológicos, que serán más evidentes cuanto más alta sea la categoría taxonómica a la que se adscriben (nótese la importancia del concepto de *Bauplan* o plan morfológico desde esta acepción; Arthur, 2000). Es decir, la disparidad aumentará cuanto mayor sea la escala taxonómica de que se trate. Asumiendo que la forma orgánica puede ser clasificada atendiendo a sus características tipológicas (p. ej. la jerarquía lineada clásica, los fenogramas fenéticos e incluso, los cladogramas actuales con calificativos para nodos monofiléti-

cos), la distribución en el morfoespacio será discontinua (Fig. B2.1 de Alberch, 1989).

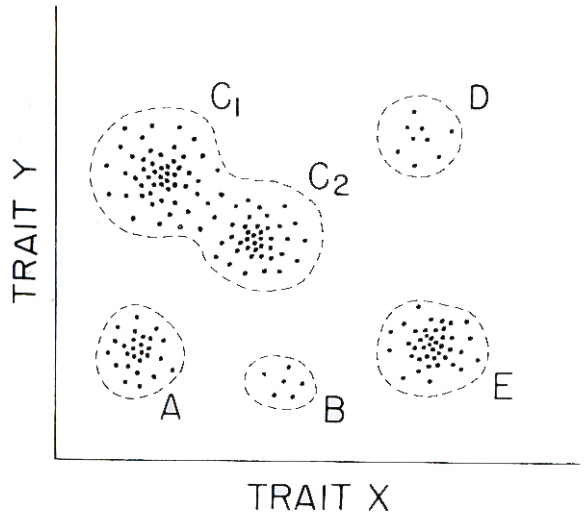

Figura B2.1. Espacio fenotípico (morfoespacio) donde se asume que la morfología de un organismo puede ser definido por la medida de dos rasgos (X, e Y). Cada punto es una morfología específica. Los espacios vacíos implican que no todas las formas existen. Las nubes de puntos representan especies (de la A a la E). C1 y C2 pueden corresponder, por ejemplo, a especies polimórficas o especies cercanamente emparentadas. Modificado de Alberch (1989).

Esta visión dicotómica de las condicionantes sobre la forma es una visión más particular de lo que Seilacher (1970; Fig. 1.1, Parte Primera de la tesis) simultaneará en su conocido triángulo de factores condicionantes sobre la morfología; en el triángulo de Seilacher los dos factores ya los hemos citado, del desarrollo y ambiental (resumidos en la dicotomía del internalismo frente al externalismo), se mezclan con el funcional. En el triángulo, el tercer vértice original representaba el factor histórico (filogenético), y posteriormente aprobaría el cuarto factor ambiental, que facilitaría diferenciarlo del biomecánico.

En presencia de restricciones (filogenéticas, estructurales u ontogenéticas) la identidad de los taxa se hará patente, y así ocurrirá para Alberch en la discontinuidad en la distribución (op. cit.; Fig. B2.1). Esta discontinuidad será mayor cuanto mayor sea la jerarquía taxonómica (es decir, cuanto mayor sea el rango taxonómico que sean analice, mayor será esta disparidad hipotética). Por el contrario, cuanto más emparentados estén los taxones las nubes de puntos que representan a los taxa en el espacio fenotípico estarán más cercanas, llegando incluso a solaparse (p. ej. en el caso de especies muy cercanas o especies polimórficas). En ausencia de restricciones (o *constraints*), la distribución que encontraríamos tendría que, por el contrario, ser completamente homogénea, pues no existiría ningún tipo de canalización.

Aún así, desde el punto de vista externalista se acepta la existencia de sesgos, y se explica la inexistencia de formas (los espacios vacíos). La ruptura de la continuidad (típicamente darviniana) se explica invocando la contingencia histórica (p. ej. existieron en el pasado pero desaparecieron, o bien son posibilidades que todavía no se han explorado). Desde el punto de vista más estrictamente internalista, el sesgo en la variación (disparidad) se entiende desde las reglas de construcción que imponga el propio programa del desarrollo (integración). Para Alberch (op. cit.), los constraints definirán el rango de morfologías posibles, siempre limitadas a los estados de equilibrio accesibles a cada sistema dinámico durante la morfogénesis (ver también; Rasskin-Gutman e Ipsizúa-Belmonte, 2004).

En términos generales, tanto la disparidad (distribución sobre el morfoespacio) como la integración morfológica (covariación de los caracteres debidas a reglas del desarrollo) se desvelan por tanto como fenómenos ligados a la noción del sesgo en la variación fenotípica a escala macroevolutiva, patente en las tendencias evolutivas (Stanley, 1979; Gould, 1990).

1.4. El cráneo y la singularización de sus partes

…the parts of an organism come unlabelled. It is then a more difficult task to reveal the underlying structural unity. K. V. Kardong. Vertebrates: Comparative Anatomy, Function, Evolution (1995)

El cráneo de un arcosaurio, como el de cualquier vertebrado, es una estructura compleja. Esta idea de complejidad implica que el cráneo será un sistema subdivisible en partes que son susceptibles de variar en sí mismas, y de covariar entre ellas. El cráneo no es un solo hueso, sino que es un complejo formado por diferentes huesos ordenados en un patrón espacial. Puesto que el cráneo es un sistema organizado por huesos, el estudio de su organización podría residir en la variación de estos. Sin embargo, existe una manera más resolutiva de entender la organización fenotípica del cráneo, desde una escala de organización mayor.

En el cráneo de un vertebrado se pueden definir y delimitar unidades mayores, más inclusivas, que también organizarán el cráneo espacialmente tal y como lo percibimos. Estas partes o unidades mayores son las *unidades esqueléticas fundamentales*, contienen distintos elementos (huesos), y añadiendo el factor dinámico de tiempo (ontogenético o evolutivo), estas unidades también son susceptibles de cambiar. La identidad de cada unidad estructural será jerárquica en cuanto a que cada unidad como tal estará configurada por varios elementos (los huesos), aunque estos también puede que no sean exclusivos de una sola parte, sino que puede que estén compartidos entre unidades dentro del sistema. La cuestión es, sin embargo, qué criterio utilizar para definir estas partes.

1.4.1. Criterios funcionales

Aunque esta visión "modular" de la organización fenotípica del cráneo tiene una larga historia, el primer enfoque que lo trata desde una perspectiva teórica es el monumental trabajo de C. J. van der Klaauw (1945, 1948, 1951, 1952) de la universidad de Leiden en Holanda, y fundador de la ecomorfología como una disciplina evolutiva (según Dressino y Lamas, 2003). Posteriormente M. L. Moss, de la universidad de Columbia en Nueva York (EE.UU), desarrollará a lo largo de toda su carrera investigadora el concepto de unidad fundamental craneal tal y como la enunciábamos anteriormente (a la que posteriormente llamará *unidad funcional*), y al estudio detallado de sus implicaciones en la organización evolutiva del fenotipo craneal (ver, Moss y Young, 1960; Moss, 1962; Moss y Salentjin, 1969; Moss y Vilmann, 1978; Moss, 1997a, b, c, d; Moss-Salentjin, 1997).

Tanto Klaauw como Moss convergen en concebir la organización fenotípica del cráneo, la emergencia y la identidad de partes diferenciables del cráneo, desde criterios funcionales. Klaauw (op. cit.) será el primero en desarrollar una Teoría Craneana Funcional vinculando la relación entre estructura y función con la presión ambiental, es decir, explicando el

cambio morfológico del cráneo desde la modulación adaptativa. De esta forma, el autor fundó un marco teórico para los estudios sobre el crecimiento y el desarrollo craneal y craneofacial. Sin embargo, para Klaauw cada unidad evolutiva del sistema (del cráneo) era delimitable atendiendo a un criterio explícitamente topográfico (donde está localizada en el cráneo) y funcional (dependiente de la función que desempeña). Sin embargo, nunca llegó a clarificar los conceptos de unidad funcional o componente funcional, que no obstante desplegaba constantemente en su monumental trabajo (ver en el mismo volumen; Klaauw, 1945, 1948, 1951, 1952).

El paso crítico que dio Klaauw fue pasar a concebir la estructura craneal como una entidad compleja y dinámica, por tanto, cambiante en el tiempo, donde el ambiente sería el motor de cambio. Así, Klaauw forja la simiente desde la que comenzarán de desarrollarse estudios evolutivos de la morfología funcional, de la morfología comparada (en especial la diferenciación entre tamaño y forma), y abrió el camino a la morfología ecológica, como denominaría a lo que actualmente conocemos como ecomorfología. En cuanto a sus investigaciones craneológicas, Klaauw estudió su propuesta sobre la evolución morfológica del cráneo en todo tipo de vertebrados, incorporando así varios ejemplos de arcosaurios, como cocodrilos, dinosaurios, y aves. En todos distinguiría dos unidades principales; una región cefálica del cráneo, asociada al sistema nervioso central, y un esqueleto facial, asociado al comportamiento trófico y asociado al aparato olfativo.

La visión "modular" del cráneo que Klaauw proponía (definir las partes del cráneo atendiendo a su función especializada) era holística, lo que implicaba que siempre tenía en cuenta la integración del sistema como algo lógico e inapelable. Aseveraba este hecho alegando que, *- a pesar que las partes mencionadas son explicadas como partes funcionales separadas, están por definición, unidas en un todo* (Klaauw, 1945; p.32; traducción de Dressino y Lamas, 2003; ver también Duijm, 1951). En su propuesta, la manera de subdividir el cráneo en partes parece que respondía más a cuestiones metodológicas que a problemas epistemológicos (holismo vs. reduccionismo, o la integración morfológica; para un desarrollo hipotético deductivo de la Teoría funcional de Klaauw, ver; Dressino y Lamas, op. cit.). Sin embargo, esta dicotomía conceptual dejaba sus aseveraciones en un terreno relativamente incierto.

Moss (p. ej. en Moss y Young, 1960) reelaborará en pasos sucesivos, durante varias décadas y en sus propios términos las ideas de Klaauw, poniendo un énfasis mayor en la asociación entre el tejido, los tejidos u órganos (p. ej. el sistema nervioso central) y el entorno óseo del cráneo para definir unas unidades. De hecho, Moss dará un cierto giro hacia el estructuralismo

frente al funcionalismo de Klaauw, como veremos más adelante. Los estudios de Moss ejercieron una fuerte influencia sobre los estudios del crecimiento craneofacial, aunque particularmente en su vertiente médica, aplicada en ortodoncia y cirugía maxilofacial. En términos generales, los estudios de Moss se centraron en el estudio del cráneo en mamíferos, y a juzgar por la literatura disponible, nunca extendió su modelo a ningún tipo de vertebrado fuera de este linaje.

Las unidades o partes del cráneo para Moss pueden delimitarse como agregados osteológicos, al igual que para Klaauw, pero las partes del cráneo, sus unidades funcionales, estarán subordinadas a la necesidad *funcional* del órgano o tejidos a los que esté asociado. Moss conjuga una compleja trama conceptual donde la función tiene una identidad abstracta; en términos generales, cada tejido tiene una función específica, y para que cada uno la pueda cumplir, todo cambiará al unísono durante la ontogenia hasta formarse. Cada unidad será diferenciable en un momento determinado. Sin embargo, Moss también parece sugerir una subordinación funcional entre tejidos, una compleja metáfora con tintes Cuvierianos donde el hueso del cráneo, cuya función se entiende que es la de proteger a los tejidos blandos, se organizará atendiendo a la necesidad funcional y regional de los tejidos con los que se asocia (el principal rector de cambio será el sistema nervioso).

Las partes, o unidades funcionales, se unificarán y delimitarán según un criterio de relación hueso-tejido blando aseverada por su función específica, aunque la variación en su expresión osteológica vendrá determinada por la necesidad de cambio de los tejidos blandos, y no del hueso en si mismo. En su propuesta genuina, el cambio se producirá epigenéticamente desde la relación estructural entre todos los tejidos (p. ej. transducción mecánica). En su propuesta más contemporánea el mecanismo estructural no se entiende como una respuesta física de empuje en si misma, sino como activador de señales que estimulan, por ejemplo, la producción de factores de crecimiento (FGFs) implicados en la proliferación de hueso, como parece ser el caso en el cierre de suturas (Aldridge et al., 2005).

Es resumen, la organización fenotípica del cráneo para Moss será jerárquica pues los huesos (las unidades elementales) serán la base material, los ladrillos con los que se construye cada parte y se consigue una arquitectura craneal coherente. El origen ontogenético del hueso, el origen y la identidad de las unidades compuestas por huesos, así como sus cambios estructurales no serán sino respuestas mecánicas inevitables a las demandas temporales y operativas de las células no esqueléticas, es decir, de los tejidos blandos, de los órganos y de su desarrollo.

Moss formulará esta noción estructural del cráneo como una hipótesis epigenética que finalmente llamará la Matriz Funcional, (la hipótesis primeramente se llamó el Análisis Craneal Funcional; Moss y Salentijn, 1969; Moss y Vilmann, 1978). El cráneo protegerá al sistema nervioso central y a otros órganos o tejidos que contiene. El desarrollo de los tejidos blandos (predominantemente del sistema nervioso central) hace que éstos cambien de tamaño y proporciones, lo que se traducirá en el cambio en los huesos como una respuesta activa que amolde su configuración a los cambios sucedidos en los órganos que protege. Las partes del cráneo irán transformándose epigenéticamente a medida que el tejido conforme el órgano, y a medida que este aumente paulatinamente de volumen y/o cambie de forma. La función para Moss implica que los factores y procesos causales de cambio serán siempre epigenéticos y de procedencia exoesquelética, es decir, la información y las causas de cambio no residirán en las células (y poblaciones celulares) esqueléticas, sino en la información emergente de los procesos epigenéticos de la matriz funcional *per se*.

Moss fue objeto de críticas por parte de algunos investigadores cultivados en perspectivas puramente holísticas, quienes consideraban que no atendía a la naturaleza integrada de las unidades funcionales dentro del sistema, al igual que se lo achacarían a Klaauw. Curiosamente será Dullemeijer (1974), discípulo de Klaauw y colega del mismo Moss, quién distinguirá entre la concepción modular-funcional del cráneo de Moss con la identidad de la integración, la resistencia al cambio estructural desde las leyes de construcción del cráneo (ver Fig. 1.3). Sin embargo, y al igual que ocurriría con Klaauw, el complejo modelo de Moss no niega la integración, simplemente la jerarquiza, aunque subordina el cambio a una necesidad funcional.

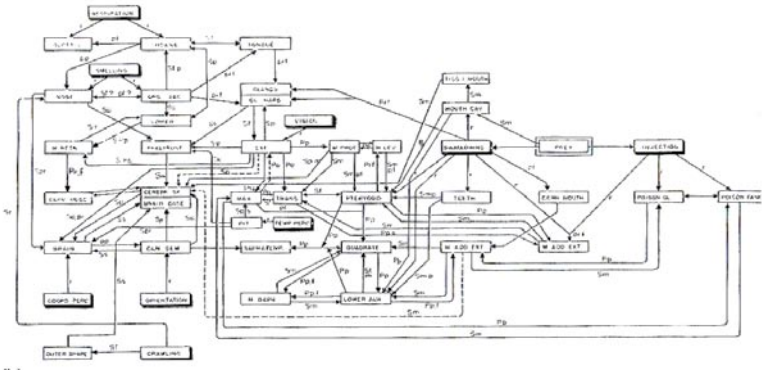

Figura 1.3. Red de conexiones estructurales y funcionales entre elementos de la cabeza en el cráneo de una serpiente. El ejemplo persigue mostrar desde la complejidad de la red lo difícil que puede ser un cambio filético. Las conexiones representan correlaciones entre todos los elementos del patrón. Original de Dullemeijer (1974).

Como adelantábamos en párrafos anteriores, la propuesta de Moss será muy valorada en el entorno de la medicina craneofacial. Apoyándose en la hipótesis de la Matriz Funcional, Enlow

(1968) y Enlow y Hans (1996) considerarán como agente causal del origen de la morfología facial tan particular en humanos al sistema nervioso central. El SNC desarrollándose exageradamente traducirá su variación al hueso circundante biomecánicamente, lo que en una comparativa macroevolutiva (entre muy distintos taxa de mamiferos) se traducirá en un descenso (ventral) del hocico hasta quedar enteramente reducido en humanos. Puesto que las partes definidas funcionalmente (o embrionariamente, según el esquema clásico de tipo de hueso; ver párrafo siguientes), están integradas, todas se verán afectadas por los cambios en el encéfalo. En definitiva, todas las partes responderán cambiando morfogenéticamente (*s.l*), resultando en la cara tan corta típica de los humanos (Fig. 1.4).

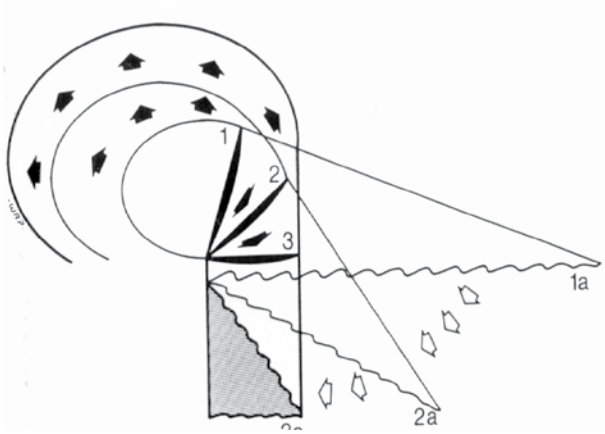

Figura 1.4. Esquema de Enlow (1968) en el que se hipotetiza la mecánica de cambio morfológico en un contexto macroevolutivo en mamíferos. Las flechas muestran el aumento cefálico para cada esquema. El primer esquema, 1a, es un mamífero con hocico y un encéfalo pequeño, y 1 marca la posición de su placa cribiforme. En 2a el hocico ha descendido hasta quedar más oblicuo, y la placa cribiforme ha sufrido la misma dirección de cambio dado que el encéfalo ha aumentado de tamaño relativo. En 3b el hocico se ha verticalizado, la placa cribiforme se ha horizontalizado completamente, y el cerebro es enorme; *viz.* caso humano.

La compleja trama epistémica de la matriz funcional ha sido revisada más recientemente en la década de los noventa (Moss, 1997a, b, c, d), transformando parte de la idea que trataba la epigénesis solo desde una visión enteramente estructuralista (típica en ese momento; ver Wilkins, 2001), a una perspectiva mecanicista más molecular. Esta transformación es equivalente a la evolución y tratamiento del concepto de morfogénesis estructuralista a la perspectiva desde la que se trata la morfogénesis actualmente. El efecto de interacción física entre partes es un aspecto de la epigénesis, mientras que otro son las relaciones de señalización molecular entre rutas del desarrollo, morfógenos y productos Hox, a las que Moss hará referencia en sus últimos trabajos.

1.4.2. Criterios ontogenéticos

Existe otra manera de distinguir las partes que organizan el cráneo de un vertebrado desde criterios que se extraen de la ontogenia temprana. Esta visión clásica tiene su raíz en los

tipos de osificación de los huesos del cráneo, aunque también llevan implícita una función y, en cierto modo, el origen regional desde las capas germinales en el embrión. Generalmente, además, pueden asociarse con una región topográfica en el cráneo adulto. Desde esta perspectiva el cráneo se divide en tres regiones; el esplacnocráneo, el condrocráneo, y el dermatocráneo (Pirlot, 1976; Romer y Parsons, 1989; Kardong, 1995). Aunque es raro encontrar trabajos que exploren la integración morfológica atendiendo únicamente a este criterio, esta distinción de partes del cráneo es un estándar descriptivo donde se apoyan las los pilares de la homología clásica.

Sin embargo, esta división no está exenta de ciertas ambigüedades descriptivas. El condrocráneo y el dermatocráneo se diferencian claramente entre sí en que el primero está compuesto por hueso de tipo condral (primero se genera un "molde" de cartílago, que después es sustituido por hueso), mientras que el segundo es hueso dérmico de naturaleza membranosa (no se forma por la sustitución de cartílago, sino que se genera directamente). El condrocráneo representa principalmente la base del cráneo y los occipitales, y es el denominado cráneo "primitivo" (DeBeer, 1937), mientras que el dermatocráneo lo encontramos distribuido por todo el cráneo (p. ej. desde la bóveda craneal a los huesos de la maxila). El esplacnocráneo, en cambio, está principalmente compuesto por huesos condrales, aunque en estadios adultos se encuentra envuelto en huesos dérmicos. Estructuralmente representa las mandíbulas y los huesos del oído. El Esplacnocráneo tiene su origen en los arcos faríngeos.

Los nuevos descubrimientos de la biología del desarrollo, por otra parte, permiten superar esta relativa imprecisión, desarrollando una nueva terminología desde la que describir las partes en las que se pueden subdividir el cráneo. Basada enteramente en la identidad celular del mesénquima embrionario (de qué poblaciones celulares emerge cada hueso), una ventaja añadida de este nuevo enfoque para nuestros intereses es que la ilustración estructural de las regiones del cráneo se ha desarrollado en el embrión de pollo (*viz.* un arcosaurio). Utilizando marcadores genéticos en el desarrollo del pollo y la codorniz, e hibridando las poblaciones celulares primigenias entre ambos embriones, se puede rastrear el destino final de cada una de ellas a cada región de mesénquima que, durante el desarrollo, dará lugar a cada hueso del cráneo (la técnica recibe el nombre de quimera codorniz-pollo; Le Douarin, 1986).

A través de estas técnicas se ha conseguido definir dos regiones claramente distinguibles a las que se denomina como región *cordal* y región *precordal* también llamada *acordal* (Couly et al., 1993; Le Douarin et al., 1993; ver Parte Segunda del volumen para más detalle y apartado 1.5 debajo). Los nombres cordal y precordal describen la localización de cada una de estas regiones en el cráneo del embrión en desarrollo con respeto a la notocorda, un importante

núcleo organizador del embrión. Así, *cordal* definirá la región que incluye los huesos que quedan justo por detrás de la extensión más rostral (anterior) de la notocorda, mientras que la precordal será la región (con sus elementos) que queda en una posición anterior esta frontera notocordal en el embrión. Esta definición territorial también puntualiza una frontera entre distintas poblaciones de células progenitoras. La región cordal surge del mesodermo (desde dos tipos particulares de mesodermo; somitico y paraxial craneal), mientras que la región precordal nace de la cresta neural craneal (también llamada cresta neural cefálica).

Cada una de estas regiones equivale a definir unas *unidades fundamentales*, tal y como se definían anteriormente, es decir, se delimitan regiones (o partes) más inclusivas del cráneo, compuestas por huesos, definibles atendiendo a un criterio común a todas. La salvedad es que el criterio no es la función (*s.l.*; ver párrafos anteriores), sino que vienen definidas por criterios de homología regionales y de identidad celular (los elementos de cada una comparten un mismo origen y se localizan en una región concreta).

Lo que resulta interesante es que cada parte definida según estos criterios tiene a su vez una equivalencia relativa a las unidades fundamentales que se definen atendiendo a criterios funcionales. Por ejemplo, la región precordal que se origina desde la cresta neural craneal coincide casi perfectamente con el esqueleto facial. A su vez, el esqueleto facial es principalmente de naturaleza dérmica, por lo que la región precordal también contiene regiones detalladas desde la naturaleza de su identidad osteológica. En el esqueleto facial, no obstante, encontramos huesos de naturaleza dérmica pero también condral, ya que la cresta neural craneal es capaz de producir ambos huesos (de hecho, solo lo hará en la región de la cabeza, y no en el post-cráneo). Es por tanto una definición más acotada que la acepción embrionaria clásica.

A la luz de todo lo expuesto, se hace patente que el cráneo es un sistema complejo, altamente organizado y funcionalmente coherente. En el cráneo de un arcosaurio podemos distinguir distintos huesos, pero podemos sobreseer que tienen una identidad particular, e incluirlos a todos como elementos constituyentes de partes o unidades más inclusivas, partes que sustentarán la organización fenotípica del cráneo. La definición de las partes, sin embargo, es una tarea complicada pues puede realizarse atendiendo a diferentes criterios para su delimitación.

Definir dos regiones o partes fundamentales, una cordal y otra precordal, implica un criterio de identidad celular (homología celular) y regional que posiblemente sea más práctico para hablar del fenómeno de integración. Aunque exploraremos la identidad estructural del cráneo

de un arcosaurio y su variación atendiendo a criterios funcionales (digamos, "clásicos"), el objetivo que perseguimos es comprobar si es posible desvelar alguno de los factores causales de aquellos fenómenos que capturamos a una escala estructural macroevolutiva (la organización fenotípica del cráneo en reptiles arcosaurios y su evolución). Contamos actualmente con la información provista por los grandes avances de la biología del desarrollo contemporánea en materia morfogenética. En efecto, es de la maquinaria morfogenética, en el desarrollo, de donde emerge la variación y la coordinación que capturamos como fenómenos estadísticos (variación y covariación).

Partiendo de la base de que la identificación celular de los orígenes de las partes craneales se ha realizado en un cráneo aviano (arcosauriano), y asumiendo como hipótesis de partida que esta delimitación es generalizable a otros representantes del mismo clado (Noden y Trainor, 2005), podremos aproximar más fielmente la fenomenología macroevolutiva a las consideraciones conceptuales y prácticas que se manejan en la biología del desarrollo contemporánea.

1.4.3. Consideraciones particulares sobre la forma y la función

Una consideración adicional a utilizar el criterio embriológico de identidad celular para reconocer las partes del cráneo es que permite realizar un compromiso estratégico; al igual que con la alometría, la función "adaptativa" puede ser tratada como un fenómeno que emerge del propio programa del desarrollo, y no como un factor causal *a priori* del cambio y de la covariación. Pensamos que desde estas bases, retirar la función como criterio o como factor principal de causa permite un desarrollo por pasos del estudio en el que la evaluación del binomio forma-función puede ser desarrollada *a posteriori*.

Este compromiso estratégico simboliza una manera de evitar las concepciones teleológicas típicamente aducidas en morfología y biología evolutiva, donde a veces parece imputarse a la emergencia orgánica una determinación final (p. ej. el epítome de; *las alas de un águila están diseñadas –por la naturaleza, para planear*; ver Nagel, 1961). Esta disociación de la función y la forma nos permite evitar la confusión y posicionarnos más cercanamente a la concepción del desarrollo y la morfogénesis desde las leyes generativas de la complejidad, la autoorganización y la emergencia (Turing, 1952; Kauffmann, 1993; Solé y Goodwin, 2002). Como apuntará A. Wagner (2006), desde este particular punto de vista, utilizar una terminología funcional puede ser útil, pero puede despertar perspicacias:

Part of the reason is that words like "function" and "problem" insinuate an intelligent agent standing behind a system's design. However, for all we know, the biological systems… emerged from the blindly groping search that characterizes all of biological evolution. … It should be understood that functional language merely provides a convenient and compact way to describe the endpoint of the convoluted paths evolution takes.

1.5. Morfología, morfometría y mecanismos de variación y covariación

La ortodoxia evolutiva evalúa la correlación entre partes o unidades desde la optimización adaptativa (Lande, 1979; Cheverud et al., 1989), y los genes siguen teniendo un papel relevante desde su interacción alélica (la pleiotropía, o cuando un gen afecta o tiene influencia sobre varios genes). A un nivel estructural, el cambio de una parte, si se observa que está acompañado por el cambio en otra, ocurrirá desde la modificación de los óptimos de adecuación o *fitness*. Efectivamente, esta es una lectura fenotípica del paisaje adaptativo de Sewall-Wright (1932), y el factor condicionante (*constraint*) implicado en el sesgo de variantes fenotípicas será la selección natural.

Desde el punto de vista del desarrollo, por el contrario, la integración se entiende como un fenómeno morfológico producto de los procesos genéticos, pero también epigenéticos, surgidos del programa del desarrollo (Magwene, 2001; Klingenberg, 2002). La integración reflejará la estabilidad de los programas del desarrollo (Waddington, 1963). En un contexto evolutivo, la mecánica de la integración se entiende como la conservación heredable de dichas pautas organizativas del programa del desarrollo, y deja a la selección natural como un operador restrictivo sólo sobre lo que ya está producido, y no como un único factor productor y único causante del sesgo.

1.5.1 Estrategia conceptual en macroevolución

El paso conceptual que nos permite traducir los fenómenos de la disparidad y de la integración morfológicas desde una perspectiva morfométrica a una mecánica epigenética es la consigna de Waddington (1975) de que -*la evolución orgánica (fenotípica) es en definitiva el producto de la evolución de su programa del desarrollo*, una idea que secundarán muchos autores (ver p. ej.; Oster et al., 1988; Alberch, 1989, 1991; ver también, Gould 2002).

Desde esta premisa se abre la puerta estratégica para el desarrollo conceptual de la tesis, pues justifica que los procesos involucrados en el programa del desarrollo puedan ser capturados desde el estudio cuantitativo de la variación y la covariación morfológica a una escala macroevolutiva. Si la disparidad y la integración son el producto de los procesos que se heredan, éstos deben tener un reflejo fenomenológico en la morfología a escala macroevolutiva. Desde la captura de los fenómenos cuantitativos podremos formular recíprocamente una serie de preguntas e hipótesis que nos permitan profundizar en su naturaleza causal.

1.5.2. Un modelo mecanístico para la integración desde la morfometría

En relación a la posibilidad de extrapolar los mecanismos de integración desde la morfología a través de la morfometría, Riska (1986) propuso un modelo teórico donde, desde una perspectiva epigenética, ponderaba el papel de la morfogénesis frente a la función (adaptación), una modelo acorde con la invitación conceptual de D'Arcy Thompson (1942) para el estudio de la morfología.

El modelo de Riska (op. cit.) estimaba que la integración entre caracteres medidos, tal y como los tasaba desde la morfometría (correlación entre variables "tradicionales", ver Marcus et al., 1996), podría explicarse desde la identidad de los caracteres que se correlacionaban. El vínculo morfológico (la correlación) dependería de un denominador común a ellos, su descendencia común partiendo de la división de un *precursor* común. Esta hipótesis estaría basada en el mismo principio de homología que se asocia a la descendencia genealógica, o filogenética entre organismos, y la equivalencia de los caracteres en el modelo, su estrecho parentesco, permitiría explicar su comportamiento coordinado. La correspondencia u homología vendría dada, no obstante, desde un criterio de origen (ontogenético) común. Del modelo se desprenden paralelamente dos alternativas que explicarían la correlación positiva o negativa entre los caracteres, dependiendo del momento y modo de fisión del precursor común (ver, Riska, 1986).

Sin embargo, la conexión en el desarrollo no es solo una causa de covariación pues otros factores externos pueden afectar a la variación coordinada (p. ej. el ambiente o la función).

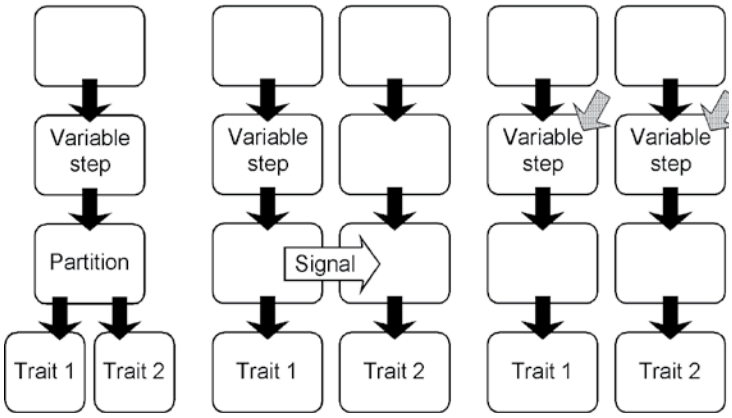

Figura 1.5. Esquema hipotético de los orígenes de la covariación entre rasgos morfológicos. Rutas morfogenéticas simuladas en; (izquierda) Conexión directa entre rutas debida a la partición de un mismo precursor, (centro) Conexión directa (flecha "Signal", o señal) entre rutas (el origen puede ser distinto). (derecha) Variación paralela de dos rutas separadas (por tanto coordinada por efectores externos al sistema en un mismo paso de la ruta; flechas en gris, p. ej. el ambiente). Modificado de Klingenberg (2004).

Para diferenciar entre estos distintos factores Klingenberg (2004) extiende el modelo de Riska y diferencia claramente entre integración *per se* como derivada de la propia morfogénesis de la covariación *en paralelo*, causada por factores que, en definitiva, están fuera del programa del desarrollo (Fig. 1.5).

Para que haya covariación es necesario que haya una fuente de variación y un mecanismo que genere una asociación regular entre las partes. Las asociaciones están generadas bien por conexiones directas de o entre las rutas del desarrollo, o por variación de rutas distintas que responden de manera equivalente a un mismo factor extrínseco. La Figura 1.5 muestra un modelo en los que los precursores embriológicos se dividen en distintos caracteres (de Klingenberg, 2004, basado en Riska, 1986).

Estos mecanismos, que parecen elementales, están envueltos en complejos procesos del desarrollo tales como el crecimiento, partición y migración de poblaciones celulares, por ejemplo de la cresta neural o del mesodermo. Por un lado (Fig. 1.5a) tenemos el origen de la covariación entre dos caracteres debida a una conexión directa que surge por la partición de un mismo precursor. La variación existente en la ruta antes de la partición se *transmite* (la heredan los *caracteres* descendientes), y puede manifestarse como una covariación entre ambos caracteres. En otro ejemplo (Fig. 1.5b), la señalización que produzca covariación puede darse entre rutas señalizadoras y equivale al también llamado *control epigenético* (Atchley y Hall, 1991). Estas señales pueden originarse en estructuras adyacentes, como por ejemplo la comunicación que puede existir entre en endodermo y la cresta neural (para más detalles, incluyendo la pleiotropía, ver; Klingenberg, 2004), o quizá, entre el sistema nervioso central y las partes del cráneo.

Lo importante es discernir entre estos dos mecanismos de integración (Figs 1.5a y b) y el fenómeno de *variación paralela*, concepto que utiliza Klingenberg (op. cit.) para diferenciar entre covariación (integración) no causada por conexiones epigenéticas directas entre rutas y poblaciones celulares, sino por factores extreínsecos al sistema (p. ej. el ambiente). La Figura 1.5c esquematiza un ejemplo de cómo un factor externo puede afectar a las rutas simultáneamente. Este factor hipotético puede afectar a uno de los pasos de cada ruta forzando una respuesta común ambas, lo que se reflejará en una covariación. Los factores que suelen causar esta covariación paralela son ambientales, como por ejemplo, la temperatura, cambios en la nutrición, etc. El ejemplo típico es el efecto que puede tener el ambiente (y en términos ambientalistas, la selección natural) sobre el fenotipo permitiendo inferencias directas como las reglas de Bergman, de Allen, o de Glogler. Estas reglas permiten

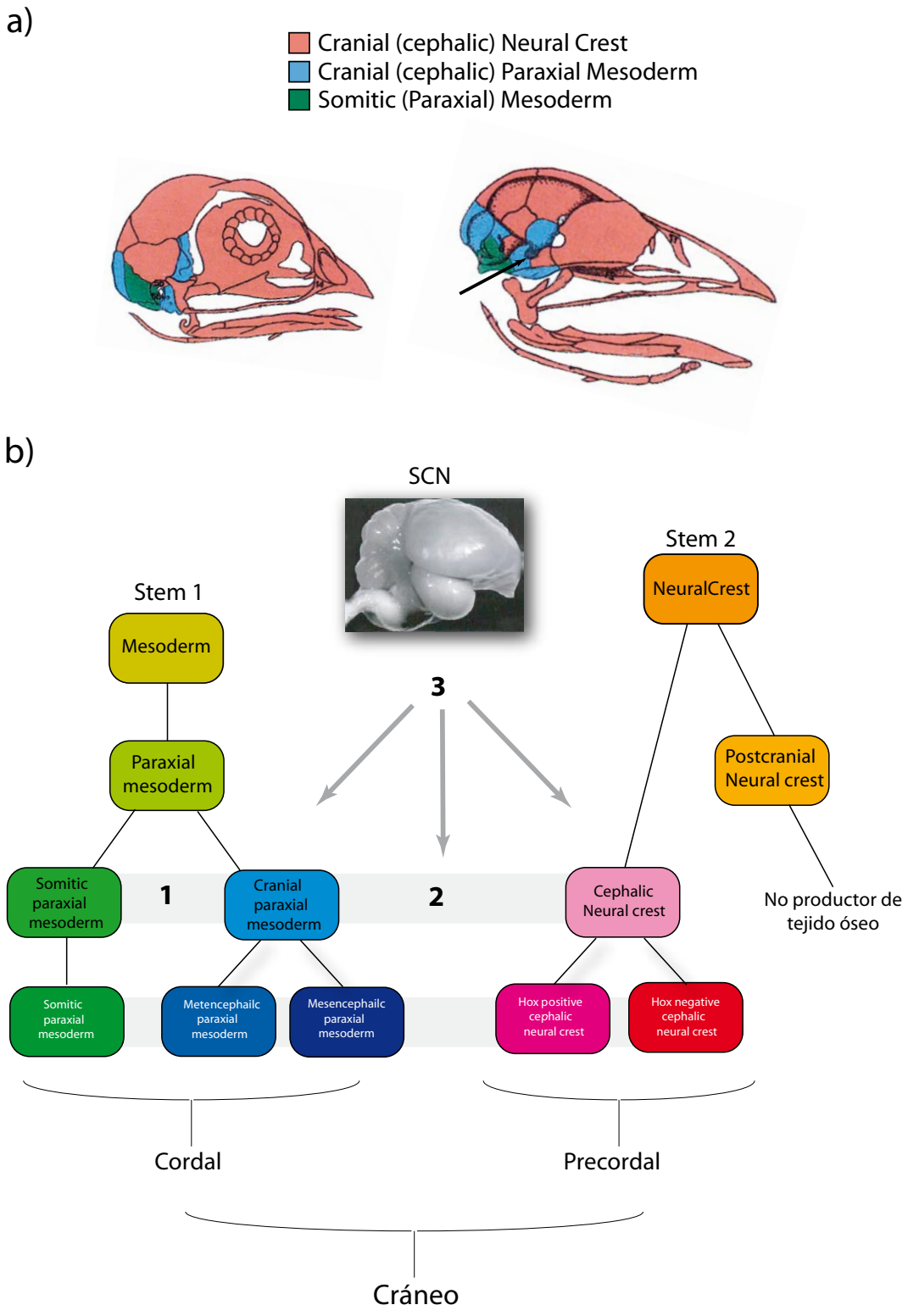

Figura 1.6. Extensión del modelo de Riska-Klingenberg (ver Fig. 1.5) a la subdivisión de partes del cráneo siguiendo un criterio de identidad celular por marcadores en quimeras de codorniz-pollo. a) Modelos de regionalización craneal según Couly et al., (1993). Izquierda, embrión de pollo en vista lateral externa. Derecha, modelo esquemático de un adulto en vista medial-sagital. Modificado de Ledouarin et al., (1993). b) Esquema hipotético equivalente a Klingenberg (2004; Fig. 1.5) de los posibles orígenes de la covariación entre unidades morfológicas del cráneo acorde con los orígenes celulares de los huesos englobados por cada región. La interacción número 1 implicaría una covariación debida a la partición de un precursor común. La conexión 2 representa la separación entre rutas de origen distinto origen, no coordinadas, o si lo están, la conexión será leve y el factor intrínseco es desconocido. La conexión 3 representa la hipótesis de un factor común intrínseco que coordina el desarrollo del cerebro y el desarrollo del cráneo. Se incluyen tres flechas ya que desconocemos si su efecto será sobre partes mesodérmicas, de la cresta neural, o de ambas.

predicciones ya que climas fríos harán covariar con un aumento de talla la reducción de las extremidades, o coloraciones cutáneas más oscuras, todo ello en en ausencia de mecanismos morfogenéticos subyacentes (Felsenstein, 2002).

1.5.3 Extendiendo los caracteres morfométricos de Riska en las configuraciones de landmarks que delimitan las partes del cráneo

La idea de partida en la que se basa el modelo de Riska anteriormente expuesto es que la integración que resulte de interacciones en el desarrollo puede estudiarse desde la covariación entre partes de una estructura completamente formada. Podemos traducir los caracteres cuantitativos del modelo de Riska (1986) en las partes o unidades estructurales en las que pronosticamos que se puede subdividir el cráneo, partes que hemos definido de varias maneras, aunque preferentemente desde un criterio ontogenético de homología (identidad) celular (las regiones cordal y la precordal que exponíamos en el apartado anterior). Morfológicamente, esperaríamos que la variación tuviese lugar dentro de las partes, entre los elementos del cada módulo identificados por un criterio de homología celular (Fig. 1.6). En efecto, la hipótesis mecanística de integración de Riska (op. cit.) preverá que la integración entre ambas unidades del cráneo será menor que la que observaremos en ellas mismas (ver también; Klingenberg et al., 2003; Fig. 1.6). La explicación desde el punto de vista morfogenético en el que se posiciona la hipótesis sería que la interpretación de las rutas (las señales que interpretarán las células durante el desarrollo) por parte de las poblaciones celulares será más parecida cuanto más emparentadas estén éstas, y menos cuanto menos emparentadas estén las poblaciones celulares.

Por ejemplo, la región cordal deriva del mesodermo, mientras que la precordal deriva de la cresta neural craneal. Por tanto, puesto que su origen parte de poblaciones celulares distintas esperaremos encontrar que la disparidad dependa más de las relaciones espaciales y topográficas entre ambas partes que de una de ellas más que de la otra (lo que, por otro lado, no implica que sean totalmente autónomas). La lectura de la señalización morfogenética (su interpretación) será distinta entre ambas (Fig 1.6).

A su vez, la región cordal contiene dos regiones distintas que derivan de dos precursores, el mesodermo somítico y el craneal paraxial, que se han escindido evolutivamente de un único precursor, el mesodermo. Aunque su identidad es distinta, su origen es común (el mesodermo), por lo que seguiremos esperando que la relación de covariación entre estas dos “subregiones” continúe siendo mayor entre ellas que con cualquier parte de la región

precordal. En términos anatómicos, la región somítica se corresponde con parte de la base del cráneo caudal y los huesos paraoccipitales, mientras que la paraxial corresponde, por ejemplo, al supraoccipital y algunos huesos de la base del cráneo, como el basiesfenoides en la Silla Turca. En definitiva, todos estos elementos conforman la mayor parte de la caja craneana (Ver Parte Segunda del volúmen). Aunque haya variación entre todos ellos, esperamos que el cambio morfológico entre todos estos elementos esté más coordinado entre sí que con elementos de la región del esqueleto facial, región que deriva de la cresta neural.

1.5.4. El sistema nervioso central

Como se resumía anteriormente es muy posible que la organización fenotípica de el cráneo y la del sistema nervioso central estén relacionadas epigenéticamente (Fig. 1.6). La cuestión, sin embargo, es si el cambio morfológico del cráneo está regido por la variación del sistema nervioso central (en un sentido más general, el cerebro), o si por el contrario, si los dos sistemas varían coordinadamente sin estar subordinado el cambio de uno (el cráneo) al cambio del otro (cerebro). Sin embargo, la dinámica de cualquiera que sea el cambio estructural, así como la relación de cambios entre ambos sistemas tiene lugar durante la morfogénesis y, desafortunadamente, solo podrá ser estudiada experimentalmente en embriones. En definitiva, no podemos abordar esta problemática desde el proyecto de tesis, ya que el nivel de análisis debe ajustarse a la información indirecta que provee la morfología. Puesto que no podemos comprobar la relación epigenética entre ambos sistemas, la estrategia a seguir es inferir la posible relación entre ambos sistemas basándonos en modelos que sean capaces de evaluar la variación coordinada que se proyecte desde la morfología. Como apuntábamos en párrafos anteriores, es posible que el sistema nervioso central esté asociado a esta organización esqueletogenética. De hecho, la cuestión es si la señalización entre rutas morfogenéticas a las que aludíamos es externa a ambos sistemas, es decir, si ambos se coordinan sistémica y sincrónicamente, o si por el contrario, es el cerebro en el desarrollo el que señaliza las rutas esqueletogenéticas dirigiendo el desarrollo y la organización del hueso circundante (la propuesta general de; Moss, 1997a, b, c, d, donde también caben factores epigenéticos de naturaleza estructural, p. ej. presión mecánica sobre el hueso circundante). Hasta este momento solo hemos desglosado información procedente del cráneo. Como

no podemos analizar la relación entre ambos sistemas en el desarrollo de manera directa, por lo que ¿cómo podemos comparar la posible asociación que exista entre la organización fenotípica del cerebro y del cráneo para proponer una hipótesis de integración entre ambos? Por un lado, conocemos la influencia de la evolución de la ontogenia en la evolución fenotípica del sistema nervioso central. Aunque se desconoce la mecánica de los procesos que intervienen en la evolución del desarrollo, se sabe que esta evolución se refleja en el "grado" de desarrollo que los recién nacidos muestran al salir del huevo. En amniotas, mientras que unos nacen casi completamente desarrollados, otros aparentan haber nacido sin desarrollarse completamente, por lo que su desarrollo continuará en el transcurso de unas etapas adicionales supervisadas por cuidados parentales. Este fenómeno ocurre en un espectro de tipos de recién nacidos llamado altricial-precocial, un espectro que responde al grado de desarrollo que muestren los embriones de cada taxón (anteriormente se diagnosticaba, principalmente en aves, como nidícolas o nidífugos respectivamente, ver Starck, 1993). El espectro altricial-precocial está delimitado por dos extremos radicales donde, en un lado están los neonatos altriciales (nidícolas), los cuales nacen indefensos, sin plumón, generalmente con los ojos cerrados, y sin ninguna capacidad motriz. Los precociales verdaderos, por el contrario, son capaces de valerse por si mismos, lo que implica que tienen casi todo el plumaje desarrollado, así como el sistema sensorial y el aparato locomotor. En realidad el espectro abarca al menos ocho categorías bien diferenciadas, y como fenómeno, se da tanto en arcosaurios como en mamíferos. En todos, la altricialidad parece ser una característica de la estrategia vital asociada a un mayor desarrollo del sistema nervioso central, tanto en términos alométricos, como de desarrollo neuronal *per se*. Por tanto, la evolución de las estrategias ontogenéticas tiene un reflejo sistémico tanto en el "grado" de desarrollo del embrión, como en última instancia en la encefalización del adulto. Puesto que, la variación fenotípica del cerebro está ligada a la evolución de la ontogénia y, a la vez, muy posiblemente con la organización craneal, puede que también haya una asociación entre la evolución de modos de desarrollo y la evolución de la organización fenotípica craneal. Revelar si existen diferencias fenotípicas craneales ligadas a la macroevolución de las estrategias ontogenéticas puede explorarse desde la aplicación de técnicas estadísticas discriminantes (de probabilidad de asignación a un grupo particular) como los Análisis de Variantes canónicos (CVA) sobre las configuraciones de landmarks de la morfometría geométrica. Si los resultados son positivos desvelaríamos el posible valor que tienen los cambios del desarrollo a nivel más sistémico, pues se

coordinarían cambios en el sistema nervioso y el sistema craneal de manera sincrónica. Por otro lado, es lógico pensar que la evaluación más inmediata para comprobar la relación estructural que pueda existir entre las organizaciones fenotípicas del cerebro y el cráneo ha de realizarse comparando morfométricamente las geometrías de ambos sistemas, y expresarla en términos de covariación estadística. De encontrar una relación directa (y como hemos apuntado en varias ocasiones, las hipótesis nulas generalmente lo prevén así), el modelo resultante aproximaría los resultados a una interpretación del desarrollo conjunto de ambos sistemas. Adicionalmente, ayudados por la extensa información que existe referente a la función de las partes que organizan el fenotipo del cerebro (*s.l.)*, sería posible manejar una hipótesis más inclusiva que explore las consecuencias funcionales de la intersección estructural entre ambos sistemas a una escala fenotípica y macroevolutiva. Realizaremos este experimento morfométricamente utilizando la técnica de Mínimos Cuadrados Parciales.

Box 3

La modularidad y el campo morfogenético en la biología evolutiva del desarrollo

El estudio de la integración y modularidad ha despertado un gran interés en la embriología contemporánea desde donde se entiende que en el desarrollo habrá un equivalente germinal de los módulos estructurales observables en el adulto, los campos morfogenéticos (Gilbert et al., 1996). No obstante la idea de módulo en biología del desarrollo es más complejo, pues se entiende que será más *un recurso que un objeto* (Gass y Bolker, 2003), pues puede incluir, un gen, un conjunto de genes, célula o poblaciones de células, así como rutas de señalización.

La biología del desarrollo contemporánea ha desarrollado con gran énfasis el concepto de modularidad en la última década asociándolo al concepto, rejuvenecido, de campo morfogenético (Gilbert, et al., 1996; Raff, 1996; Bolker, 2003), estableciendo un nuevo marco desde el que abordar la modularidad estructural desde procesos dinámicos. Desde su punto de vista, la modularidad estructural es, en definitiva, el fiel reflejo de la organización modular de su desarrollo.

Desde el desarrollo se entiende que un modulo (campo morfogenético) será relativamente autónomo y susceptible por tanto de variar sin comprometer a otros, y las fuentes de variación dependerán de factores epigenéticos (interpretación de la señalización celular por parte de las poblaciones o la interacción entre ellas, y entre ellas y su entorno). Lo que en principio puede resultar antagónico, pues es difícil de comprender que algo esté integrado y sea modular a la vez (Eble, 2004), adquiere sentido desde la embriología, donde la integración en el desarrollo se da por un hecho inevitable. En definitiva se asume (y demuestra) que en el desarrollo no existe ningún proceso que sea totalmente autónomo (Noden y Trainor, 2005).

Una cuestión que resulta interesante es que en morfología se entiende que será una fuente de variación (variación de cada módulo y entre módulos del sistema). En teoría y biología de sistemas, en vez de verse como un reflejo del proceso evolutivo, la modularidad se entiende como un mecanismo efectivo para amortiguar el efecto de perturbaciones, como por ejemplo mutaciones o delecciones, y es lo que mantiene estable al sistema en el tiempo.

La noción de campo morfogenético, por su parte, tiene una larga historia en la embriología clásica (ver, p. ej.; Weiss, 1939; Needham, 1936, 1950; Spemann, 1938; Oppenheimer, 1966). En la biología del desarrollo actual se considera que los campos morfogenéticos son regiones embrionarias precursoras de partes específicas en un organismo en desarrollo y que, una vez se han establecido, tienen una cierta autonomía con respecto a otras partes que también se estén desarrollando (Gilbert et al.,1996). Un factor critico de para la iniciación e identificación de un campo morfogenético (también llamados campos primarios, secundarios o terciarios, según la escala de la que se trate; Carroll et al., 2004) son las rutas de señalización intercelular.

Carroll et al. (2004) definen como campo morfogenético *primario* al embrión en desarrollo, mientras que un campo morfogenético *secundario* será, por ejemplo, una extremidad. Puesto que es una organización jerárquica, puede existir un campo *terciario*, etc.

La identidad celular no es imprescindible para diferenciar un campo morfogenético (Klingenberg, 2004), aunque si que habrá fronteras entre distintas poblaciones que partan de diferencias entre sus propiedades (*viz.* existe una compartimentación que especifica las células en cada campo). El código de genes selectores dentro del campo morfogenético tiene influencia sobre el patrón de la estructura final mediando en las tasas de proliferación celular relativa y en el alineamiento de éstas (epigénesis). Este patrón previo se traducirá en última instancia en la geometría de la estructura final, diferenciando tejidos y participando en el movimiento morfogenético de regiones o partes dentro del área (p. ej. mediante dobleces, deformaciones, alargamientos, etc.). Aunque esta parte es menos conocida, es muy posible que tenga una influencia decisiva sobre la interacción de las estructuras morfológicas.

SEGUNDA PARTE

2.1 Morfología descriptiva del cráneo

*…Thus, I conceive, the study of the mode in which the skulls of vertebrate animals are developed, demonstrates … that they are all constructed upon one plan; that they differ, indeed, in the extent to which this plan is modified….*T. H. Huxley. On the Theory of the Vertebrate Skull (1858)

El cráneo de un arcosaurio mantiene el plan estructural común a todos los vertebrados, siendo una estructura tridimensional que queda dividida en dos mitades simétricas por un plano medial sagital. A continuación resumimos, en primer lugar, la composición osteológica general del cráneo de Archosauria, así como la identidad de sus regiones más inclusivas. Seguidamente pasamos a resumir los aspectos más importantes del desarrollo craneal, desde la visión clásica hasta las acepciones más contemporáneas que explican la identidad embriológica de cada hueso. Pasamos después a resumir la asociación estructural del cráneo y el sistema nervioso central, y por último, destacamos los aspectos más generalizados del cambio morfológico en el cráneo como un adelanto a la variación morfológica que esperamos encontrar desde los análisis métricos.

2.1.1. Anatomía del cráneo en un arcosaurio.

En la figura 2.1 se muestra un esquema original del un cráneo de *Tyrannosaurus rex* (AMNH 5027), tal y como lo preparó, fotografió y esquematizó para su descripción H. F. Osborn (1905). Utilizamos este cráneo como modelo general para el cráneo en Archosauria. Otros ejemplos pueden verse en cada capítulo de la tercera parte del volumen.

En la figura el cráneo de *T. rex* muestra su lado izquierdo (Fig. 2.1, superior), y debajo del original se incluye un esquema (también de Osborn, op. cit.) que permite ver cada hueso singularizado con los huesos colindantes por sus suturas. La Fig. 2.2a muestra la región interna del cráneo del mismo dinosaurio, su endocráneo, donde se alberga el sistema nervioso central y donde se pueden observar también más detalles de la composición osteológica del cráneo en Archosauria. Esta región queda expuesta despues de realizar un corte medial sagital, trabajo que realizó Osborn (op. cit.) sobre otro ejemplar original (AMNH 5029). El AMNH 5027 se encuentra expuesto en la sala de dinosaurios terópodos de la misma institución en la ciudad de Nueva York (EE.UU.).

En la vista lateral del cráneo la región más anterior es la región *rostral*. Ésta queda delimitada por los premaxilares (fusionados en una sínfisis), a los que siguen, ventral y cauldamente, los maxilares, y dorsal y caudalmente, los nasales (nótese que el plural afirma la paridad de estos huesos, aunque sólo trabajemos con cada uno del par desde la vista lateral). Los maxilares y premaxilares son los huesos portadores de dientes, que en arcosaurios tienen una inserción típicamente tecodonta (sin raíz, y de recambio constante).

Encontramos más caudalmente los huesos prefrontales y lacrimales, a los que siguen los frontales, más dorsalmente, y los yugales, en posición ventral. La región más afín al sistema

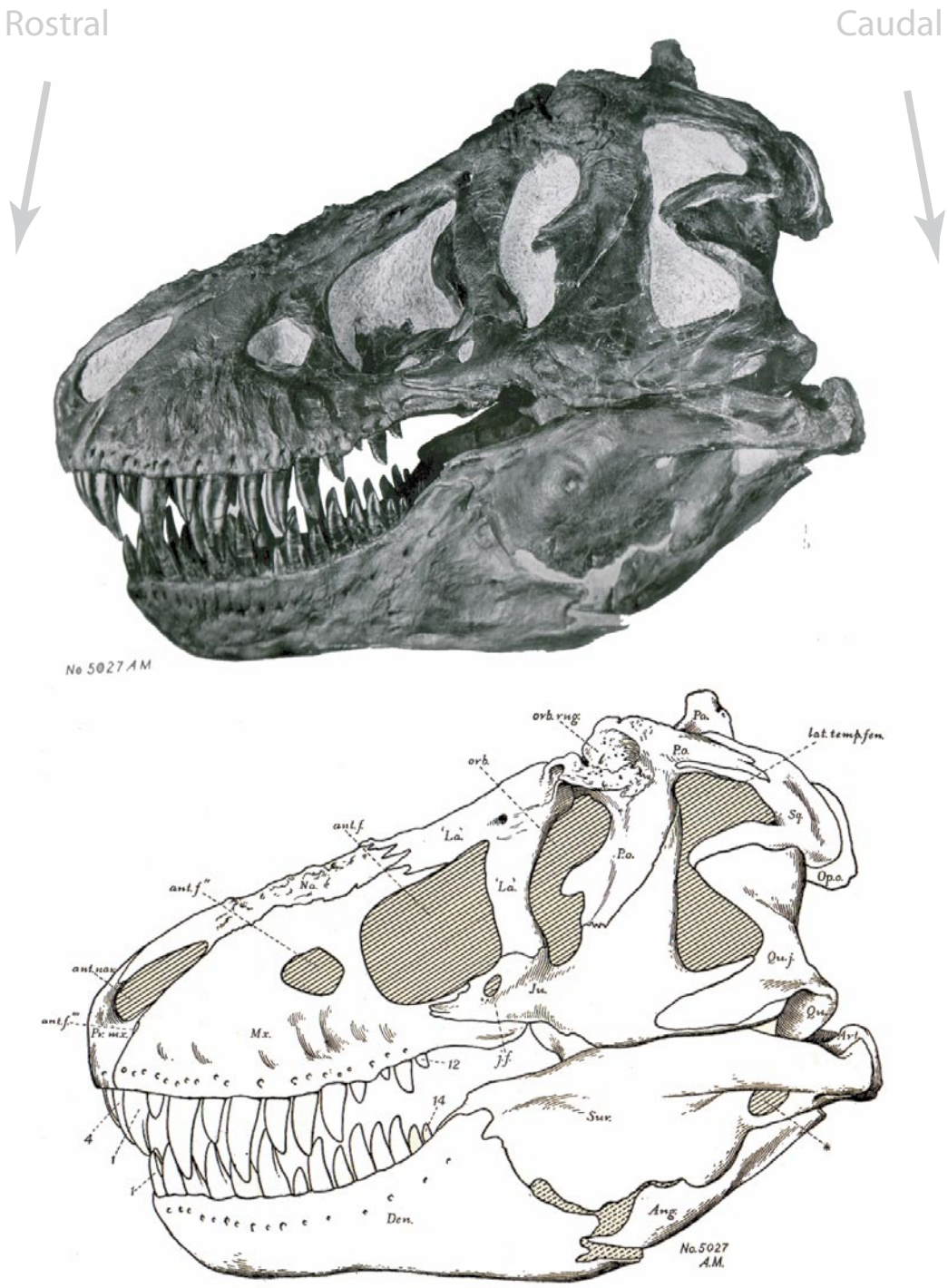

Figura 2.1. Vista lateral del cráneo de T. rex según Osborn (1905). (Arriba) Cráneo original (AMNH 5027). Las flechas diferencian las regiones anterior (rostral) y posterior (caudal). (Debajo) Esquema del mismo cráneo (original de Osborn, op. cit.). Las abreviaturas son; Pr.mx=premaxila, Mx=maxila, Na=nasal, Ant.nar=narina, La=lacrimal, Ju=yugal, J.f.=fenestra yugal, Po=postorbitario, Orb.rug=rugosidad orbital, Pa=parietal, Lat. Temp. Fen.=Fenestra temporal lateral, Sq, escamoso, Quj.=cuadratoyugal, Op.o.=opistótico, Qu.=cuadrado. En mandibula; Art. =articular, Ang.=angular, Sur.=surangular, Den.=dentario. Las flechas señalan con ant. f., las distintas aperturas rostrals (ant. f=fenestra anteorbitaria, ant.f"=fenestra maxilar, y ant.f'"=fenestra premaxilo-maxilar). Los números indican la posición de los dientes (maxilares y mandibulares). En mandibula, *=apertura (fenestra) mandibular.

nervioso es la caja craneana, también llamada neurocráneo, se localiza caudalmente a la rostral, y se compone de los parietales y escamosos, en la región más dorsal y lateral respectivamente, y los huesos cuadrado y cuadratoyugal, siendo la región ventral del yugal

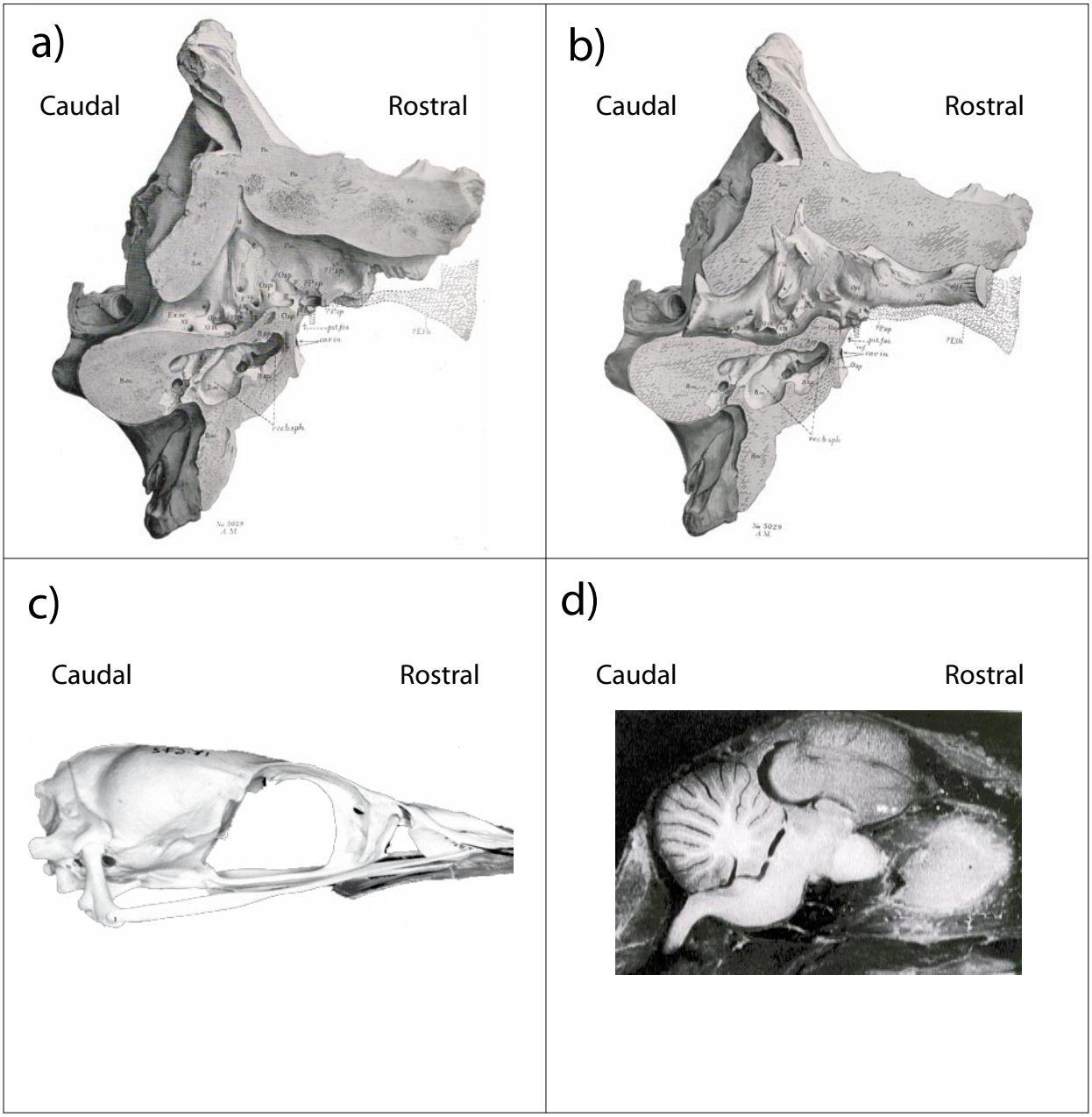

Figura 2.2. a) Vista medial sagital de la caja craneana de T. rex (AMNH 5029; Osborn 1905). b) Misma vista medial sagital con un molde del endocráneo superpuesto simulando el sistema nerviso central. Nótese que no se sabe realmente si el SNC ocupaba, o no, toda la cavidad. c) Vista externa de caja craneana de *Phalacrocorax* para resaltar como se evidencia la forma del SNC desde el exterior del cráneo. d) Corte medial sagital del cráneo fresco de una gaviota (*Larus*), donde se puede ver la asociación del SNC con el cráneo circundante en un ave actual (Fotografía original de Dubbeldam, 1968).

el punto de articulación con la mandíbula.

Las paredes caudales del cráneo pueden verse en el corte medial sagital (Fig. 2.2a), y en ella se diferencian los occipitales, un conjunto de huesos que se denominan según su localización espacial. Así, tenemos el supraoccipital, en la región dorsal fusionado en el plano medial sagital. Más ventralmente le siguen los paraoccipitales, uno a cada lado del foramen mágnum, espacio de paso para la medula espinal que dejan todos los occipitales, incluyendo al más ventral, el basioccipital.

En el esquema también se distingue fácilmente una apertura anterior, la narina, y otra, la órbita ocular la cual alberga el ojo, que generalmente es grande con respecto al resto del cráneo en cualquier representante del grupo. Justo por delante de ésta y detrás de la narina se localiza una apertura muy grande, denominada fenestra anteorbitaria, una apertura del cráneo diagnóstica de archosauria (la fenestra mandibular, es otro rasgo diagnóstico del grupo, y se trata de una apertura relativamente pequeña delimitada por los huesos angular y el surangular, en la mandíbula). En el cráneo, más caudalmente, puede distinguirse otra apertura, la fenestra (lateral) temporal, aunque esta puede desaparecer en algunos taxa, como por ejemplo, en aves (para más detalle ver también).

En vista lateral podemos distinguir el complejo facial. En él, el rostro está delimitado anteriormente por la premaxila y caudalmente por los huesos prefrontal y/o el lacrimal, huesos que definen el margen anterior de cada órbita. El plan general del cráneo arcosauriano en vista lateral deja la órbita ocular en una situación topográficamente intermedia entre el rostro y la caja craneana, definida ésta última por el límite caudal de la órbita, generalmente definido por el hueso postorbitario (ver, Klaauw, 1945, 1948, 1951, 1952; Witmer, 1995, 1997). Estas tres unidades unifican el cráneo, aunque también son definidas, en conjunto, como el complejo, o el sistema craneofacial. Es difícil definir objetivamente qué es el complejo facial en reptiles arcosaurios, pues cualquiera que sea el taxón, éste incorpora o puede incorporar la órbita ocular (por ejemplo, en mamíferos el término incluye también el jugal, hueso que define la extensión ventral de la órbita en todo Archosauria).

2.1.2. Unidades del cráneo, su desarrollo y criterios de homología

En la Teoría Vertebral del cráneo clásica se ve al cráneo como un sistema ordenado y segmentado en varias vértebras modificadas dispuestas en serie (Fig. 2.3). La idea general de este modelo fue propuesta por el morfólogo alemán Goethe, aunque parece que quién la promulgó en el ámbito científico fue, posteriormente, R. Oken. Geoffroy Saint-Hillaire (Fig. 2.4), autor coetáneo, extendería en Francia la propuesta, y así mimo, R. Owen, haría lo mismo en Inglaterra sentando, a la par, las bases de homología propuestas por Saint-Hillaire en su noción de arquetipo (Fig. 2.5). En la propuesta del arquetipo subyace la idea de que todos los vertebrados están construidos a partir de la modificación de un plan unitario común a todos.

Owen estudió también el desarrollo de los huesos del cráneo, definiendo las tres regiones embrionarias que lo componen (el condrocráneo, el dermatocráneo y el esplacnocráneo;

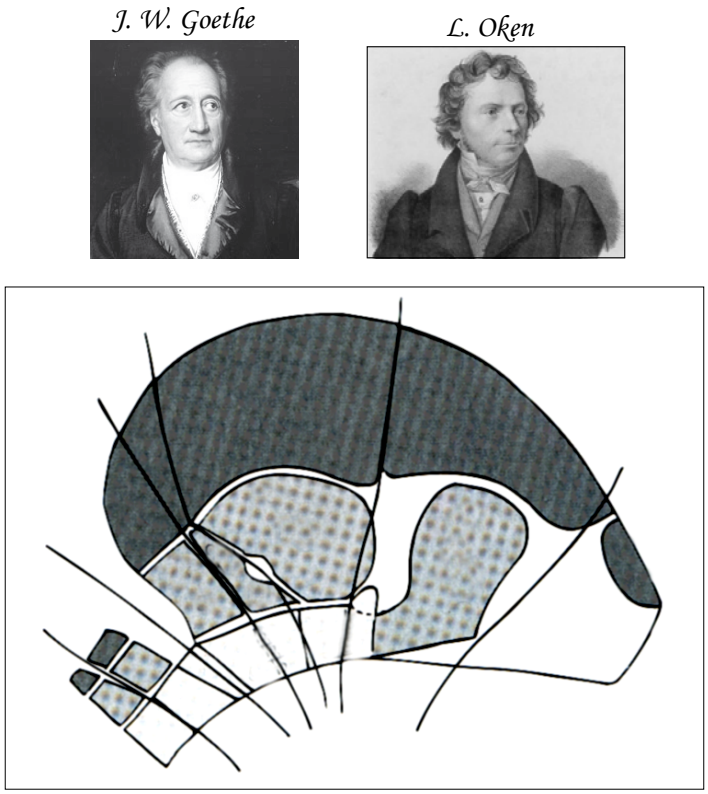

Figura 2.3. (Superior) Imágenes de Goethe, a la izquierda, y Oken, a la derecha. (Debajo) Esquema de la Teoría Vertebral del Cráneo según ambos autores. Modificado de Kardong (1995).

Fig. 2.6).

El condrocráneo engloba a todos los huesos del cráneo de origen condral, es decir, aquellos huesos cuya osificación parte de un precursor cartilaginoso el cual es posteriormente sustituido. El hueso dérmico es un tipo de hueso que, por el contrario, no deriva de un precursor cartilaginoso previo, sino que se forma directamente. El esplacnocráneo contiene ambos tipos de huesos, y su distinción viene determinada directamente por la región desde la que se origina, los arcos branquiales.

El condrocráneo (también llamado neurocráneo por su asociación con el sistema nervioso) contiene a los huesos occipitales, y aquellos que rodean a las cápsulas sensoriales, tales como la mayoría de huesos esfenoidales y la cápsula ótica. El resto de huesos serán por tanto de naturaleza dérmica (Fig. 2.6).

Desde esta regionalización se sustentará la homología osteológica de los huesos en todo Craniata, y puede encontrarse descrita en detalle en los trabajos monumentales de G. de Beer (1937), o de Hanken y Hall (1993), entre otros. En estas referencias se detalla también el desarrollo primigenio del cráneo, que es común, en términos generales, a todos los vertebrados. En la Figura 2.7 se resume la secuencia del desarrollo de las estructuras primordiales de naturaleza condral (trabéculas, paracordales y cápsulas óticas) que preceden a la aparición secuencial de los huesos dérmicos. Su pronta aparición y su naturaleza condral hace que se consideren los cimientos que sustentarán al futuro cráneo.

Desde su propuesta, la *Teoría Vertebral* del cráneo ha prevalecido durante siglos, e implica una noción de modularidad en cuanto a que, según el morfólogo W. Bateson (1894), el cráneo surgiría de una diversificación de *partes seriadas homólogas*. El modelo contemporáneo, en cambio, difiere de la teoría clásica en un aspecto fundamental y tiene sus inicios en uno de los discursos *Croonianos* más aclamados de Huxley (*On the Theory of the Vertebrate Skull*;

Étienne Geoffroy Saint-Hilaire

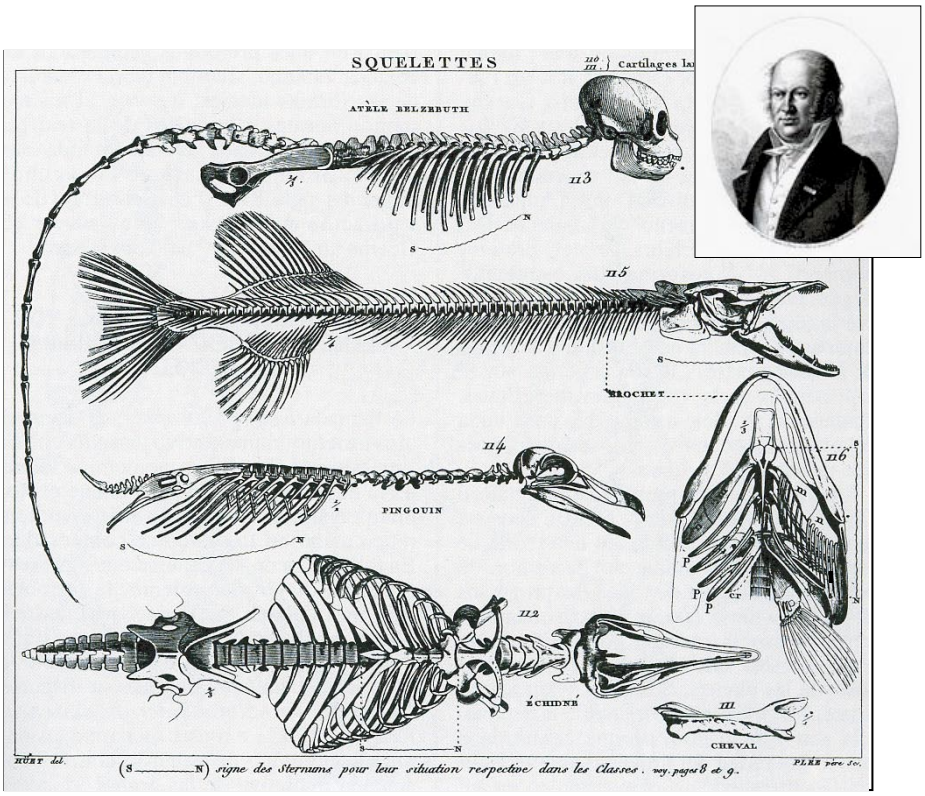

Figura 2.4. Imagen de Saint-Hillaire. (Debajo) Esquema del autor mostrando su hipótesis de homología entre distintos vertebrados. En ella se compara el esqueleto y la disposición de un primate, arriba, seguida hacia abajo, de un pez osteictio, después de un ave, y finalmente una ballena. Modificado de López Piñero (1992).

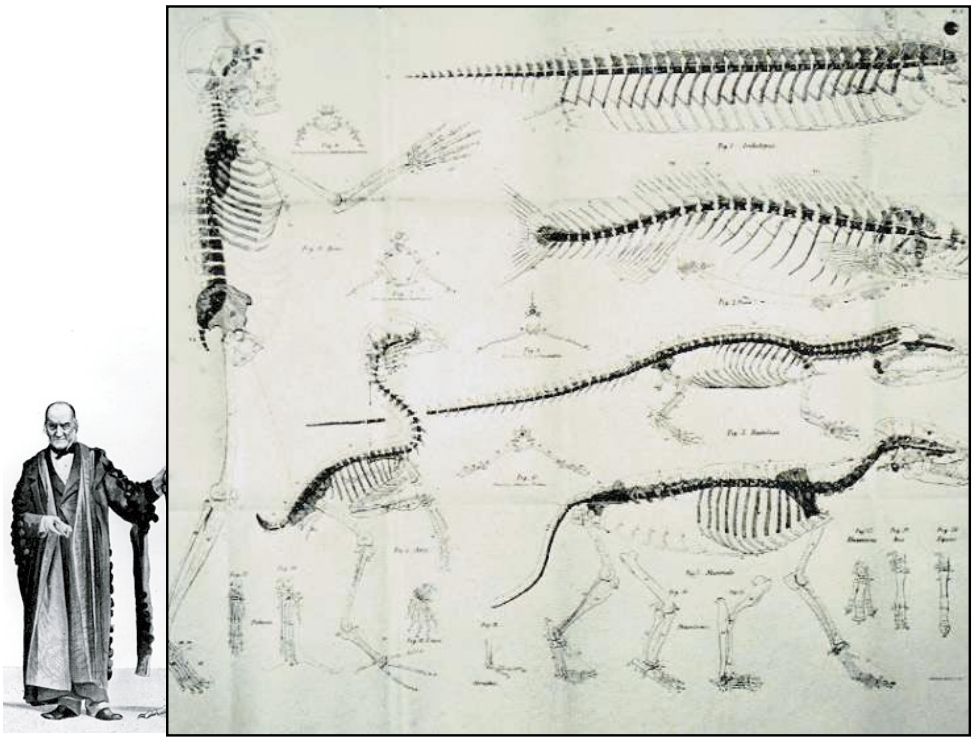

Rihard Owen

Figura 2.5. Imagen de Owen junto a su esquema del Arquetipo (forma superior-derecha del dibujo). El resto de esqueletos corresponde a un humano (izquierda), un ave, un pez, un cocodrilo y un perro. El eje axial está oscurecido mostrando la extensión de hueso condral. Original tomado de López Piñero (1992).

1858). Huxley defendió que la región facial del cráneo surge *de novo* y, por tanto, no es una vértebra, sino una sustancia desconocida o inusual, de origen no "vertebral".

La visión actual es que los conjuntos de células embrionarias que caracterizan esta región surgen en la interfase entre el ectodermo y el mesodermo, casi como una nueva capa germinal (Stone y Hall, 2004). Estas poblaciones celulares son la Cresta Neural, y su génesis es, en efecto, una novedad crucial en la historia evolutiva de los cordados (Northcutt y Gans, 1983; Gans y Northcutt, 1983). Sin embargo, la noción de que la región cordal, en sentido general, es una vértebra muy modificada ha sido demostrada recientemente, y por tanto, permanece intacta en la actualidad.

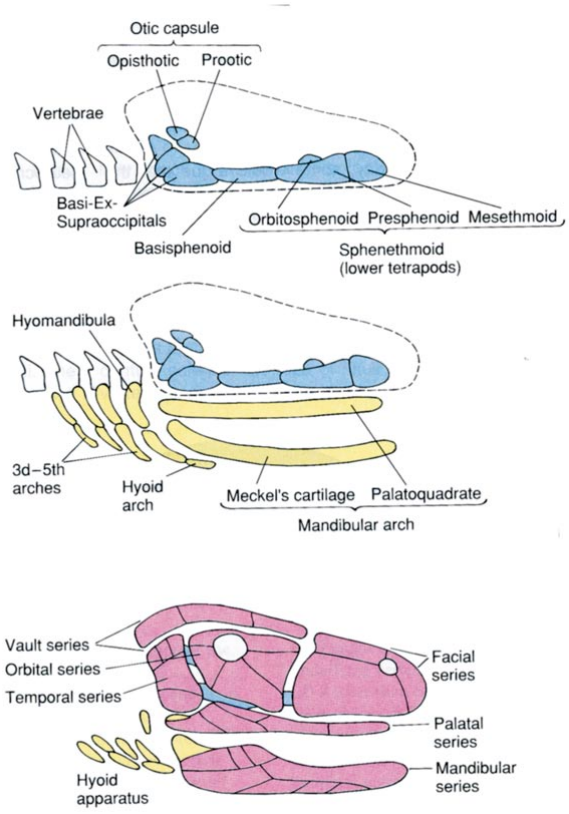

Figura 2.6. Las tres partes del cráneo según tipo de osificación y función relativa. En azul, condrocráneo (conforma, como un zócalo, las partes caudal y ventral que sustenta al sistema nervioso central dentro de la caja craneana). En amarillo, el esplacnocráneo, y en rojo, el dermatocráneo. Compárese también con figura 2.8, más adelante. Original de Kardong (1995).

En definitiva, la visión estructural contemporánea del cráneo implica una región "vertebral" más caudal unida a una derivada de la cresta neural. La diferencia, por tanto, radica en que no existe una segmentación, sino una distinción entre dos regiones que configuran todo el sistema craneal cuya identidad primigenia es distinta (su mesénquima primordial).

Las técnicas modernas de marcación celular (las quimeras; LeDouarin, 1986; o de marcaje viral, ver p. ej., Evans y Noden, 2006), son las que han permitido mostrar con claridad las fronteras que separaran estos dos grandes dominios del cráneo. La distinción se realiza atendiendo a la identidad celular del mesénquima precursor de los huesos que encontramos en la morfología de un cráneo adulto.

Concretamente, existe una definición de dos territorios distintos que se separan por la identidad de estas células, según deriven de la cresta neural o del mesodermo. Couly et al., (1993) y LeDouarin et al., (1993) describen una región *cordal* que se localiza en el embrión temprano, caudalmente a la porción más anterior de la notocorda (también la definen como

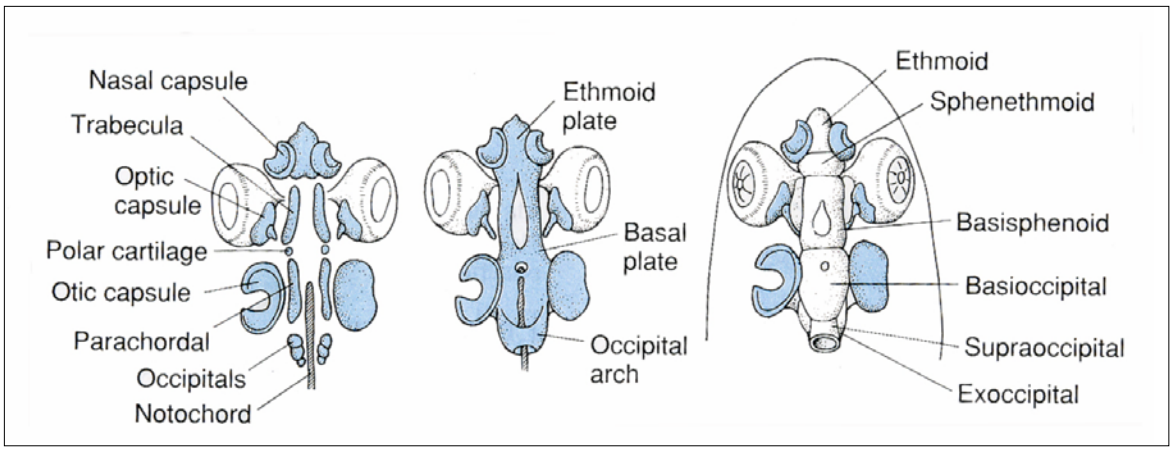

Figura 2.7. Distintas estructuras primigenias en el desarrollo temprano del condro- o neurocráneo. Original de Kardong (1995).

región "*Acordal*"; Fig. 2.8). De hecho, la notocorda en el embrión es un centro organizador que entra en el cráneo y llega justo hasta casi la mitad de lo que será la fosa pituitaria, y por tanto, esta zona será un punto frontera clave entre ambos dominios. El mesénquima, precursor de esta región caudal al límite anterior de la notocorda, tiene un origen mesodérmico, aunque dentro de la región habrá elementos derivados del mesodermo somítico (también llamado paraxial), y del mesodermo craneal paraxial.

Por otra parte, la región *precordal* será aquella que se localizará anterior a la frontera impuesta por la notocorda, y comprende elementos mesenquimales que se diferenciarán en células cuyo origen es la cresta neural craneal.

Couly et a., (op. cit.) explican cómo la identificación de estas regiones surgió de observar mutaciones homeóticas de complejos implicados en la génesis de los elementos axiales (vértebras cervicales), cómo éstas afectaban también al atlas y al axis, e incluso cómo su efecto se extendía a huesos embebidos en la caja craneana (el basiocipital), lo que sugería un origen morfogenético común a todos ellos.

Después de varios experimentos se pudo demostrar que el mesodermo somítico (paraxial), además de ser un componente celular post-craneal, contribuye en gran medida a la construcción del cráneo. Por otra parte, se ha descubierto que otras poblaciones celulares del

Figura 2.8. (Arriba) Vista lateral del condrocráneo de un pollo en el estadio E9 mostrando el origen de cada una de las cápsulas. La línea negra marca la notocorda. 1. Cápsula nasal, 2. capsula orbital, 3. cápsula ótica (pars ampullaris), 4. cápsula ótica (pars cochlearis), 5. arco occipital, 6. exocipital, 7. basioccipital, 8. supraoccipital, 9. septo interorbitario, 10. cartílago hioideo, 11, cartílago de Meckel, 12. cartílago cuadratoarticular, 13. basiesfeoides (a), basipostesfenoides, (b) basipreesfenoides. (Izquierda) Esquema del cráneo completo de un ave. La flecha indica el límite más anterior de la notocorda en la fosa pituitaria. A) Vista lateral externa, B) vista lateral interna (medial sagital). Código de colores igual que arriba. Los huesos son, 1. angular, 2. basibranquial, 3. basihial, 4. ceratobranquial, 5. columela (a) y cápsula ótica (b), 6. dentario, 7. epibranquial, 8. entogloso, 9. etmoides, 10. exooccipital, 11, frontal, 12. septo interorbitario, 13. yugal, 14. maxila, 15. cartílago de Meckel, 16. cápsula nasal,.....

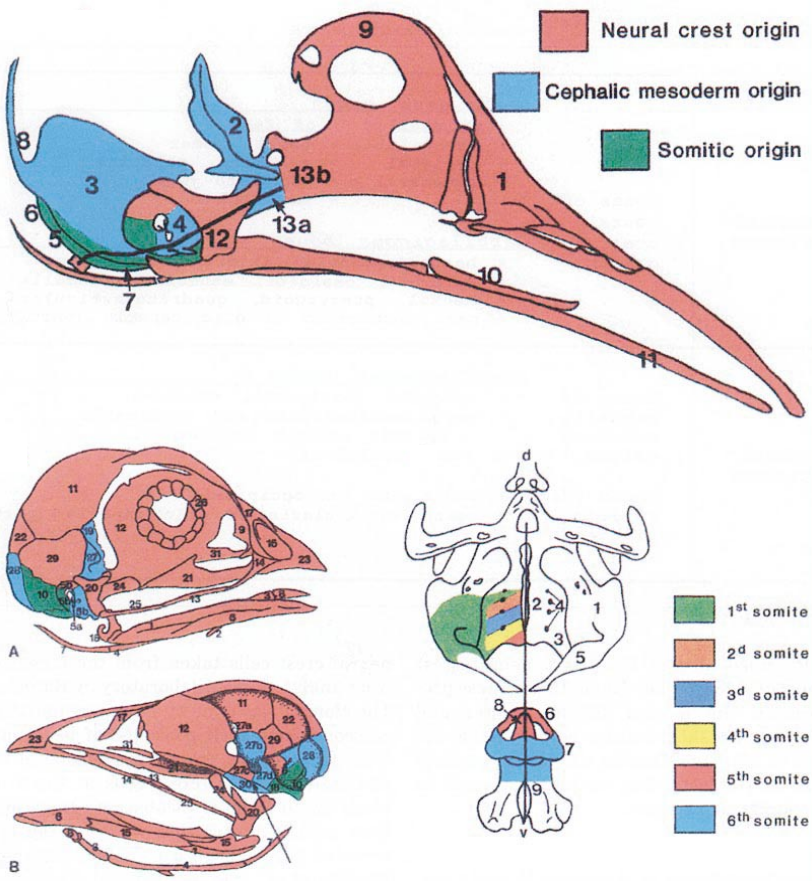

T.....
ORIGIN OF CEPHALIC SKELETON

"ACHORDAL" SKELETON	Bones of neural crest origin	*Membranous bones* : - *of skull* : • frontal • parietal • squamosal - *of face* : • nasal, vomer • maxillar, palatine • quadrato-jugal • mandibular *Cartilaginous bones* • basipresphenoid, interorbital septum • sclerotic ossicles, ethmoid, columella • Meckel, pteryogoid, quadrato-articular • pars cochlearis of otic capsule (partly)
"CHORDAL" SKELETON	Bones of cephalic mesoderm origin	*Cartilaginous bones* : • sphenoid (basipost-, orbito-) • pars canalicularis and cochlearis of otic capsule (partly) • supra-occipital
	Bones of somitic origin	• basi- and exo-occipital • pars canalicularis of otic capsule (partly)

.....17. nasal, 18. basioccipital, 19. postorbital, 20. cuadrado, 21. palatino, 22. parietal, 23. premaxila, 24 pterygoides, 25. cuadratoyugal, 26. osículos escleróticos, 27. esfenoides (a) orbitoesfenoides, (b) pleuroesfenoides, (c) basipreesfenoides, (d) basipostesfenoides, 28. supraoccipital, 29. escamoso, 30. temporal, 31. vomer. (Derecha) Esquema de la vista dorsal del condrocráneo aviano embrionario (en estadio E3) mostrando la contribución de cada somito a; 1. la cápsula ótica, 2. el basioccipital, 3. el exoocipital, 4. raíces del nervio hipogloso, 5. el supraoccipital, 6. arco anterior, 7. arco posterior del atlas, 8. odontoides de la apófisis del, 9. el eje axial. A línea negra en el eje sagital representa la notocorda. La tabla resume los mismos huesos según tipos. Toda la figura, su texto y la tabla son originales de LeDouarin et al., (1993).

mesodermo se han especializado en la producción de mesenquima craneal, el mesodermo paraxial craneal o cefálico (Hacker y Guthrie, 1998).

Igualmente, la cresta neural craneal es específica de esta región del cuerpo (el cráneo), pues es la única capaz de generar hueso, bien condral o dérmico (Couly et al., 1993). La diferenciación del mesodermo paraxial en el cráneo viene determinado por su identificación *in situ*, por las rutas que sigue desde los rombómeros junto a la cresta neural craneal, por su identidad genética y porque además de hueso, está implicado en la formación del tejido muscular de la cara y del cuello.

Los huesos que contienen cada una de estas regiones están descritos en la Fig. 2.8, junto al esquema coloreado que muestra la delimitación de las fronteras mayores entre regiones (Nota: la figura es la original de LeDouarin et al., 1993).

2.1.3. Relación estructural entre el cráneo y el sistema nervioso central (SNC)

La evolución fenotípica del cráneo, y más particularmente de la región cefálica, parece estar íntimamente coordinada con la evolución fenotípica del sistema nervioso (Fig. 1.8b). Para Moss y Vilmann (1978):

...the skull as a whole and each of its skeletal components must satisfactorily meet all functional demands instantaneously placed upon it at every developmental stage.

Demostrar que el hueso tenga que seguir unas pautas de cambio dictadas por el SNC no es una tarea sencilla, lo que por otra parte no hace que la relación estructural entre ambos sistemas sea dudosa. Por ejemplo, el SNC deja su impronta casi perfecta dentro de la caja craneal, tal y como se muestra en la Figura 2.2, aun cuando puede que el SNC no ocupe toda la cavidad, como en el caso de los cocodrilos actuales. En cambio, en aves, el SNC ocupa completamente la cavidad, y su relación con el hueso circundante es tan estrecha que es posible percibir los bultos cerebrales desde la periferia externa de la caja craneana (Fig. 2.2c, d)

En el SNC está constituido por el encéfalo y la médula espinal (Fig. 2.9). El encéfalo, parte del sistema nervioso central, situado en el interior del cráneo, comprende el cerebro, el cerebelo y el tronco encefálico. El cerebro se divide en dos hemisferios. En casi todos los arcosaurios el cerebelo se encuentra detrás de los hemisferios cerebrales. Consta de dos partes, como el cerebro, unidas por una masa central. El cerebelo es el órgano destinado a coordinar y

armonizar los movimientos. Cuando se priva de cerebelo a un animal la vida continúa pero sus movimientos no se coordinan, perdiendo la capacidad de andar o volar si se trata de un ave. El bulbo raquídeo o médula oblonga es una prolongación de la médula espinal y es el órgano que establece una comunicación directa entre el cerebro y la médula. Al mismo nivel de la médula oblonga se entrecruzan los nervios que provienen de los hemisferios cerebrales.

El encéfalo consta de tres pártes: 1. Prosencéfalo: Que consta de otras dos partes A) El Teléncefalo es el Cerebro, y se encarga de la visión, la sensación, la audición, la olfacción, y

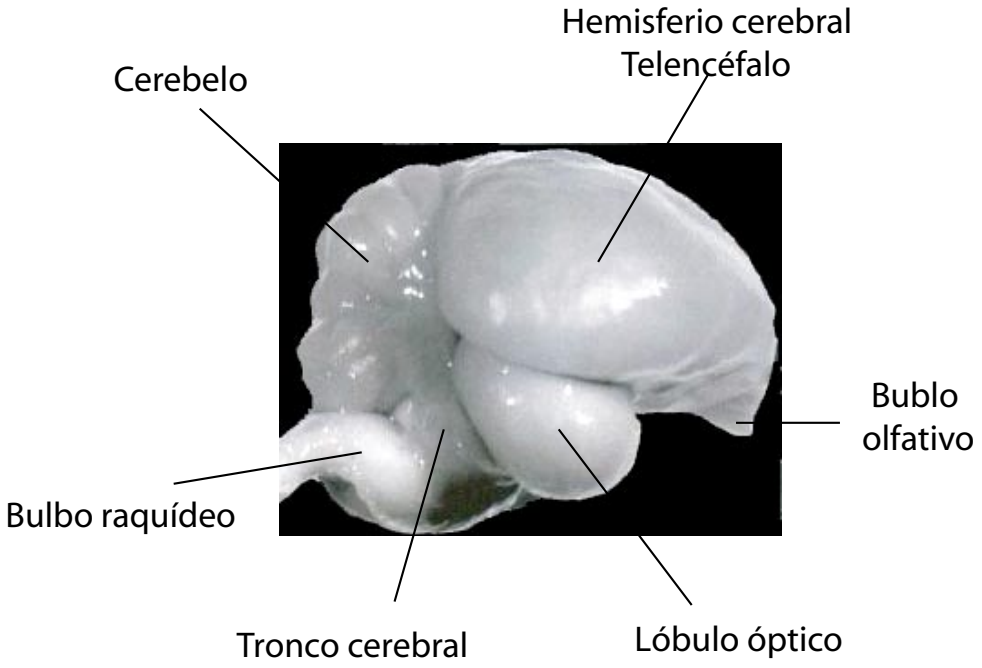

Figura 2.9. Sistema nervioso central de un paseriforme (Neornithes) en vista lateral, mostrando sus unidades fundamentales (o funcionales).

el aprendizaje. B) El Diencéfalo es el Tálamo: Zona de control maximo de las sensaciones, también es el centro regulador de las emociones (Sistema Límbico) y control físico Epitálamo.

2. Mesencéfalo es el cerebro Medio, y posee los tuberculos cuadrigéminos que son cuatro, dos ópticos y dos olfativos. Controla la vigilia y el sueño. 3. El Rombencéfalo consta de, A) Metencéfalo o Cerebelo: Control movimiento (muscular), postura, y B) Mielencéfalo, o Bulbo Raquídeo: Control de las funciones básicas como digestión y la respiración.

La región del endocráneo que subyace a todo el SNC se conoce como la base del cráneo (Fig. 2.2c), y se diferencia del "suelo" craneal, que se localiza exteriormente y en que este último generalmente lo conforma el basiesfenoides, aunque en el caso particular de las aves

esta región está cubierta por una lámina de hueso dérmico, llamada Lámina Paraesfenoidal (Baumel y Witmer, 1993). Desde su relación espacial con el SNC, la base del cráneo puede dividirse en dos partes, una caudal que se asocia topográficamente con el bulbo raquídeo (parte craneal de la medula; Fig. 2.9) y con la pituitaria, por delante. La otra parte, más anterior, es la región de la base del cráneo que subyace al telencefalo, y coincide con los paraesfenoides y lateroesfenoides. Esta región puede no osificar en aves modernas. La medula continúa su curso hacia el post-cráneo a través del foramen mágnum, apertura que dejan los huesos occipitales.

El cerebelo, dorsal a la médula, está rodeado caudalmente por los occipitales, dorsalmente por los parietales y lateralmente por los escamosos. Parte de los parietales y los frontales rodean al resto del SNC (mesencéfalo y telencéfalo). Los nervios principales del cráneo salen por distintos forámenes entre los que destacamos el foramen óptico, (por donde sale el nervio óptico a la órbita ventralmente al telencefalo), y el foramen olfativo, (salida del nervio olfativo desde la región anterior del telencefalo), también desde la caja craneana a la órbita. Las distintas ramificaciones del nervio trigémino salen por distintos forámenes entre los que destaca el foramen oval (vía de paso para el nervio mandibular).

2.1.4. Relaciones espaciales entre las partes del cráneo.

La exploración de la morfología craneal en Archosauria, en esta memoria, se realiza en norma lateral, tal y como se mostraba en las figuras anteriores. Las herramientas analíticas más desarrolladas de la morfometría geométrica están principalmente desarrolladas para trabajar en dos dimensiones. Dadas estas limitaciones prácticas, trabajar en la vista del cráneo lateral permite capturar una mayor cantidad de información, como lo demuestran las investigaciones más fructíferas en craneología Fig. 2.10).

Como se ha podido observar, hemos omitido la inclusión de la mandíbula. En un principio la mandíbula se excluyó por tratarse de un elemento del cráneo aislado y móvil. Un elemento móvil dificulta el análisis geométrico, a menos que se consiga una posición de estabilidad como consenso común para todos los taxa estudiados. La mandíbula tiene que ser estudiada como un elemento aislado. Otro motivo que nos llevó a excluir la mandíbula es que la mayoría de las veces se encuentra mal preservada (o no se conoce) en algunos fósiles, lo que sesgaría la muestra si la incluyésemos. En el caso de las aves, además, es muy difícil decidir un conjunto de landmarks que sean suficientemente informativos para analizar su variación morfológica.

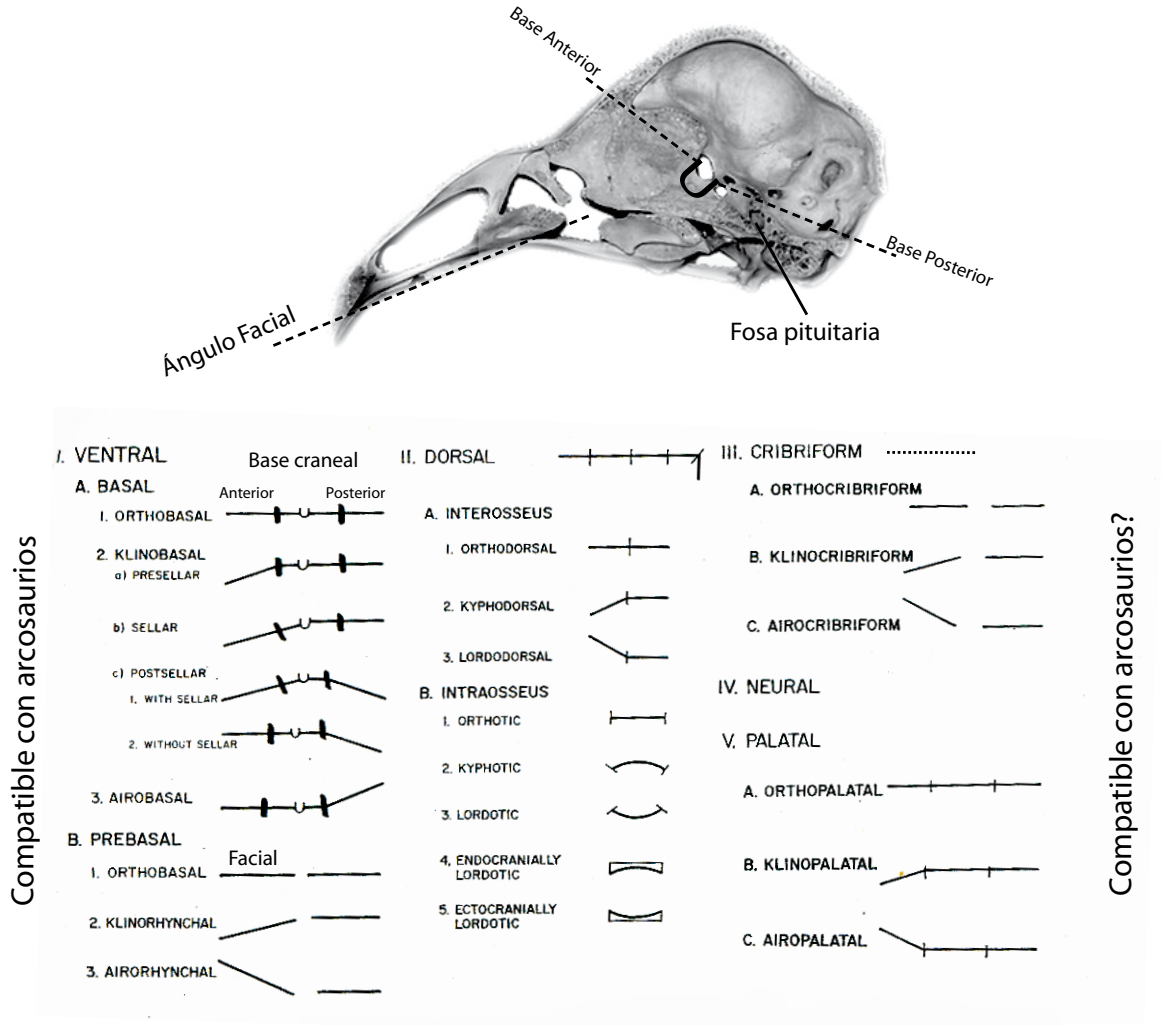

Figura 2.10. Esquema representativo de las distintas posiciones relativas (angulares) entre distintas partes craneales (las también llamadas "flexiones") El cráneo del ave (arriba) representa algunos de los planos desde los que se capturan las variaciones angulares. I. Ventral, A. basal= a los Pre y Basi esfenoides, y al basioccipital (izquierda es anterior, derecha, caudal; la U es la fosa hipofisiaria). B. Ventral Prebasal= esqueleto facial (izquierda) frente a su relación angular con Base del cráneo entera. Otras opciones puede que no ocurran en reptiles arcosaurios. Esquema modificado de Moss y Vilmann (1978).

El objetivo es realizar todo el trabajo en dos dimensiones utilizando para ello todas las herramientas disponibles que permitan comprobar las hipótesis propuestas. A la luz de los resultados obtenidos, el trabajo futuro se dedicará a explorar los mismos eventos en tres dimensiones, así como a incluir la mandíbula y explorar su variación y su asociación con la variación global del cráneo. El compromiso de trabajar en dos dimensiones es capturar la máxima información desde el plano lateral externo del cráneo, o el plano medial sagital (endocráneo), aunque también perdiendo parte la información del plano coronal (transverso, es decir, anchura del cráneo), o información sobre algunos elementos presentes en el planos particulares, principalmente del ventral.

No obstante, en todos los estudios realizados siempre se ha intentado capturar el máximo de información de estos planos infiriéndolos perpendicularmente a las dimensiones desde las que se ha trabajado. Así, siempre tenemos parte de la información contenida en elementos

cuya extensión real se da en otros planos distintos al lateral. Este es el caso, por ejemplo, de los huesos de la región occipital, o de parte de los palatinos (ver, Figs. 2.1 y 2.2).

Los cambios morfológicos que se capturan a una escala comparativa son marcadamente visibles en vista lateral desde la relación angular entre distintas partes del cráneo. Evolutivamente estos cambios son equivalentes (convergentes) entre mamíferos y reptiles arcosaurios. Clásicamente todos estos cambios se han determinado como "flexiones" o "estiramientos" por esa apariencia que confieren al cráneo (Gaup, 1906; Marinelli, 1928; Duijm, 1951; Hofer, 1952; Lang, 1952; Fig. 2.10).

Como resumen general esquematizamos en la Figura 2.10, la propuesta de Moss y Vilmann (1978) de todas las combinaciones posibles que pueden encontrarse en mamíferos, y que quizá puedan ser extendidas a reptiles y aves (ver también; Hofer, 1952). Se distingue entre partes como la base del cráneo (zona "ventral basal" sensu Moss y Vilmann, op. cit.) región que es de gran interés para la primatología contemporánea (Lieberman et al., 2000a, b). En esta región se distinguen dos zonas, una anterior y otra posterior, y la variación se observa como la relación angular entre las dos partes (flexión de la base del cráneo). En otra escala, también se mide la relación angular entre las partes facial y la base del cráneo, lo que los autores llaman la zona prebasal. Es importante destacar que cada tipo de modificación recibe un nombre específico (ver texto en pié de Fig. 2.10).

Nuestro objetivo es identificar este tipo de cambios estructurales en el cráneo arcosauriano desde la morfometría geométrica (el uso de configuraciones de landmarks), lo que impone dos diferencias particulares con respecto a la manera de proceder de los trabajos clásicos. Éstos basaban todas sus mediciones en referencia a un plano basal, plano que es, o ha de ser, común a todos los cráneos comparados. Un ejemplo clásico es el discutido Plano de Francfort (de Beer, 1937), o el Plano Visual Neutral (Enlow y Hans, 1996). Esta *posición estable* del cráneo es una medida de referencia desde la que establecer el resto de las medidas. El problema es que si éste reside entre partes del sistema, su estabilización anulará la variación de éstas trasladándola al resto de medidas que se realicen (ver p. ej. la Superposición por Coordenadas de Forma, para un caso similar). Fijar un plano sólo tendrá sentido en un cráneo si las partes que contiene no varían; en la conjetura de Rabey (1968) de que en su transformación, *-¡todos los elementos de un cráneo se mueven!* (exclamaciones del autor; ver también, Duijm, 1951).

A parte de permitir visualizar el cambio morfológico, la propuesta morfométrica desde la superposición Procrustes en morfometría geométrica es que se utilice como referencia la

media que minimiza la distancia entre las configuraciones de landmarks tras eliminar el efecto de la rotación. Así, la variación de forma se captura desde su independencia de la rotación ("postura") del cráneo. Discutimos éstos y otros aspectos de variación morfológica en el Capitulo 3 (Parte Tercera del volumen).

2.2 Aproximación cuantitativa a la morfología; Morfología Teórica y Morfometría Geométrica

-When the mind of early [humans] began to consider the natural forms…they drew pictures and carved impressions of what [they] saw. G. Rabey. 1968. Morphanalysis.

A continuación se resume como se llega a una métrica de la forma, así como ciertos aspectos de su evolución que más nos conciernen respecto a los métodos que se aplican a lo largo de todo el trabajo. Los métodos en particular se tratan en los apartados que suceden a la introducción histórica.

2.2.1 Hacia una geometría de la forma orgánica

En la historia del ser humano un paso trascendental fue transcribir a dibujos y esculturas las imágenes del mundo que le rodeaba. La representación de la forma humana y la captura de su armonía en un sentido puramente estético es la que dirigirá el desarrollo de una estrategia métrica encaminada al análisis reflexivo de la forma en el mundo orgánico (ver un resumen en; Rabey, 1968, también; Buscalioni et al., 2005).

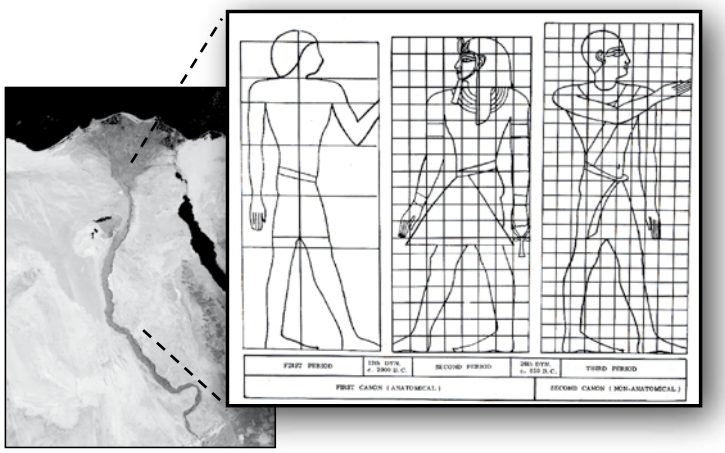

Figura 2.11. Cánones y proporciones en el arte egipcio. Nótense los cambios en la referencia según las etapas históricas (debajo de las figuras, de izquierda a derecha). Modificado de Rabey (1968).

Hace más de 4000 años los egipcios medían el mundo a su alrededor utilizando unidades anatómicas (p. ej. el ancho de la mano y sus múltiplos). Para decorar las tumbas de sus faraones, los artistas desarrollaron un sistema de proporciones, posiblemente el primero, para representar al cuerpo humano. La representación artística de la figura humana se basaba en un conjunto de leyes fijas basado en proporciones que, de hecho, asentaría su propio canon estético. Para refrendar el canon se utilizaba una plantilla en forma de malla (Fig. 2.11), que contenía un completo sistema fijo de proporciones. Desde esta referencia siempre conseguirían repetir correctamente la forma del cuerpo humano.

El estudio y uso de la proporción humana alcanzará un cenit estético en la Grecia antigua, y sus cánones se emplearán en la Roma clásica varios siglos después. Euclides de Alejandría sistematizará y sintetizará el acervo helénico en materia matemática en una geometría basada en teoremas derivados de un sistema axiomático finito; con él nace la geometría euclidiana. Algunos artistas del renacimiento, bien instruidos en matemáticas, aplicarán las

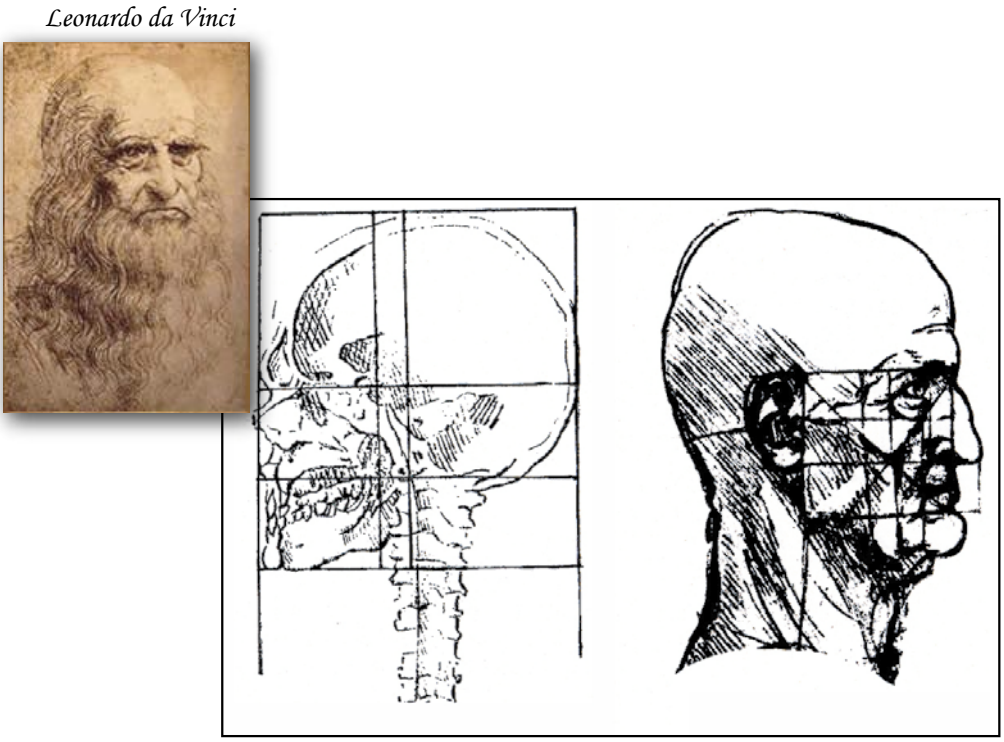

Figura 2.12. Esquemas de Leonardo como ejemplo de la búsqueda de la búsqueda de armonía natura en la cabeza humana. Modificado de Rabey (1968).

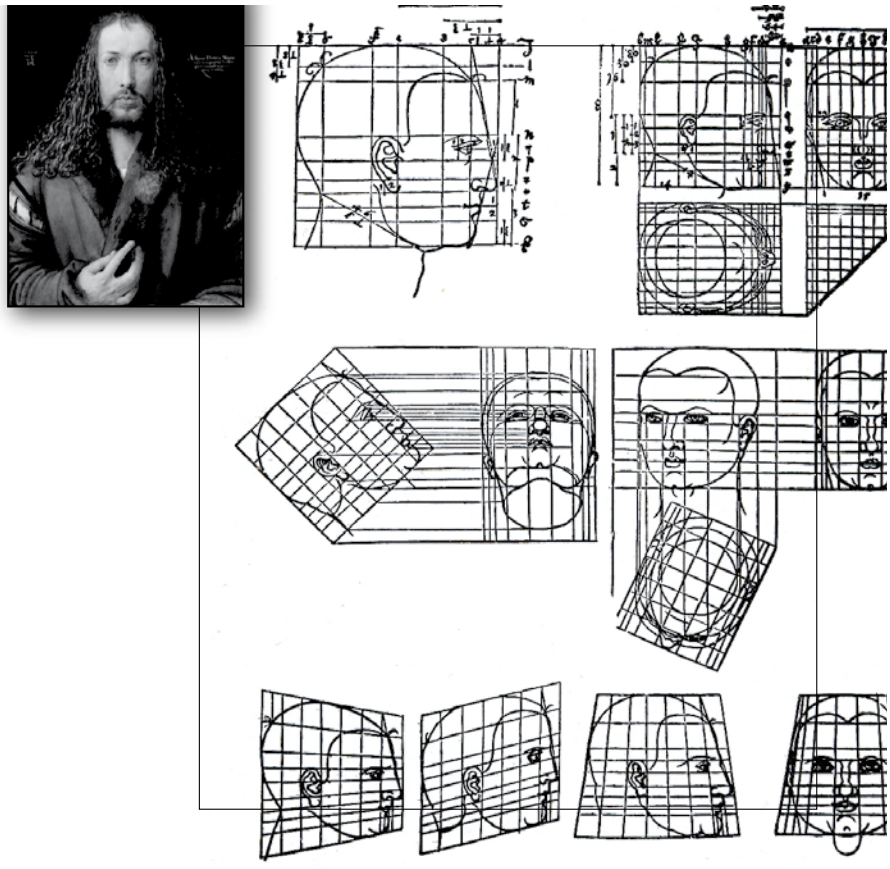

Figura 2.13. Esquemas del sistema de coordenadas de Alberto Durero (1528). La malla conecta partes anatómicas, para algunos, la puerta al trabajo de D'Arcy Thompson y aun mundo totalmente nuevo para la morfología. La diferencia esencial con las coordenadas cartesianas; Durero utiliza líneas para unir distintas perspectivas pero las mallas carecen de una referencia de base, mientras que el sistema cartesiano parte de una base (y una malla uniforme), y la transformación se entiende desde la referencia. Es el paso clave para tornar el método en un sistema analítico. Modificado de Rabey (1968).

proyecciones de la geometría euclidiana al arte, y retomarán el interés en las proporciones humanas, haciendo de nuevo hincapié en la importancia de conseguir unos estándares anatómicos "verdaderos". Destacan de esta época grandes maestros como Leonardo da Vinci (1452-1519; Fig. 2.12) o Alberto Durero (1471-1528; Fig. 2.13) quienes además comenzarán a utilizar mallas como referencia de coordenadas. El uso de mallas alcanza su máxima expresión en el sistema de coordenadas Cartesiano (de *La Geometrie* de R. Descartes, en 1637), un sistema que consigue combinar el lenguaje matemático y el geométrico, permitiendo la expresión simbólica del algebra en figuras geométricas y viceversa.

Nacida del arte, la medición del cuerpo humano comenzará a utilizarse en medicina donde se empieza a desarrollar una analítica práctica para la diagnosis (p. ej. en la obstetricia, la ortodoncia, o la neurología). Despertado el interés científico por la materia, serán la anatomía comparada, sobre todo en el campo de la antropología, quienes se apropien de las técnicas cada vez más sofisticadas para capturar las diferencias taxonómicas con precisión, y comenzar a comprender las reglas de transformación morfológica.

El uso de de la morfometría ha tenido desde entonces un uso cada vez más amplio en biología, extendiéndose de los vertebrados a los de invertebrados, aunque teniendo un especial impacto en la craneología. Por ejemplo, el anatomista holandés Petrus Camper (1722-1789), trabajó en el desarrollo de sistemas de planos para comprender los cambios anatómicos que observaba en distintos grupos de vertebrados. Camper es conocido particularmente por proponer el *ángulo facial*, un ángulo con el que se podía relacionar la forma de la cara con la de la región frontal del cráneo y desde la relación discernir entre rasgos representativos de distintas etnias humanas. La propuesta más errática (y en la que confiarían siglos despues, y sin éxito, algunos sectores creyentes en las capacidades de la eugenesia) fue que el escalar del ángulo sirviera para asociar la forma del cráneo al grado psíquico de inteligencia (ver Gould, 1981).

Los datos métricos que se comenzaron a incluir a lo largo del s. XIX eran sobre algún rasgo fácilmente mesurable, y se incluían en la forma de una media representativa para ser, posteriormente, comparada con otros grupos taxonómicos (Bookstein, 1998). El impulso conceptual de la morfología analítica viene de D'Arcy Wentworth Thompson en su *On growth and form* (Thompson, 1942), y concretamente en su propuesta de la transformación de las coordenadas cartesianas (Fig. 2.14).

La deformación de las coordenadas, basada en la teoría matemática de las transformaciones, permite ver la diferencia objetiva entre dos formas: una malla cartesiana (ortogonal) delimita

aspectos de una forma que se usa como referencia y que se deformará tras transformarla a las coordenadas de otra (siempre y cuando el nivel de semejanza u homología sea lógico; Fig. 2.14). Para D'Arcy Thompson el morfólogo puede limitarse a estudiar la deformación de las coordenadas para entender el mecanismo que ha causado la transformación, y en principio, también cuantificar el cambio.

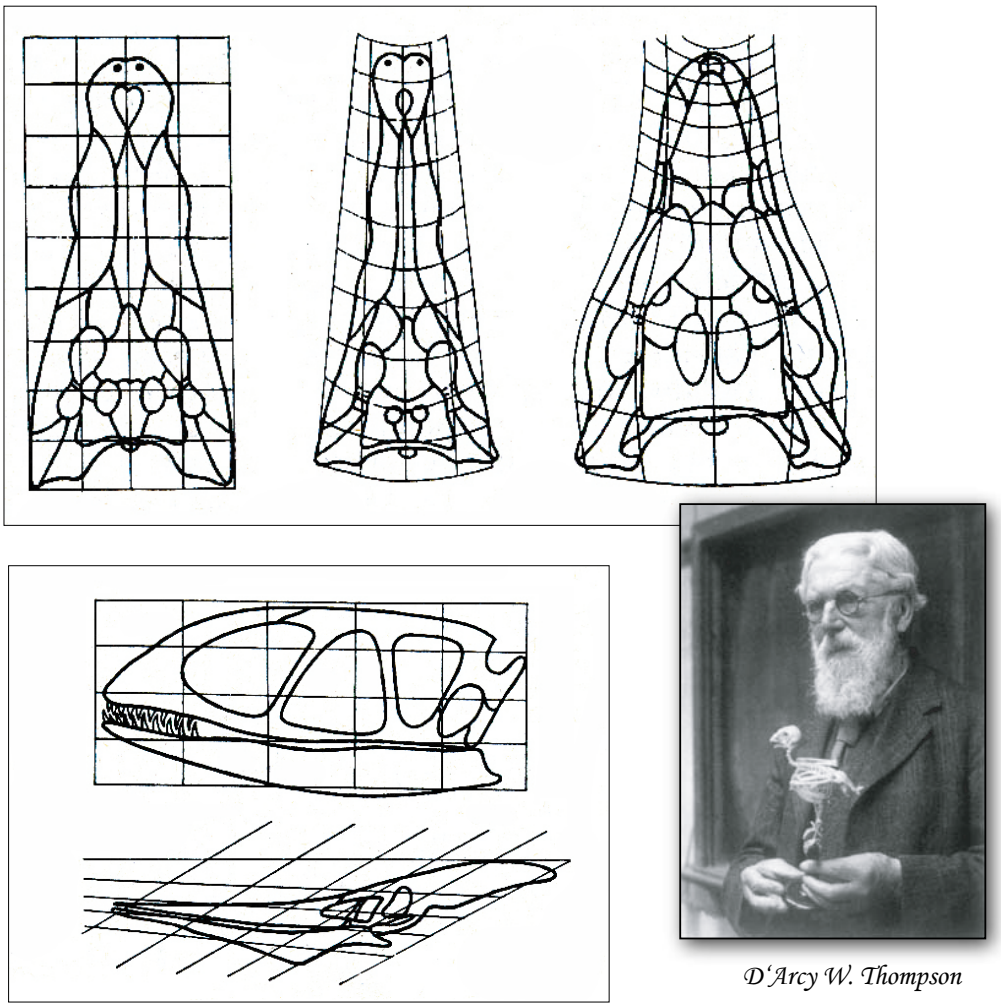

Figura 2.14. Esquema de las coordenadas cartesianas de D'Arcy Thompson (1942).(Arriba) La referencia es el ejemplar de la izquierda (*Crocodilus porosus*), y la malla no está deformada. En el centro la referencia se deforma a *C. americanus*, y en la derecha con *Notosuchus terrestris*. (Debajo) La referencia es el pterosaurio basal *Eudimorphodon* (Triásico), y la malla se deforma hacia el pterosaurio más derivado *Pteranodon* (Cretácico).

Thompson, a su vez, fue mentor de J. S. Huxley, probablemente uno de los biólogos más implicados en el desarrollo de un cuerpo de investigación en biometría, y un protagonista emblemático del Neodarwinismo naciente en el primer tercio del s. XX. Gran parte de su obra, estimulada por los trabajos de su mentor, estaba dedicada casi enteramente al estudio cuantitativo y analítico de la forma orgánica (ver, p. ej. *Problems of relative growth*; Huxley,

1932). La diferencia objetiva entre ambos autores radica en la consideración de los escalares utilizados para el análisis. Mientras que las coordenadas de Thompson perseguían abarcar toda la forma, Huxley se centrará en la variación de las partes desde mediciones singulares (especialmente longitudes).

El análisis cuantitativo de la forma orgánica del s. XX pierde el hilo de la propuesta de D'Arcy Thompson para seguir las pautas de Huxley marcadas para el estudio de la alometría (crecimiento diferencial de las partes), pues éstas se amoldaban a las nociones evolutivas Darvinistas y Mendelistas de la época (que, por otra parte Thompson rechazaba). En materia estadística se consigue en ese siglo un mayor rigor matemático pues es también un momento de auge en el desarrollo de la matemática estadística. Se desarrollan metodologías complejas como el cálculo de los coeficientes de variación y correlación, el análisis de la varianza o de métodos más sofisticados multivariantes como el análisis de componentes principales (ver revisión del tema y autores en, Adams et al., 2004).

A partir de la segunda mitad de siglo XX nacerán dos metodologías. Una, la morfometría geométrica, quién intentando retomar la doctrina holística de Thompson revolucionará la aplicación del método (Rohlf y Marcus, 1993), consiguiendo combinar la transformación geometría y la estadística del cambio de forma, y mostrándolas a través de un potente motor visual. Otra, la morfología teórica, disciplina que se pondrá a la vanguardia del estudio de la transformación morfológica (Rasskin-Gutman, 1995; Eble, 2000), en la búsqueda de sus procesos y sus leyes siguiendo la estrategia singular de simular la forma desde la concepción del morfoespacio.

2.2.2 Morfología Teórica

2.2.2.i La disciplina

La morfología teórica es una metodología relativamente joven, y es más una herramienta conceptual que una técnica que debamos desglosar exhaustivamente para comprender sus objetivos y su manera de proceder. De hecho, es en su sencillez y su carencia de subterfugios matemáticos de donde parten su elegancia y su eficacia. Conceptualmente la morfología teórica se ocupa de ofrecer un modo de operar para el estudio de la morfología desde la modelización de un aspecto morfológico a través del morfoespacio (Rasskin-Gutman, 1995). Desde él, el objetivo es analizar la naturaleza de las restricciones impuestas por las propiedades de los modelos que generan, y a su vez, estudiar la lógica de las transformaciones proyectada sobre los aspectos de la ontogenia, la filogenia y la función. Igualmente, McGhee

(1999) resume estos objetivos conceptuales en una práctica; 1) simular matemáticamente la morfogénesis orgánica, y 2) explorar el posible rango de variabilidad morfológica que la naturaleza es capaz de construir (ver también; Raup y Michelson, 1965; Reif y Weischampel, 1991; Hickman, 1993).

Por tanto, la morfología teórica nace del interés en hallar leyes que describan y expliquen la generación de la forma orgánica (Rasskin-Gutman, 1995). En esencia, la meta es revelar principios geométricos comunes en lo que en principio puedan parecer morfologías completamente divergentes. Analizar el posible espectro de la forma orgánica a través de la construcción de un morfoespacio hipotético, es para McGhee (op. cit.), la mayor contribución de la morfología teórica al estudio de la evolución.

La línea que separa la morfología teórica de la morfometría (*s.l.*) puede parecer bastante fina pues ambas escuelas son principalmente matemáticas y hacen un uso extensivo de ordenadores. Sin embargo sus objetivos son fundamentalmente distintos; la morfología teórica está únicamente interesada en la simulación y no en la cuantificación exhaustiva de la forma orgánica a la que se encomienda la morfometría. Para McGhee (op. cit.):

-Theoretical morphology is concerned with a minimum number of parameters, or with the simulation of the morphogenetic process itself that produced the form under study, and is not concerned with the production of a precise mathematical characterization or picture of any given existent form.

Así, la creación y el examen de las formas no existentes es clave desde el punto de vista de la morfología teórica, quién además, persigue la construcción de morfoespacios, también comunes con la morfometría, pero basa su construcción en la simulación de los parámetros elegidos y no desde medidas empíricas. De esta segunda aserción parte la distinción práctica entre el morfoespacio teórico, terreno de la morfología teórica, y el morfoespacio empírico de la morfometría.

2.2.2ii. Morfoespacio

El concepto de morfoespacio teórico parte de la formulación del *Paisaje Adaptativo* de S. Wright (1932; Fig. 2.15): la abstracción de todas las posibles combinaciones de genes de un organismo en un espacio multidimensional que contendrá, además, todas las combinaciones posibles de genes ausentes en el organismo. El marco de este hiperespacio englobará todas las combinaciones de genes (y fenotipos) posibles permitiendo plantearse desde el, por qué

algunas si existen frente a otras que, aun siendo matemáticamente predecibles, no se han producido en la naturaleza. Wright (op. cit.) atribuiría la distribution sobre su espacio a la deriva génica principalmente, y la adecuación (*fitness*) vía la selección natural explicaría los sesgos en la distribución (no aleatoria).

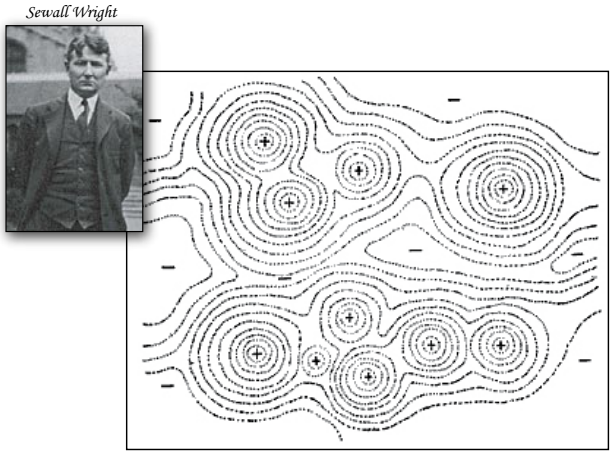

Figura 2.15. Paisaje adapatativo de S. Wright (1932). En el paisaje de combinaciones génicas, símbolos positivos son los "picos" adaptativos, y los negativos los "valles". Los contornos simbolizan el fitness adaptativo.

Un morfoespacio teórico es el equivalente fenotípico del paisaje adaptativo, y representa una contrapartida formal a un esquema basado exclusivamente en la reducción del organismo a su genotipo como agente susceptible de evolucionar. Una de las criticas al paisaje de Wright era que su abstracción dejaba de lado a la morfología. El paleontólogo G. G. Simpson (1944) construyó una primera versión del paisaje adaptativo en un espacio fenotípico donde los ejes eran ya caracteres. Su "espacio fenotípico" le serviría para explicar su hipótesis de evolución cuántica. Raup y Michelson (1965) sentarán las bases conceptuales de la morfología teórica moderna (y su nombre), así como la identidad del morfoespacio teórico despues de la publicación de sus simulaciones por ordenador del enrollamiento de conchas (ver orígenes en Raup, 1962, 1969; Fig. 2.16).

Un morfoespacio teórico puede definirse como un hiperespacio geométrico *n*-dimensional producido por la variación sistemática de los parámetros de un modelo geométrico de la forma (McGhee, 1999). En su formulación original (Raup y Michelson, 1965), al igual que el paisaje adaptativo, el morfoespacio teórico tiene la habilidad de mostrar los picos y los valles adaptativos a partir de las formas existentes y no existentes.

Una diferencia que debemos resaltar son las diferencias entre las nociones y aplicaciones de un morfoespacio teórico y un morfoespacio empírico. El morfoespacio empírico, a diferencia del teórico, está basado en datos reales, por lo que en realidad representa un subconjunto de las posibilidades expresadas por el teórico. Su generación generalmente deriva del análisis de datos desde la estadística multivariante, por lo que se ha convertido en patrimonio de la morfometría.

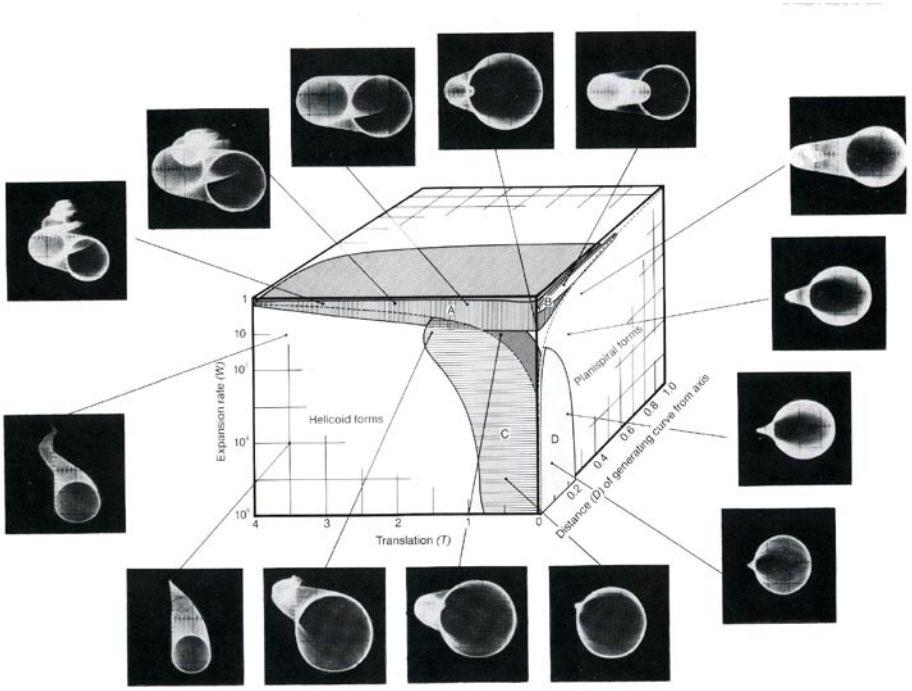

Fig. 2.16. Distribución de formas (empíricas) en el morfoespacio de Raup (1969). Las regiones marcadas son; A. gasterópodos, B. cefalópodos enrollados, C. bivalvos, D. braquiópodos. Extraído de Raup y Stanley (1978).

Una diferencia que deriva de su propia definición es que el morfoespacio empírico es totalmente dependiente de la muestra, tanto en número de ejemplares, como de variables medidas en los organismos. Generalmente (aunque no siempre) un morfoespacio empírico suele derivarse de la descomposición *n*-dimensional de la variación mediante métodos de ordenación (p. ej. un PCA). Estos métodos son sensibles a los *outliers* (datos extremos), por lo que las dimensiones del espacio vendrán definidas (y estarán ordenadas) por estos con respecto a su desviación de la media (ponderada). Sin embargo, los extremos son formas naturales, por lo que en términos macroevolutivos (escala a la que es más posible detectarlos) son también informativos. Siempre habrá que tener en cuenta por qué los extremos son morfológicamente extremos, y cual es su efecto en la construcción del morfoespacio. Si la distribución que tengan las formas reales en el espacio de ordenación (morfoespacio empírico) no se ve afectada especialmente por esos extremos, entonces tendrá un sentido morfológico y podrá ser interpretada. De hecho, desde su construcción podemos saber qué variables intervienen en cada una de las dimensiones, por lo que el morfoespacio empírico podrá mostrar formas posibles que puedan o hayan podido existir aún cuando su construcción dependa de los datos que lo producen.

Una propuesta práctica que se sugiere para la aplicación de morfoespacios, sin embargo, es la utilización simultánea de ambos tipos, bien combinada, o bien simultánea (viz. generar un morfoespacio híbrido). Del mismo modo, es posible hacer una lectura casi equivalente

de un morfoespacio empírico a la de uno teórico, siempre y cuando se tengan en cuenta sus posibles limitaciones del primero; *-"Empirical morphology", in turn, remains necessary for the proper quantification of temporal patterns of disparity...* (Eble, 2000).

La disparidad es un atributo de la distribución de formas en un morfoespacio. La evaluación de la integración morfológica sobre un morfoespacio, sin embargo, es más descriptiva que analítica, en tanto y en cuanto no existe una medida *ad hoc* de la covariación. La evaluación de la integración se extrae de la identidad de las nubes de puntos (la distribución no aleatoria de los taxa) dentro del morfoespacio, siguiendo una pauta descriptiva y tipológica (siguiendo un criterio más acorde con la noción de unidad taxonómica, ver; Alberch, 1989), que parta de una hipótesis elaborada previamente.

Por ejemplo, desde la formulación de un morfoespacio para analizar una morfología se espera encontrar un código geométrico que engarce con una hipótesis de identidad taxonómica (o, tipológica). Si ésta se encuentra, es decir, si de todas las posibilidades de organización propuestas en teoría se dan sólo unas y en una región concreta de la distribución, la identidad del taxón se justifica desde la integración. Si hay integración, ésta se reflejará en una distribución concreta susceptible de predecirse desde *leyes* geométricas (p. ej. fórmulas) que predigan esa posición.

En el primer estudio que se detalla en la parte tercera de la presente tesis se construye un morfoespacio teórico basado en una métrica proporcional del cráneo. El morfoespacio teórico se basa en el uso de un diagrama triangular desde el que se plantea el número *n* de combinaciones teóricamente posibles de las proporciones del rostro, la órbita ocular y la caja craneana en arcosaurios. Las proporciones teóricas se contrastan con las proporciones reales de los cráneos en distintos grupos de arcosaurios, fósiles y actuales.

Posteriormente, los trabajos que se realizan se basan enteramente en la aplicación de la morfometría geométrica, aunque haciendo una traducción literal del espacio de forma en morfoespacios, que basados en a superposición de landmarks Procrusteana, son todos de naturaleza empírica.

2.2.3 Morfometría geométrica

La morfometría es una herramienta diseñada para extraer información sobre la forma y su desarrollo (Huxley, 1932; Roth y Mercer, 2000). Operativamente, la morfometría es el estudio de la variación de la forma (del inglés *shape*), y su covariación con otras variables (Bookstein, 1991; Dryden y Mardia, 1999).

Como adelantábamos anteriormente, la morfometría se desarrolla desde la aplicación de análisis estadísticos multivariantes a conjuntos de medidas como por ejemplo, altura, longitud o anchura. Entre las décadas de los ochenta y noventa del s. XX se da un giro hacia un nuevo paradigma desde el que analizar la forma (Rohlf, 2002). Nace una morfometría capaz de capturar la geometría de la forma, y capaz de incluirla y mantenerla en todos los pasos estadísticos de los análisis estadísticos. El origen de la metodología nace motivado por las mallas deformadas de Thompson (1942; Fig. 2.14). El desarrollo de sus nuevas propiedades, capaces de capturar la forma, hace que esta nueva morfometría sea tildada de *geométrica*. Su recepción fue acogida como una "revolución" para el mundo del análisis morfológico (Rohlf y Marcus, 1993).

A diferencia de la morfología teórica, la morfometría geométrica se basa en una matemática relativamente compleja (está basada enteramente en el álgebra matricial), y aunque sus objetivos y su manera de proceder son intuitivos (es una herramienta muy visual), es necesario esclarecer sus bases fundamentales, aunque por limitaciones del texto nos veamos a hacerlo de manera sucinta. De hecho, en la última década se han sucedido grandes e importantes avances en el desarrollo de esta materia, avances que han conseguido generalizar sus estándares conceptuales y prácticos. Sugerimos, Bookstein (1991) como lectura sobre su base histórica y el desarrollo de las técnicas, y Goodall (1991) en particular para la metodología Procrustes. Marcus et al. (1996) y Zelditch et al. (2004) son muy interesantes como material introductorio desarrollado *in extenso*, así como para ver el amplio espectro de posibles aplicaciones. Dryden y Mardia (1999) realizan una síntesis detallada de la estadística aplicable al estudio de la forma, y Small (1996) da un estudio detallado de la noción y tipos de espacios de forma. Todas estas citas resumen las referencias bibliográficas más importantes disponibles hasta la fecha. A continuación detallamos los antecedentes más inmediatos que permitan al lector familiarizarse con, y hacer una lectura práctica de, los resultados obtenidos en la tesis desde la aplicación metodología.

2.2.3.i. Morfometría tradicional y morfometría geométrica

Tras el advenimiento de la morfometría geométrica, la morfometría basada en longitudes, proporciones o ángulos pasa a ser una "morfometría multivariante" o "tradicional" (ver también; Marcus, 1990). Ambas se diferencian en aspectos, que por otra parte, son fundamentales. La clave que diferencia las dos aproximaciones es la capacidad de la morfometría geométrica, como su nombre indica, de capturar la geometría de la forma e incorporarla en los análisis, de mantenerla, y de permitir visualizarla en todo momento

desde cualquier operación que se realice.

Los métodos morfométricos tradicionales están basados en la aplicación de análisis multivariantes sobre colecciones de medidas, generalmente distancias longitudinales, proporciones, o ángulos. Las medidas serán repetibles pero no están exentas de cierta arbitrariedad (muchas veces pueden no estar fundamentadas en algún criterio de homología). Al mismo tiempo, las medidas tradicionales sólo capturan una parte de la información, pues no registran de ninguna manera la relación espacial entre las medidas.

Por ejemplo, supongamos que queremos medir la anchura y la altura de dos vasos con un diseño particular, uno cuadrado y de otro que sea más rectangular (Fig. 2.17a). Teniendo en cuenta que comparamos vasos se pueden comparar las medidas sin atender a sus formas. Sin embargo, perderemos la identidad geométrica de cada uno de los vasos, redonda o cuadrada, ya que éstas no contienen ninguna información a este respecto (Fig. 2.17b). Por otra parte, la altura y la anchura son obvias, pero al medir, cada investigador podrá situar el calibre según decida, siempre que lo haga entre dos puntos uno en la base y otro en el extremo superior o en alguna región del vaso que capture su diámetro máximo. Sin embargo, medir altura no indica dónde tiene que ponerse exactamente el calibre para medir esa longitud. La morfometría geométrica surgió como una metodología que supliera estas dos carencias esenciales para el estudio de la morfología.

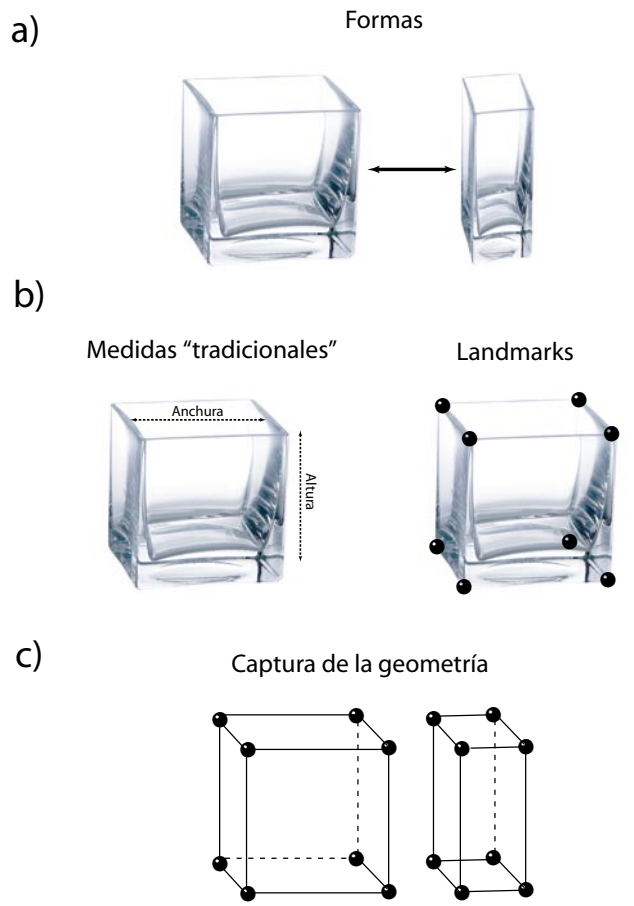

Figura 2.17. Ejemplo para mostrar las diferencias entre la morfometría tradicional y la geométrica desde la forma de dos vasos de vidrio.

Por definición, la morfometría geométrica comprende un conjunto de métodos desarrollados para la adquisición, el procesado, y el análisis de variables de forma que retienen toda la información geométrica contenida en los datos (Slice, 2005). Siguiendo con el sencillo

ejemplo anterior, la morfometría geométrica es capaz de capturar la altura y la anchura de los vasos a la vez que la forma geométrica de ambos vasos. La forma se captura registrando los vértices de cada vaso (p=8 en total, cuatro en la apertura del vaso y cuatro en la base; Fig. 2.17c), asignando con unas coordenadas (x, y, z, por tratarse de una forma tridimensional) a cada uno de ellos. Esas coordenadas son los *landmarks*, y los análisis tendrán en cuenta (de hecho, se basarán en ellos) y mantendrán siempre las relaciones espaciales entre esas coordenadas que capturan la geometría de los vasos del ejemplo.

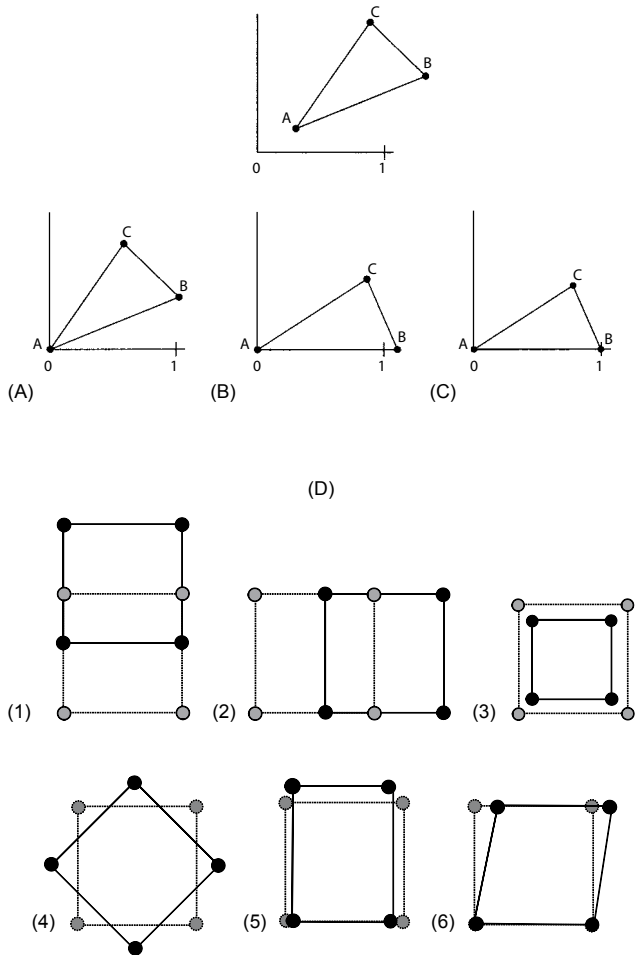

Figura 2.18. Operaciones afines que no alteran la forma geométrica, A) traslación, B) rotación, y C) re-escalado. Otra forma de representarlo todas las transformaciones afines, es; (1) y (2) traslación, (3) escalado, (4) rotación, (5) y (6) componente uniforme. Todos los ejemplos de Zelditch et al. (2004).

La morfometría geométrica, en definitiva, lleva consigo una nueva definición de forma (del inglés, *shape*, difícil de traducir en español, puede ser figura o configuración) y de tamaño. Utilizaremos la letra cursiva al referirnos a *shape* en el contexto de la morfometría geométrica. Así, la *forma* será un aspecto de la configuración de landmarks que no se corresponda, ni con el tamaño o escala (*size*), ni con la *posición* de la configuración, ni con la *orientación* (todos ellos factores afines que no afectan en realidad a la forma; Fig. 2.18). Su definición es matemática (geométrica concretamente. Así mismo, existe una estimación particular del tamaño, el *Centroid Size* o "Tamaño del centroide", que se extrae de la propia configuración de landmarks. Este tamaño es en realidad la *escala* de la configuración, y corresponde a la raíz cuadrada de la suma de todas las distancias al cuadrado entre todos los landmarks de la configuración (Bookstein, 1991)

Las medidas longitudinales tradicionales tienden a estar siempre correlacionadas con el

tamaño, y aunque se han desarrollado muchos métodos para evitar esta inconveniencia, nunca se ha alcanzado una congruencia entre los resultados obtenidos desde cada uno (Adams et al., 2004). Un segundo formalismo de la morfometría geométrica que también la separa de la tradicional, y solventa su limitación, es que el tamaño del centroide (*centroid size*), será ortogonal a la forma salvo en el caso de la alometría. Esto permitirá, además, analizar la alometría de una forma particular, sentando unas bases nunca antes realizadas (ver más adelante la exclusión del tamaño de la forma).

Así mismo, los métodos tradicionales a la hora de exponer los resultados sólo permiten visualizar las relaciones estadísticas de las variables numéricamente o a partir de gráficos de dispersión. La morfometría geométrica añade a su operatividad analítica un potente motor visual, el cual permite representar las estimaciones realizadas como una expresión directa de la geometría de las formas en estudio (se podría ver directamente la diferencia geométrica entre los vasos del ejemplo anterior; Fig. 2.17).

2.2.3.ii Landmarks

La morfometría geométrica nace estimulada por el reto conceptual de D'Arcy Thompson (1942) en el que se propone comparar morfologías desde el punto de vista de la transformación geométrica. Los investigadores que intentaron aplicar la propuesta a problemas biológicos reales encontraron, en cambio, que la propuesta primigenia era "impracticable" por carecer de una referencia empírica y singular que marcase cada una de las estructuras que hacían deformarse a la malla (Bonner, 1980). Los landmarks representan un paso crucial para solventar esa necesidad, y serán la clave que permita rastrear la diferencia de forma (Bookstein, 1991, 1996).

Cada landmark representa la localización singular de una estructura en la forma en estudio, y el registro de varios landmarks sobre varias estructuras representa una configuración de coordenadas de la geometría global (Fig.2.19). Cada estructura se registra en términos de coordenadas cartesianas (por tanto, con respecto a unos ejes de coordenadas en 2D, x, e y, o en 3D añadiendo una coordenada adicional z). Los landmarks registrarán numéricamente las coordenadas que capturen la suficiente información (más homogéneamente) sobre la geometría de la forma de interés. Los landmarks tienen que ser "homólogos" en algún sentido para asegurar su repetición en toda la muestra. Para nuestros intereses, la homología ha de ser biológica.

El primer paso es localizar los landmarks en la forma y describirlos anatómicamente,

comprobar si pueden repetirse en toda la muestra, y asignarles un número que será su seña de identidad geométrica de homología (p. ej. el landmark 1 localizará siempre la misma estructura –y siempre será el 1, en todas las formas que se comparen).

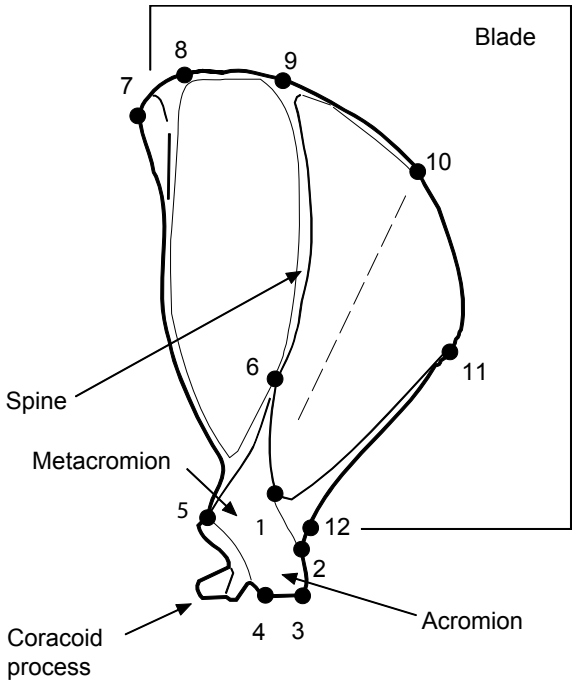

Figura 2.19. Distintos tipos de landmarks capturando los rasgos distintivos más característicos de una escápula de ardilla. Original de Zeldtich et al. (2004).

Así mismo, los landmarks pueden diferir en la calidad de la información que codifican. Bookstein (1991) define tres tipos de landmarks; tipo I, serán aquellos que se registren en la yuxtaposición exacta de tejidos, como puede ser por ejemplo, el punto localizable entre la intersección de suturas. Tipo II serán aquellos que, por ejemplo, se localicen en una región de máxima curvatura y que, a su vez, estén asociados a una estructura local reconocible anatómicamente, mientras que los tipo III son generalmente considerados deficientes pues corresponderán a puntos extremos, como por ejemplo, el extremo distal de una estructura. Su deficiencia radica en que contienen información útil solo con respecto a una distancia remota con la estructura (Fig. 2.19), aunque esta definición es en cierto modo ambigua.

Una definición alternativa y quizá menos restrictiva es la de Marcus et al., (1996). Los landmark tipo I serán aquellos cuya equivalencia de espécimen a espécimen esté fundamentada por la mayor evidencia local, por ejemplo, el encuentro entre estructuras (valdría el ejemplo de suturas). Tipo II serán landmarks que sean repetibles y equivalentes atendiendo a una evidencia geométrica, como por ejemplo, el extremo de la prominencia de un hueso. La propuesta es que, además, se pueden hacer híbridos entre los dos tipos. Un tipo III sería un landmark inválido que no cumpliese alguna de estas dos normas, como por ejemplo un landmark de contorno (imagínese un landmark entre el 9 y el 10 de la figura 2.19). Lo importante en cualquiera de las dos definiciones es que cada landmark lleve asociada a una definición anatómica concreta.

Ya hemos adelantado que el análisis morfológico exige que el criterio de homología para

definir cada landmark sea biológico. En un sentido evolutivo, por tanto, un landmark será un punto de correspondencia coincidente en cada individuo de una muestra entre y dentro de una población (Zelditch et al., 2004). En esta memoria los landmarks se utilizan en un contexto macroevolutivo, donde la homología es entendida como a la correspondencia de estructuras entre organismos de un mismo clado monofilético (Archosauria). Los landmarks que utilizamos localizan siempre en nuestra muestra zonas morfológicamente homólogas e invariantes (véase Parte Tercera, capítulos 2, 3, y 4). Por ejemplo, forámenes de salidas o entradas de nervios, puntos estratégicos de frontera, bien entre distintas regiones definidas por criterios de identidad celular, o criterios topográficos (región facial, órbita, etc.).

La captura de landmarks tiene que realizarse mediante un soporte digital. Para operar en dos dimensiones se suele trabajar sobre fotografías, mientras que en tres dimensiones se puede trabajar desde imágenes (p. ej. de escáners CT o láser), o bien capturando las coordenadas directamente sobre el cráneo (p. ej. con un Microscribe). El trabajo que presentamos se ha realizado en dos dimensiones pues la mayoría de las herramientas estadísticas de la morfometría geométrica están desarrolladas para trabajar en estas dimensiones. La manera más ágil y económica de realizar las fotografías de los individuos de la muestra es con una cámara digital, y la captura de las coordenadas, de los landmarks se realiza a través de programas informáticos (p. ej. el más extendido es TPSdig, aunque existen muchas otras posibilidades). En nuestro caso todos los estudios se han realizado en dos dimensiones utilizando una cámara digital y siguiendo un protocolo estricto de su ajuste, distancia y localización del objeto frente al objetivo, para evitar sobre todo cualquier efecto de deformación que pudiera ejercer la lente sobre la forma del cráneo (ver, Marugán-Lobón y Buscalioni, 2004; Zelditch et al., 2004).

2.2.3.iii Métodos de Superposición de configuraciones de landmarks

-There are three elements in the Procrustes story, the unfortunate traveller, who we might label X_1, The Procrustean bed X_2, and the treatment, T, meted out of ranking, hammering, or amputation., J. C. Gower and G. B. Dijksterhuis; Procrustes Problems (2004)

La morfometría geométrica que utilizamos en el presente estudio se centra en la superposición de configuraciones de landmarks siguiendo los procedimientos Procrustes, basada en el criterio de superposición de mínimos cuadrados (Gower, 1975). Los datos con los que contamos en la tesis son en dos dimensiones, por lo que resumimos los conceptos de este tipo de superposición centrándonos únicamente en su vertiente bidimensional. La matemática de las metodologías en tres dimensiones es muy similar a excepción de las

Coordenadas de Forma de Bookstein, que difieren sustancialmente (Bookstein, 1991). Para comprobar las diferencias y algunos ejemplos de los procedimientos Procrustes en tres dimensiones ver por ejemplo, Gunz (2005).

Existen otras metodologías morfométricas como los análisis de contornos, los elementos finitos, o las distancia entre landmarks (EDMA; Lele y Richtsmeier, 1991). Cualquiera de estas metodologías es útil para el estudio de la forma, ya que su realización puede suplementar las carencias o limitaciones de las otras, siempre dependiendo del contexto comparativo en el que se apliquen. Este es el caso, por ejemplo, del análisis resistente (Resistant Fit Theta Rho Análisis, o RFTRA; Siegel y Benson, 1982), un método procrusteano que explicaremos más adelante y que aplicaremos (en su versión generalizada; Rohlf y Slice, 1990; GRF) por sus habilidades para detectar cambios localizados, cuestión que también detallaremos más adelante.

A excepción de la superposición Procrustes basada en mínimos cuadrados ninguna técnica ha sido considerada dentro del denominado *consenso morfométrico* de Bookstein (1996b). Esto implica que ninguna de ellas está basada en la "teoría de la forma" explorada por Kendall (1977), un geómetra que persiguiendo dar una definición del Espacio de Forma ha conseguido justificar, desde sus axiomas, una noción de distancia y de forma particulares (ver, BOX 4). Estar fuera de la teoría no es un problema a la hora de utilizar el método analítico distinto al ajuste por mínimos cuadrados para comparar configuraciones de landmarks (formas). La ventaja de trabajar basándose en la propuesta axiomática de Kendall, en cambio, justifica un rigor matemático necesario para aplicar modelos de estadística multivariante (Bookstein, 1996a; Rohlf, 1999; Rohlf, 2000).

Una vez digitalizados los landmarks, los datos quedan registrados como coordenadas en una matriz, y se procede a superponerlos para minimizar la distancia entre cada landmark homólogo de cada una de las configuraciones. Esto se realiza en la superposición Procrustes trasladando, rotando y escalando las configuraciones, lo que retira el "efecto" de estas transformaciones afines (o uniformes), convirtiendo las antiguas coordenadas en otras nuevas. Estas nuevas coordenadas quedarán dentro del espacio de forma (Rohlf, 1995), y las distancias que separen a los landmarks homólogos serán las diferencias entre las formas comparadas. Así, lo que en realidad se hace con estos tres movimientos matriciales es minimizar la distancia entre landmarks geométricamente homólogos retirando tres factores que en realidad no afectan a la forma (p. ej. rotar una figura no cambia su forma, al igual que trasladarla, o escalarla homogéneamente). La resultante son unas nuevas variables que

serán invariantes a estos tres factores.

Existen tres formas de realizar este movimiento analítico desde el álgebra matricial; mediante Coordenadas de Forma que citábamos recientemente (*Bookstein*-Shape Coordinates; Bookstein, 1991), el Ajuste Resistente (RFTRA; Benson et al., 1982; Siegel y Benson, 1982) y el ajuste por Mínimos Cuadrados (LS, de Least Squares; Gower, 1975). Los dos últimos, en realidad, se aplican desde su versión generalizada (*G*), lo que permite la comparación entre más de dos formas frente a una referencia, que será la mediana de la muestra para el *G*-RFTRA (Rohlf y Slice, 1990), y la media para el *G*-LS (Gower, 1975). Los mínimos cuadrados a los que se refiere el método son distintos a los utilizados en estadística convencional, por lo que el G-LS ha pasado a reconocerse más generalmente como el Análisis Procrustes General, o GPA (*General Procrustes Análisis*; Gower, op. cit.).

2.2.3.iii.a. Coordenadas de Forma

Aunque exploradas primero por Galton (1907) para comparar perfiles humanos la primera década del s. XX, la formalización de las Coordenadas de Forma vendrá de la mano de F. L. Bookstein en la década de los noventa (el método también se conoce como de Registro en Dos Puntos; Bookstein, 1991). Este método ya no está tan extendido como en sus inicios, pero claramente representa el método más intuitivo para demostrar el concepto de superposición de coordenadas (Fig. 2.18). Aunque en este estudio hemos realizado varias comparaciones utilizando esta técnica de superposición, no mostramos sus resultados. Únicamente la explicamos como una manera de aproximarse al concepto de superposición de configuraciones de landmarks.

Las configuraciones de coordenadas de landmarks que representan las geometrías de las formas estudiadas se superponen trasladándolas, rotándolas y escalándolas dos coordenadas fijas (0,0) y (0,1). Estas coordenadas representan los extremos de una línea fija horizontal entre dos landmarks (llamada *línea base*), donde la elección de los landmarks que se fijarán en estas coordenadas depende del criterio experimentador. Los residuos que queden (la distancia entre cada landmark homólogo de cada configuración) serán los datos de *forma* (el residuo es la diferencia de coordenadas entre landmarks geométricamente homólogos entre configuraciones que resta de trasladar, rotar y escalar las configuraciones a la línea base).

Un problema que tiene esta técnica es que al fijar dos puntos de la configuración la variación que éstos contienen se anula por completo (los landmarks elegidos pierden toda su variación pues se localizan todos en la misma coordenada), pero sin embargo, su variación no desaparece. Por el contrario, lo que ocurre es que su variación (varianza en términos

estadísticos) se traslada a los demás puntos. Si la elección de la línea base no ha sido correcta, la variación (varianza) que se capture entre los demás landmarks puede ser errónea, es decir, la variación que observemos en otros landmarks puede no ser únicamente suya, sino que contenga también la de las estructuras representadas por los landmarks fijados.

Aunque la elección de los landmarks a fijar debería realizarse atendiendo a un criterio biológico (quizá arbitrario), la recomendación práctica es que se escojan puntos más extremos de la configuración, pues dicha elección hará que la varianza se reparta más homogéneamente entre todos los puntos de la configuración. No obstante, esta manera de elegir la línea base es intuitiva, y no existe un criterio consensuado sobre como realizar la elección de la línea base.

2.2.3.iii.b. Superposición Procrustes

En vez de utilizar solo dos landmarks como registro para superponer los landmarks, las superoposiciones Procrustes utilizan toda la configuración. Cuando la superposición Procrustes se realiza por el método de Mínimos Cuadrados, la distinción clave es que el criterio utilizado para minimizar las diferencias entre las configuraciones de landmarks es lo que actualmente se conoce como *Distancia Procrustes*. Basándose en mínimos cuadrados para estimar los parámetros para la localización, orientación y escalado, el método minimiza la suma de distancias cuadradas entre los puntos correspondientes de las configuraciones (Gower, 1975; Slice, 2005). El método se denomina GPA (de General Procrustes Analysis), lo que hace que se excluya al Ajuste Resistente de los métodos Procrustes como se venía haciendo hasta aproximadamente los años 90 (ver más adelante). Veamos por qué:

Los pasos que se realizan para la superposición para una muestra de *N* individuos se resumen en: 1) Centrar cada configuración de landmarks en el origen restando las coordenadas de su centroide de las coordenadas (X, e Y, en 0,0; también puede hacerse en 3D) de cada landmark de la configuración. Los landmarks reflejarán su desviación del centroide. 2) Escalar las configuraciones de landmarks a la unidad (Tamaño del Centroide, CS=1), dividiendo cada coordenada de cada landmark por el centroide de su configuración (escalado). 3) Elegir una configuración de referencia (por consenso, la primera de la muestra), y rotar la segunda para minimizar las distancias cuadradas sumadas entre landmarks homólogos (en todos) entre ambas (rotación). El álgebra matricial de estas operaciones puede verse en Rohlf (1990).

Cuando hay varias configuraciones la primera referencia es el primer individuo (podría ser cualquiera en realidad), pero después, se calcula la media que pasará, por *consenso*, a ser la referencia. Todas las configuraciones se rotan frente al consenso (la media) de nuevo, y la operación se repite tantas veces como sea necesario hasta que se consigan dos medias

iguales. La cantidad de cálculos matriciales que se realizan justifica por qué es muy útil realizar estos cómputos con ordenadores relativamente potentes. Actualmente este proceso, que conlleva un número elevado de operaciones con matrices (y muchos landmarks), se realiza en mucho menos de un segundo.

El método GPA es el aplicado en el conjunto de datos obtenidos para los cráneos de la tesis. En principio, GPA consigue evitar el problema de traslado y dispersión de la varianza que presenta el método de Coordenadas de forma de Bookstein. La excepción a la norma, no obstante, aparecerá cuando exista una región (uno o más landmarks) que cambien de manera localizada con respecto a los demás. GPA es muy sensible a este fenómeno estructural, y cuando ocurre, el efecto que tiene sobre el GPA es que en la superposición los mínimos cuadrados distribuirán la variación localizada entre los landmarks de la configuración, al igual que ocurría con las Coordenadas de forma, y por tanto, sesgará los datos.

La Superposición Generalizada de Ajuste Resistente (Generalised Resistant Fit superimposition, o *GRF*; Siegel y Benson, 1982) surgió como una objeción a esta sensibilidad del GPA sobre los cambios localizados, y por eso también lo hemos utilizado en algunas secciones experimentales de la tesis.

El método de GRF también minimiza la diferencia entre landmarks de distintas configuraciones, y por ello, se aunaba en la metodología Procrustes (ver. p. ej. Chapman, 1990), pero actualmente se excluye puesto que su criterio de optimización no utiliza la distancia Procrustes como criterio de optimización. Por el contrario, el método se basa, primero, en distancias, y segundo, en la iteración de medianas.

El método, por otra parte, es "resistente" a cambios localizados, cambios que en la jerga morfométrica se denominan *Efecto Pinocho*, haciendo alusión al crecimiento localizado de la nariz de este personaje de cuento (término propuesto por Ralph Chapman, de la universidad de Idaho, EE.UU.). En términos estadísticos, el GRF es robusto frente a los extremos que haya en los datos (*outliers*), lo que en la superposición se traduce en que el método es relativamente insensible a los cambios localizados. La robustez se debe a que en vez de la media, el método se basa en el uso de la mediana, un estadístico de tendencia central que por definición es insensible a valores extremos (es el estadístico equivalente al percentil 50).

La superposición en GRF no está basada en un método analítico, sino que la rotación, el escalado y la traslación se basan en métodos estrictamente numéricos, concretamente en distancias e iteración de medianas, no de medias. Sus pasos son; 1) para el escalado, se calcula una pareja de distancias entre landmarks de dos configuraciones y se calcula la proporción de cada una. Después, para cada landmark se calcula la mediana de las proporciones de

cada segmento que radie desde cada landmark, lo que da una proporción para cada uno. Finalmente se calcula la mediana de las medianas calculadas en el paso anterior, escalar que además servirá como el factor que se utiliza de escalado (todas las coordenadas de la segunda forma estarán escaladas a ese escalar. 2) El ángulo de rotación puede determinarse de la misma manera desde los segmentos utilizados en el paso (1). Primero se calculan los ángulos entre los segmentos, y los pasos sucesivos buscan la mediana de los ángulos asociados con cada landmark, y la mediana de las medianas. Al igual que en GPA, se reproduce un método iterativo que compute la referencia consenso y superponga todas las configuraciones a ella. Como apuntábamos, la principal ventaja del GRF frente al GPA es su efectividad para caracterizar cambios localizados (el efecto Pinocho), un aspecto de la variación que es posible encontrar, por ejemplo, si se comparan formas relativamente distintas como puede ser el caso de la alometría, o al comparar formas a escalas macroevolutivas. Sin embargo, la desventaja es que su criterio de superposición no se ajusta a la métrica de la distancia Procrustes, por lo que carece de un motor axiomático que sustente el uso de la estadística multivariante en sus datos (ver Box 4).

2.2.3.iv. La función de interpolación del Thin Plate Spline (TPS)

La aplicación de la función de suavizado o interpolación del Thin Plate Spline (TPS; Bookstein, 1989; 1991) fue propuesta como una manera de emular la elegancia visual de las deformaciones de mallas cartesianas propuesta por D'Arcy Thompson (1942; Fig. 2.14). Así, la función de interpolación del TPS se utiliza para describir cambios de forma por medio de deformaciones entre dos configuraciones de landmarks distintas (Fig. 2.20).

La función, tomada de Duchon (1976), es la solución fundamental para la ecuación biharmónica:

$$U(r)=r^2 \ln r$$

Dadas unas coordenadas, una combinación pesada de TPS centrados en cada coordenada da la función que pasa exactamente a través de cada puntos minimizando, a la vez la Energía de Doblado (*Bending Energy*, BE).

El nombre de TPS se refiere a una analogía física que implica el doblado de una malla muy fina de metal. La función se utiliza para calcular la deformación desde una forma referencia, "clavada" (virtualmente) en esa malla virtual, a una forma objetivo tal y como lo propuso Thompson (op. cit.). La función se traduce en la deformación de la malla desde la interpolación de la referencia al objetivo (Fig. 2.20). La BE, es equivalente a una *energía de*

deformación, y equivale en magnitud a la cantidad de "esfuerzo" que hay que realizar para deformar la malla de una forma a otra; si es entre landmarks distantes entre si, la energía será baja, mientras que si la distancia es pequeña, la energía será mucho mayor (ver también; Rohlf, 1993).

Un ejemplo para percibir lo que ocurre es imaginar que la malla es un trozo de tela. En ella

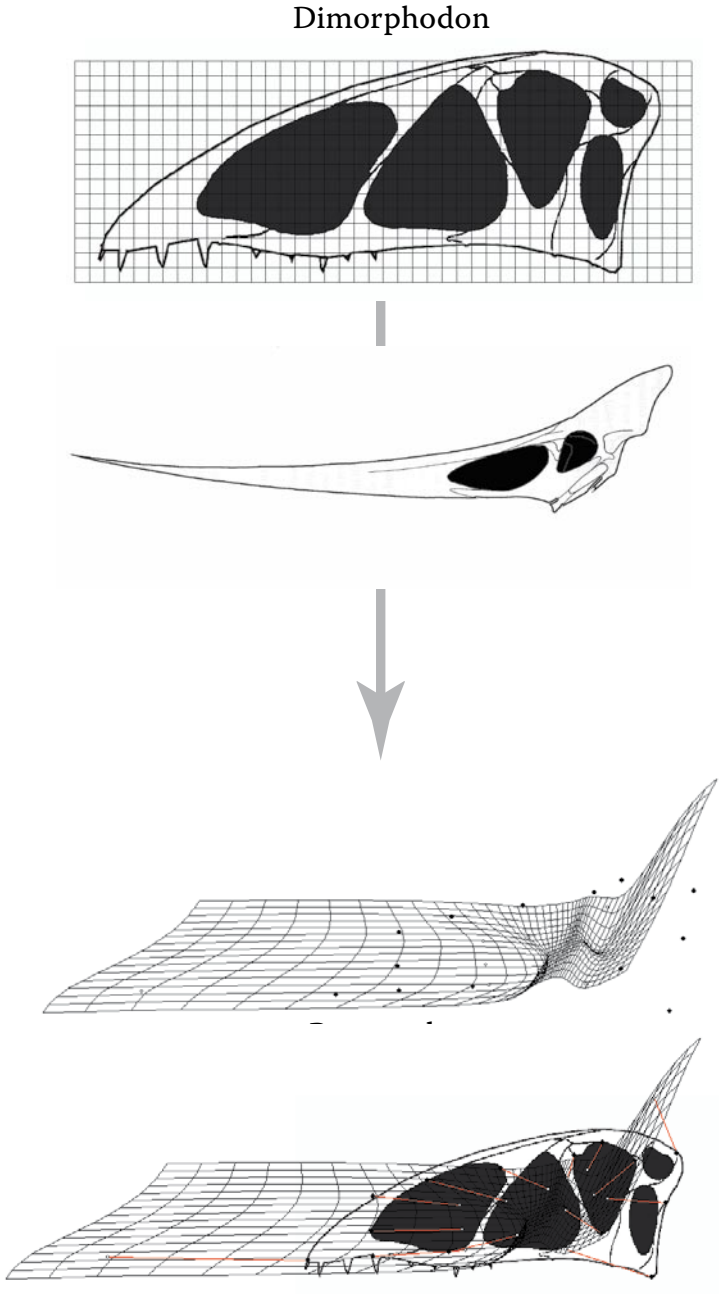

Figura 2.20. Deformación de la malla utilizando la función de interpolación del TPS después de superponer dos cráneos de pterosaurios desde el GPA con el programa Morpheus et al., (Slice, 2002). La referencia es el pterosaurio *Dimorphodon* (Triásico), y el objetivo es *Pteranodon* (Cretácico) Compárese con las mallas de deformación de Thompson (Figura 2.14). El ejemplo muestra como el cambio de forma se localiza desde la utilización de landmarks. La malla muestra que además de cambio uniforme existe cambio más localizado, por ejemplo en la altura de todo el cráneo, aunque sobre todo en la región de la fenestra antorbitaria, donde la malla se comprime drásticamente. Parte de la superposición implica algo de rotación del cráneo. Lamentablemente no se puede mostrar, ni tampoco el original de *Pteranodon*, pues el software no rota la fotografía, lo que hace que no coincida bien con las zonas de deformación de la malla que se muestran. La imagen inferior pretende complementar esta carencia. Nótese que los cráneos no están a escala, y que GPA los ha escalado (*Dimorphodon* es mucho más grande en la figura de arriba y se escala al cráneo de *Pteranodon*, debajo).

clavamos unas chinchetas representado los landmarks. Si queremos mover dos chinchetas, veremos que la fuerza que se hace para desplazar dos chinchetas lejanas es infinitamente menor que entre dos chinchetas que estén mucho más próximas entre si, debido a la

superficie de tela que tenemos que mover.

Aunque la matriz de energía que se calcula no tiene ningún valor en el espacio de forma, sí que lo tiene a la hora de calcular un tipo de variables imprescindibles para los cálculos estadísticos, los llamados *Partial Warps* (PW). Los PW contienen la descomposición del cambio de forma no homogéneo entre las configuraciones de landmarks que se comparen. La identidad de cada PW viene definido por la cantidad de BE que se le atribuye, es decir, si se trata de diferencias entre landmarks distantes (baja BE) o entre landmarks cercanos (alta BE). Los PW se ordenan jerárquicamente de menor a mayor escala.

Un análisis factorial de la matriz de energía de deformación de la configuración referencia descompondrá su variación en provee los *Partial Warp Scores*. Estas serán las nuevas variables de forma y son descriptores de ésta basados en la referencia y responden al llamado componente *no uniforme*. Su particularidad es que mantienen los grados de liberad necesarios (y propios) para realizar cualquier análisis estadístico (ver Zelditch et al., 2004).

A esta serie de nuevas variables hay que sumarle el componente *uniforme*, también llamado *afín*, cambio que afecta homogéneamente a toda la configuración de landmakrs (ver Rasskin-Gutman, 1995). De todos los cambios afines, los de traslación, escalado y rotado ya se han quitado en la superoposición, por lo que restan dos, el cizallado y el estirado (o compresión). En términos de la BE necesaria para deformar la malla, el componente uniforme es el cambio de mayor escala, puesto que afecta a toda la configuración de landmarks homogéneamente. Por tanto, la BE es nula. Cualquier cambio de forma tiene una componente de cambio y otro afín, por lo que ambos tienen que ser incluidos en los análisis (ver relative warps, más abajo).

Existen varias formas de calcular el componente afín, y ninguna parece diferir claramente de las demás (Rohlf y Bookstein, 2003). La nueva matriz que contiene los datos de forma (las variables PW más el componente uniforme) se conoce como *Weight Matrix*, o matriz de pesado (*W*), y es la que contendrá todas las variables de forma que se utilizarán en cualquier análisis multivariante. El método se apoya en una matemática compleja; Bookstein (1991) detalla su formalismo, y en Zelditch et al., (2004) se desglosan en términos más generales.

2.2.3.v. Herramientas estadísticas relacionadas con el estudio propuesto

La morfometría geométrica cuenta con un aparato propio de estadística multivariante. Como ya se mostraba anteriormente la manera de rastrear la variación de forma en una muestra es desde la aplicación de un análisis de componentes principales (PCA), el cual reduce la dimensionalidad de la variación en el espacio tangente (lineal), y ordena la variación en

un orden decreciente (de mayor a menor) varianza de forma. Los *Relative Warps* (RW; Bookstein, 1989; Rohlf, 1993) son la herramienta exploratoria emblemática en morfometría geométrica, y se utilizan para este fin. Los RW (cuya traducción es difícil), son en esencia un PCA pero basado en el uso del Thin Plate Spline (TPS). La particularidad que los diferencia de un PCA es que permiten hacer una selección de la escala a la que tasar la variación morfológica previa al análisis, pues el cálculo de los autovalores se realiza sobre las nuevas variables de forma (viz. sobre la matriz W, o los Partial Warp scores más el componente uniforme; ver apartado sobre el TPS en párrafos anteriores).

La escala, en efecto, es una medida de la cantidad de energía de deformación (de la *bending energy*, BE, necesaria para deformar la malla). La escala es inversamente proporcional a la cantidad de energía aplicada; una escala alta es de baja energía (poca "fuerza" para deformar la malla), mientras que una escala pequeña requiere valores escalares mucho más altos. El control sobre la escala se establece en tres valores categóricos de un parámetro α; cuando $\alpha=0$ se opera incluyendo ambas escalas, y es lo más recomendado para cualquier estudio general comparativo. Si $\alpha=1$ se incluirá sólo la escala grande, mientras que a $\alpha=-1$, se trabajará a escalas pequeñas. Nótese que a cualquier valor distinto de cero la variación podrá (y deberá) ser localizada, por lo que no se podrá incluir el componente uniforme (solo se incluirá en $\alpha=0$).

La sugerencia es que en estudios comparados α se mantenga siempre a cero, pues permite incluir el componente uniforme en los análisis, y por tanto, toda la información posible sobre la geometría de la forma. Igualmente, algunos estudios recientes han demostrado que variando el valor de α, es decir, analizando las distintas escalas de variación de la forma pueden encontrarse congruencias entre el desarrollo, la filogenia y la integración (Nicola et al., 2003), aunque las restricciones de los análisis fuerzan estas exploraciones a muestras muy controladas en laboratorio.

En general, los RW son una manera de aproximarse a la variación de la muestra de una manera sencilla, ya que además, permiten visualizar el cambio de forma correspondiente a cada uno de los ejes de valores de los autovalores mediante la interpolación que permite en TPS entre el espacio tangente y el espacio de Kendall (Rohlf, 2002). En el presente trabajo utilizaremos los análisis para prospectar la disparidad de *forma*, por tanto asumiendo que tanto el espacio de Kendall como su proyección tangente al plano Euclideo (y el PCA) son morfoespacios empíricos basados en la métrica particular de la morfometría geométrica.

Toda la estadística que se utiliza en morfometría geométrica se basa en modelos multivariantes ya que el compromiso de la técnica es tratar siempre las configuraciones de

landmarks en conjunto, es decir, nunca se calcula ni tasa el cambio de forma en landmarks aislados. Así, el análisis de la varianza se realizará siempre desde modelos basados en MANOVA, y la covariación con variables independientes y grupos podrá realizarse desde modelos generales lineales (análisis de Pendientes Comunes, etc.), como la MANCOVA. En uno de los capítulos utilizamos estos modelos para identificar diferencias de forma en el cráneo aviano utilizando una covariable (categórica) que diferencia entre formas altriciales y precociales.

Así mismo, la alometría se estudia desde modelos multivariantes de regresión lineal frente a variables independientes (p. ej. centroid size; CS). La particularidad de todos estos análisis es que, gracias a la función de interpolación del TPS, se puede visualizar el cambio geométrico (las diferencias entre las configuraciones, como deformaciones de la malla en función a las covariables independientes.

Una cuestión importante a este respecto, que avanzamos en este trabajo y que rara vez se trata en textos especializados, es que el CS es una medida de escala óptima para el estudio de la morfometría geométrica, pero no es la única medida de tamaño que se puede utilizar. Hemos reunido una colección de pesos (masas) corporales de aves actuales en la literatura que hemos contrastado con el valor del centroide, y con los que, además, hemos realizado varios análisis de alometría craneal.

Otra metodología propia de la morfometría geométrica son los Mínimos Cuadrados Parciales entre dos bloques (*Two Block Partial Least Squares*, o 2BPLS; Rohlf y Corti, 2000). La técnica de 2BPLS permite comprobar la organización y magnitud de covariación entre dos matrices de datos, siendo una siempre dependiente de la matriz *W* (landmarks), pero otra de variables "tradicionales" u otra *W*, siempre que represente, cualquiera de ellas, una estructura diferente.

Este método es idóneo para explorar hipótesis de integración morfológica. Los 2BPLS se basan en la descomposición de valores singulares (*Singular Value Decomposition*, SVD, o valores de descomposición singulares), para calcular las funciones, en este caso de covariación entre los bloques (las matrices que se comparan). Al igual que los RW, el método expresa los resultados en orden decreciente, aunque de covariación en vez de variación. También permiten visualizar el cambio de forma en términos de deformación de la malla, por lo que los modelos de covariación pueden verse empíricamente. Utilizaremos estas técnicas para el mapeado de las posibles unidades que subyacen a la organización fenotípica del cráneo, comparando medidas tradicionales del endocráneo con configuraciones de landmarks, y de cambios proporcionales del sistema nervioso central con el cráneo en aves actuales.

En cualquiera que sea el método analítico que se utilice (a excepción de los relative warps, que es una técnica exploratoria, y no confirmatoria), el criterio de significación estadístico debe ser analizado siempre con modelos de aleatorización y permutación. Generalmente aplicaremos un nivel de probabilidad $P<0.01$, lo que el número de permutaciones siempre será de 999, aún cuando el software especializado (la serie TPS de F. J. Rohlf) lleva por defecto un nivel inferior (generalmente 99). Los modelos de significación se realizan siguiendo a Goodall (1991).

Box 4

Anotaciones sobre la Teoría de la forma de Kendall. Distancia Procrustes y Espacio de Forma

La definición de *forma* en morfometría geométrica menciona que la escala (*size*, o CS) es un efecto que hay que retirar de la forma para poder capturar las diferencias geométricas (Kendall, 1977). La *forma*, por tanto, ha de ser independiente de la escala. En definitiva, la *forma* en morfometría geométrica será "*el filtrado que contiene toda la información geométrica cuando los efectos de la localización, la escala y la rotación se han retirado*" (Kendall, op. cit.).

Despues de digitalizar, los landmarks quedan registrados como coordenadas en una matriz de *K* filas (número de landmarks) y *M* columnas (coordenadas), donde *M* en dos dimensiones será siempre 2 (X-, Y-). El primer espacio conceptual en el que esas coordenadas se encuentran es el denominado Espacio de Configuraciones, que por definición contiene a todos los posibles conjuntos de matrices *KxM* conteniendo, a su vez, a todas las posibles configuraciones de landmarks imaginables de *K* y *M* (como curiosidad, nótese cierta analogía con la noción de morfoespacio teórico). Atendiendo a un número de formas *i*, con un número determinado de landmarks *p* con unas coordenadas *k* (Rohlf, 1996), si tenemos, por ejemplo, p=10 landmarks, un Espacio de Configuración 10x2 será aquel que contenga todas las configuraciones posibles definibles por 16x2 landmarks en 2D. Cualquier configuración de *K* landmarks con *M* coordenadas puede ser imaginado como un punto (que representará a una forma individual, o lo que es lo mismo, a cada configuración de landmarks) en el espacio de *KxM* dimensiones.

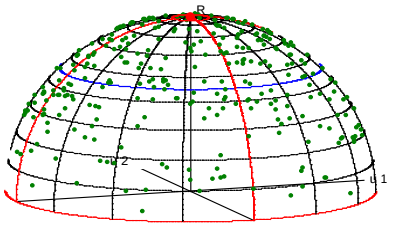

Figura B4.2. Espacio de Pre-forma con 500 triángulos generados aleatoriamente con una distribución isotrópica (sin error). Los puntos son las formas (en este ejemplo, los triángulos). Calculado y dubujado con TPStri (v1.22; Rohlf, 2006).

Tras la translación de las coordenadas de los centroides y del escalado la matriz de configuración (la matriz *KxM*) siguiendo los pasos de la superposición Procrustes, esta pasa a localizarse en un espacio llamado de *Pre-forma* (Preshape Space), que se diferencia del espacio de configuraciones en que las configuraciones ya están ordenadas, es decir, todas las configuraciones de landmarks carecen de dos dimensiones de la forma, traslación y el tamaño (la rotación todavía no se ha retirado, por lo que la distancia entre landmarks homólogos todavía no se ha minimizado del todo). Siguiendo el criterio de superposición, todas las formas están localizadas en una misma región (el origen de coordenadas, *x*- 0, *y*-0) y, además están escaladas a la unidad. Las dimensiones de este espacio son menores (hemos perdido tres), por lo que quedan *KM-(M+1)=KM-M-1* dimensiones. Para cualquier configuración de landmarks en 2D, el espacio de preforma siempre tendrá *2K-3* dimensiones. Una se pierde de fijar el centroide a uno, al eliminar la dimensión de escala, y otras dos se pierden al centrar las configuraciones (para describir la localización).

Dentro de este espacio de preforma (Fig. B4.1) el orden se define por series de fibras que contienen las configuraciones (cada fibra una forma distinta) ya centradas en el origen y escaladas, a CS=1. Las fibras se definen según un orden de rotación de las configuraciones (cada una continúen configuraciones iguales que solo difieren en rotación). Como la rotación no se ha retirado de la forma todavía no hemos

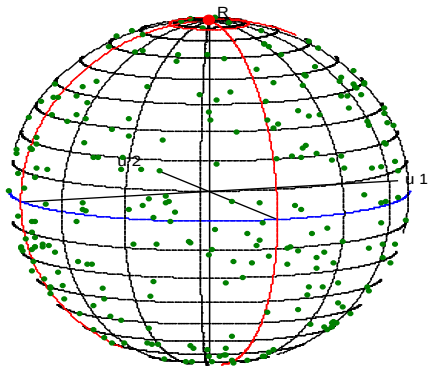

Figura B4.3. Espacio de forma (Kendall) con 500 triángulos generados aleatoriamente con una distribución isotrópica (sin error). Los puntos son las formas (en este ejemplo, los triángulos). Calculado y dubujado con TPStri (v1.22; F. J. Rohlf).

cumplido la definición de *forma* de Kendall.

El espacio de Kendall de *forma*, se alcanza una vez se hayan retirado todos los factores no asociados a la forma (traslación, escalado y rotación). El espacio es una construcción geométrica multidimensional donde, cada punto representa la forma de una configuración de landmarks (una forma). Sus dimensiones, tras alinear las configuraciones retirando la rotación son, 2K-4 (en 2D), de donde una (-1) se resta del escalado (como se expresó anteriormente), dos de la traslación (-2), y una de la rotación (-1).

Desde una perspectiva estadística, las distribuciones isotrópicas de landmarks alrededor de la media resultan en una distribución isotrópica de los puntos que representan a los individuos de la muestra en un espacio tangente al espacio de forma (Fig. B4.2; Rohlf, 1996). Sin embargo, el espacio de Kendall no es Euclideo (no es lineal). Para las formas geométricas más sencillas, triángulos, el espacio puede visualizarse como una esfera. Para más de tres landmarks el espacio es mucho más complejo, y debido a su no-linearidad, la estadística es también particular y más compleja (ver, Small, 1996).

La solución operativa para trabajar estadísticamente con los datos es utilizando el análisis de componentes principales sobre un espacio tangente al de Kendall. Siguiendo el ejemplo más sencillo, usando triángulos, se toman las dispersiones de puntos del espacio esférico donde cada punto refleja la variación de la muestra, y se proyecta a un espacio Euclídeo, representado por un plano tangente de la misma manera que un cartógrafo proyecta un mapa de un globo a un papel plano (B en la figura 3.16). Así, las coordenadas de las configuraciones (triángulos) dejan de tener una referencia en la esfera y sus coordenadas pasan al Plano Tangente (Euclídeo). Mientras no se produzca mucha distorsión (lo que ocurriría si se proyecta un área grande de la esfera, o lo que es lo mismo, si la variación de la muestra es muy grande), se puede aplicar casi todo tipo de estadística multivariante (Rohlf, 1996).

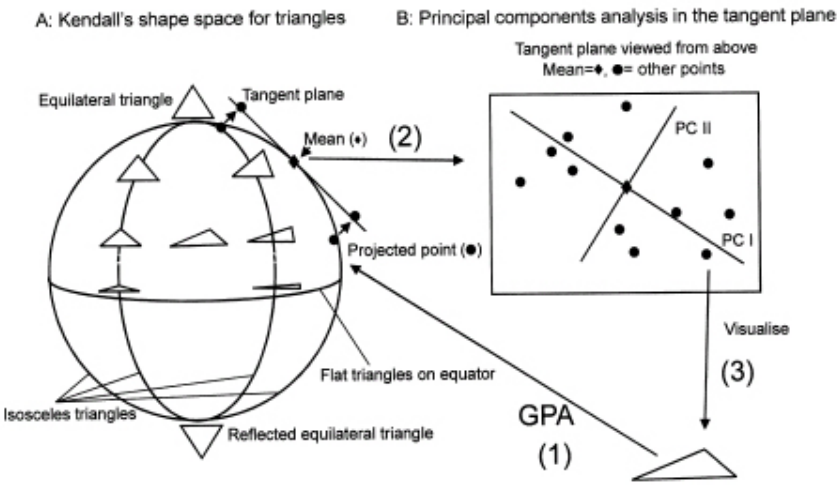

Figura B4.2. . a) Esquema aproximativo del espacio de Kendall para triángulos. Los triángulos equiláteros caen en los polos, por lo que el "hemisferio" sur es un reflejo del norte. La esfera está dividida en doce medias lunas (fibra, ver texto; luna=figura plana rodeada por dos arcos circulares de radio desigual); si los ápices del triángulo no están registrados y las reflexiones se ignoran todos los triángulos caen en una media luna. Los triángulos isósceles caen a lo largo de las líneas dividiendo las lunas. B) Esquema indicando la proyección de puntos que representan triángulos en el espacio de Kendal dentro del espacio Tangente respecto al triángulo medio (consenso; ver flechas), y los componenetes principales de variación entre las formas de triángulos (PC 1 y PC2). Los números representan los pasos seguidos; 1) GPA para registrar las figuras en el espacio de Kendall, 2) Proyección de los puntos al Espacio Tangente desde la media. Se realiza el PCA, y 3) la visualización de la variación de forma se observa desde el PCA mediante una proyección reciproca que permite visualizar la forma en vez de valores escalares. Original de O'Higgins y Jones, (1999). Ver también un resumen en Rohlf (2002).

En el caso de estudio que planteamos en esta tesis, la escala macroevolutiva de variación de los cráneos podría plantear algún problema de proyección, pues los cráneos podrían ser muy distintos entre si. Sin embargo (ver Parte Tercera, Capitulo 2), la proyección entre espacios puede realizarse sin ningún problema. F. J. Rohlf suele explicar que la incoherencia entre espacios se daría, por ejemplo, si comparásemos teratologías muy marcadas.

Las coordenadas Procrustes en el espacio tangente pueden estimarse como el vector *KxM* de las desviaciones de la media. El vector de las coordenadas en el espacio tangente es de rango KM-m-m(m-1)-1, por lo que se puede utilizar un PCA para extraer el mismo rango de autovalores, que a su vez, serán los componentes principales de la variación de forma (O'Higgins y Jones, 1999; Fig. B4.3).

TERCERA PARTE

3.1 Disparity and geometry of the skull in Archosauria (Reptilia: Diapsida)

Marugán-Lobón J. & A. D. Buscalioni.

Paper Published in the *Biological Journal of the Linnean Society*

Biological Journal of the Linnean Society, 2003, **80**, 67–88. With 9 figures

Disparity and geometry of the skull in Archosauria (Reptilia: Diapsida)

JESÚS MARUGÁN-LOBÓN* and ÁNGELA D. BUSCALIONI

Departamento. Biología, Unidad de Palaeontología, Facultad Ciencias, Universidad Autónoma de Madrid, 28049 Cantoblanco (Madrid), Spain

Received 27 June 2002; accepted for publication 5 February 2003

A metric comparison of 155 fossil and extant species in lateral view based on the proportions of three homologous units (braincase, orbit and rostrum) reveals the existence of an archosaurian skull geometry. An empirical morphospace depicting skull proportions shows that the most variable unit is the rostrum. Three skull types based on rostral proportion are proposed: meso-, longi- and brevirostral. These types depend, on one hand, on a direct numerical relationship between the braincase and the orbit, with a mean ratio of 1:1; never surpassing a 2:1 or 1:2 ratio limit. On the other hand, skull types show a significant negative correlation between braincase and rostrum proportions. Close relationships have been obtained between orbit and the rostrum, although with lower significance and a geometric meaning specific to each group. Skull types depend mainly on the proportional relationship between the rostrum and the braincase. Mesorostral types account for more natural occurrences within morphospace, implying a plesiomorphic condition in Archosauria. Skulls with highest longirostral values (flying forms) display a more restrictive braincase–orbit ratio relationship. Brevirostrals are limited to the smallest skull lengths, up to approximately 180 mm. 85% of brevirostral modern birds have altricial post-hatchling development. General allometric pattern is very similar for all sampled archosaurs, although giant taxa (i.e. non-avian theropods) display a different type of skull proportional growth, closer to isometry. Results reveal the existence of a constructional skull geometry, highlighting the importance of the deviance of the structural design from adaptive explanations on craniofacial morphology in macroevolution. *Biological Journal of the Linnean Society*, 2003, **80**, 67–88.

ADDITIONAL KEYWORDS: macroevolution – morphospace – theoretical morphology.

INTRODUCTION

At present, close to 10 000 extant species (9951 birds and 27 crocodiles) represent the archosaur lineage which, along with the vast number of extinct species studied and described, has probably been one of the most diverse groups of vertebrates on the planet. Occupying almost the entirety of existing habitats during the Mesozoic (fresh and salty aquatic, aerial and terrestrial mediums), archosaur morphology can be characterized, among other features, by extreme skull diversity in shape and size (Witmer, 1995). This diversity matches the high disparity in overall size these organisms can and could reach, where, for instance, skull sizes range from the 30 mm of hummingbirds (Trochilidae) up to the approximately 1800 mm displayed by the huge *Giganotosaurus carolinii* (Calvo & Coria, 1998). The spectrum of cranial shapes is also highly varied, from the widespread platirostral condition in modern crocodiles, through the oreinirostral of certain extinct crocodiles and dinosaurs, to the well-known beaked modern birds.

A relationship between habitats and cranial diversity has often been suggested, and the evolution of the rostral shape has usually been considered dependant only on adaptation, either trophic, ethological or both (Proctor & Lynch, 1993 for modern birds, and an overview in Brochu, 2001 for modern crocodiles). In accordance with this functional paradigm, the facial system has been analysed thoroughly, although strictly in terms of the properties of its discrete conforming elements (Lewontin, 2000); thus functional constraints have been historically well explored in the archosaurian cranial anatomy (Busbey, 1995 on modern croco-

*Corresponding author. E-mail: jesus.marugan@uam.es

diles). Furthermore, this approach has led to the facial skeleton being viewed as an independent structure within the skull (Zusi, 1993), whereas the rostrum has only occasionally been evaluated in close relation to other parts of the skull complex.

Our objective is to explore skull disparity and its possible geometric basis, including analysing the rostrum within the skull of the archosaurian lineage. We have considered two-dimensional classic morphometrics, in lateral view. According to our method, the skull, taken as bone tissue, incorporates three anatomical units: facial skeleton (rostrum), cranial box (braincase), and orbits. Our starting hypothesis suggests the occurrence of a geometric pattern in the archosaurian skull, forecasting that, despite skull disparity (in terms of overall size, rostral proportion, and even braincase lateral extent), a set of relationships will underlie phylogenetic and functional factors in the archosaurian skull design. Thus, this study intends to gain insights on macroevolutionary patterns for the archosaurian skull, highlighting the existence of morphological limitations due to structural constraints between the rostrum, braincase and orbital proportions.

Theoretical morphology and its operative tool, the morphospace, is the instrument we have used to investigate the natural limits of the skull geometry in the clade Archosauria. Within this theoretical background, the creation of a hybrid morphospace, mixing information from both theoretical and empirical approaches, has developed into a fruitful exploratory tool (see Rasskin-Gutman, 1995; McGhee, 1999; Chapman & Rasskin-Gutman, 2001; Rasskin-Gutman & Buscalioni, 2001) which has yielded prospective macroevolutionary hypotheses and predictions. Morphospace analysis sets the context in which to pose questions about how the distribution of organic shapes occurs in nature by means of an evaluation of the extent of occupied space, and how a particular geometry is conformed against all possible combinatory occurrences (Fig. 1). Our evolutionary analysis of the skull patterns was undertaken horizontally (Wagner,

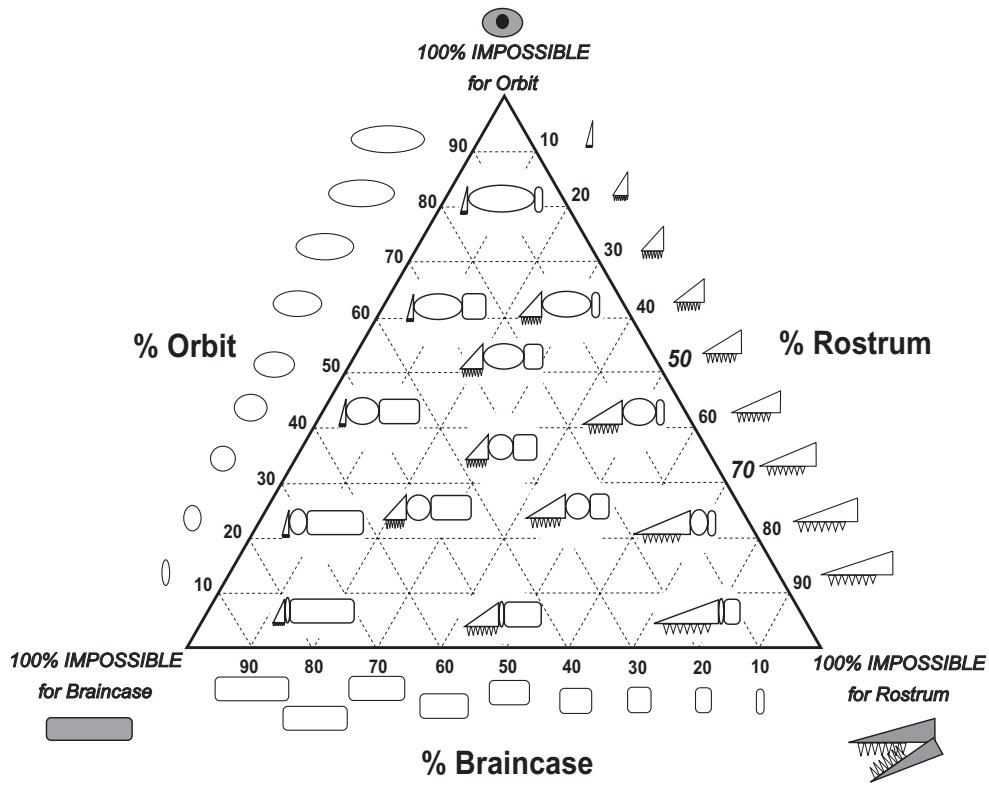

Figure 1. Theoretical morphospace of skull proportions. The triangular diagram shows all the possible combinations theoretically achievable. On each axis are percentages for rostrum (R), the orbit (O) and the braincase (B). Note that the skull theoretical designs are all of the same height and only vary on their horizontal length. Impossible theoretical and natural occurrences are represented by the apices of the triangle (meaning 100% of appearance of one unit alone) and by the midpoints of the sides of the triangle (50% each for two units). All possible combinations gather within the range delimited by the area of the triangle where they can be infinite, and strictly between the three elements.

2001) throughout the clade Archosauria (i.e. *Euparkeria*, *Scleromochlus* + Pterosauria, Ornithischia, Sauropodomorpha, non-avian and avian theropods). Our objective was to develop a model of skull variation in archosaurs by means of a simple metric statement. Data was explored statistically to test for allometry between pairs of anatomical skull units (rostrum, orbit and braincase) in order to reveal the possible factors underlying their macroevolutionary patterns.

The geometry of the skull

Geometric statements on the amniote skull can be advanced intuitively. For example, Gould (1993) summarizes the history and works by Petrus Camper (1722–1789), an anatomist whose research revealed a relationship between the cranial vault and the anterior face in humans. In order to quantify this relationship, Camper defined the 'Facial Angle', whose values depict a negative covariation between both cranial structures. The Facial Angle soon became a widespread morphometric tool for anthropologists although, ludicrously, it also provided the first anthropometric device for the endorsement of racist prejudices. Throughout the mid-20th century, Weidenreich (1941 *fide* Gould, 1977), best known for the development of the multiregional hypothesis on human origins, claimed that large-brained dogs have relatively small faces. He argued that the brain would exert pressure upon the entire skull, inhibiting development of the jaws during ontogeny. From this point of view, the geometry of the skull acquires developmental foundations through the pattern of soft tissue exerting pressure on the hard tissue (see also de Beer, 1937; Herring, 1993).

Having probably considered these approaches, Enlow & Azuma (1975) and Enlow & Hans (1996) defined a model to explain patterns of craniofacial growth in mammals. Using a set of perpendicularly paired planes (the cribiform vs. the facial planes, and the pterygomandibular vs. the orbital axis), the authors linked the rostrum, neurocranium and orbit areas, emphasizing the importance of understanding the human face as a complex structure subordinated to the development of the nervous system. On the same basis, they suggest a morphocline from any long-snouted mammal to the short appearance of the human face. By empirically quantifying the angles between said planes, their morphometrics bear evidence to an invariance of values in mammals. They therefore considered that in order to keep these relationships between angles constant, an increase in the volume of the brain which pushes the cribiform plate forward must also flex and drag the facial complex backward, thus reconfiguring it to conform the craniofacial variations displayed by the mammalian skull.

THE SAMPLE AND THE METRICS

The Appendix shows the list of the archosaurian species sampled. The whole sample consists of 155 specimens belonging to five monophyletic groups (*Euparkeria*, *Scleromochlus* + Pterosauria, Ornithischia, Sauropodomorpha, Theropoda – including Aves). Several authors have successively verified the monophyly of these groups; a taxonomically congruent dendrogram including all groups is depicted in Figure 2. Throughout the study we use the terms 'theropods' and 'birds' paraphyletically only for the sake of simplicity when comparing groups, although by 'theropods' we mean strictly all extinct avian and non-avian theropods, while 'birds' is used to express all extant avian theropods. The sample includes both extinct and extant species; the former were measured on casts from real specimens available at the Universidad Autónoma de Madrid or were taken from literature. The results obtained were also used to check the reliability of skull reconstructions. Extant birds were measured from actual skulls from the MNCN (Museo Nacional de Ciencias Naturales) and MAUV collections (Museo Anatómico de la Universidad de Valladolid), and measurements for a few avian species were taken from the literature. The sample was restricted to include only adults or, in a few cases, subadults, while the use of juveniles was avoided.

Measurements

The skull as we consider it concerns the bony architectural complex formed by three adjacent units: braincase, orbit and rostrum. We measured the geometry of the skull by quantifying the proportions of its parts with regards to the full skull length in lateral view (Fig. 3A). These cranial units and their boundaries may be considered homologous, at least in Archosauria (Witmer, 1997).

The rostrum has been described as a structure departing from the orbital region (Witmer, 1995), or the region anterior to the orbits (Busbey, 1995). The rostrum is limited anteriorly by the tip of the premaxilla, and is caudally bounded by the anterior-most part of the orbits (Starck, 1979; Zusi, 1993; Kardong, 1999). The bony orbit in Archosauria is aligned between the rostrum and the braincase, surrounded mainly by dermal bones (Baumel & Witmer, 1993). The orbit is enclosed by the lachrymal, post- and prefrontal, and postorbital bar (including also part of the jugal). It houses the ocular globe (occulus *sensu* Martin, 1985), and the orbital contents (referring to constitutive tissues *sensu* Witmer, 1997).

The braincase is an alternative and broader term for the neurocranium. Braincase consists of the set of fussed osteological pieces immediately surrounding

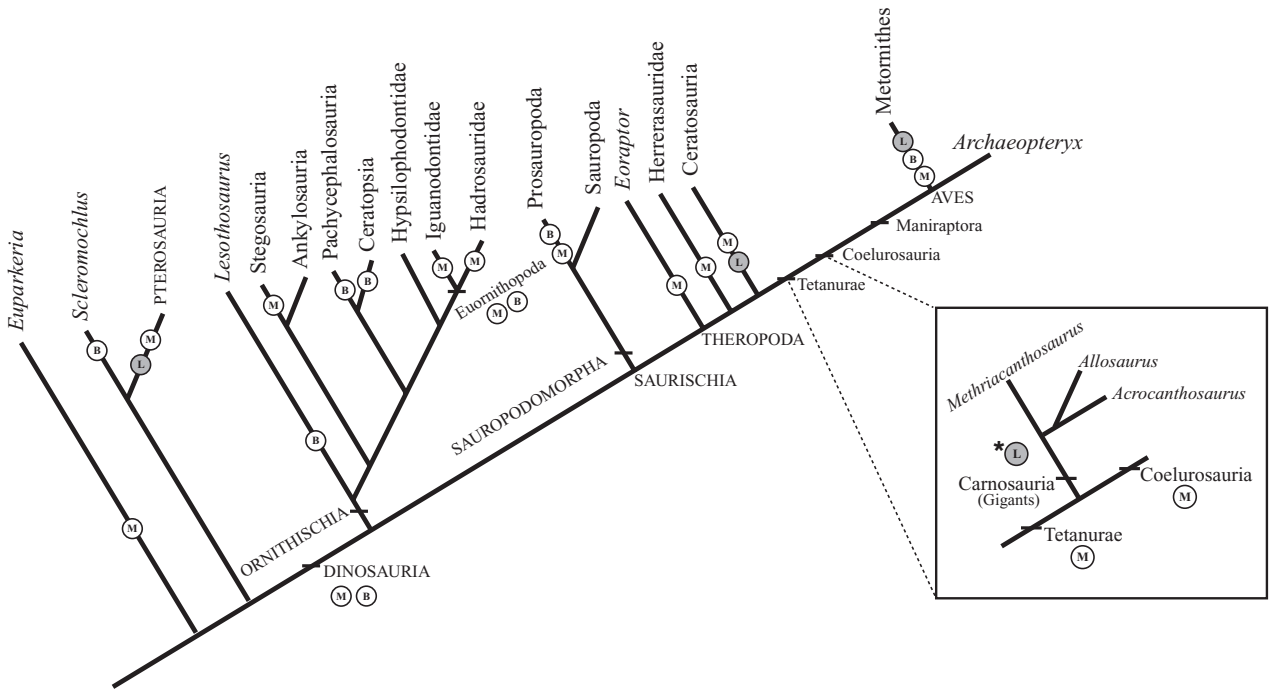

Figure 2. Dendrogram showing the analysed groups. We have depicted the major clades of Dinosauria based on the following phylogenetic relationships: Ornithischia on Benton (1990), Sauropodomorpha on Wilson & Sereno (1998). Theropoda including Aves on Holtz (1998), Sereno (1999), and Padian (2001). Throughout the dendrogram, rostral types on each terminal taxon have been mapped where; B = brevirostral, M = mesorostral and L = longirostral. Box shows carnosaurian taxa emphasizing that giant theropods display a special longirostral condition.

and including the encephalon. It is tapped by dermal, chondrocranial, and even splachnocranial elements (Kardong, 1999). We have chosen the term braincase because it excludes the optic capsules, which are treated separately in the study.

Four homologous points or landmarks have been defined as the crucial boundaries for each structure. All measurements have been taken in lateral view, representing the length of each anatomic unit (abbreviated as B, O and R; Fig. 3A), where distances are obtained between landmarks projected perpendicularly to a baseline (BL) defined from the premaxillary symphysis to the ventral surface of the quadrato-mandibular articulation. Proportions are the ratio between the lengths of each structure and the total length of the baseline, used herein as a comparative numerical constant for each specimen.

Landmarks have been defined as follows. The premaxilary symphysis (1) delimits the rostral anterior margin, and is easily found in every group. The lacrymal bone (*os lacrimale*) (2) is a shared landmark, defining the posterior boundary of the rostrum and the anterior edge of the orbit. It can be anatomically controversial due to a disputable homology between dinosaurs and birds. However, based on topographic and transformational criteria, Baumel & Witmer (1993) offer arguments in favour of homology. The authors claim that the lacrymal always represents the boundary for the anteorbital fenestra in all archosaurs, including birds, and that in all dinosaur ancestors of birds, the progressive reduction in prefrontal covaries with an increase of the lacrymal. We have located this landmark in birds from the orbitonasal foramen (*Foramen Orbitonasalis Medialis*) ascending dorsally to reach the posterior edge of the lacrymal bone at the beginning of its cranial thickening.

The postorbital bar (3) is also a shared landmark limiting the orbit and braincase. We have located the point in birds at the postorbital process. We assume the homology of this postorbital process in birds (compounded by the laterosphenoid, squamosal and frontal bones) and the postorbital bar in the remaining archosaurs (postorbital plus, to a greater or lesser degree, the ascending ramus of the jugal; Baumel & Witmer 1993). The point in birds coincides with the pathway delivered by the external ramus (*nervus Supraorbitalis*, probably *n. Temporalis Superficialis sensu* Ghetie *et al*., 1981), on its way over the temporal surface (consisting in the squamosal and parietal bones). In *Scleromochlus* + Pterosaurs, the landmark is located at the intersection between jugal and postorbital sutures, according to reconstructions in Wellnhofer (1978,

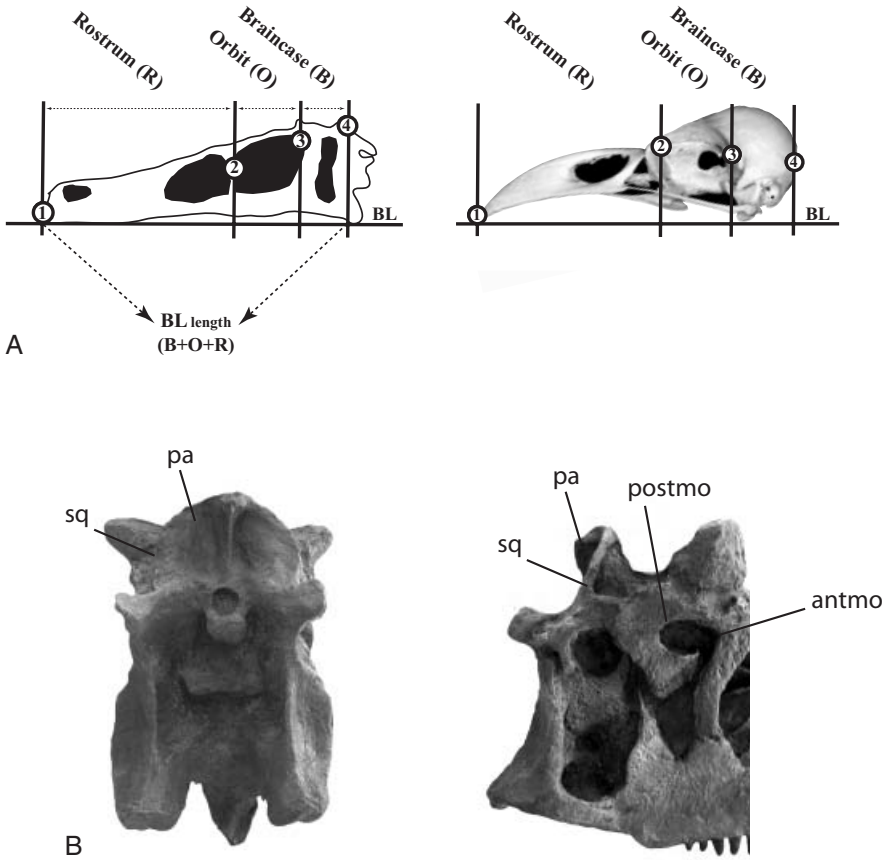

Figure 3. (A) Lateral view of the schematized theropod dinosaur *Velociraptor mongoliensis* and modern bird *Corvus corax*, with landmarks and measures taken for R (rostrum), O (orbit) and B (braincase). BL denotes baseline length (B + O + R). (B) Occiput and lateral view of theropod dinosaur *Carnotaurus sastrei* (cast), illustrating the occiput concavity (see text). Abbreviations: antmo, most anterior margin of the orbit; pa, parietal; postmo, most posterior margin of the orbit; sq, squamosal.

1991). In Sauropodomorpha, Ornithischia and Theropoda it is located dorsally where the postorbital bar inflects toward the frontal.

The caudal-most point of junction between parietal and squamosal (4) marks the posterior end of the braincase. In birds, the point coincides with the sagittal point of the occipital crest (*Prominentia cerebellaris*). This point represents the caudal limit of the brain, marking it quite precisely, as the braincase may conform closely to the size and shape of the brain, at least in birds (Zusi, 1993; Feduccia, 1999). In the remaining groups, however, any estimation of the total brain length from the braincase will probably be approximate.

Note that for some specimens (*Allosaurus fragilis* and *Carnotaurus sastrei*; a drawn example of a sagittal scheme can be found in Norman, 1986 for *Iguanodon atherfieldensis*) the landmark, from a lateral view, appears not to embrace the total length of the brain (*Carnotaurus*; Fig. 3B). However, from an occipital view, the bony occipital region is concave, where the occipitals correspond to the caudal wall of the brain. When viewed laterally, part of the squamosal and the paraoccipital process exceed the position of the landmark caudally, thus hiding this concavity, but the landmark precisely defines the caudal boundary of the brain at the junction between the parietal and squamosal.

SKULL PROPORTIONS: MORPHOSPACES

THE THEORETICAL MORPHOSPACE

The theoretical morphospace (Fig. 1) is built onto a triangular diagram showing all the theoretically possible combinations between the percentages of braincase (B), orbit (O) and rostrum (R). The diagram includes a grid of 100 subtriangles in order to quantify occupied space, and axes are each split into 10% units. Note that the theoretical skull designs displayed have been schematized and forced to be the same height; hence,

types only vary in their horizontal proportions. Impossible theoretical or empirical occurrences correspond to the apices of the triangle, meaning 100% of appearance of one unit alone. Another impossibility would be a shared 100% between only two units. All possible combinations fall within the area of the triangle, where the variations in combination of skull types are unlimited.

THE EMPIRICAL MORPHOSPACE

The empirical morphospace on a triangular diagram yields an extremely useful exploratory tool for studying the relative contribution of three elements simultaneously (Gatesy & Middleton, 1997; Gatesy & Middleton, 1999). The cluster over the empirical morphospace occupies 18 subtriangles of the grid (Fig. 4A), 18% of the total depicted diagram. The cluster as it is plotted goes from approximately the centre of the diagram, down to its bottom right apex, defining a tight region. Two main axes can be defined over the region (Fig. 4B). The main one, or the longest, spans the values corresponding to the higher range of the rostrum, the most variable unit. Furthermore, with extreme values defining its limits between 90% (plotted value for *Pteranodon ingens*) and 30% (from *Falco tinnunculus*), the rostrum has a total range of 60%, whereas orbit and braincase do not surpass 20% ranges.

Along this main long axis over the region there is an operative expression for the rostral variation over the morphospace (Fig. 4B). The cluster can be split into three hexagons (H1, H2 and H3) in the diagram where each includes a categorical rostral range of proportion. We have adopted the terms used by Busbey (1995) for rostral qualification applied to archosaurs (brevi-, meso- and longirostral). Thus, three rostral types of the same range units are defined: 30–50% for the brevirostral (on H1), 50–70% for the mesorostral (on H2), and 70–90% for the longirostral (on H3). Likewise, each type is included within its corresponding hexagon (Fig. 4A,B).

Orbital and braincase follow a ratio of 1:1, from a B/O ratio with a mean value = 0.97 (Fig. 4B). The cluster's long midline passes through every hexagon centroid (where B/O mean value = 1). The traced bisector over the diagram matches the long midline axis of the cloud, splitting it in two almost symmetrical parts. Each part of the divided region represents the proportional relationship between B and O. The contours of the hexagons delimit the total variance ranging between 1:1 and maximums close to 2:1 and 1:2. This can be expressed as follows; none of the structures will be twice the value of the other in total length or proportion. The short axes of the region also graphically display this relationship (Fig. 4B).

The edges of the operative hexagons define the borders between the empirical and the theoretical morphospace. The most brevirostral skull (30% rostrum) never surpasses a braincase and orbit value in an interval between 30 and 40%. The most longirostral one (90% rostrum) never surpasses less than a 5% for either braincase or orbit, displaying the smallest variance for the B/O relationship (Fig. 4A). The mesorostral condition, on the contrary, yields the maximum spectrum of variance in the occupied hexagonal area, although it never surpasses the 1:2 or 2:1 B/O relationship.

Furthermore, in terms of the space occupied by groups and their distribution, all groups are represented within the mesorostral-qualified hexagon (Fig. 5 shows how mesorostrality is represented by 60% of the total sample, and with far more occurrences than either the longirostral (22%) or brevirostral (18%) conditions). The brevirostral condition comprises birds, which are the most frequently represented with 14% of total brevirostral type occurrences, followed by ornithischians with approximately 9%. Pterosaurs are only represented by their sister taxa *Scleromochlus taylori* and theropods are only represented by *Oviraptor philoceratops*.

The mesorostral condition includes the basal *Euparkeria*, together with representatives of all groups, though mesorostral theropods and birds are dominant, both reaching around 30% of total occurrences. The longirostral condition is clearly dominated by the presence of pterosaurs (18%) followed by birds and theropods (approximately 9% and 7%, respectively), where the latter are gigantic representatives of the clade. Sauropodomorphs lack this rostral condition and birds, although present in clearly lower numbers than pterosaurs, can reach up to almost the same rostrum lengths as the former. Ornithischians only have one representative (*Ouranosaurus*) that is almost over the border between both meso- and longirostral conditions (rostrum = 70.5%).

Figure 4. Empirical morphospace. (A) Plotted skull proportions where rostral borders are represented from the boundaries delimited by rostral percentage values. Mammals are plotted for contrasting purposes, displaying a different geometric relationship between skull units against that of archosaurs. (B) Schematic drawing for the operative expression of the rostral variation in hexagons (H1 = brevi-, H2 = meso-, and H3 = longirostral). Dashed ellipse represents the cluster, long axis crosses hexagon along 1:1 mean B:O ratio. Upper and lower dashed parallel lines represent maximum B:O ratios (limits). (C) B:O plot for each rostral type. Note outliers above and below maximum–minimum ratios.

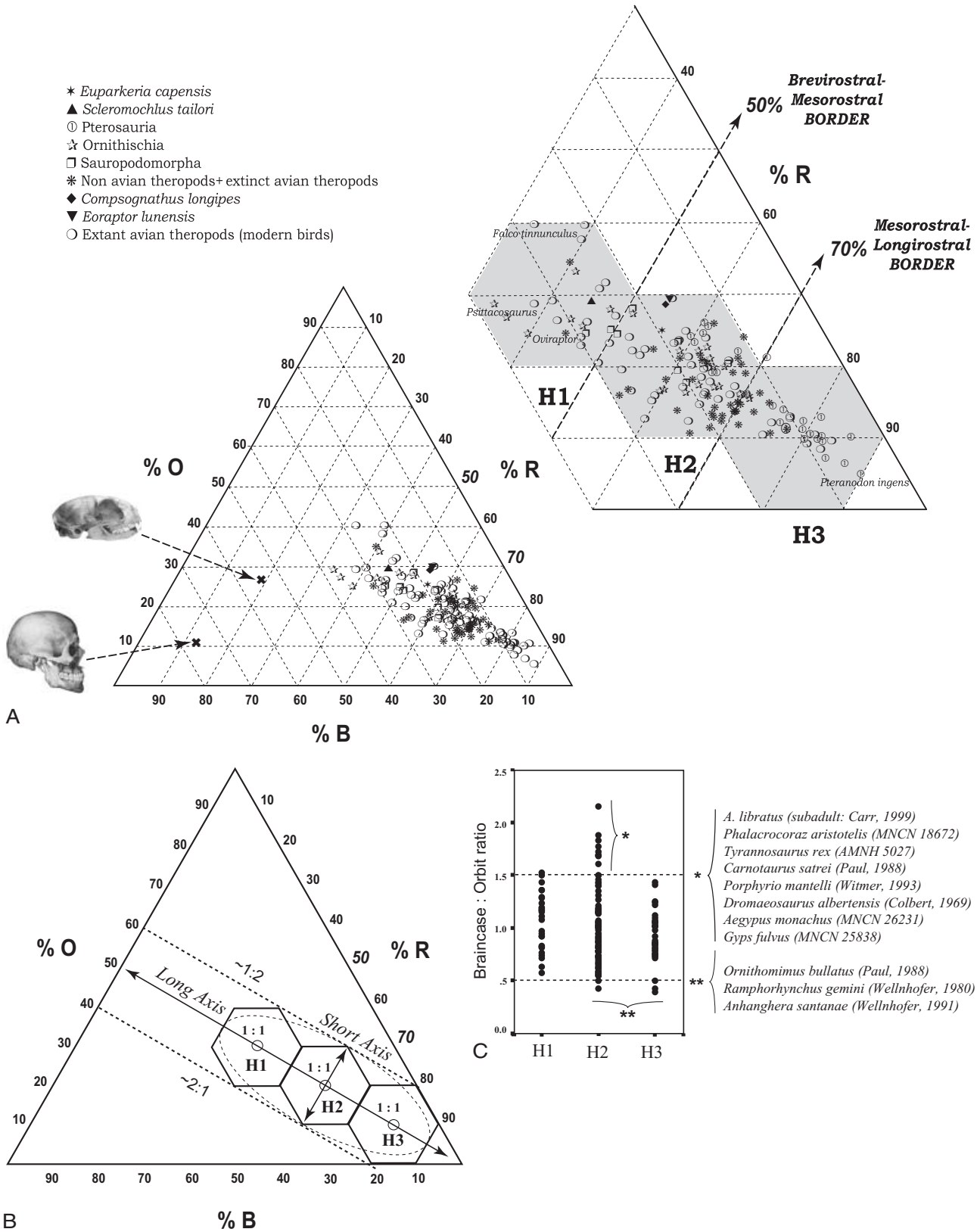
✶ Euparkeria capensis
▲ Scleromochlus tailori
① Pterosauria
☆ Ornithischia
❒ Sauropodomorpha
❋ Non avian theropods+ extinct avian theropods
◆ Compsognathus longipes
▼ Eoraptor lunensis
❍ Extant avian theropods (modern birds)
Brevirostral-Mesorostral BORDER
50%
% R
Mesorostral-Longirostral BORDER
70%
Falco tinnunculus
Psittacosaurus
Oviraptor
Pteranodon ingens
H1
H2
H3
% O
% B
A
Long Axis
Short Axis
~1:2
~2:1
1 : 1
B
Braincase : Orbit ratio
C
A. libratus (subadult: Carr, 1999)
Phalacrocoraz aristotelis (MNCN 18672)
Tyrannosaurus rex (AMNH 5027)
Carnotaurus satrei (Paul, 1988)
Porphyrio mantelli (Witmer, 1993)
Dromaeosaurus albertensis (Colbert, 1969)
Aegypus monachus (MNCN 26231)
Gyps fulvus (MNCN 25838)
Ornithomimus bullatus (Paul, 1988)
Ramphorhynchus gemini (Wellnhofer, 1980)
Anhanghera santanae (Wellnhofer, 1991)

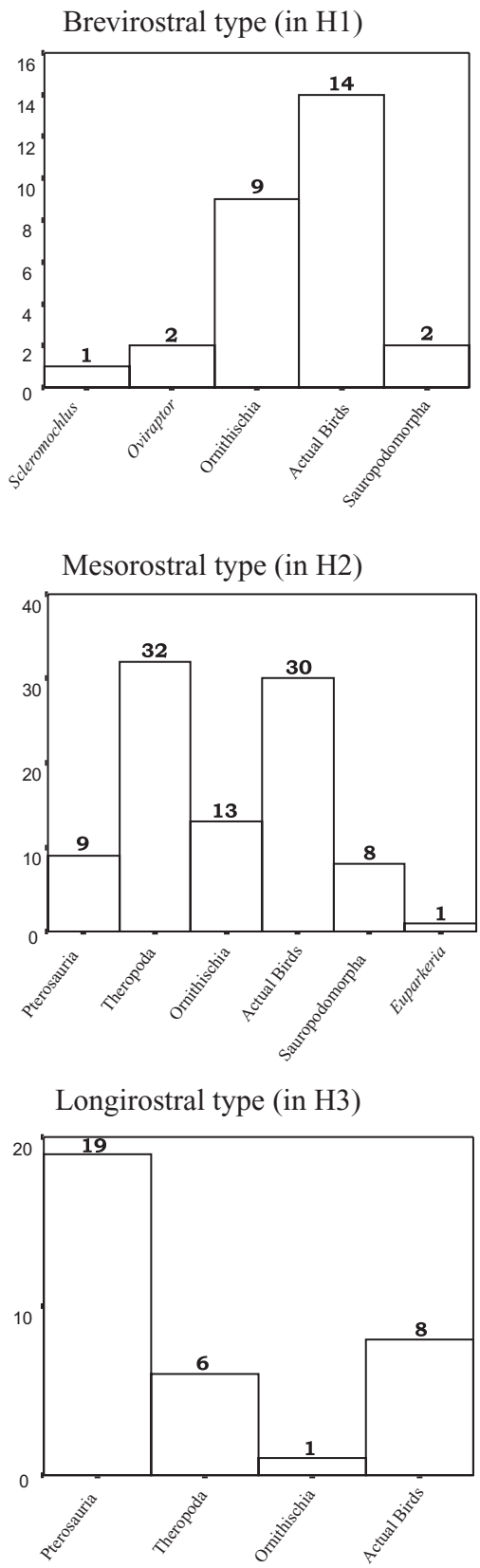

Figure 5. Histograms for frequency of rostral types over the empirical morphospace. Mesorostral is the most frequent condition. Brevirostrals theropods include two specimens but only *Oviraptor* is cited (*Compsognathus* (Paul, 1988) could be wrongly positioned, see text).

REGRESSION ANALYSES

We plotted two bivariate scatterplots to test correlations by applying least-square regression models to compare ratios. Results (Fig. 6) show a strong significant negative correlation ($r = -0.893$; $P < 0.01$) between braincase proportion and rostrum proportion, with a relatively high value of regression when analysing the whole sample ($R^2 = 0.80$; $y = -1.555x + 91.045$). Analysis of variance (ANOVA) confirms that the model is highly significant for braincase proportion to explain most of the variation in rostrum proportion (d.f. = 151; $F = 609.62$, $P < 0.01$).

When analysed separately, pterosaurs, ornitischians and sauropodomorphs behave likewise. Birds display an even higher significant negative correlation ($r = -0.89$; $R^2 = 0.75$). Values rise to $R^2 = 0.84$ and $r = -0.90$ by removing only three outliers from Falconiformes (*Falco tinnunculus* and *Falco subbuteo*: Falconidae, and *Pernis apivorus*: Accipitridae). These are discussed separately below since they clearly fall outside the graphic tendency line defined for the whole group. The index for theropods is the lowest, but still maintains the significant negative correlation ($P < 0.01$; $r = -0.69$; $R^2 = 0.48$).

The relationship between O and R (Fig. 6A) also shows a high negative correlation ($r = -0.88$), although with a lower determination coefficient ($R^2 = 0.78$) for the overall sample, although for individual groups the regression index values vary greatly. Pterosaurs have the highest index ($R^2 = 0.91$), followed by birds ($R^2 = 0.81$). Theropods and ornitischians ($R^2 = 0.71$ and $R^2 = 0.72$, respectively), and sauropodomorphs display the lowest correlation values ($R^2 = 0.52$; refer to Table 1 for regression equations and Pearson's correlation coefficients).

TEST FOR SIZE

To test for size effects, we have checked allometries strictly on adults and a few subadults, searching for covariation between changes in different traits across the branches of a phylogeny (Klingenberg, 1996). Principal component analysis (PCA) and residuals were applied to test for such allometries in our sample.

For PCA by means of a covariance matrix, log-transformed variables were analysed (see Table 2). We performed two tests, a general one and a partial

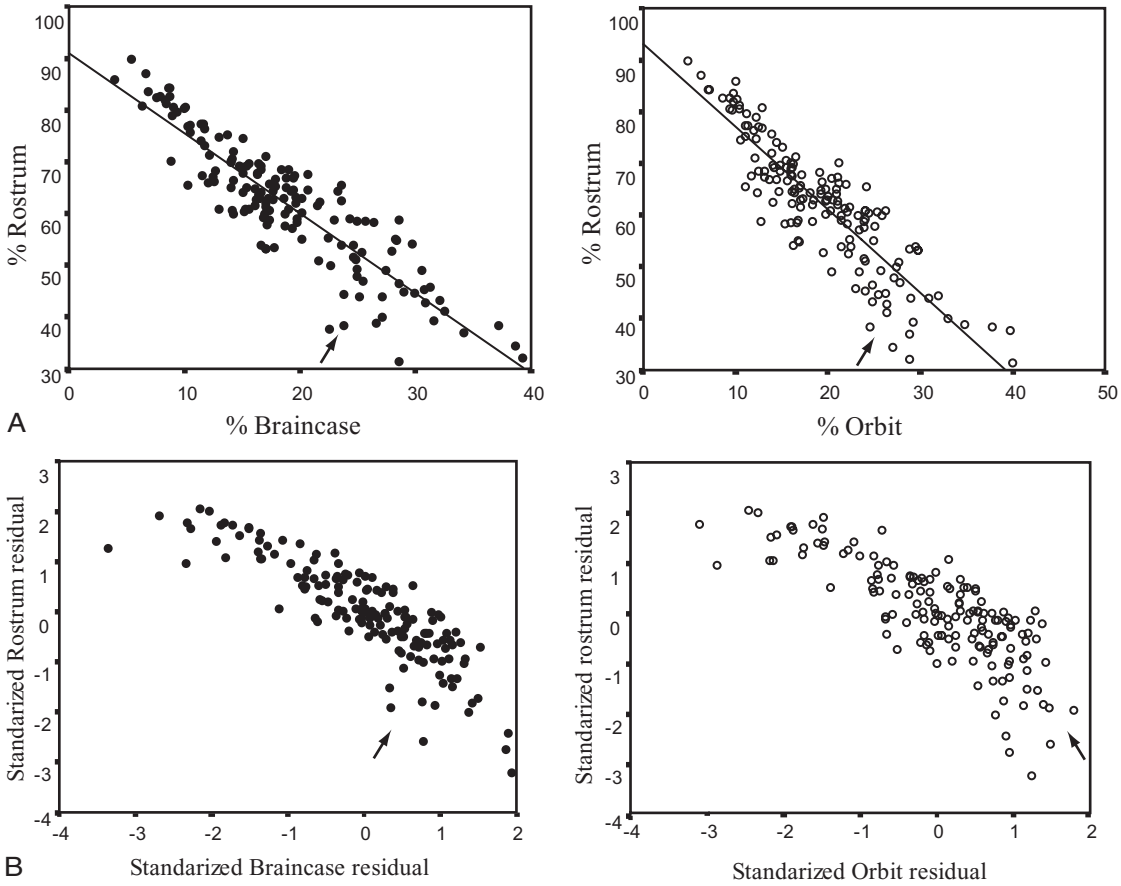

Figure 6. Regressions. (A) Scatterplot for braincase and orbit against rostrum proportions. Regression equation between braincase and rostrum with $R^2 = 0.80$ is $y = -1.555x + 91.045$. Equation for orbit against rostrum, with $R^2 = 0.78$ is, $y = -1.614x + 93.335$. Symbols are chosen according to rostral types, although taxa overlap over the region as in empirical morphospace. Arrow points to Falconiformes' outlier taxa. (B) Scatterplots for residuals yield the same strong negative correlation between skull anatomical units.

second one by groups. In the general analysis, overall Component 1 reveals size and rostral variation. It accounts for 88.96% of the total explained variance (Table 2), with the highest loading on log R and lowest on log O. Disparity in size within the sample is accounted from the largest (1355 mm) to the smallest (26.6 mm) individual (Fig. 7). Component 2 accounts for 8.992% of the variance, where log R, with negative sign and the highest value, is followed in the same factor but with opposite sign by log B. Component 3 explains only 2.04% of the variance, accounting for the highest loadings between log B and log O with opposite sign.

When analysed by groups (Table 2), only the first two components of PCA are described herein since only allometries are checked. Component 1 in every group maintains the highest loading on log R, whereas loadings over log B and log O vary. In ornithischians and sauropodomorphs log O has slightly higher loadings (sauropodomorphs have higher values, although the relatively small size of the sample must be taken into account). Pterosaurs, theropods and birds have higher loading values on log B. However, the most striking issue is that besides these subtle loading differences, ornithischians and theropods have all their variables loading quite similarly for size. It is also worth mentioning that, for Component 1, birds account for 75% of explained variance, against 90% of total explained variance displayed by the remaining groups.

For results obtained in Component 2, loadings can be classified differently: ones with log B and log O are the highest and similar in value (pterosaurs and birds), and the remainder with only high loadings on log B (ornithischians, theropods and sauropodomorphs), where log O loadings are low (very close to zero).

When proportions are plotted against total baseline length by groups (Fig. 7), as size increases in the scat-

terplots, rostrum proportion increases with convex asymptotic curves, whereas curves for braincase and orbit proportions decrease with concave asymptotic curves. However, whilst all groups behave similarly, theropods, and to some extent ornithischians, yield a different slope when reaching large sizes. In fact, when surpassing sizes of approximately 200 mm, slopes begin to straighten out to reach almost zero, while they remain invariable up to the largest measurements of total baseline. As an exploratory tool for comparative purposes, tests for residuals have been also checked. Standardized residuals were obtained

Table 1. Equations for each group between braincase–rostrum and orbit–rostrum proportions (%); r = Pearson's correlation coefficient. All coefficients are significant at $P < 0.01$

Clade	B–R equation	Correlation coefficient (r)	O–R equation	Correlation coefficient (r)
Pterosauria	$y = 98.456 - 2.188x$	–0.932	$y = 97.032 - 1.558x$	–0.969
Ornithischia	$y = 88.255 - 1.430x$	–0.944	$y = 98.283 - 1.993x$	–0.866
Sauropodomorpha	$y = 83.168 - 1.29x$	–0.918	$y = 96.398 - 1.740x$	–0.776
Theropoda	$y = 81.957 - 0.998x$	–0.615	$y = 82.902 - 1.08x$	–0.787
Aves	$y = 91.979 - 1.599x$	–0.870	$y = 89.437 - 1.507x$	–0.890

Table 2. Principal components obtained data for $\log_{10}$-transformed variables (B = braincase, O = orbit, R = rostrum)

		Component		
General sample		1	2	3
Archosaurs	Explained variance (%)	88.9648	8.9924	2.0428
	log B	0.942	0.300	–0.153
	log O	0.951	0.210	0.228
	log R	0.940	–0.341	–0.019
Pterosauria	Explained variance (%)	90.2181	7.5309	2.2510
	log B	0.929	0.326	–0.172
	log O	0.908	0.299	0.292
	log R	0.972	–0.236	–0.003
Ornithischia	Explained variance (%)	93.8286	5.3036	0.8678
	log B	0.909	0.416	–0.037
	log O	0.982	–0.020	0.189
	log R	0.988	–0.149	–0.050
Sauropodomorpha	Explained variance (%)	95.1031	3.1051	1.7919
	log B	0.922	0.387	0.020
	log O	0.974	–0.094	0.207
	log R	0.992	–0.068	–0.106
Theropoda	Explained variance (%)	94.2946	3.9519	1.7535
	log B	0.963	0.270	–0.027
	log O	0.960	–0.082	0.269
	log R	0.982	–0.167	–0.088
Aves	Explained variance (%)	75.9139	17.9131	6. 1730
	log B	0.648	0.664	–0.373
	log O	0.632	0.618	0.468
	log R	0.974	–0.229	–0.003

Figure 7. Proportions of each group plotted against total baseline (BL) length. Note that in theropods, the braincase displays a lower slope than the remaining groups. Above approximately 200 mm, theropods are a good example of lowering to almost zero slope value. Arrow in Aves points to *Diatryma* as a special case for size within the group.

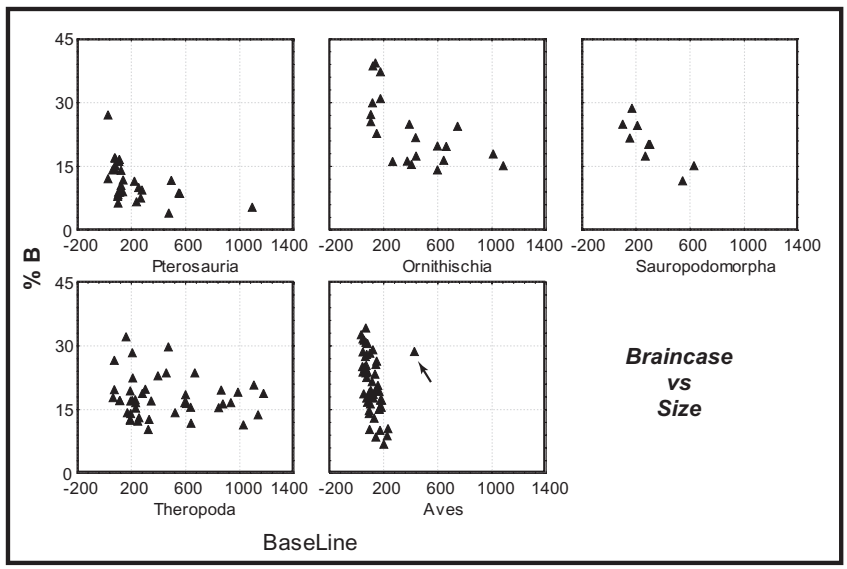
% B
Pterosauria
Ornithischia
Sauropodomorpha
Theropoda
Aves
Braincase
vs
Size
BaseLine

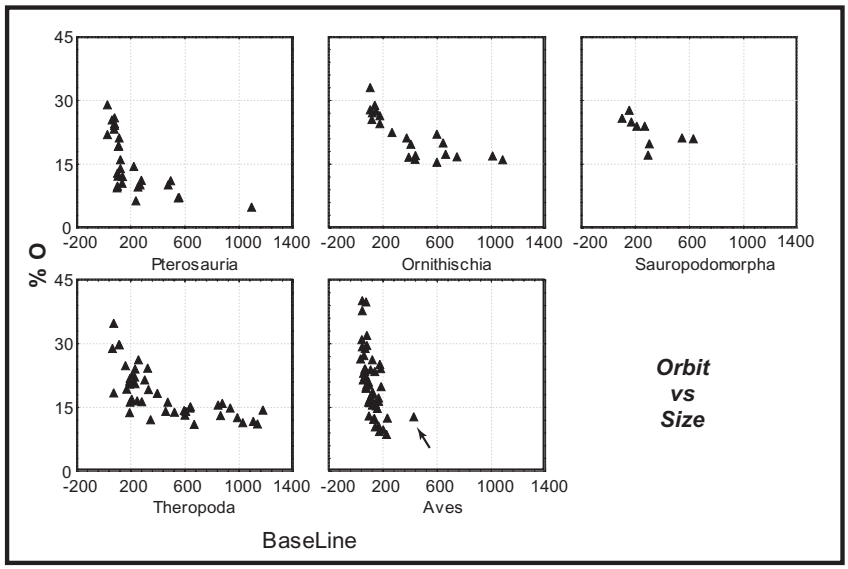
% O
Pterosauria
Ornithischia
Sauropodomorpha
Theropoda
Aves
Orbit
vs
Size
BaseLine

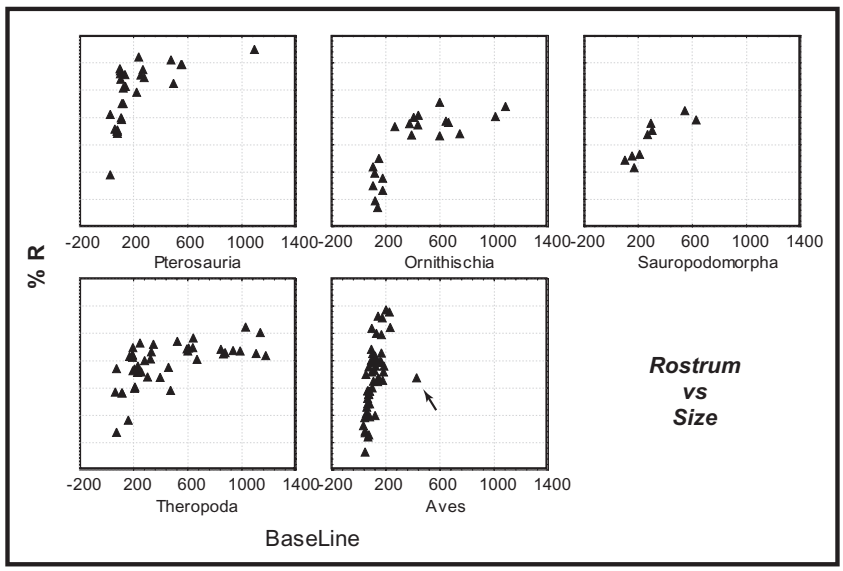
% R
Pterosauria
Ornithischia
Sauropodomorpha
Theropoda
Aves
Rostrum
vs
Size
BaseLine

from total skull length with the same log-transformed variables used for PCA (Fig. 6B).

OUTLIERS

Some particular outliers were excluded when analysing data. It must be noted that all measured taxa were plotted on the empirical morphospace, so as to amplify the total extent of natural occurrences. Thus, not even outliers violate the numerical frontiers defined for natural occurrences over the morphospace.

Detected outliers need to be specified separately due to the relevance they might have in calculations. The sample is a mixture of both reconstructions and real material, which allows us to keep track of measurement errors and test accuracy. Reconstruction errors were considered and deleted in the rare cases where, when comparing two samples of a same individual, one of the pair was behaving extremely differently to either the other in the pair, or to the whole sample.

Extreme quantitative values in braincase proportion were detected in psittacosaurs (*Psittacosaurus meileyungensis* and *Psittacosaurus sinensis*), whilst Falconiformes (*Falco tinnunculus* and *Pernis apivorus*) gave extreme orbit proportions. If only Falconiformes are subtracted, psittacosaurs appear as outliers for the smallest rostrum proportion values, while if both are deleted the sample becomes homogenous enough to lack outliers for any of the proportions. All these outliers characterized by their extreme values were included in the analyses.

When tested by groups, only theropods have extremes; for the three proportions, *Oviraptor philoceratops* (from Barsbold, Maryanska & Osmólska, 1990) and *Compsognathus longipes* (from Paul, 1988). The latter was disregarded for calculations because when it was compared to *Compsognathus longipes* (from Norman, 1990), the former did not yield extreme values, whereas Paul's (1988) was an extreme for the three proportions. Besides, for rostrum proportion it yielded values more than three interquartile ranges away from the box for rostrum proportion of its own group.

For the same tests applied to the Braincase/Orbit relationship (Fig. 4C), noticeable outliers are *Phalacrocorax aristotelis* (MNCN18672) and *Carnotaurus sastrei* (from Paul, 1988), both being extremes for higher ratio values, followed by *Diatryma gigantea* (from Witmer & Rose, 1991), *Albertosaurus libratus* (from Carr, 1999) and *Tyrannosaurus rex* (Osborn, 1905 and Czerkas & Czercas, 1990). *Phalacrocorax* was expected to be an outlier due to problems with data acquisition for the braincase, whilst *Albertosaurus* could arguably be a subadult (Carr, 1999). *Tyrannosaurus* (AMNH 5247) can be considered an adult (T. D. Carr, pers. comm.), and was left in for analyses. *Carnotaurus* (from Paul, 1988) could be considered a wrong reconstruction and was excluded from analysis because a cast from the real skull had also been sampled without yielding any detectable extreme values. *Diatryma gigantea* cannot be compared to any similar specimen and has therefore been included. *Dromaeosaurus albertensis* (from Colbert & Russel, 1969) metrics behave differently to the rest of the sample and can be contrasted against Currie's (1995) reconstruction, which does not yield any conspicuous differences. The former *Dromaeosaurus* was also disregarded. Other examples (Fig. 4C) are outliers for the Braincase/Orbit ratio, i.e. *Porphyrio mantelli* (from Witmer, 1991), compared to a natural specimen *Porphyrio porphyrio* (MNCN 23433), although they have all been included in analyses.

DISCUSSION

Morphospace is a tool that extracts the extent of occurrences from the combination of the three proportions obtained within the skull. These proportions have shown a precise positioning over the empirical morphospace, defining a tight region, where a pattern of rostral conditions can also be confirmed. Although the rostrum is one of the most variable characters of the archosaurian skull (see also Witmer, 1997), it has been possible to approach a geometric pattern in terms of the negative covariation between braincase and the rostrum, finding that rostral variation can be stated in terms of a linear equation. In addition, analysis of the orbit has revealed its important role within skull morphology, which has lead us to postulate that the three anatomical units studied must be integrated modules.

As archosaur skulls can be classified according to their rostral condition, this seems to be dependent upon a proportional relationship between the braincase and orbit. Thus, brevirostral, mesorostral and longirostral become defined by a metric trade-off between the three cranial modules. A trophic device, the rostrum, turns out to be morphologically harmonized with other elements endowed with completely different functions (vision and motor co-ordination, for instance). Yet, along the geometric pattern between the anatomical skull modules in all archosaurs, slight shifting from the general model might be grounded either on functional or developmental constraints (Schwenk & Wagner, 2001).

A shifting from the model can be detected in birds, where the regression index for rostrum–braincase can be significantly increased by excluding only a few falconiform taxa (Fig. 6A), the most 'orbitalised' organisms in terms of a trait within the model (see Outliers above). While functional and physiological constraints

have been largely described for the orbit (Martin, 1985), less attention has been paid to developmental explanations. *Falco tinnunculus* and *Pernis apivorus* occupy a position of extreme brevirostrallity within the morphospace. Developmental timing or heterochrony might require more attention following the finding that only brevirostral types, at least the actual birds, are mainly altricial organisms (Fig. 8). In fact, when developmental condition is checked in hatchlings, precocial condition happens to be restrained to meso- and longirostral types, while altriciality seems to cover the entire rostral type spectrum. This is to be expected, since altriciality is the most widespread development condition in birds (Starck, 1993). Although it would seem more feasible to suggest that shifts in developmental timing would affect orbit proportion and its relationship with the remaining anatomical units within the skull, further analysis would be required to support this developmental effect.

Among all the rostral types, mesorostral is the one with the highest number of occurrences in all the sampled groups. Within a phylogenetic framework, mesorostrallity implies the plesiomorphic condition, as it is the broader type in Archosauria (see Fig. 2), although the brevirostral type is also at the basal node of all Dinosauria groups considered. Mesorostral and brevirostral yield a similar range of variation between orbit and braincase. On the other hand, longirostral seems to be a derived condition, being restricted to a narrower interval towards a 1:1 braincase–orbit trait (Fig. 4C). Mesorostrallity embraces the complete size spectrum of skull length (Fig. 9), while above log-baseline = 2.25 (approximately 180 mm in length), there are no brevirostral types and, on the contrary,

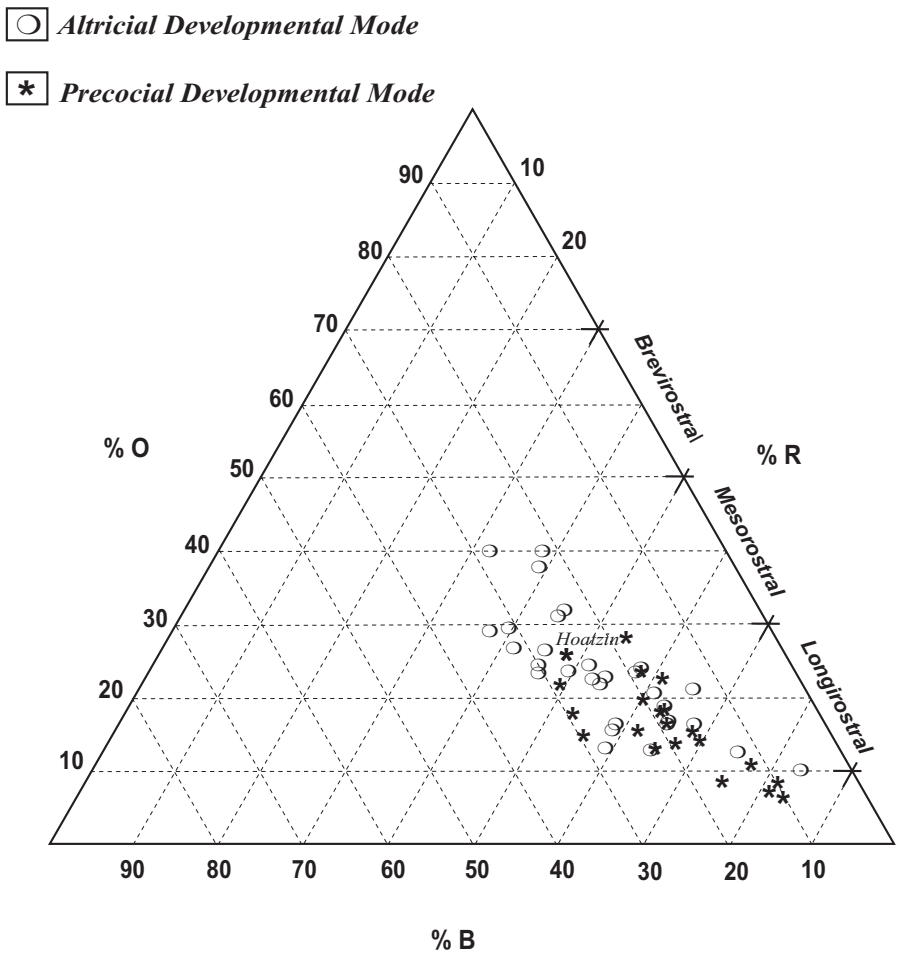

Figure 8. Distribution of developmental types in modern birds (characterization extracted from Starck, 1993). Special cases are *Hoatzin* and *Chauna torcuta* (from Witmer & Rose, 1991); slight brevirostrals (47.9 and 49.1 respectively) and precocials. Interestingly, it is difficult to assign the hoatzin to a developmental type (Nice, 1962 *fide* Starck & Ricklefs, 1998).

below 2.00 (approximately 100 mm) no longirostral types occur in our sample.

When rostral size proportion is tested against size (baseline length) in every group, the rostrum always displays a positive growth according to size acquisition. For both braincase and orbit, in contrast, there is a shift to negative slopes with increased sizes. Nevertheless, a divergence in the static allometry pattern occurs in theropods since proportions tend to be held quite constant, displaying an almost isometric behaviour (especially in regard to the braincase proportion) when reaching certain sizes. Although maintaining the general rule of the negative allometry of the rostrum against the braincase, size acquisition affects the braincase and, to a lesser degree the rostrum, which is mainly displayed when reaching approximately 220–240 mm of total baseline length. This singular growth pattern demonstrates the difficulties in trying to differentiate between ontogenetic stages in theropods (see Carr, 1999 for a thorough study describing *Nannotyranus* as a juvenile *Tyrannosaurus*).

Within a phylogenetic framework, contrasted evolutionary allometry might isolate theropods from the remaining clades of the Dinosauria lineage. This feature could be treated as an autapomorphy of non-avian theropods, as opposed to its descendant branch (Methornites). Birds, in contrast, retain the common allometric condition present in the remaining sampled groups.

While the most common occurrences reveal a negative correlation between the rostrum and orbits, this latter anatomical module suggests a further interpretation of the skull's pattern of variation. Principal components yield a clear distinction between pterosaurs and birds on the one hand, where orbit and braincase load almost equally for Component 2, and the remaining groups, where the orbit does not affect proportions. Pterosaurs and birds can be classed as flyers, with a higher grade of encephalization and orbitalization (King & King, 1979). Thus, functional convergence offers a meaningful explanation for this result, as the dendrogram reveals. (Fig. 2).

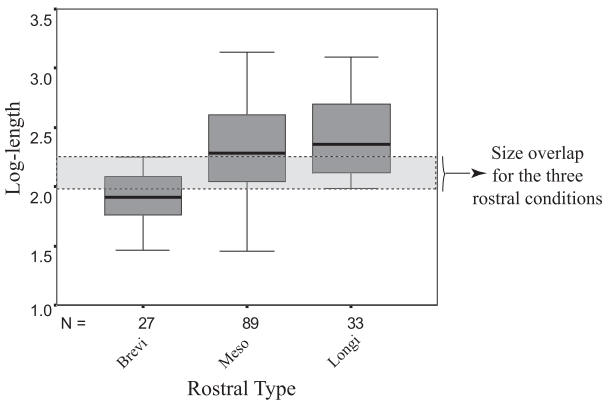

Figure 9. Box and whiskers plot displaying how size is distributed along the three rostral conditions. Shaded stripe denotes matched overlapping lengths within the sample.

Finally, a steady geometrical skull pattern along the archosaurian lineage can supply an extremely useful tool when testing for the accuracy of reconstructed fossil taxa, as well as an accurate predictive tool when trying to reconstruct incomplete specimens, a common occurrence in palaeontology. A generalized equation for regression provides a premise of a common skull proportion pattern within the group, leading to a comprehensive way to reconstruct skulls found incomplete. As analysis shows, reconstructions are amazingly accurate. Nevertheless, a metric rule that reinforces accuracy also enhances reliability.

CONCLUSIONS

This study has primarily demonstrated the strikingly conservative pattern of skull proportions in the archosaurs studied. The rostrum is geometrically linked principally to the braincase, where mesorostrallity is the basal condition in Pterosauria and Dinosauria. With regards to this point, we have found that predictions on the relation between the braincase and facial complex proposed by Enlow (Enlow & Azuma, 1975; Enlow & Hans, 1996) in mammals is a premise that may be extended to archosaurs. If we plot mammals in the empirical morphospace (Fig. 4A) we see clearly that, despite the relationship that should exist between braincase and rostrum, mammals occupy a distinct position, implying they have different skull geometry with a lineage-specific organization. In terms of proportion and according to the way we have operated (in two dimensions), the braincase is much larger than the orbit in the cat (*Felis catus*), while in humans the braincase can be eight times as large as the orbit. This could be partially explained by encephalization, although this issue needs further exploration with a less restricted methodology. This study has been carried out strictly in two dimensions as a preliminary approach. Three dimensional analyses will allow us to explore how volume as a parameter is related to size and how its changes, regarding the orbit and/or the brain, will affect the whole craniofacial complex. 3D geometric morphometrics will provide a detailed description of localized changes in each module which will also enable the prediction of skull configuration trends. Such trends will provide information on the dynamics that uphold the constructional geometric rule found in archosaurs.

Approaches to a transverse comparison within major clades such as Archosauria or Mammalia yield insights

into macroevolutionary patterns. Results have revealed the existence of archosaurian skull geometry as a constant constructional morphological organization, where three integrated modules follow a variation rule. The permanence of this underlying skull geometry highlights an independence from other sources of variation, such as changing adaptive conditions.

Modular behaviour has also been stated in developmental studies; for example, extirpating the orbits in chick embryos resulted in disturbances to the braincase (Herring, 1993). This general model pursues a constructional explanation to explore the effect the variation of the modules might exert over the whole, thus extracting partially hidden information (Dullemeijer & Zweers, 1997). This information helps unveil the phenotypic invariants otherwise inconceivable since studies of morphological changes are always carried out on discrete elements to construct phylogenies. We understand that particularizing the units of study provides for good explanatory formulas, although yielding only partial solutions. For instance, few examples have been cited with regard to the rostrum and the orbits, where explanations have described their sizes and/or shapes as merely functional devices. Instead, within a general constructional framework, the study of covariation among modules takes a step further in understanding the common causal patterns and processes observed in macroevolution.

We have arrived at an assessment of three rostral conditions: brevirostral, mesorostral and longirostral, defining them as a metric trade-off among the cranial modules, where we stress the geometrical constraints of these rostral conditions resulting in braincase:orbit ratio values limited to a range of 2:1 to 1:2. Among the three rostral types, the most longirostral (pterosaurs and birds) show a more restrictive braincase:orbit ratio value, that is, restrained closer to a 1:1 ratio relationship. The largest number of occurrences within longirostral species belongs to pterosaurs and birds, between which a convergent pattern appears. Thus, we suggest that encephalization should never be decoupled from orbitalization, in order to understand this convergent condition in flying archosaurs.

Rostral types are expressed differentially according to size (total skull baseline length). Brevirostrals never reach a size above 180 mm. Regarding size, we also find that gigantism (i.e. theropods) resembles a proper type of proportional growth which maintains the size acquisition close to isometry.

The present paper introduces the possibility of exploring the evolutionary variation of the amniote skull by studying the existence and role of the evolutionary modular units integrating the morphology of the skull. Further research should include the use of 3D geometric morphometrics, and the broadening of the sample, both in number of clades and specimens, which will expand the limits of empirical morphospace to display the realm of natural archosaurian skull occurrences. Additionally, the study of ontogenetic trajectories will clearly help to characterize the dynamics of localized skull changes, while also allowing the testing of the role of development in their explanation.

ACKNOWLEDGEMENTS

The authors acknowledge Josefina Barreiro at the Museo Nacional de Ciencias Naturales de Madrid (CSIC), and Dr Fancisco Pastor at the Museo de Anatomía de la Universidad de Valladolid, for granting access to specimen collections. Also Drs Jorge Morales, Nieves López, and Blanca Ruiz Zapata, for their comments on the initial phases of this study, Markus Bastir, Susan Evans, and Antonio Rosas for their suggestions on the elaboration of the manuscript and final corrections, and Thomas Carr who provided with tyrannosaurids and with helpful comments about them. Juan Carlos Pavón and Aitor Arauz-Chapman helped with the English revision of the manuscript. J. Marugán-Lobón is supported by the Spanish Ministerio de Educación, Cultura y Deporte, F.P.U. funds, reference AP2001-0912, under the project DGCYT BTE2001-0185-C0201/.

REREFENCES

Attridge J, Crompton AW, Jenkins FA Jr. 1985. The Southern African Liassic prosauropod *Massospondylus* discovered in North America. *Journal of Vertebrate Paleontology* **5** (2)**:** 128–132.

Baker R, Williams M, Currie P. 1988. *Nannotyrannus*, a new genus of pygmy tyrannosaur from the Late Cretaceous of Montana. *Hunteria* **1:** 1–30.

Barsbold R, Maryanska T. 1990a. Ornithomimosauria. In: Weischampel DB, Dodson P, Osmólska H, eds. *The Dinosauria*. Berkeley: University of California Press, 409–415.

Barsbold R, Maryanska T. 1990b. Segnosauria. In: Weischampel DB, Dodson P, Osmólska H, eds. *The Dinosauria*. Berkeley: University of California Press, 409–415.

Barsbold R, Maryanska T, Osmólska H. 1990. Oviraptorosauria. In: Weischampel DB, Dodson P, Osmólska H, eds. *The Dinosauria*. Berkeley: University of California Press, 409–415.

Baumel JJ, Witmer LM. 1993. *Osteologia*. In: Baumel JJ, Evans HE, Van den Berge JC, eds. *Handbook of avian anatomy: nomina anatomica avium*, 2nd edn. *Publications of the Nuttal Ornithological Club* 23: 45–132.

de Beer GR. 1985. *The development of the vertebrate skull*, 3rd edn. Chicago: The University of Chicago Press.

Benton MJ. 1990. Origin and interrelatonships of dinosaurs. In: Weischampel DB, Dodson P, Osmólska H, eds. *The Dinosauria*. Berkeley: University of California Press, 11–30.

Benton MJ. 1997. Origin and evolution of dinosaurs. In: Farlow JO, Brett-Surman MK, eds. *The complete dinosaur*. Indianapolis: Indiana University Press.

Benton MJ. 1999. *Scleromochlus taylori* and the origin of dinosaurs and pterosaurs. *Philosophical Transactions of the Royal Society of London B* **334:** 1423–1466.

Brochu CA. 2001. Progress and future directions in archosaur phylogenetics. *Journal of Palaeontology* **75** (6)**:** 1185–1201.

Busbey AB. 1995. The structural consequences of skull flattening in crocodilians. In: Thomason J, ed. *Functional morphology in vertebrate paleontology*. Cambridge, MA: Cambridge University Press, 173–193.

Calvo JO, Coria R. 1998. New specimen of *Giganotosaurus carolinii* (Coria & Salgado, 1995), supports it as the largest theropod ever found. *Gaia* **15:** 117–122.

Carr TD. 1999. Craniofacial ontogeny in Tyranosauridae (Dinosauria: Coelurosauria). *Journal of Vertebrate Paleontology* **19 (3):** 494–520.

Chapman RE, Raskin-Gutman D. 2001. Quantifying morphology. In: Briggs DEG, Crowther PR, eds. *Palaeobiology 2*, London: Blackwell Science Ltd, 489–492.

Charig AJ, Milner AC. 1997. *Baryonyx walkeri*, a fish eating dinosaur from the wealden of Surrey. *Bulletin of the Natural History Museum, Geology* **53:** 11–70.

Colbert EH. 1989. The Triassic dinosaur *Coelophysis*. *Museum of Northern Arizona Bulletin* **57:** 1–160.

Colbert EH, Russel DA. 1969. The small Cretaceous dinosaur *Dromaeosaurus*. *American Museum Novitates* **2380:** 1–49.

Currie PJ. 1995. New information on the anatomy and relationships of *Dromaeosaurus albertensis* (Dinosauria: Theropoda). *Journal of Vertebrate Paleontology* **15** (3)**:** 576–591.

Currie PJ. 1997. Raptors. In: Padian K, Currie PJ, eds. *Encyclopedia of dinosaurs*. London: Academic Press, 626.

Currie PJ, Carpenter K. 2000. *Acrocanthosaurus atokensis* from Antlers Formation, Oklahoma, U.S.A. *Geodiversitas* **22** (2)**:** 207–246.

Czerkas SJ, Czercas SA. 1990. *Dinosaurs: a global view*. Surrey: Dragon's World Ltd.

Dullemeijer P, Zweers GA. 1997. The variety of explanations of living forms and structures. *European Journal of Morphology* **35** (5)**:** 354–364.

Enlow DH, Azuma M. 1975. Functional growth boundaries in the human and mammalian face. In: Langman J, ed. *Morphogenesis and malformation of the face and the brain.* New York: The National Foundation, 217–230.

Enlow DH, Hans MG. 1996. *Essentials of facial growth*. London: W.B. Saunders Co.

Feduccia A. 1999. *The origin and evolution of birds*, 2nd edn. New Haven: Yale University press.

Galton P. 1974. The ornithischian dinosaur *Hypsilophodon* from the Wealden of the Isle of Wight. *Bulletin of the British Museum of Natural History, Geology* **25** (1)**:** 1–152.

Galton PM. 1985. Cranial anatomy of the prosauropod dinosaur *Sellosaurus gracilis* from the Middle Stubensandstein (Upper Jurassic) of NordWürrtenberg, West Germany. *Stuttgarter Beiträge zur Naturkunde B* **118:** 1–29.

Galton PM. 1990. Basal Sauropodomorpha-Prosauropoda. In: Weischampel DB, Dodson P, Osmólska H, eds. *The Dinosauria*. Berkeley: University of California Press, 579–592.

Gatesy SM, Middleton KM. 1997. Bipedalism, flight, and the evolution of theropod locomotor diversity. *Journal of Vertebrate Paleontology* **17** (2)**:** 308–329.

Gatesy SM, Middleton KM. 1999. Theropod hind limb disparity revisited: a response. *Journal of Vertebrate Paleontology* **19** (3)**:** 602–605.

Ghetie V, Chitescu ST, Cotofan VY, Hillebrand A. 1981. *Atlas de Anatomía de las Aves Domésticas.* Madrid: Paraninfo-Acribia.

Gilmore CW. 1920. Osteology of the carnivorous dinosauria in the U.S National Museum, with special reference to the genera *Antrodesmus* (*Allosaurus*) and *Ceratosaurus*. *United States National Museum Bulletin* **110:** 1–159.

Gould SJ. 1977. *Ontogeny and phylogeny*. London: The Belknap Press of Harvard University Press.

Gould SJ. 1993. *Brontosaurus y la Nalga del Ministro. Reflexiones sobre historia natural.* Madrid: Circulo de Lectores.

Herring SW. 1993. Epigenetic and functional influeces on skull growth. In: Hanken J, Hall B, eds. *The skull*, Vol. 2. Development. Chicago: The University of Chicago Press.

Holtz TR Jr. 1998. A new phylogeny of the carnivorous dinosaurs. *Gaia* **15:** 15–61.

Kardong KV. 1999. *Vertebrados: Anatomía comparada, función y evolución.* Madrid: McGraw-Hill Interamericana.

Khun O. 1976. Thecodontia. In: Kuhn O, Wellnhofer P, eds. *Enciclopedia of paleoherpetology*. Vol. 13. Stuttgart/New York: Gustav Fisher Verlag, 1–136.

King AS, King DZ. 1979. Avian morphology: general principles. In: King AS, Mclelland J, eds. *Form and function in birds.* London: Academic Press, 1–38.

Klingenberg CP. 1996. Multivariate allometry. In: Marcus LF, ed. *Advances in morphometrics*. New York: Plenum Press.

Lewontin RC. 2000. *Genes, organismo y ambiente. Las relaciones de causa y efecto en biología.* Barcelona: Gedisa.

Madsen JH Jr. 1976. *Allosaurus fragilis*. A revised osteology. *Utah Geological and Mineral Survey Bulletin* **109:** 1–163.

Martin GR. 1985. Eye. In: King AS, Mclelland J, eds. *Form and function in birds*. London: Academic Press, 311–374.

Maryanska T. 1990. Pachycephalosauria. In: Weischampel DB, Dodson P, Osmólska H, eds. *The Dinosauria*. Berkeley: University of California Press, 564–577.

Mazzetta GV, Fariña RA, Vizcaíno SF. 1998. On the paleobiology of the South American horned theropod *Carnotaurus sastrei* Bonaparte. *Gaia* **15** (185)**:** 192.

McGhee GR Jr. 1999. *Theoretical morphology. The concept and its applications. Perspectives in paleobiology and Earth history*. New York: Columbia University Press.

Morony JJ, Bock WJ, Farrand J. 1975. *Reference list of the birds of the world*. New York: Department of Ornithology American Museum of Natural History.

Nice MM. 1962. Development of behaviour in precocial birds. *Transactions of the Linnean Society* **8:** 1–211.

Norman D. 1984. On the cranial morphology and evolution of Ornithopod dinosaurs. *Symposia of the Zoological Society of London* **52:** 521–547.

Norman D. 1986. On the anatomy of *Iguanodon atherfieldensis* (Ornithischia: Ornithopoda). *Bulletin Institute Royal de Sciences Naturelles du Belgique* **56:** 281–372.

Norman D. 1990. Problematic Theropoda: 'Coelurosaurs'. In: Weischampel DB, Dodson P, Osmólska H, eds. *The Dinosauria*. Berkeley: University of California Press, 280–305.

Norman D, Hilpert KH, Holder H. 1987. Die Wilbertierfauna von Nehden (Sauerland), Westdeutschland. *Geologie und Palaeontologie Westfalense* **8:** 1–77.

Norman D, Weischampel DB. 1991a. Feeding mechanisms in some small herbivorous dinosaurs: processes and patterns. In: Rayner JMV, Wooton RJ, eds. *Biomechanics in evolution*. Cambridge: Cambridge University Press, 161–181.

Norman D, Weischampel DB. 1991b. Iguanodontidae and related ornithopods. In: Weischampel DB, Dodson P, Osmólska H, eds. *The Dinosauria*. Berkeley: University of California Press, 510–533.

Osborn HF. 1905. *Tyrannosaurus* and other Cretaceous carnivorous dinosaurs. *Bulletin of the American Museum of Natural History* **21:** 259–265.

Ostrom JH. 1970. Stratigraphy and paleontology of the Cloverly Formation (Lower Cretaceous) of the Bighorn Basin area, Wyoming and Montana. *Peabody Museum of Natural History Bulletin* **35:** 1–234.

Padian K. 2001. Cross-testing adaptive hypothesis: phylogenetic analysis and the origin of bird flight. *American Zoologist* **41:** 598–607.

Paul GS. 1988. *Predatory dinosaurs of the World. A complete illustrated guide*. New York: New York Academy of Sciences.

Paul GS. 1993. Are the *Syntarsus* and the Whitaker Theropods the same genus?. *New Mexico Museum of Natural History and Science* **3:** 397–402.

Proctor NS, Lynch PJ. 1993. *Manual of ornithology. Avian structure and function*. New Haven: Yale University Press.

Rasskin-Gutman D. 1995. Modelos geométricos y Topológicos en Morfología. Exploración del morfoespacio afín. Aplicaciones en paleobiología. Unpublished DPhil Thesis, Universidad Autónoma de Madrid.

Rasskin-Gutman D, Buscalioni AD. 2001. Theoretical morphology of the Archosaur (Reptilia: Diapsida) pelvic girdle. *Paleobiology* **27** (1)**:** 59–78.

Russel DA. 1970. Tyrannosaurids from the Late Cretaceous of Western Canada. *National Museum of Natural Sciences Publications in Paleontology* **1:** 1–30.

Schwenk K, Wagner GP. 2001. Function and the evolution of phenotipic stability: Conecting pattern to process. *American Zoologist* **41:** 552–563.

Sereno PC. 1990. Psittacosauridae. In: Weischampel DB, Dodson P, Osmólska H, eds. *The Dinosauria*. Berkeley: University of California Press, 579–592.

Sereno PC. 1991a. Basal Archosaurs. Phylogenetic relationships and functional implications. *Journal of Vertebrate Paleontology* **11:** 1–53. (suppl. 4)

Sereno PC. 1991b. *Lesothosaurus*, 'Fabrosaurids' and the early evolution of Ornithischia. *Journal of Vertebrate Paleontology* **11** (2)**:** 169–197.

Sereno PC. 1999. The evolution of dinosaurs. *Science* **284:** 2137–2147.

Sereno PC, Novas FE. 1993. The skull and neck of the basal theropod *Herrerasaurs ischigualastensis*. *Journal of Vertebrate Paleontology* **13** (4)**:** 451–476.

Sereno PC, Sichin C, Zhenqun C, Chenggan R. 1988. *Psittacosaurus meileyungensis* (Ornitischia: Ceratopsia), a new psittacosaur from the Lower Cretaceous of North-Eastern China. *Journal of Vertebrate Paleontology* **8** (4)**:** 366–377.

Sereno PC, Zhimin D. 1992. The skull of the basal stegosaur *Huayangosaurus taibai* and a cladistic diagnosis of Stegosauria. *Journal of Vertebrate Paleontology* **12** (3)**:** 318–343.

Starck D. 1979. Cranio-cerebral relations in recent reptiles. In: Gans C, Northcutt RG, Ulinski P, eds. *Biology of Reptilia*, Vol. 9A. London: Academic Press, 1–38.

Starck JM. 1993. Evolution of avian ontogenies. In: Power DM, ed. *Current ornithology*, Vol. 10. New York: Plenum Press, 275–366.

Starck JM, Ricklefs RE. 1998. Patterns of development: the altricial-precocial spectrum. In: Starck JM, Ricklefs RE, eds. *Avian growth and development*. New York: Oxford University Press, 3–30.

Upchurch P. 1995. The evolutionary history of sauropod dinosaurs. *Philosophical Transactions of the Royal Society of London Series B* **349:** 365–390.

Wagner PJ. 2001. Constraints in the evolution of form. In: Briggs DEG, Crowther PR, eds. *Palaeobiology 2*, London: Blackwell Science Ltd., 152–156.

Weischampel DB, Gregoriscu D, Norman DB. 1991. The Dinosaurs of Transylvania. *National Geographic Research and Exploration* **7** (2)**:** 196–215.

Weischampel DB, Horner JR. 1990. Hadrosauridae. In: Weischampel DB, Dodson P, Osmólska H, eds. *The Dinosauria*. Berkeley: University of California Press, 534–561.

Wellnhofer P. 1978. Pterosauria. In: Kuhn O, Wellnhofer P, eds. *Enciclopedia of paleoherpetology*. Stuttgart/New York: Gustav Fisher Verlag, 1–82.

Wellnhofer P. 1991. *The illustrated encyclopaedia of pterosaurs*. London: Salamander Books Ltd.

Wild R. 1978. Die flugsaurier (Reptilia: Pterosauria) aus der Oberen Trias von cene bei Bergamo, Italien. *Bolletino della Società. Paleontologica Italiana* **17** (2)**:** 176–256.

Wilson JA, Sereno PC. 1998. Early evolution and higher-level phylogeny of sauropod dinosaur. *Journal of Vertebrate Paleontology* **18** (1)**:** 68. (Suppl. 2)

Witmer LM. 1995. Homology of facial structures in extant Archosaurs (Birds and Crocodilians), with special reference to paranasal pneumacity and nasal conchae. *Journal of Morphology* **225:** 269–327.

Witmer LM. 1997. The evolution of the antorbital cavity of archosaurs: a study in soft-tissue reconstruction in the fossil record with an analysis of the function of pneumacity. *Journal of Vertebrate Paleontology* **17** (Suppl. 1)**:** 1–73.

Witmer LM, Rose KD. 1991. Biomechanics of the jaw apparatus of the gigantic Eocene bird *Diatryma*: implications for diet and mode of life. *Paleobiology* **17** (2)**:** 95–120.

Zusi RL. 1993. Patterns of diversity in the reptilian skull. In: Hanken J, Hall B, eds. *The skull, patterns of structural and systematic diversity*, Vol. 2. Chicago: The University of Chicago Press.

APPENDIX

List of species, measures and proportions studied. Abbreviations: B = braincase, O = orbit, R = rostrum, BL = baseline (B + O + R), Len = total skull length (note in some instances how it can slightly differ from BL because of caudal distance between landmark 4 and total dermatocranium extent), Cast = casts from real taxa. MAUV = Museo de Anatomía de la Universidad de Valladolid, MNCN = Museo Nacional de Ciencias Naturales de Madrid, UAM = Universidad Autónoma de Madrid, LH = Colección Las Hoyas (UAM), exp = in exposition. Major clades are grouped following references in Figure 2 (dendrogram). Bird families following Morony, Bock & Farrand (1975). (EUPAR = *Euparkeria*, SCLER = *Scleromochlus*, PTERO = PTEROSAURIA, LESOT = *Lesothosaurus*, STEGO = STEGOSAURIA, PACHY = PACHYCEPHALOSAURIA, CERAT = CERATOSAURIA, HYPSI = HYPSILOPHODONTIDAE, IGUAN = IGUANODONTIDAE, HADRO = HADROSAURIDAE, PROSA = PROSAUROPODA, SAURO = SAUROPODA, EORAP = *Eoraptor*, HERRE = HERRERASAURIDAE, CERAT = CERATOSAURIA, TETAN = TETANURAE, CARNO = CARNOSAURIA, COELU = COELUROSAURIA, MANIR = MANIRAPTORA, STRUT = STRUTIONIDAE, RHEID = RHEIDAE, DROMA = DROMAIIDAE, SPHEN = SPHENICIDAE, PROCE = PROCELARIIDAE, SULLI = SULLIDAE, PHALA = PHALACROCORACIDAE, CICON = CICONIDAE, THERE = THERESKIORNITHIDAE, PHOEN = PHOENICOPTERIDAE, ANHIM = ANHIMIDAE, ANATI = ANATIDAE, ACCIP = ACCIPITRIDAE, FALCO = FALCONIDAE, OPIST = OPISTHOCOMIDAE, GRUID = GRUIDAE, RALLI = RALLIDAE, OTIDA = OTIDAE, RECUR = RECURVIROSTRIDAE, BURHI = BURHINIDAE, SCOLO = SCOLOPACIDAE, LARID = LARIDAE, ALCID = ALCIDAE, PSITT = PSITTACIDAE, TYTON = TYTONIDAE, STRIG = STRIGIDAE, RHAMP = RHAMPHASTIDAE, PICID = PICIDAE, LANII = LANIIDAE, ARDEI = ARDEIDAE, CORVI = CORVIDAE, DIATR = *Diatryma*).

APPENDIX *Continued*

Taxa	In or from:	B (mm)	O (mm)	R (mm)	Len.	% B	% O	% R	BL
Euparkeria capensis (Eupark)	(Khun, 1976)	16.8	20.78	45.83	95.5	20.1	24.9	55	83.4
Scleromochlus taylori (SCLER)	(Benton, 1999)	7.83	8.38	12.73	28.94	27.1	29	44	28.9
Araripesaurus santanae (PTERO)	(Sereno, 1991a)	12.37	14.35	110.73	137.5	9	10.4	80.6	137.5
Pteranodon ingens (PTERO)	(Wellnhofer, 1978)	58.58	52.46	982.6	1094	5.36	4.8	89.9	1093.6
Ornithodesmus latidens (PTERO)	(Wellnhofer, 1978)	48.37	39.68	471.5	559.6	8.64	7.09	84.3	559.6
Ornithocheirus compressirostris (PTERO)	(Wellnhofer, 1978)	25.41	24.49	204.29	254.2	9.99	9.63	80.4	254.2
Gallodactylus suevicus (PTERO)	(Wellnhofer, 1978)	16.29	16.72	106.18	139.2	11.7	12	76.3	139.2
Pterodactylus antiquus (PTERO)	(Wellnhofer, 1978)	9.6	13.09	85	107.7	8.92	12.2	78.9	107.7
Germanodactylus cristatus (PTERO)	(Wellnhofer, 1978)	13.25	17.56	95.55	126.4	10.5	13.9	75.6	126.4
Rhamphorhynchus gemmingi (PTERO)	(Wellnhofer, 1978)	10.35	24.62	81.65	116.6	8.88	21.1	70	116.6
Scaphognathus crassirostris (PTERO)	(Wellnhofer, 1978)	18.58	21.51	71.66	111.8	16.6	19.3	64.1	111.8
Dorygnathus banthensis (PTERO)	(Wellnhofer, 1978)	17.57	20.05	87.73	125.4	14	16	70	125.4
Campylognathoides liassicus (PTERO)	(Wellnhofer, 1978)	13.95	19.9	48.89	82.73	16.9	24.1	59.1	82.7
Dimorphodon macronyx (PTERO)	(Wellnhofer, 1978)	25.61	32.33	165.88	223.8	11.4	14.4	74.1	223.8
Pterodaustro guinazui (PTERO)	(Wellnhofer, 1978)	15.77	15.02	207.96	238.8	6.6	6.29	87.1	238.8
Ctenochasma gracile (PTERO)	(Wellnhofer, 1978)	8.53	10	84.23	102.8	8.3	9.74	82	102.8
Gnathosaurus subulatus (PTERO)	(Wellnhofer, 1978)	26.34	31.3	223.9	281.5	9.36	11.1	79.5	281.5
Dorignathus banthensis (PTERO)	(Wild, 1978)	11.42	20.69	48	80.11	14.3	25.8	59.9	80.1
Campylognathoides liassicus (PTERO)	(Wild, 1978)	9.15	16.45	39.35	64.96	14.1	25.3	60.6	65.0
Eudimorphodon ranzii (PTERO)	(Wild, 1978)	13.32	18.23	47.07	78.62	16.9	23.2	59.9	78.6
Ornithodesmus latidens (PTERO)	(Wellnhofer, 1991)	48.35	38.71	466.66	553.7	8.73	6.99	84.3	553.7
Ctenochasma gracile (PTERO)	(Wellnhofer, 1991)	8.05	9.52	83.99	101.6	7.93	9.37	82.7	101.6
Anurognathus ammoni (PTERO)	(Wellnhofer, 1991)	3.46	6.27	18.87	28.6	12.1	21.9	66	28.6
Scaphognathus crassirostris (PTERO)	(Wellnhofer, 1991)	17.69	21.04	71.11	109.8	16.1	19.2	64.7	109.8
Pterodactylus antiquus (PTERO)	(Wellnhofer, 1991)	6.6	13.27	83.73	103.6	6.37	12.8	80.8	103.6
Eudimorphodon ranzii (PTERO)	(Wellnhofer, 1991)	12.49	20.12	49.68	82.29	15.2	24.5	60.4	82.3
Gnathosaurus subulatus (PTERO)	(Wellnhofer, 1991)	20.41	27.25	222.75	270.4	7.55	10.1	82.4	270.4
Criorhynchus sp. (PTERO)	(Wellnhofer, 1991)	57.84	54.61	383.29	495.8	11.7	11	77.3	495.7
Anhanguera santanae (PTERO)	(Wellnhofer, 1991)	18.95	48.06	410.5	477.5	3.97	10.1	86	477.5
Lesothosaurus diagnosticus (LESOT)	(Sereno, 1991)	34.09	41.18	75.02	150.3	22.7	27.4	49.9	150.3
Huayangosaurus taibai (STEGO)	(Sereno & Zhimin, 1992)	43.12	59.93	164.46	267.5	16.1	22.4	61.5	267.5
Prenocephale prenes (PACHY)	(Maryanska, 1990)	66.57	43.86	68.47	178.9	37.2	24.5	38.3	178.9
Stegoceras validum (PACHY)	(Maryanska, 1990)	54.63	46.68	75.62	176.9	30.9	26.4	42.7	176.9
Psittacosaurus sinensis (CERAT)	(Sereno, 1990)	46.92	32.84	41.71	121.5	38.6	27	34.3	121.5
Psittacosaurus youngi (CERAT)	(Sereno, 1990)	28.94	35.2	42.56	106.7	27.1	33	39.9	106.7
Psittacosaurus meileyungensis (CERAT)	(Sereno *et al.*, 1988)	54.82	40.2	44.66	139.7	39.2	28.8	32	139.7
Hypsilophodon foxii (HYPSI)	(Norman, 1984)	35.43	30.12	52.71	118.3	30	25.5	44.6	118.3
Hypsilophodon foxii (HYPSI)	(Galton, 1974)	27.41	29.91	50.45	107.8	25.4	27.8	46.8	107.8

APPENDIX *Continued*

Taxa	In or from:	B (mm)	O (mm)	R (mm)	Len.	% B	% O	% R	BL
Iguanodon atherfieldensis (IGUAN)	(Norman *et al.*, 1987)	76.67	74.99	289.84	441.5	17.4	17	65.7	441.5
Iguanodon atherfieldensis (IGUAN)	(Norman & Weischampel, 1991b)	95.57	70.86	272.85	439.3	21.8	16.1	62.1	439.3
Iguanodon bernissartensis (IGUAN)	(Norman & Weischampel, 1991b)	182.02	124.76	440.48	747.3	24.4	16.7	59	747.3
Ouranosaurus nigeriensis (IGUAN)	(Norman & Weischampel, 1991b)	84.83	92.37	422.42	599.6	14.2	15.4	70.5	599.6
Tenontosaurus tilletti (IGUAN)	(Ostrom, 1970)	61.12	79.39	235.98	376.5	16.2	21.1	62.7	376.5
Parasaurolophus Walkeri (HADRO)	(Weischampel & Horner, 1990)	118.18	131.93	348.59	598.7	19.7	22	58.2	598.7
Edmontosaurus saskatchewanensis (HADRO)	(Weischampel & Horner, 1990)	105.8	128.42	409.61	643.8	16.4	20	63.6	643.8
Anatosaurus copei (HADRO)	(Weischampel & Horner, 1990)	163.66	173.12	746.88	1084	15.1	16	68.9	1083.7
Prosaurolophus sp. (HADRO)	(Weischampel & Horner, 1990)	130.62	114.82	419.38	664.8	19.7	17.3	63.1	664.8
Saurolophus angustirostris (HADRO)	(Weischampel & Horner, 1990)	62.54	80.01	264.06	406.6	15.4	19.7	64.9	406.6
Telmatosaurus transsylvanicus (HADRO)	(Weischampel *et al.*, 1991)	97.78	65.16	229.91	392.9	24.9	16.6	58.5	392.9
Edmontosaurus regalis (HADRO)	(Norman, 1984)	180.89	170.46	659.07	1010	17.9	16.9	65.2	1010.4
Sellosaurus gracilis (PROSA)	(Galton, 1985)	52.4	50.88	109.58	229.7	24.6	23.9	51.5	212.9
Anchisaurus sp. (PROSA)	(Norman & Weischampel, 1991a)	25.69	26.52	50.84	109.2	24.9	25.7	49.3	103.1
Plateosaurus sp. (PROSA)	(Norman & Weischampel, 1991a)	46.85	64.59	158.47	318.9	17.4	23.9	58.7	269.9
Massospondylus sp. (PROSA)	(Norman & Weischampel, 1991a)	48.11	46.55	78.32	168.4	28.6	24.9	46.6	173.0
Plateosaurus sp. (PROSA)	(Galton, 1990)	59.51	50.49	185.82	330.4	20.1	17.1	62.8	295.8
Massospondylus sp. (PROSA)	(Attridge *et al.*, 1985)	33.68	43.03	79.11	182.1	21.6	27.6	50.8	155.8
Brachiosaurus bancai (SAURO)	(Upchurch, 1995)	95.13	132.13	403.25	638.5	15.1	21	64	630.5
Camarasaurus lentus (SAURO)	(Upchurch, 1995)	61.09	59.87	182.84	334.4	20.1	19.7	60.2	303.8
Diplodocus longus (SAURO)	(Upchurch, 1995)	63.1	115	366.8	550.8	11.6	21.1	67.3	544.9
Eoraptor lunensis (EORAP)	(Benton, 1997)	19.61	34.1	61.02	131	17.1	29.7	53.2	114.7
Eoraptor lunensis (EORAP)	Cast (UAM-Exp)	32	31.96	52.69	131	27.42	27.38	45.14	116.7
Herrerasaurus ischigualastensis (HERRE)	(Sereno & Novas, 1993)	59.81	64.93	178.85	303.6	19.7	21.4	58.9	303.6
Ceratosaurus nasicornis (CERAT)	(Gilmore, 1920)	59.32	42.12	247.56	349	17	12.1	70.9	349.0
Carnotaurus sastrei (CERAT)	(Paul, 1988)	123.37	81	269.66	570	29.7	16.2	54	474.0
Carnotaurus sastrei (CERAT)	Cast (UAM-Exp)	108.62	64.33	287.06	591.5	23.6	14	62.4	460.0
Carnotaurus sastrei (CERAT)	(Mazzetta *et al.*, 1998)	91	72.6	233.27	396.9	22.9	18.3	58.8	396.9
Coelophysis bauri (CERAT)	(Colbert, 1989)	37.39	26.43	129.01	192.8	19.4	13.7	66.9	192.8
Syntarsus rhodensis (CERAT)	(Colbert, 1989)	24.39	40.97	128.13	193.5	12.6	21.2	66.2	193.5
Syntarsus colberti (CERAT)	(Paul, 1993)	30.42	41.03	177.85	249.3	12.2	16.5	71.3	249.3
Syntarsus colberti (CERAT)	(Paul, 1993)	27.53	31.91	137.12	196.6	14	16.2	69.8	196.6
Syntarsus rhodensis (CERAT)	(Paul, 1993)	24.16	39.78	130.6	194.5	12.4	20.5	67.1	194.5
Syntarsus kayentakatae (CERAT)	(Paul, 1993)	35.8	44.01	129.8	209.6	17.1	21	61.9	209.6
Baryonyx walkeri (TETAN)	(Charig & Milner, 1997)	130.59	131.48	585.26	880.7	15.4	15.5	69.1	847.3
Daspletosaurus torossus (COELU)	(Russel, 1970)	155.83	138.35	642.17	936.4	16.6	14.8	68.6	936.4
Nannotyranus lancensis (COELU)	(Baker *et al.*, 1988)	98.47	84.37	411.13	594	16.6	14.2	69.2	594.0
Tyrannosaurus rex (COELU)	(Czerkas & Czercas, 1990)	228.83	129.27	746.58	1105	20.7	11.7	67.6	1104.7
Tyrannosaurus rex (COELU)	(Carr, 1999)	74.52	72.81	377.91	525.2	14.2	13.9	72	525.2
Albertosaurus libratus (COELU)	(Carr, 1999)	157.9	73.58	437.32	668.8	23.6	11	65.4	668.8

Daspletosaurus torossus (COELU)	(Paul, 1988)	188.23	123.72	676.14	1107	19	12.5	68.4	988.1
Tyrannosaurus rex (COELU)	(Paul, 1988)	221.22	169.08	786.49	1355	18.8	14.4	66.8	1176.8
Abelisaurus sp. (CERATO)	(Czerkas & Czercas, 1990)	117.37	116.83	795.6	1030	11.4	11.3	77.3	1029.8
Albertosaurus libratus (COELU)	Cast (UAM)	100	85	423	670	16.4	14	69.6	608.0
Albertosaurus libratus (COELU)	(Paul, 1988)	111.03	79.331	412.43	678	18.4	13.2	68.4	602.8
Albertosaurus libratus (COELU)	(Paul, 1988)	143.01	139.48	594.16	1040	16.3	15.9	67.8	876.7
Albertosaurus arctunguis (COELU)	(Paul, 1988)	168.86	112.78	581.83	970	19.6	13.1	67.4	863.5
Allosaurus fragilis (CARNO)	(Madsen, 1976)	99.45	94.96	445.55	640	15.5	14.8	69.6	640.0
Acrocanthosaurus atokensis (CARNO)	(Currie & Carpenter, 2000)	155.99	125.38	856.25	1253	13.7	11	75.3	1137.6
Metriacanthosaurus shangyouensis (CARNO)	(Paul, 1988)	75.14	96.68	468.61	816	11.7	15.1	73.2	640.4
Compsognathus longipes (MANIR)	(Norman, 1990)	11.77	19.07	35.4	66.24	17.8	28.8	53.4	66.2
Compsognathus longipes (MANIR)	(Paul, 1988)	20.184	26.404	29.412	76	26.6	34.7	38.7	76.0
Gallimimus bullatus (COELU)	(Barsbold & Maryanska, 1990a)	42.33	63.86	227.31	333.5	12.7	19.2	68.2	333.5
Ornithomimus samueli (COELU)	(Paul, 1988)	33.63	67.8	157.44	258	13	26.2	60.8	258.9
Ornithomimus bullatus (COELU)	(Paul, 1988)	33.43	78.83	213.63	330	10.3	24.2	65.6	325.9
Ornithomimus edmontonicus (COELU)	(Paul, 1988)	35.76	56.2	142.13	234	15.3	24	60.7	234.1
Pelecanimimus poliodon (COELU)	LH 7777 (UAM)	24.5	33.18	114.28	175.4	14.2	19.3	66.5	172.0
Erlykosaurus andrewsi (MANIR)	(Barsbold & Maryanska, 1990b)	39.79	50.82	139.28	229.9	17.3	22.1	60.6	229.9
Oviraptor philoceratops (MANIR)	(Barsbold *et al.*, 1990)	52.01	40.18	69.84	162	32.1	24.8	43.1	162.0
Dromaeosaurus albertensis (MANIR)	(Colbert & Russel, 1969)	59.33	35.37	114.7	209.4	28.3	16.9	54.8	209.4
Dromaeosaurus albertensis (MANIR)	(Currie, 1995)	47.49	47.26	116.69	211.4	22.5	22.4	55.2	211.4
Velociraptor mongoliensis (MANIR)	(Paul, 1988)	38.6	47.78	146.51	249	16.6	20.5	62.9	232.9
Velociraptor mongoliensis (MANIR)	(Currie, 1997)	14.69	13.74	46.46	74.89	19.6	18.4	62	74.9
Velociraptor mongoliensis (MANIR)	Cast (UAM-Exp)	33.28	42.69	119.58	208.7	17	21.8	61.2	195.6
Deynonychus antirrhopus (MANIR)	Cast (UAM-Exp)	53.25	46.25	184.3	318	18.8	16.3	64.9	283.8
Diatryma gigantea (DIATR)	(Witmer & Rose, 1991)	122.51	54.529	251.48	449.8	28.6	12.7	58.7	428.5
Strutio camellus (STRUT)	MAUV-Exp.	30.509	44.501	102.7	177.7	17.2	25	57.8	177.7
Rhea americana (RHEID)	MAUV-Exp.	32.2	37.168	117.71	187.1	17.2	19.9	62.9	187.1
Dromicellus novaholandie (DROMA)	MAUV-Exp.	27.633	43.97	111	182.6	15.5	24.1	60.8	182.6
Spheniscus demersus (SPHEN)	MAUV-Exp.	24.81	19.61	70.8	115.2	21.5	17	61.4	115.2
Calonectris diomedea (PROCE)	MNCN 18656	20.8	17.15	68.8	106.8	19.5	16.1	64.5	106.8
Fulmarus glacialis (PROCE)	MNCN 18653	18.8	19.99	59.95	98.73	19	20.3	60.7	98.7
Sula bassana (SULLI)	MAUV-Exp.	17.01	16.84	70.51	178.9	16.3	16.1	67.6	104.4
Morus bassanus (SULLI)	MNCN 18671	32.51	27.75	108.87	169.1	19.2	16.4	64.4	169.1
Phalacrocorax aristotelis (PHALA)	MNCN 18672	32.28	17.16	89.35	138.8	23.3	12.4	64.4	138.8
Egretta garcetta (ARDEI)	MNCN 18681	16.95	15.91	97.83	130.7	13	12.2	74.9	130.7
Ciconia ciconia (CICON)	MNCN 18696	24.37	28.92	178.74	232	10.5	12.5	77	232.0
Thereskiornis aethiopicus (THERE)	MNCN 23422	17.73	16.33	141.09	175.2	10.1	9.32	80.6	175.2
Platalea leucorodia (THERE)	MAUV-Exp.	19.89	19.536	187.99	227.4	8.75	8.59	82.7	227.4
Phoenicopteryx ruber (PHOEN)	MNCN 23527	25.25	17.69	125.13	168.1	15	10.5	74.5	168.1
Chauna torcuata (ANHIM)	(Witmer & Rose, 1991)	24.725	16.524	39.796	81.47	30.5	20.4	49.1	81.0
Anser caerulescens (ANATI)	MAUV-Exp.	21.21	21.63	77.07	119.9	17.7	18	64.3	119.9
Branta canadensis (ANATI)	(Witmer & Rose, 1991)	21.67	18.783	80.522	124.5	17.9	15.5	66.6	121.0

APPENDIX *Continued*

Taxa	In or from:	B (mm)	O (mm)	R (mm)	Len.	% B	% O	% R	BL
Marmaroneta angustrirostris (ANATI)	MNCN 18723	13.87	15.2	65.02	94.09	14.7	16.2	69.1	94.1
Acipiter gentilis (ACCIP)	MNCN 25522	24.18	20.39	26.14	70.7	34.2	28.8	37	70.7
Aquila crisaetus (ACCIP)	MNCN 19124	35.57	32.13	54.96	122.7	29	26.2	44.8	122.7
Aegypus monachus (ACCIP)	MNCN 26231	39.8	23.09	88.12	151	26.4	15.3	58.4	151.0
Pernis apivorus (ACCIP)	MAUV-Exp.	16.751	29.586	28.117	74.46	22.5	39.7	37.8	74.5
Gyps fulvus (ACCIP)	MNCN 25838	36.69	22.82	83.7	143.2	25.6	15.9	58.5	143.2
Buteo buteo (ACCIP)	MNCN 21065	19.59	26.32	36.55	82.46	23.8	31.9	44.3	82.5
Falco tinnunculus (FALCO)	MNCN 26465	13.19	18.5	14.5	46.2	28.6	40	31.4	46.2
Falco subbuteo (FALCO)	MAUV-Exp.	11.19	17.74	18.08	47.02	23.8	37.7	38.5	47.0
Opisthocomus hoazin (OPIST)	(Witmer & Rose, 1991)	14.69	16	28.22	58.95	24.9	27.2	47.9	58.9
Grus grus (GRUID)	MNCN 18498	25.47	28.93	114.35	168.8	15.1	17.2	67.8	168.8
Rallus aquaticus (RALLI)	MNCN 18802	10.16	11.63	32.6	54.39	18.7	21.4	59.9	54.4
Porphyrio porphyrio (RALLI)	MNCN 23433	21.43	14.97	40.41	76.81	27.9	19.5	52.6	76.8
Porphyrio mantelli (RALLI)	(Witmer & Rose, 1991)	27.94	16.58	54.36	101.2	28.3	16.8	55	98.9
Coccothraustes vespertinus (RALLI)	(Witmer & Rose, 1991)	11.532	9.3388	14.567	35.81	32.5	26.4	41.1	35.4
Otis tarda (OTIDA)	MAUV-Exp.	27.04	32.7	79.81	139.6	19.4	23.4	57.2	139.6
Recurvirostra avoceta (RECUR)	MNCN 18847	9.96	12.52	74.49	96.97	10.3	12.9	76.8	97.0
Burhinus oedicnemus (BURHI)	MNCN 23802	13.4	23.74	43.22	80.37	16.7	29.5	53.8	80.4
Limosa limosa (SCOLO)	MNCN 18823	12.09	14.87	115.96	142.9	8.46	10.4	81.1	142.9
Larus ridibundus (LARID)	MNCN 19995	13.51	15.13	47.99	76.63	17.6	19.7	62.6	76.6
Larus argentatus (LARID)	MNCN 18878	33.12	23.64	103.81	160.6	20.6	14.7	64.7	160.6
Fratercula arctica (ALCID)	MNCN 18865	16.55	15.78	37.81	70.14	23.6	22.5	53.9	70.1
Aratinga guarouba (PSITT)	MAUV-Exp.	17.51	12.892	25.545	55.95	31.3	23	45.7	55.9
Amazona ochrocephala (PSITT)	(Witmer & Rose, 1991)	21.798	17.01	31.99	71.15	30.8	24	45.2	70.8
Tito alba (TYTON)	MNCN 19205	16.37	14.26	35.72	66.35	24.7	21.5	53.8	66.4
Bubo bubo (STRIG)	MNCN 20384	13.4	19.98	62.23	95.61	14	20.9	65.1	95.6
Asio otus (STRIG)	MNCN 23117	17.97	15.31	32.12	65.4	27.5	23.4	49.1	65.4
Strix aluco (STRIG)	MNCN 23238	18.41	16.13	38.15	72.69	25.3	22.2	52.5	72.7
Athene noctua (STRIG)	MNCN 19235	15.02	13.9	18.63	47.55	31.6	29.2	39.2	47.6
Ramphastus tucanus (RHAMP)	MAUV-Exp.	13.935	19.72	170.03	203.8	6.84	9.68	83.5	203.7
Picus viridis (PICID)	MNCN 19093	16.74	16.17	34.51	67.42	24.8	24	51.2	67.4
Lanius senator (LANII)	MAUV-Exp.	11.273	13.845	19.749	44.86	25.1	30.9	44	44.9
Corvus corax (CORVI)	MNCN 26548	20.55	26.2	63.18	109.9	18.7	23.8	57.5	109.9
Corvus crassirostris (CORVI)	(Witmer & Rose, 1991)	23.245	23.133	78.715	124.9	18.6	18.5	62.9	125.1

3.2. Insights on avian skull shape macroevolution on the basis of Geometric Morphometric procedures

3.2.1 Introduction

This chapter summarizes some of the most relevant aspects of the phenotypic organization of the avian skull at a macroevolutionary scale. The quest might not be so edifying in the sense that avian skull shape disparity was already characterized by us elsewhere on similar morphometric basis (Marugán-Lobón and Buscalioni, 2004). However, such study was only preliminary since we did not utilize the main tools of geometric morphometrics in their full extent, nor thereby fulfilled its principal commitment, which is to tackle with biological processes (Gould, 1966; Gould 1971; Bookstein, 1998; Gayon, 2000; Roth and Mercer, 2000), via testing the covariance of shape with other independent variables (e.g. size). This chapter is the doorway for the thesis into studying skull morphology on the basis of geometric morphometric procedures.

Thus, we explore the organizational nature of the avian skull phenotype, showing and re-interpreting its patterns of disparity with a large macroevolutionary sample. However, this chapter also deals with some operational issues that we found important when applying geometric morphometrics for the study of the evolutionary morphology in the skull of avians, issues which mostly have to do with the strong variation accounted by the facial skeleton in these organisms. This will be explained in forthcoming paragraphs. Heretofore, evolutionary allometry is tested, testing shape evolution of the avian skull as a function of size to test for their covariation.

Avian skull shape disparity will be first characterized using multivariate methods of shape analysis such as relative warps analysis (see; Rohlf, 1993). These will be performed onto the shape variables obtained applying the Least Squares superimposition criterion (*General Procrustes Analysis*, or GPA; Gower, 1975; Adams et al., 2004). Shape variation will be visualized using the Thin Plate Spline interpolation function, and therefore, principal shape variables will be, once transformed, the partial warp scores plus the uniform component embedded in the weight matrix.

These shape variables symbolize salient features of the avian skull geometry on its lateral and external view by means of a configuration of p=12 landmarks that are repeatable across all the skulls. The landmarks were elected on the basis of biological and not geometrical homology (i.e. same structural and anatomical correspondence among the skulls of the monophyletic clade, and avoiding the use of geometric quasi-landmarks; see Dryden and Mardia, 1999; O'Higgins and Jones, 1999). The sample comprises N=172 skulls of birds, a

number that almost doubles the sample used in our previous survey, and the number reflects the inclusion of at least one representative of each of the approximately 80% of described modern avian families (the sample spans across 100% of Orders, and the families that are missing belong mostly to Order Passeriformes; see Appendix 1).

When exploring the shape variation of the avian skull statistically we expect to find two types of characteristic morphological changes among avian taxa (see, Marugán-Lobón and Buscalioni, 2004). One regards the relative antero-caudal proportion of the beak (which we will refer to as the *rostrum*, because the beak, more properly, incorporates the non-osseous ramphoteca; Zusi, 1993). These marked proportional changes of the rostrum should be dominant at a macroevolutionary scale of comparison (i.e. must cope with a larger magnitude of statistical variance across avian taxa, since we are dealing with a factor analysis, i.e. relative warps analysis; Bookstein, 1989; Rohlf, 1993).

Subsequently, a series of topographical arrangements between the facial skeleton and the

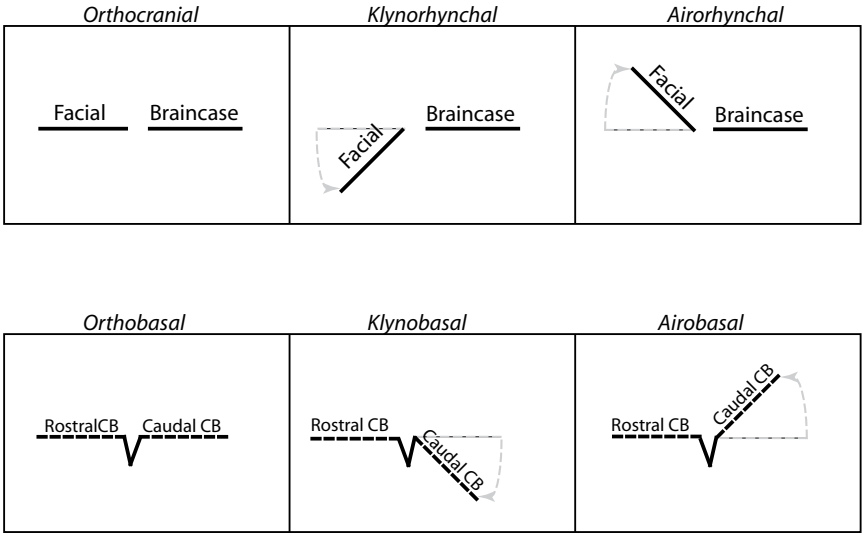

Figure 1. (Above) Craniofacial arrangements between braincase and facial skeleton. (Below) Cranial base arrangements between its anterior (laterosphenoid) and posterior (basisphenoid) portions. The split between parts is at fossa hypophysiaria. Models and names are after Moss and Vilmann (1978), but see also Hofer, (1952).

region of the braincase should follow rostral proportional variation, contained within the second vector of the analysis. Some of these different positional relationships might be convergent among most amniote vertebrates (Hofer, 1952; Moss and Vilmann, 1978; Marugán-Lobón and Bastir, 2005), and are expressed in angular terms because they regard the orientation between such structures in reference to one same plane of the skull in lateral

view (see e.g., Duijm, 1951; Moss and Vilmann, 1978; and Fig. 2.10, in the second part of the thesis). Given these angular relationships, the evolutionary topographic changes that take place between the facial skeleton and the braincase across taxa convey varied "angled" appearances to each skull, and are thereby expressed in terms of relative "flexures". Overall, avian skull disparity was previously found to be constrained between two principal extremes, one being "flexed" because of the angled relationship between the facial skeleton and the braincase, and one "extended", being both the facial skeleton and the braincase in one same plane.

The extended cranial type (sensu Duijm, 1951) is so-called *Orthocranial* (Hofer, 1952), which was afterwards generalised as *Orthobasal* by Moss and Vilmann (1978), because both the facial skeleton and the cranial base lie in the same plane (Fig. 1). We will use the former to avoid confusions with Orthobasal, meaning a flat cranial base (cf. Fig. 1). Opposed, a flexed appearance of the skull is called *klynorhynchal* (Hofer, op. cit.; Moss and Vilmann, op. cit.) because of the downwards orientation of the facial skeleton in contrast with the braincase (Fig. 1). A third craniofacial alternative is *Airorhynchal*, in which the facial skeleton might be elevated instead of downwards oriented, and has been advocated as a special case typical of Loons (Hofer, op. cit.).

We expect to find that a larger avian taxonomic sample will span the maximal skull disparity of the clade within morphospace. However, the hypothesis is that major features of avian skull disparity should notwithstanding remain rooted on these kinds of morphological evolutionary changes, the ones just exposed (rostral proportion and craniofacial arrangements), and not others.

One practical issue that we will explore in parallel to morphological evolution of the skull is the possible incidence of the local variation of the rostrum on the analyses based on the Least Squares superimposition criterion (GPA). In effect, GPA is very sensitive to localized shape variation. For instance, it is interesting that in awareness of the effect that the extension of the rostrum may impose to statistical and metric analyses, studies based on more traditional methods (such as length measurements), tend to avoid the inclusion of the beak in the data-matrix (see e.g., Brooke et al., 1999). Excluding beak variation implies neglecting bones such as the premaxillae, nasals and perhaps even part of the maxillae. The effect of avoiding these bones in craniofacial studies of, say, in mammals; would be dramatic since we would miss the anatomy of one third of the face.

It is important to test how analytical outcomes may differ if including or excluding the

rostrum (note, however, that if the rostrum is excluded there is still some rest of the facial skeleton that can be incorporated in the analyses). Moreover, we already addressed some important findings regarding the evolution of the facial skeleton in archosaurs in which the most striking feature was their rostral proportioning (Marugán-Lobón and Buscalioni, 2003, 2004; see Chapter 1 in this third part of the thesis). Thus, we will perform separate analysis including and excluding the rostrum in order to explore and disclose the possible effect that avian rostral variation may exert on GPA, and the consequences that incorporating it may have when applying the least squares criterion.

It is reciprocally important to assume that such information may be crucial to investigate rostral variation as an evolutionary phenomenon, thus being important to seek for a rationale that explains the whole situation. The possible limitations of the technique against a localized source of morphological variation may eventually lead to stumble onto a hypothesis that explains the strong variability, and the evolution, of the avian rostrum.

Additionally, allometry is expected to be somehow related to all of the above described macroevolutionary aspects of morphological evolution of the avian skull (see Marugán-Lobón and Buscalioni, 2004; Table 2, p. 166). In our preliminary approach we foresaw that rostral variation (proportional antero-caudal stretching) apparently correlated with size (at $p<0.01$), whereas the different arrangements between skull parts (i.e. craniofacial arrangements) did also correlate with size, but at lower confidence levels of statistical significance ($p<0.05$).

However, the values of centroid size (CS) that were used to test for the correlation between morphological variation and size incorporated the rostrum. This is again an operationally important aspect of the analyses in the sense that centroid size, being the square root of the sum of squared distances of a configuration of landmarks from their centroid, is highly dependent on the configuration itself. The strong antero-caudal extension of the rostrum in many birds may affect centroid size estimations of scale since a long rostrum may make the configuration (the skull) appear larger when it might just be longer. The question is thus, whether such reported correlation between rostral proportion and CS (including the rostrum) was more a matter of a geometric artefact than a morphological or evolutionary certainty.

To explore this question we first look at some of the properties of the size scalars that will be used for allometric statistics, calculating two different estimations of skull centroid size, *with* and *without* the rostrum (this latter incorporating the braincase and only part of the facial skeleton, as suggested for disparity analyses in the relative warps; see above and Fig.

2). The values for each CS will be calculated from the original individuals of the sample by means of common geometric morphometric procedures (e.g. using the TPS series of software). The effect of the rostrum on CS calculations will be tested comparing both size estimations against each other, and the hypothesis is that, possibly, CS with the rostrum is biased by its relative stretching.

Interestingly though, different size variables other than CS are seldom used in geometric morphometric studies, which is likely due to the prompt attainment of the latter, plus its useful geometric and statistical properties against shape variables (see e.g. Bookstein, 1991). For the sake of operational and morphological curiosity we also collected a series of avian somatic body masses from literature (Dunning, 1993). With this we aim exploring the statistical relationship between CS and body mass, aiming to gain a glimpse on the relationship between such different size estimations. In principle, the comparison should nevertheless yield a strong equivalency between size measurements, despite their different dimensionality.

Once size measurements have been studied, we will proceed to test the hypothesis of allometric shape change that may be related to macroevolutionary aspects of avian skull morphology. This will be performed from two different statistical perspectives, one exploratory and one confirmatory. Tests will notwithstanding be performed against the two different and independent estimators of size, CS and body mass.

One common way of exploring the relationship between shape variation and size is by building a correlation matrix between the scores of the eigenvectors of a principal components analysis and size (herein, though, not a PCA but a relative warps analysis) (O'Higgins and Jones, 1998). This procedure provides a numerical way of viewing how spread is size across dimensions of shape variation, by means of the numerical value of Pearson's coefficients. Because visualization of the results is an important maxim in geometric morphometrics, we have implemented this procedure with graphical colour-graded contours capable of reflecting the correlations.

The use of a smoothing mathematical equation (Distance-Weighted Least Squares; see e.g. McLain, 1974) enables portraying the relationship of one independent variable, herein size, as a function of two other variables, herein the scores of two eigenvectors, all in one same plot. The equation yields the contours which add the third continuous variable (size) into the scatter-plot. In fact, the drawing is in reality a three dimensional graph that is collapsed into two dimensions to fit the depiction of a common scatter-plot. The contours are drawn

in a graded scale of colours according to the degree of estimated correlation between the independent variable and the scores of the two axes of the scatter-plot (note, however, that these can be any kind of variables).

It is important to highlight that this procedure is just a graphic depiction, and is by no means equivalent to Size-Shape space (Mitteroecker et al., 2004). It is just a way to graphically explore salient patterns (e.g. allometric) that may emerge from the relationship between three variables at once, despite its drawing relies on the outcomes of a smoothing polynomial equation. It is also noteworthy that two variables used in our example represent the distribution of the individuals of the sample on tangent shape-space (ordered by the relative warps analysis), but can be any other, and the third variable can actually be any type of independent and continuous one. We opted for size because it would be a nice graphical portrayal from which to view the effect of allometry onto the relative warps analyses.

We have thereafter applied confirmatory statistics to properly testing for evolutionary allometry (i.e. tests of evolutionary allometry among adults inter-specifically; Klingenberg, 1996), putting avian skull shape variables as a function of size (i.e. CS and mass) by means of common multivariate regressions. Placing a null hypothesis at this point is not straightforward apart from expecting that size may be associated with some morphological aspects of the avian skull in this macroevolutionary context. Results could be biased because all previous tests of allometric associations with avian shape macroevolution were performed against CS values which included the rostrum. Whether previously envisaged allometric trends were an artefact is likely, but we will not be able to asses so until all surveys about the incidence of incorporating of the rostrum in CS calculations have been evaluated.

Overall, the scope of the study aims understanding the most relevant aspects of avian skull morphological evolution at a macroevolutionary scale. This includes testing for the variation at the braincase, at the facial skeleton, and of the skull as a whole when treating the morphological association between each other within the system. On the other hand, however, the study deals with important methodological issues which entail the application of GPA to avian skull morphology, and its resolution at macroevolutionary scales of comparison (studies which are seldom carried out; Marcus et al., 2000). This approximation carries with it, at the same time, the operational effect that the rostrum may have on the analytical outcomes if only applying GPA based on the Least Squares criterion.

Results should shed a glimpse on the way we understand the phenotypic organization of the avian skull at a macroevolutionary scale. This implies a phylogenetic contextualization of

shape disparity, the contrast of convergences within (empirical) morphospace (shape space), and to think of hypotheses that are sensible for explaining phenomena of morphological evolution such as allometry and phenotypic integration.

3.2.2. Materials and Methods

The phylogenetic relationships among modern birds (Neornithes) are still debated. The most extended agreement is that the most basal clades within Neornithes are Paleognathae (Ostriches and allies). The next dichotomy is the clade Neoaves, which splits into Galloanseres (Gamefowl and Waterfowl), as a sister clade of a still largely unresolved polytomy for remainder clades (see BOX 1). These more inclusive clades are the ones that will be categorized to address the evolutionary distribution within morphospace.

The pool sample comprises avian skulls of a large number of taxa, both in terms of number of individuals and in the taxonomic range it spans (N=172 individuals, all avian orders and ca. 80% of described avian families; see Appendix 1 for species, labels and institutions).

All skulls are of adult birds and were digitized in lateral view. Anatomy and landmarks (LM) are depicted in two separate pictures in Fig. 2a, and the anatomical correspondence of the landmarks is listed in Table 1. Image unwarping, a technique proposed to aid visualizations of morphological change, is used It allows transforming the image of each specimen to create images with landmarks that align with those in the reference. The term unwarping is used because each specimen is treated as a transformation of the reference. Bookstein (1991) gives an algorithm to construct an average image corresponding to the landmark location in the reference shape, and Rohlf (2002) develops the mathematics and rationale of estimating landmark configurations from multivariate results. Additionally, Rohlf (*op. cit.*) discloses in detail the algorithm and how the TPS function is used to map the correspondence of pixels between images. The algorithms are implemented in TPS super (v1.14; see Rohlf, 2002).

Additional to General Procrustes Superimposition techniques (GPA based on the Least squares superimposition criterion) the generalized version of Resistant Fit Theta-Rho Analyses (RFTRA) based on iterations of the median (Siegel and Benson, 1982; Rohlf and Slice, 1990) is also used for explorative purposes (i.e. testing for the effect of localized variation of the rostrum).

Size estimators are centroid size and body mass. Centroid size (CS) is the squared root of the sum of all the squared distances between each configuration of landmarks (Bookstein, 1991). We have calculated CS of the whole skull (p=12 landmarks), and what we call the *cranium*

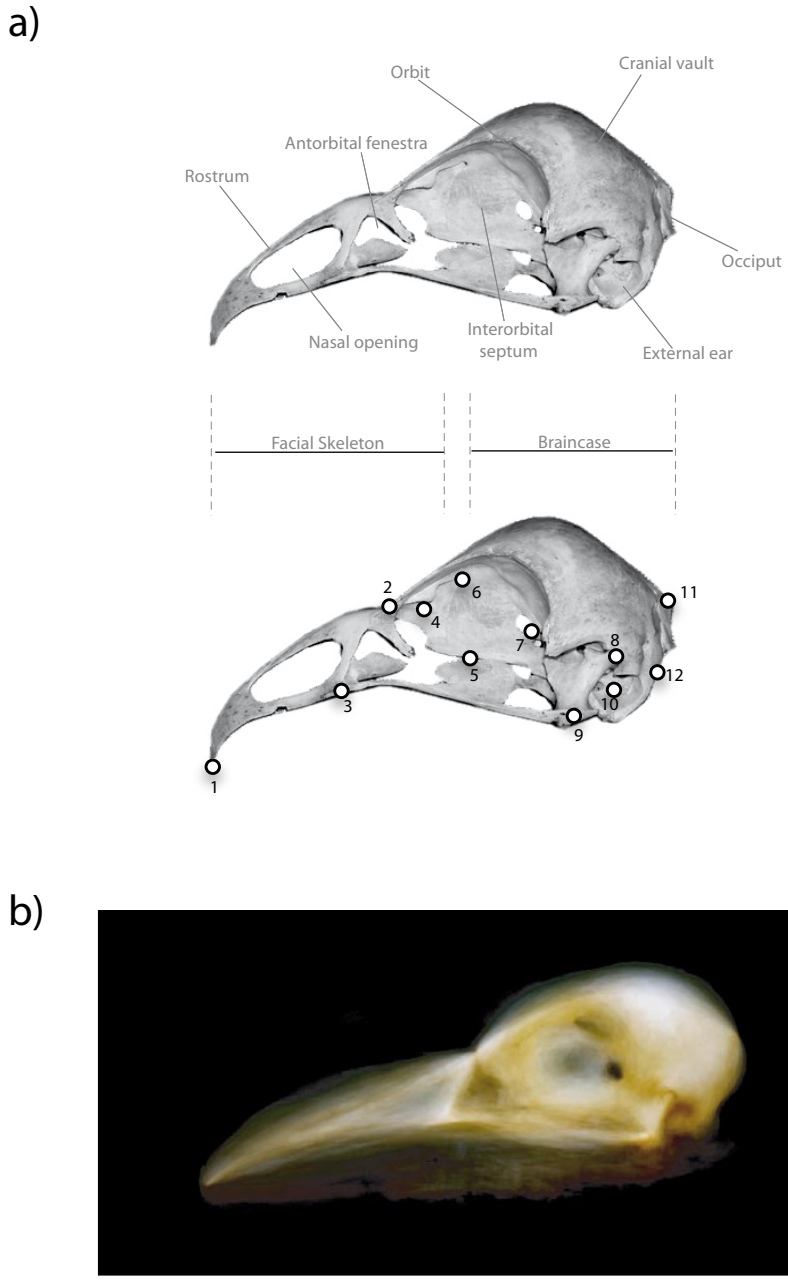

Figure 2. a) Skull in lateral view of *Chauna torcuata.* (Above) Skull with some common anatomical names. (Below) Landmark series delimiting salient features of the skull (see Table 1 for labelling). b) Unwarped consensus (average) of N=170 bird skulls after GPA superimposition. Halo around the image is the residual of the superimposed of images.

(*p*=11 landmarks), which represents the rest of the skull (braincase and facial skeleton) that remains when deleting the rostrum (LM 1; Fig. 2a). The second independent measurement of size is body mass and was collected from literature (Dunning, 1993). Whenever a match was not perfectly possible for particular species body mass was elected for the closest species. This approximation could thus be misleading because of a large mismatch between the weight and the original species, or because this way of estimating size may be highly dependent on the life stage of the organism at the moment of weighting (e.g. mass could vary

dramatically depending on reproductive moment, or migratory status; Dunning, *op. cit.*). Analyses against CS will aid foreseeing their usefulness.

Skull centroid size (CS) and cranial centroid size (CS-c, without the rostrum) are used as log-transformed and labelled *logCS* and *logCS-c* respectively, and body mass data (W) was

Table 1. List and description of landmarks

Number	*Anatomical description*
1	Premaxillary symphysis at the tip of the rostrum
2	Joint (in lateral view) of the nasal and lacrimal bones (e.g. craniofacial hinge)
3	Anteriormost edge of antorbital fenestra projected perpendicularly to rim of maxilla
4	Orbitonasal foramen (N. I)
5	Intersection between the palatines at the choana dorsally with mesethmoid
6	Foramen of the olfactory nerve (N.I)
7	Foramen of the optic nerve (N. II)
8	Insertion of quadrate to squamosal in braincase
9	Articulation between quadrate and jugal bar
10	External ear (centroid of Auditory Meatus)
11	Caudalmost junction of parietal and squamosal
12	Mid-point of foramen magnum

transformed first to its cube root and thereafter to its logarithm (labelled as *logW*).

Shape disparity is analysed reducing the dimensionality of shape variables (Partial Warp scores and the uniform component) using relative warps analyses (RW), which is equivalent to a principal components analyses that allows weighting the bending energy matrix at different scales (landmark distance within the configuration, changing the α parameter; see Rohlf, 1993). Herein all explorations are performed at α=0 because it allows to include the uniform component which is more convenient for explorations (see Rohlf and Corti, 2000). In order to explore the association with size and skull shape one method used is by constructing a correlation matrix between the eigenvector scores and each of the size scalars. This correlation matrix is calculated though additionally, we portray a contour plot that aids visualizing the association of size variables over the factor distribution viewed therein. The algorithm used is the distance-weighted least squares method which is implemented in the Statistica package (v. 6.0; Statsoft, 2001). This algorithm fits a Z-axis to an already existing pair of X-Y coordinates axes, aiming to show the relation of Z (herein the independent variables are the different size estimators; CS and body mass, though each in separate depictions) as

a function of X and Y with a non-linear function. This function is a polynomial (second-order) regression which is calculated for each value on the X variable scale to determine the corresponding Y value such that the influence of the individual data points on the regression decreases with their distance from the particular X value (an algorithm similar to the one used by this procedure is described by McLain, 1974)

Common multivariate regressions are also used to test shape variation as a function of each of the independent size estimations (independent variables). These analyses are performed by regressing all shape variables (partial warp scores and the uniform component) against each size estimate (CS and body mass).

Landmark digitalization, Procrustes superimpositions and the thin plate spline procedures, projection of shape-space to tangent-space, relative warps analysis, and multivariate regressions were performed using F. J. Rohlf's TPS*series* of morphometric software (TPSdigit v1.14, TPSrelw v. 1.42; TPSsmall v1.20; TPSregr v.1.12). Generalized RFTRA (GRF) superimposition was performed with IMPcoordGen from the IMP series (v.6f; Sheets, 2001).

3.2.3. Results

3.2.3.i Superimpositions and shape variables

The landmark configuration performs well when capturing the geometry of the avian skull. This is viewed in the way the averaged image draws the consensus (the mean) with the unwarping technique (Fig. 2b). Notice that aside skull's geometry the image captures other qualitative aspects of the skull after superimposing all the images of the individuals of the sample. For instance, it shows the common non-ossification of the laterosphenoid at the opening above the optic foramen, or that of the interorbital septum. Likewise, it captures the roundness of the braincase or the extent of the orbital opening. These are traits are visually appealing and may be of morphological utility, but notice that they are not captured by the landmark configurations.

Rostral variation is obviously dominant in the analyses (Fig 3). In order to ease some interpretations we adapt the terminology of Longi, Meso and Longirostral that was previously used in Chapter 1 of this part of the thesis (Marugán-Lobón and Buscalioni, 2003). This typology allows distinguishing between three groups of skulls in terms of rostral proportion, where longirostrals have a rostrum>70% of the cranium, mesorostrals between 70-50%, and

a)

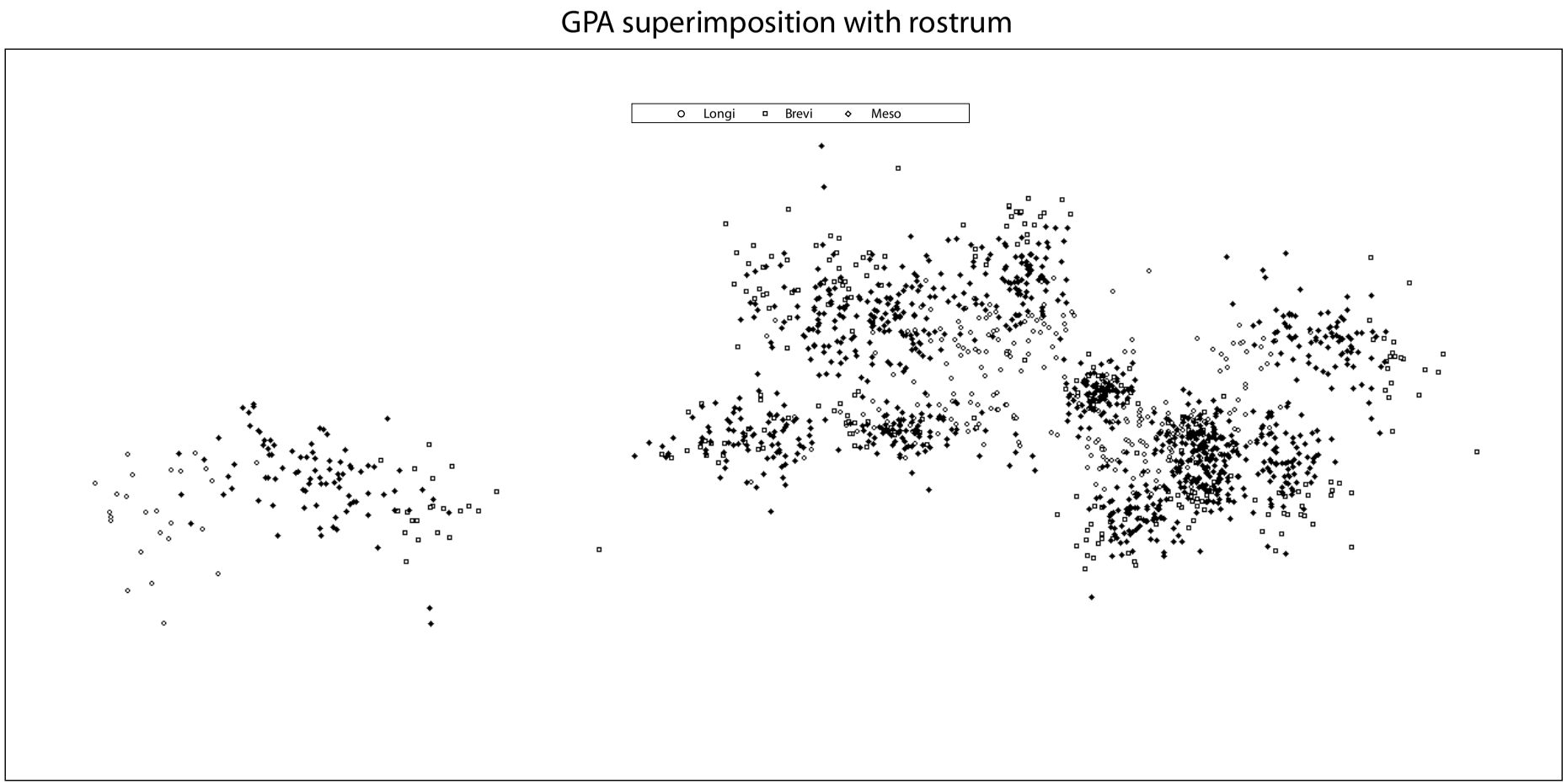

b)

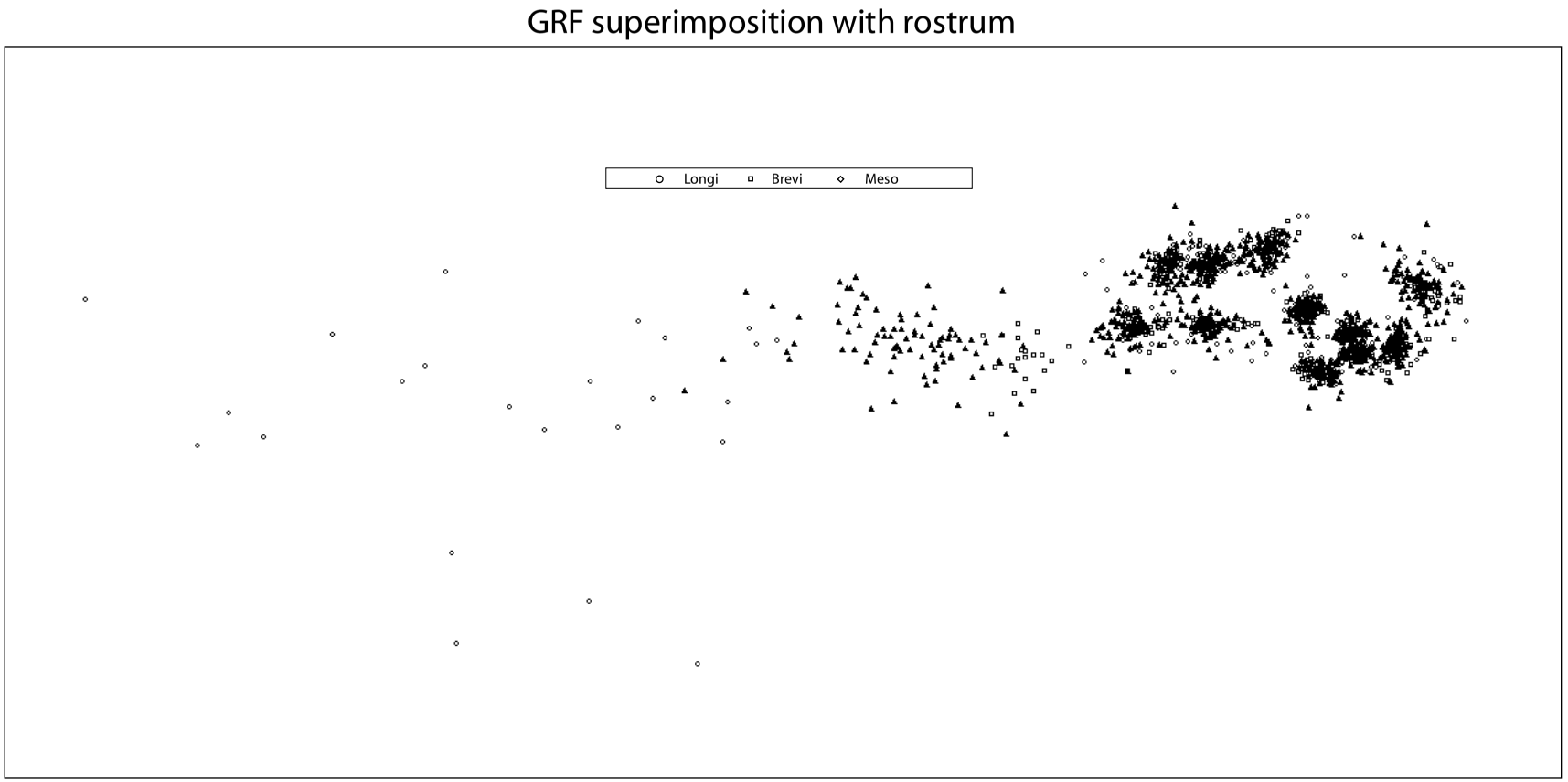

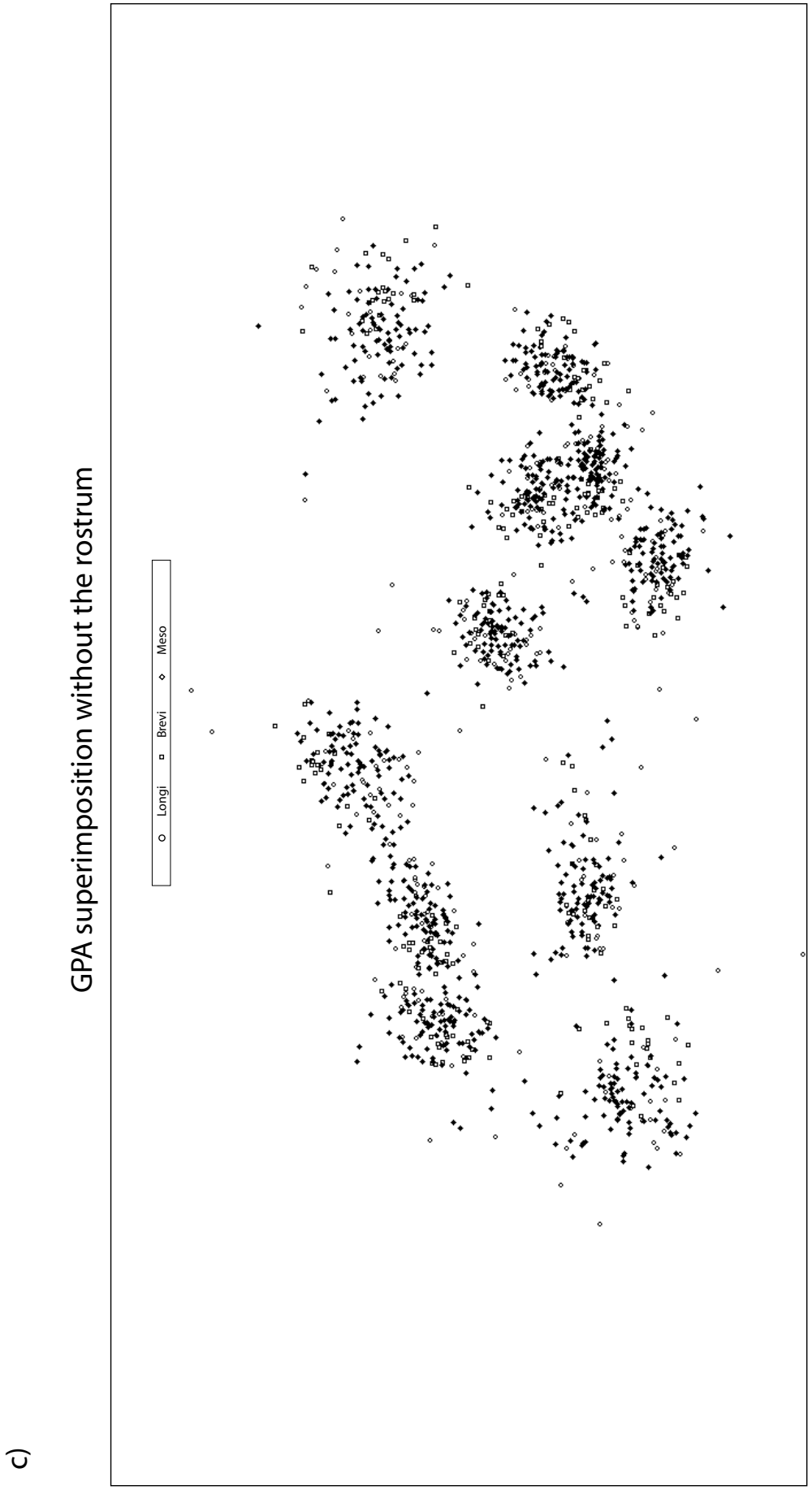

Figure 3. Superimposition residuals, a) after GPA (Least Squares), b) after GRF, and c) after GPA but excluding the tip opf the facial skeleton (the rostrum, landmark 1). Circles are longirostrals, squares are brevirostrals, and diamonds are mesorostrals.

brevirostrals<50%.

It is straightforward to see from figure 3 that the GPA procedure can be strongly affected by the localized variation between landmarks (LM) 1, 2 and 3 (compare Figs. 3a, b, and c),

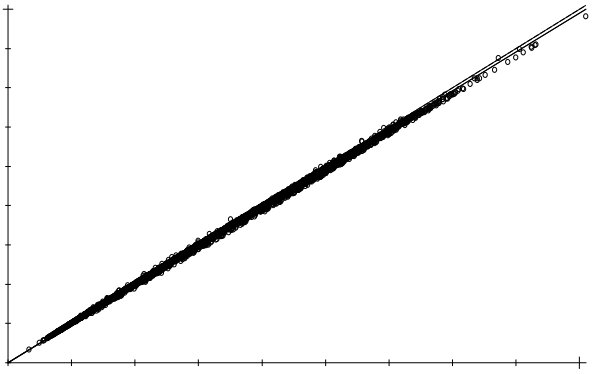

Figure 4. Projection of Kendall's Shape Space onto Tangent Space. The scatter-plot represents the distances in the tangent space against Procrustes distances (geodesic distances in radians). The dashed line shows a slope of 1 through the origin, and a least-squares regression line through the origin (shown in black). In principle, data in which the variation in shape is small both lines should superimpose. Here, there is some deviation, yet not very marked. Moreover, when shape variation is not small enough the relationship of the data points should not be linear.

since longirostrals appear to have relatively smaller cranial (Fig. 3a, longirostrals in white circles).

Figure 3b shows the result of a generalized resistant fit superimposition (GRF) which shows that the rostrum has a strongly marked localized variation, and therefore, that it causes a "Pinocchio" effect on the Least Squares superimposition. Furthermore, when another least squares superimposition is performed over the cranium alone (i.e. no rostrum, thus excluding LM 1; Fig. 3c) the superimposition is markedly congruent with the GRF superimposition shown in figure 3b, in which landmarks are equivalently clustered around their means (compare again all Figs. 3a, b, and c; notice the difference in the clusters when the rostrum is included in Fig. 3a).

In spite of the localized variation at the rostrum, shape variation across avian taxa captured by GPA (least squares) adequately approximates the linear tangent space (Euclidean) to the non-lineal Kendall's shape (a Least-Squares regression between Euclidean distance and Procrustes distance with rostrum, shows a r>0.9999; Fig. 4; please note that we only show when rostrum included assuming that any other superimposition should be unquestionably transposable between spaces).

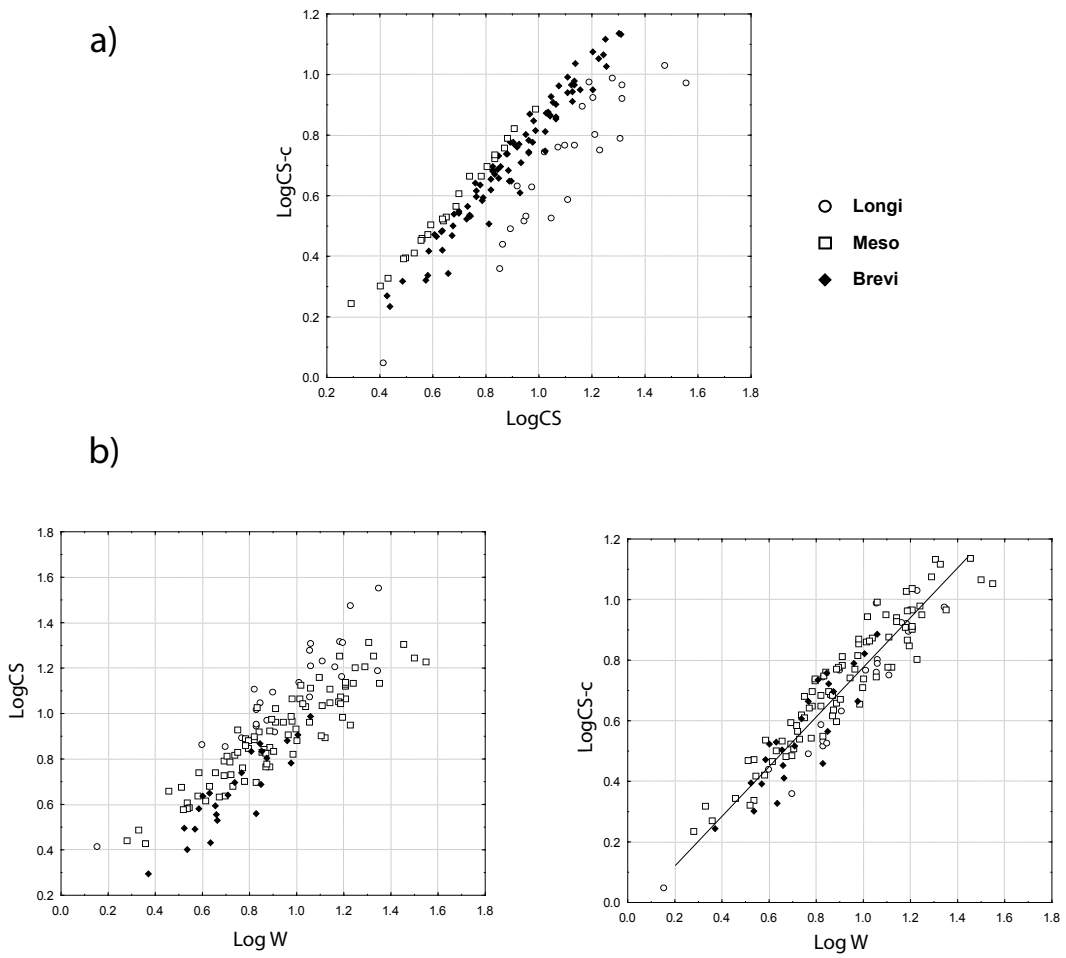

Figure 5. Scatter-plots an regressions between different size measurements. a) Scatter-plot comparing loc CS (with rostrum, x-axis) against log CS-c (no rostrum, y-axis). Notice how points deviate from the mean the larger the value of log CS, i.e. the larger the length of the rostrum. b) (Left) Scatter-plot comparing log W (body mass) with log CS, and (right), comparing log W with log CS-c, and regression between both variables.

3.2.3.ii Size variables

When comparing *logCS* of the skull (including the rostrum) with *logCS-c* (the suffix *–c* is labelling the exclusion of the rostrum out of the configuration of landmarks) it is possible to see how the former (*logCS*) is clearly associating larger scale values to specimens with longer rostra (Fig. 5a). This can also be seen in Figure 5b, in which *logCS* and *logCS-c* are both compared to *logW* (left and right respectively). Therein, *logCS-c* is linearly related and the distribution of taxa within the plot is more homogeneous across the scatter as a function of body mass (R^2 = 0.8779; *logCS*-c = -0.0084 + 0.78**logW*).

3.2.3.iii Major trends of shape variation of the avian skull

Depictions of these results are shown in figure 6a and 6b, where the latter accompanies the reading translating the deformation grids into skull "morphs" (unwarped estimates) to ease interpretations. Results of relative warps analysis on the full configuration of landmarks

based on Procrustes superimposition verify the inkling of a marked localized variation at the rostrum and its effect that were viewed on the superimposition residuals. Notice, for instance, the marked stretching of the grid when the rostrum elongates, a change in the grid that is also accompanied by a marked decrease in the overall diminishing of the whole skull (it appears much smaller; Fig 6a, b the pair above).

Rostral variation accumulates a 65.68% explained variance in the first eigenvector, and associates visually longer rostra with proportionally smaller crania. At the same time smaller rostra match with much more larger crania (Fig. 6a, b). There are several longirostral specimens (skulls) but the bird at the extreme of the axis (with the longest rostrum) is the pelican (gen. *Pelecanus*; 87% of rostral proportional length to total length of the cranium). This contrasts with the polarized situation of the most brevirostrals, a dwarf parrot (*Micropsitta*) followed by a hawk (*Falco*), both with rostral proportions close to 40%.

The second eigenvalue explains 12.91% of total variance which may not be small if considering the large variance accumulated by the first vector, and the explained variance of the following one, relative warp three (RW3), which falls down to 4.79%. This second source of morphological variation (RW2) makes the grid to bend homogeneously in two opposed directions among the two polarized extremes of the axis (Fig. 6a, b, pair below of RW 1). If referenced from the bottom (ventral to the depiction of the grid and the skull) the grid is bent concave at positive scores and convex for negative ones.

The bending of the grid coincides in what has been previously amended as flexed or extended skulls; when the grid is bent concave (positive scores) the morphological outcome coincides with the flexed appearance of the skull in lateral view (Fig. 6a, which is commonly diagnosed with the term klynorhynchal (cf. Fig. 1). That is, the facial skeleton is oriented obliquely downwards, while on the contrary, when the grid is bent convexly (referenced as well ventrally) the configuration of the skull appears to be orthocranial, whereby the facial skeleton and the braincase are both aligned in the same plane (compare the dashed line linking LM 6, 7, 12 which lets infer the position of the cranial base which lies within the braincase).

Most shape changes seem to be due to rostral rearrangements. Particular morphological changes that accompany the concave bending of the whole spline in positive values coincide, however, with the deformation (compression) of the grid around the area of the orbit (mostly affecting the jugal bar; LM 3 and 9, Fig. 6a, b). At the same time, some deformation also takes place across the region of the braincase, particularly between the laterosphenoid, the optic

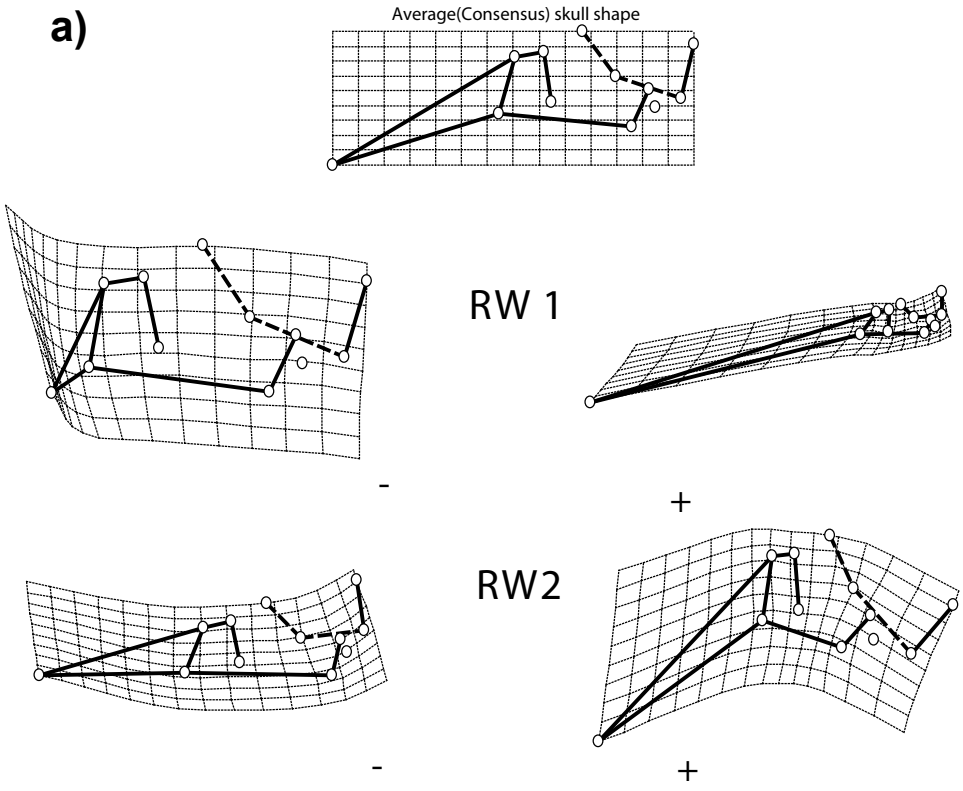
a)
Average(Consensus) skull shape
RW 1
-
+
RW2
-
+

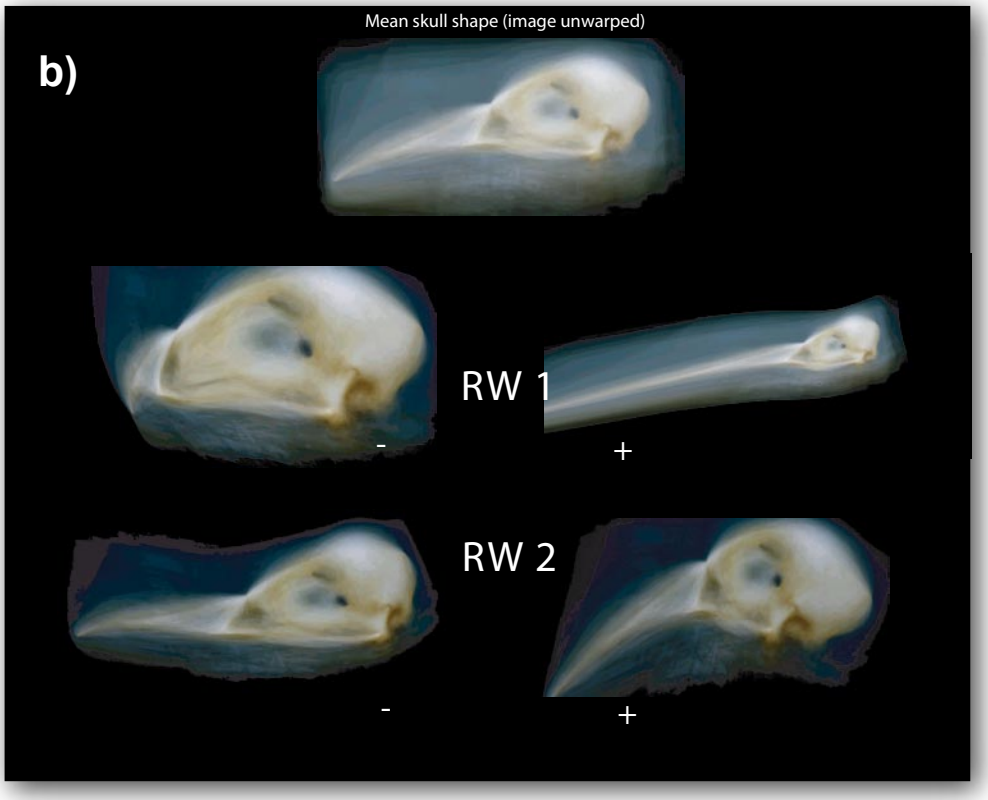
b)
Mean skull shape (image unwarped)
RW 1
-
+
RW 2
-
+

c)

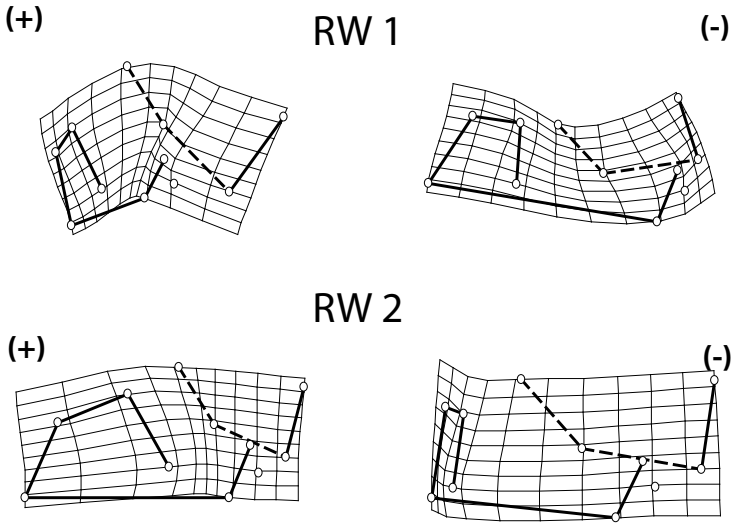

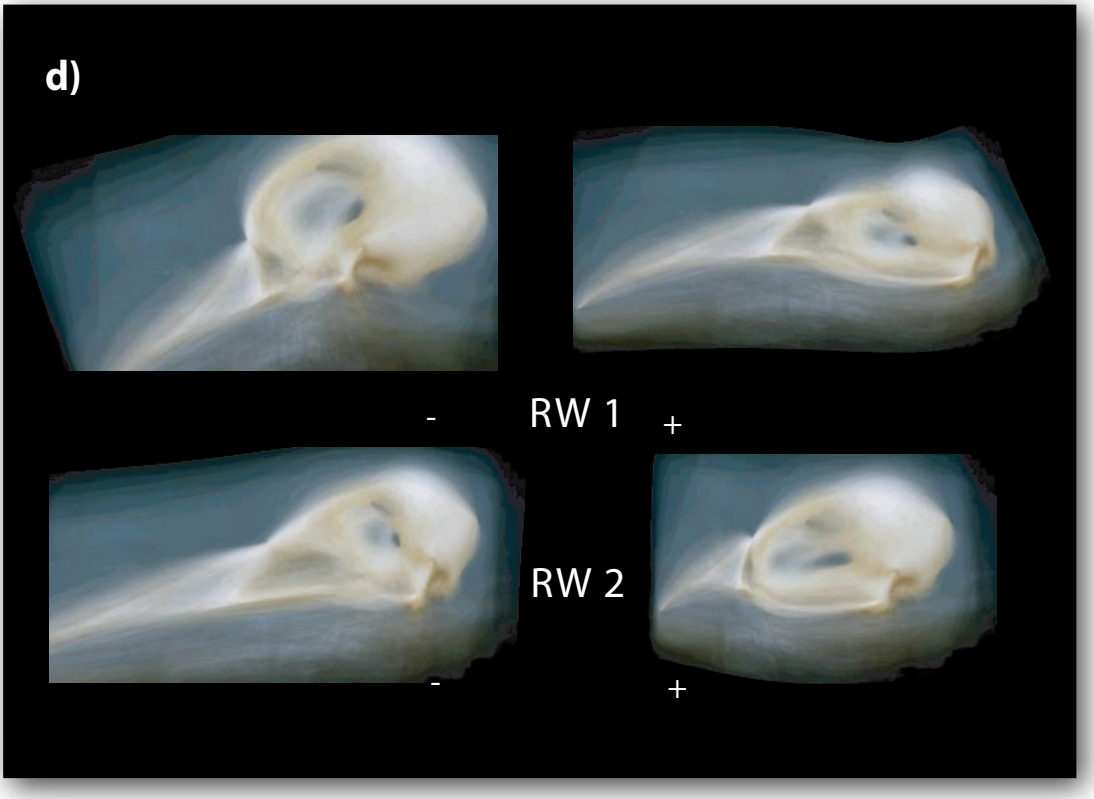

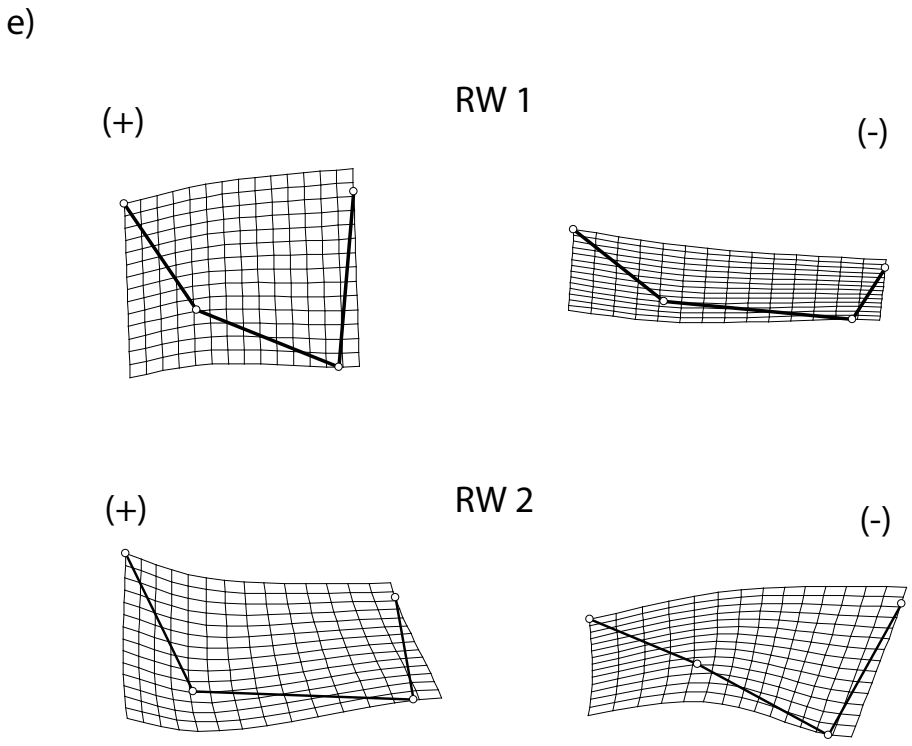

Figure 6. Deformation grids and images showing the extremes of the axes on each relative warps analysis. a) Analysis including the beak (rostrum). Above is the average, and below, ordered left to right (or right to left) are extremes of positive (+) and negative (-) scores. When using grids lines link landmarks to ease visualization. Dashed lines show that the cranial base is inferred. a) First RW 1, in which most marked changes correspond to proportion of the rostrum. Notice the marked stretching and shrinking of the braincase. RW 2 follows just below, denoting craniofacial arrangements. b) This figure is equivalent to a), but instead of using deformation grids it uses images unwarped (modifications of the average image shown in Fig. 2b) to the extreme axes shown above. c) Analysis excluding the beak (rostrum). Also ordered left to right (or right to left) are extremes of positive (+) and negative (-) scores. First RW 1 now denotes craniofacial arrangements. Notice how orthocranials are best seen as airorhynchals (see dashed lines for cranial base in 6c). RW 2 in this analysis accounts for facial changes, mostly in the antorbital fenestra. The rostrum is only included by defect, but is not incorporated in the analyses. e) Deformation grids of the braincase alone to show how the cranial base may be changing (only by inference).

foramen and the foramen magnum (LM 5, 7, 12; Fig. 6a, b). In the polarized situation, where the spline is more convex, it coincides with an antero-caudal stretching of the jugal bar.

The third eigenvalue explains solely a 4.79% of morphological variance and accounts for a marked antero-caudal and stretch or compression of the antorbital fenestra (LM 2, 3, 4, 11). There are several coincidences of the shape changes it accounts for in the ones encountered in other analyses which will therefore be shown and disclosed in following paragraphs (see below).

If analyzed without landmark 1 (the tip of the rostrum) we lose the possibility of using the longi- to brevirostrality descriptors of facial change when the rostrum is excluded. The first source of shape difference in this new situation is, however, equivalent to relative flexure or extension of what we now call the cranium (including the rostrum we call it the skull; Fig. 6c). That is, shape changes encountered now by RW 1 without the rostrum (tip of the facial

skeleton) are morphologically equivalent to those found in the RW 2 of the first analysis (compare Figs 6a, b with 6c, d).

Thus, the positive scores of RW 1 now account for a flexed cranium (a concavely bent grid), in which the facial skeleton orients downwards. It is with no doubt a Klynorhynchal cranial type. On the contrary, the convexly bent grid at negative scores coincides does not coincide now with an orthocranial, since the facial skeleton does not orient in the same plane with the braincase any more, but it may even seem to point more upwards. This is best seen if the position of the braincase is referenced from the cranial base, which can be roughly inferred within the braincase (see dashed lines linking LM 6, 7, and 12).This would mean that the extreme cranial type is now an Airorhynchal.

The second eigenvalue in this analysis is almost identical to the RW 3 when the rostrum was excluded; it explains 16.97% of morphological variance and accounts for a marked antero-caudal and stretch or compression of the antorbital fenestra (LM 2, 3, 4, 11; Fig. 6c, below RW 1; Note that these changes are equivalent to RW3 in the previous analysis, which incorporated the rostrum).

Overall, all analyses highlight the strong effect that the rostrum has in the analyses. The rostrum is morphologically dominant in terms of stretching and compressing antero-caudally, and it causes the grid to bend convexly or concavely. When the rostrum is not incorporated in the analyses there are still facial skeleton parts upon which to compare it against the braincase. Some new findings come along, among which the most striking are that the flexed to non flexed skull appearances are all embedded within one same spectrum of variation. Klynorhynchal is equivalent to the flexed types and settle one extreme, whereas Airorhynchal (rostrum elevated), and not Orthobasal (or Orthocranial), set up the opposite morphological extreme among avians, despite the fact that when incorporating the rostrum the extreme appears to be an orthocranial. For simplicity we will commonly use the term flexed when referring to klynorhynchal whereas extended will be used to refer airorhynchals, and only specify the terms when needed (e.g. to differentiate between orthocranials and airorhynchals).

3.2.3.iv Distribution in (Tangent) shape space and its association with size

Because of the differences found between the analyses performed, two different distributions will be explored; relative warps in which the rostrum was included, and when it was excluded. Thus, scatter-plots differ in that ones correspond to shape changes of the skull depicted in

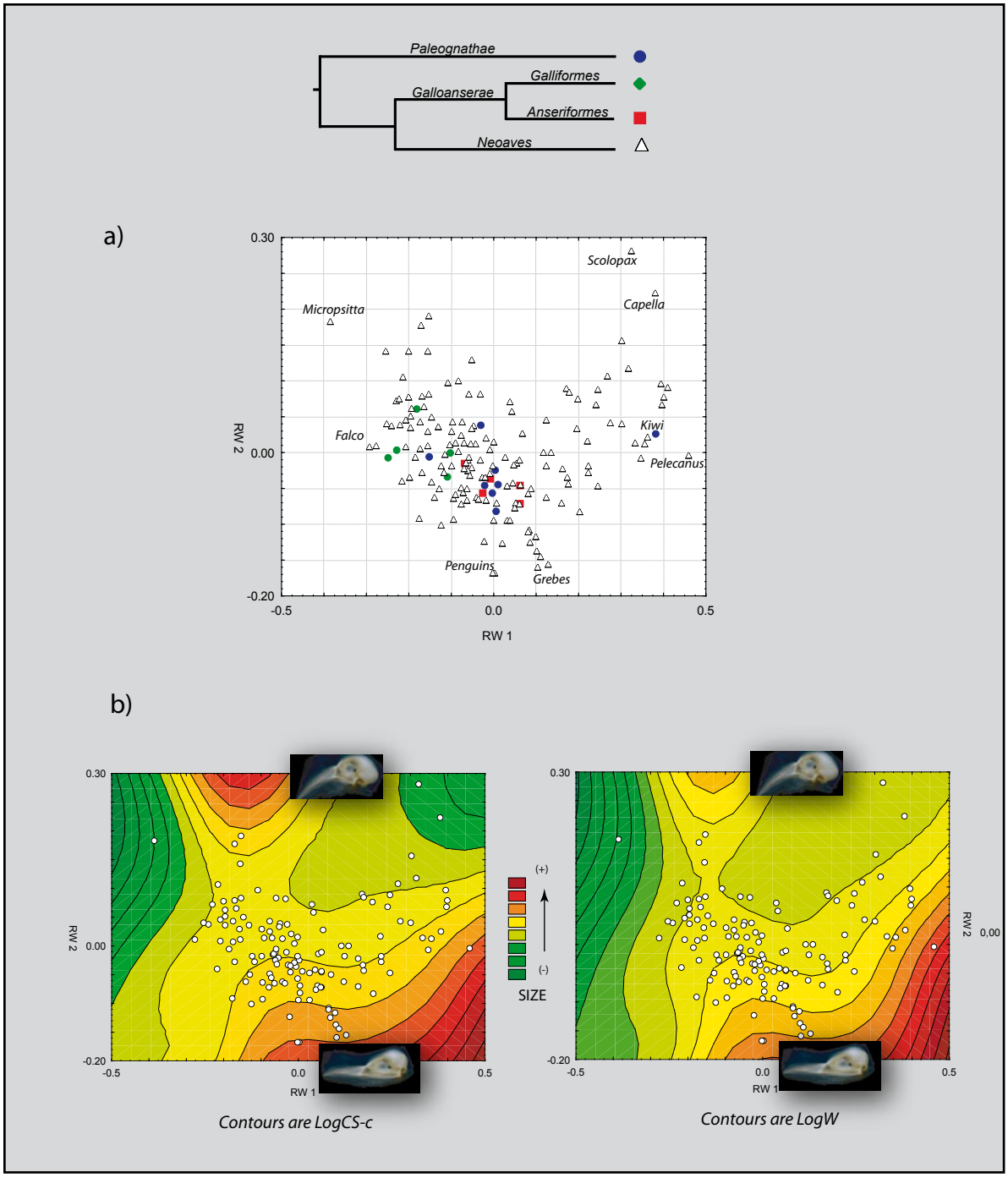

figure 6a and 6b, or figures 6c and 6c respectively.

In first place, when including the rostrum (Fig 7a), the extreme brevirostral and flexed skull in morphospace belongs to a dwarf parrot, *Micropsitta*, and the opposed extreme is a pelican (*Pelecanus*). Most points (individuals) tend to distribute more concentrated within a region that corresponds to meso- and brevirostrality. When including the rostrum we found that the extreme negative scores corresponded to skulls more extended in appearance (orthocranial), depite in reality, they are airorhynchal. The skulls in the extremes of the axis

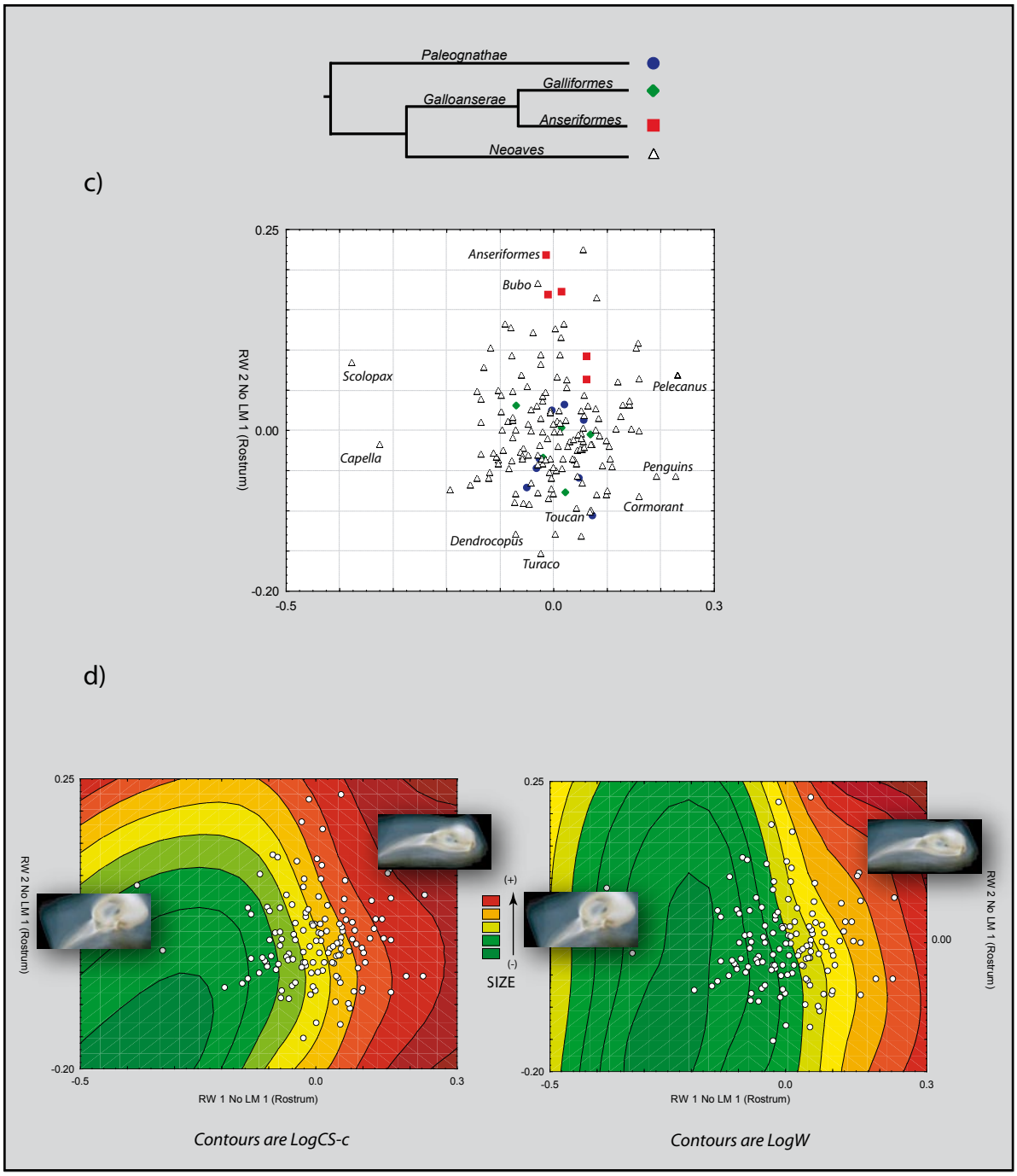

Figure 7. Shape Space (Morphospace, scatter-plots) occupancy by taxa, clades, and size. Above cladograma shows major phylogenetic relationships among Neornithes (the basal HTU). a) Relative warps analysis including the rostrum. b) Contour plot over morphospace (colour grading represent size, see centre of figure). Images of skulls are unwarped morphs at extreme axis of RW 2 (craniofacial arrangements). Left is for contours of logCS-c and right for log W. c) and d) are equivalent but represent relative warps analysis excluding the rostrum. Images are now on RW 1 (craniofacial arrangements).

of RW 2 are mesorostral birds such as penguins (*Spheniscus* and *Pigoscelis*), a loon (*Gavia*), and a murre (*Uria*). Opposed in the axis (positive scores), the scatter is far less populated by individuals and dispersion is more accentuated. The most extreme flexed birds (the extreme klynorhynchal skull) are a woodcock (*Scolopax*), followed by a common snipe (*Capella*),

and both are longirostrals. The scatter shows that longirostrals, however, can be flexed or extended across the whole extension of RW 2. In other words, longirostrality can take place regardless the klynorhynchal to orthocranial craniofacial arrangement. On the contrary, mesorostrals seem tend to be orthocraniality (likely, though, airorhynchal) given that the upper part of the graph (positive scores in RW 2) is far less populated by points. Equivalently, brevirostrals appear to concentrate in areas of a more marked cranial flexure.

In this morphospace, basal clades tend to cluster more closely and around to the consensus (mean), thereby being mostly mesorostrals, although few tend to brevirostrality, and only one Paleognathae, the Kiwi, is far from their distribution towards a region of a marked longirostrality. Likewise, basal clades tend to be more orthocranial than either klyno- or airorhynchal Galliformes cluster closely among them and somewhat further from the consensus than the Anseriformes. Derived clades (Neoaves) thus occupy the largest extent of morphospace since they overlap in the regions of more basal clades while expanding the morphological boundaries of shape space much further into regions of more klynorhynchal and airorhynchal configurations.

It is notwithstanding difficult to address whether any particular logic associates the function of rostral proportion to the distribution over morphospace since there is a great deal of convergence (seen on the overlapping of taxa). For instance, longirostrals can be pelicans, woodcocks, ibises or hummingbirds, all of which are birds that share the trait but specialise in completely different foraging strategies. Only Airorhynchals seem to converge in that they are all marine forms.

Table 2 summarizes the correlation matrix between the eigenvalues on each to the three size variables (i.e. *logCS-c*, and *logW*). In the same way as what the correlation matrix points out, when size (note that we omit *logCS* which incorporates the rostrum, cf. Fig. 5 and results above) is mapped onto this first scatter with contours, the plot hints for a salient pattern in which size increase tends to be more related with negative scores of RW 2, thus with more extended cranial shapes (Fig. 7b, left). This pattern is seen from the colour grading of the contours which matches size increase in such a way that smaller values are greener, then pass to more yellow, then more, orange, more red, and finally more brown as size values increase.

As shown above, more the skull is extended the more the tendency to be mesorostrals and to be larger. Because longirostrals can be either flexed or extended (klynorhynchal, orthocranial or airorhynchal), since they span across the entire RW 2 axes, there is no particular size that

matches them. In principle, rostral proportion would seem no to correlate with size (e.g. body mass). Most brevirostrals, on the contrary, seem to tend to be flexed and associate to

	Log W	Log CS	Log CS-c	RW 1	RW 2	RW 3	RW 1 nr	RW 2 nr	RW 3 nr
Log W	1,00	*0,88*	*0,94*	0,12	*-0,27*	-0,17	*0,57*	0,21	*-0,23*
Log CS	*0,88*	1,00	*0,90*	*0,47*	-0,21	-0,19	*0,60*	*0,23*	-0,21
Log CS-c	*0,94*	*0,90*	1,00	0,05	*-0,33*	-0,20	*0,65*	*0,25*	-0,17
RW 1	0,12	*0,47*	0,05	1,00	0,03	0,00	0,16	0,03	-0,14
RW 2	*-0,27*	-0,21	*-0,33*	0,03	1,00	-0,02	*-0,71*	-0,04	-0,01
RW 3	-0,17	-0,19	-0,20	0,00	-0,02	1,00	0,10	*-0,98*	-0,01
RW 1 Nbk	*0,57*	*0,60*	*0,65*	0,16	*-0,71*	0,10	1,00	-0,01	0,09
RW 2 Nbk	0,21	*0,23*	*0,25*	0,03	-0,04	*-0,98*	-0,01	1,00	0,04
RW 3 Nbk	*-0,23*	-0,21	-0,17	-0,14	-0,01	-0,01	0,09	0,04	1,00

Table 2. Correlation matrix between relative warp scores (nr=no rostrum), log CS, log CS-c, and log W. Significance of Pearson's r is at P<0.01 (in italics and underlined).

smaller sizes.

In the second analytical case, the scatter which corresponds to analyses without the rostrum (LM 1), extreme birds for relative craniofacial arrangements remain almost the same (Fig. 7c, d). The exception to the rule is the pelican, which was previously an extreme longirostral only, and is now also an extreme extended one (note that now this is along with a penguins which were the original extremes when the rostrum was included; note that both are large birds). Extremes for flexed skulls are now outliers and remain being the woodcock and the snipe. Extremes for the next eigenvalue (RW 2, accounting for reduced antorbital fenestra, for negative scores) are mostly forms with particularly specialised beaks, such as the turaco (*Musophaga*), the tucanet (*Aulacorhynchus*) or the woodpecker (*Dendrocopus*). In the opposed side extremes are swans and ducks with the intermission of one owl (*Bubo*; remainder Strigiformes have large fenestrae, and lie close but are not extremes).

Basal clades, again, are located close to the consensus (mean), thus remain being more orthocranial. Anseres are notwithstanding extremes lying further because of their particularly large antorbital fenestra (RW 2).Some forms of Paleognathae, such as the Rhea or the emu (*Dromaius*) tend to cluster down to more negative scores (i.e. relatively smaller fenestrae).

The contour plots show that *logCS-c* and *logW* are equivalent and associate again to cranial architecture in terms of more or less craniofacial flexure or extension (Fig. 7d, left and right); the larger the size the tendency is again towards a more extended craniofacial appearance of the cranium, that is, towards orthocraniality and its extreme case, airorhynchy (see above

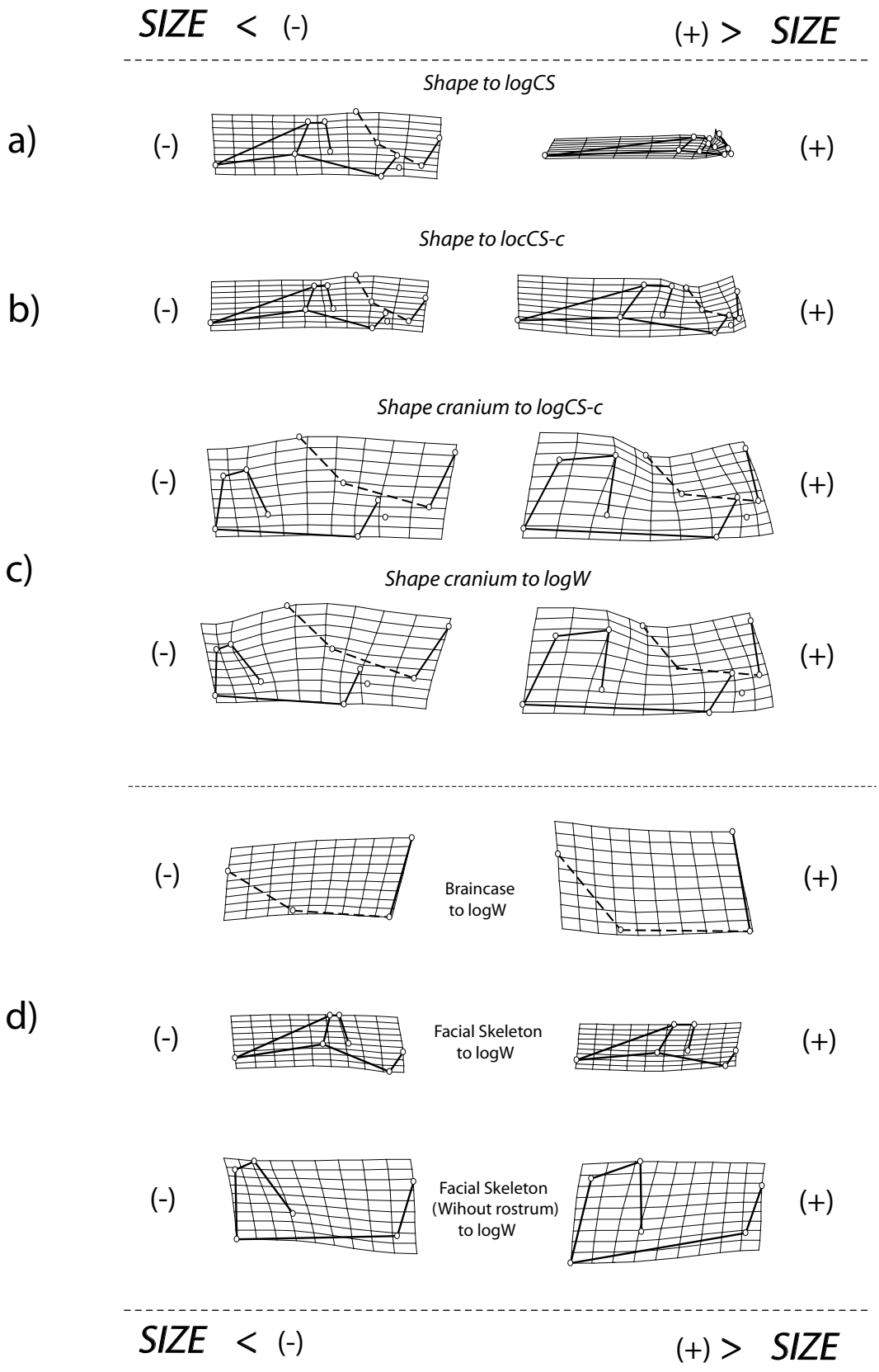

Figure 8. Evolutionary shape allometry (multivariate regressions against size) of the avian skull. Figures show deformations (shape change) as a function of size. (+; right) is largest size, (-; left) is smallest size a) Shape changes of the skull (including the rostrum) as a function of log CS. b) The same as the latter but against log CS-c. c) Cranial shape (without the rostrum) against log CS-c (above) and against log W (below). d) braincase alone against size (above), facial skeleton against size (middle), and facial skeleton without the rostrum against size (size generalization is valid for both logW and logCS-c, since they give nearly-identical outcomes).

for other shape changes associated). Thus, size is an underlying factor associated to the distribution of cranial shapes within shape-space.

3.2.3.v Evolutionary shape allometry

Any multivariate regression of shape variables as a function of on each of the size measurements are statistically significant at $P<0.01$ (see summary of results in Table 3, and

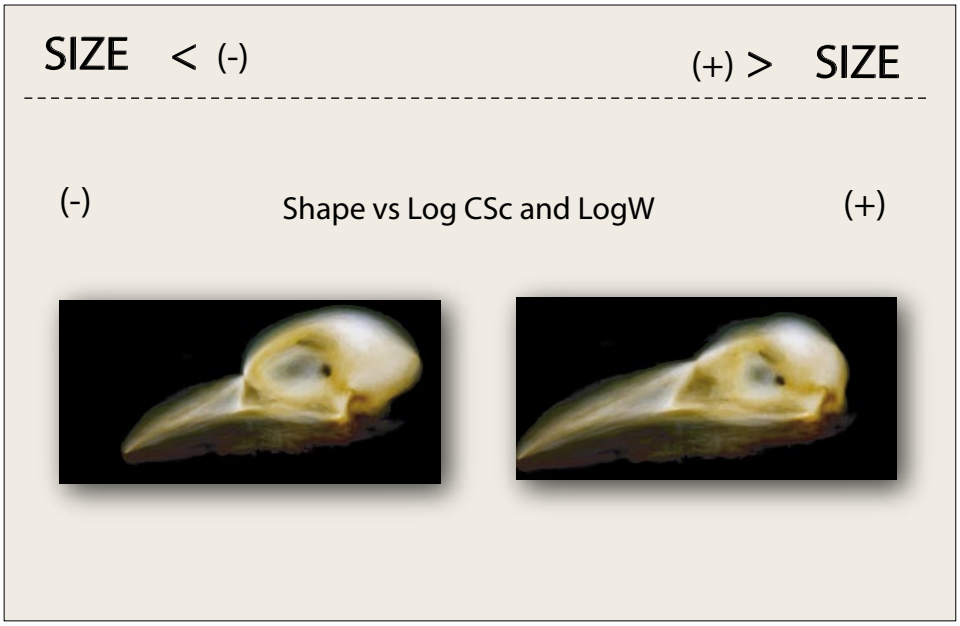

Figure 9. Evolutionary allometry as seen on an unwarped average to extreme sizes (small and large). This figure is the same as Fig. 8c but using images instead of deformation grids. Notice the marked changes in the orientation of the foramen magnum, and the beak (rostrum) is only left by defect of the original picture (thus, it is not included in the analysis).

Figs. 8 and 9, the latter which resumes the most important aspects of shape allometry with unwarped images). The effect of rostral proportional size on logCS is markedly noticeable due to the deformation it causes from its regression onto the shape of the braincase (8a). It shows that longer rostra yield larger CS values and shorter rostra lower CS values. Therefore, CS correlates well with shape changes in the exact same way, therefore biasing the results. In effect, the relative antero-caudal proportion of the rostrum appears to be allometrically dissociated both from *logCS-c* (cranium) and *logW* in accordance to what the correlation matrix and the contour plots were already suggesting (cf. Fig. 7) The effects of *logCS-c* and *logW* on cranial shape are also reasonably equivalent between them and their relationship with skull shape changes.

When the configuration of landmarks without LM 1 (rostrum) is tested as a function of size, larger sizes (and body masses) equate with relatively smaller braincases and homogeneously larger facial skeletons (Fig. 8c), the latter which seems to be also related to somewhat smaller orbits (i.e. considering that LM 4 and 7 let infer roughly the antero-caudal extent of the orbital cavity). Conversely, smaller sizes yield cranial shapes with proportionally larger braincases and smaller antorbital fenestrae which would coincide with proportionally larger orbits. There are also shape changes that associate with this covariation pattern within the braincase, such as the relative position of the supraoccipital (LM 11 and 12), and (though by inference), and to the cranial base (LM 6, 7, 12; note the dashed lines linking the landmarks therein). Larger sizes seem to associate with more convex cranial bases (Airobasal, in principle; cf. Fig. 1), whereas smaller sizes tend to yield more flat cranial bases (orthobasal; Fig. 1). In the facial skeleton, relatively larger sizes associate as well to a marked antero-caudal stretching of the jugal in lateral view and, in relation to relative proportion of the orbit, to a homogeneous enlargement of the antorbital fenestra.

Overall, the proportion of the rostrum is not allometrically associated with size at a macroevolutionary scale, nor does the evolutionary attainment of either more flexed or more extended craniofacial configurations *per se*. That is, the allometric association of size with skull or cranial shape change across avian taxa does not relate with the way in which the facial skeleton is oriented with respect to the braincase, despite the fact that relative warps analyses would seemed to suggest so.

Instead, multivariate regressions show that allometric changes are those which associate with shape change within the braincase, quite possibly (although by inference; see dashed links between landmarks in all figures) the cranial base and, without doubt, at the supraoccipital. This can be better observed in the morphs of figure 9 (notice there how size increase or decrease associates with the relative orientation of the caudal part of the braincase, particularly with the supraoccipital bone, and with the relative orientation of the foramen magnum).

Finally, if cranial parts are treated as separate configurations of landmarks (separate parts of the skull; Fig 8d), shape changes will differ from those observed if all parts are treated as a unique configuration (the skull; Fig. 8 a, b, c). For instance, size relates to shape changes of the skull in such a way that larger birds tend to have smaller braincases and larger facial skeletons, but if the braincase is treated separately, its changes as a function of size will not reflect its overall proportion (relative size), but the different arrangements between its

elements.

3.2.4 Discussion

3.2.4.i Technical issues

The usefulness of geometric morphometrics in morphological studies relies in its analytical power which is largely enriched with its high-end graphical visualizations of shape change using the Thin Plate Spline interpolation function (TPS; Bookstein, 1991).

This function allows mimicking the deformation grids proposed by D'Arcy Thompson (1942). However, a visual limitation of using the grid alone is that the location of the landmarks does not provide a very realistic depiction of the form being studied. Practitioners of morphometrics are used to these types of abstractions, and therefore to deduce at a glance what analyses are telling. This is perhaps quite in agreement with the arguments of Thompson when he was stating that the grid would suffice to speak about morphological change in a mathematical sense. However, this may also overlook that non-specialist readers may be also interested in the study but may also need to take an additional work-step in order to familiarize with what results are expressing.

A solution to this is to include an image of the organism in the background of the plot registered with respect to the landmark configuration. Image *unwarping* is a technique of the visual imagery of geometric morphometrics that allows transforming the image of each specimen to create images with landmarks that align with those in the reference. This way, for instance, the consensus (grand mean; Fig. 2b) can be visualized as a virtual skull-like depiction, and by the same way as the ones applied to deform the grid, the morphed mean can be re-transformed into shapes expressing the statistical results such as the scores of a RWA or the shape changes resulting from multivariate regressions (see Figs 6b, d, and Fig. 9).

Using unwarped images is commonly underused, despite its potential is quite evident. Moreover, its graphical capabilities are not only effective but also quite captivating. Additionally, the use of static pictures can be extended to animated frames, which are especially communicative in live presentations to any type of audiences.

In this chapter one commitment was to survey the analytical compromises of studying avian skull disparity on the basis of General Procrustes Analysis (GPA). Evaluating the performance of shape analysis at a macroevolutionary scale is important because these types

of studies are still rather unusual in geometric morphometrics literature, and therefore, there is still a need of a experimental work which helps envisaging the operational vs. informative trade-offs the technique may carry with it.

Geometric morphometrics based on Procrustes superimposition, and particularly the use of the Thin Plate Spline (TPS), was initially conceived as a tool for intra-population or intra-specific analyses of shape variation (Bookstein, 1989; Rohlf, 1993). The interpolation function may not be useful if shape differences are abrupt (non-gradual), as they may be in some instances if taxa compared are markedly different (Zelditch et al., 2004). We have seen that this is not the case for avian taxa since beak variation, the largest potential source of error, takes place in a gradient, from proportionally smaller to proportionally larger in the antero-caudal axis.

Other more general problems that could arise at high taxonomic scales of comparison lie at the core of the technique, that is, on landmark digitalization which is exemplified in the impossibility of repeating landmarks among specimens, for instance, if there is any type of evolutionary loss of an element or a structure. This has not been the case either in this study, entailing that geometric morphometrics can be used for the study of avian morphological evolution at a macroevolutionary scale.

However, a second and associated problem, and perhaps more crucial, is when macroevolutionary changes yield patterns of very large and localized variation on particular features. For instance, one of these features has been already studied in mammals (Marcus et al., 2000), a study which the authors found that the marked repositioning of the nasal opening in dolphins was very marked if compared to other terrestrial mammals. This made dolphins explore a quite distant area within shape space, which is the same as saying that they will be far apart from remainder mammalian skull shapes in terms of Procrustes distances.

However, the magnitude of this shape variability was found not to affect the analyses because it did not surpass the limits of a reliable orthogonal projection from shape space to tangent space (a magnitude of larger than $\pi/4$). Despite this marked differences in the position of the nasal opening within the skull in dolphins, Marcus et al. (*op. cit.*) demonstrated that the orthogonal projection to tangent space was still feasible. This is also the case of our bird sample despite the marked rostral variation in certain birds such as, for instance, pelicans, hummingbirds, or kiwis (Fig. 4).

Rostral variation in birds is a matter of extreme elongation, which is best seen on the far

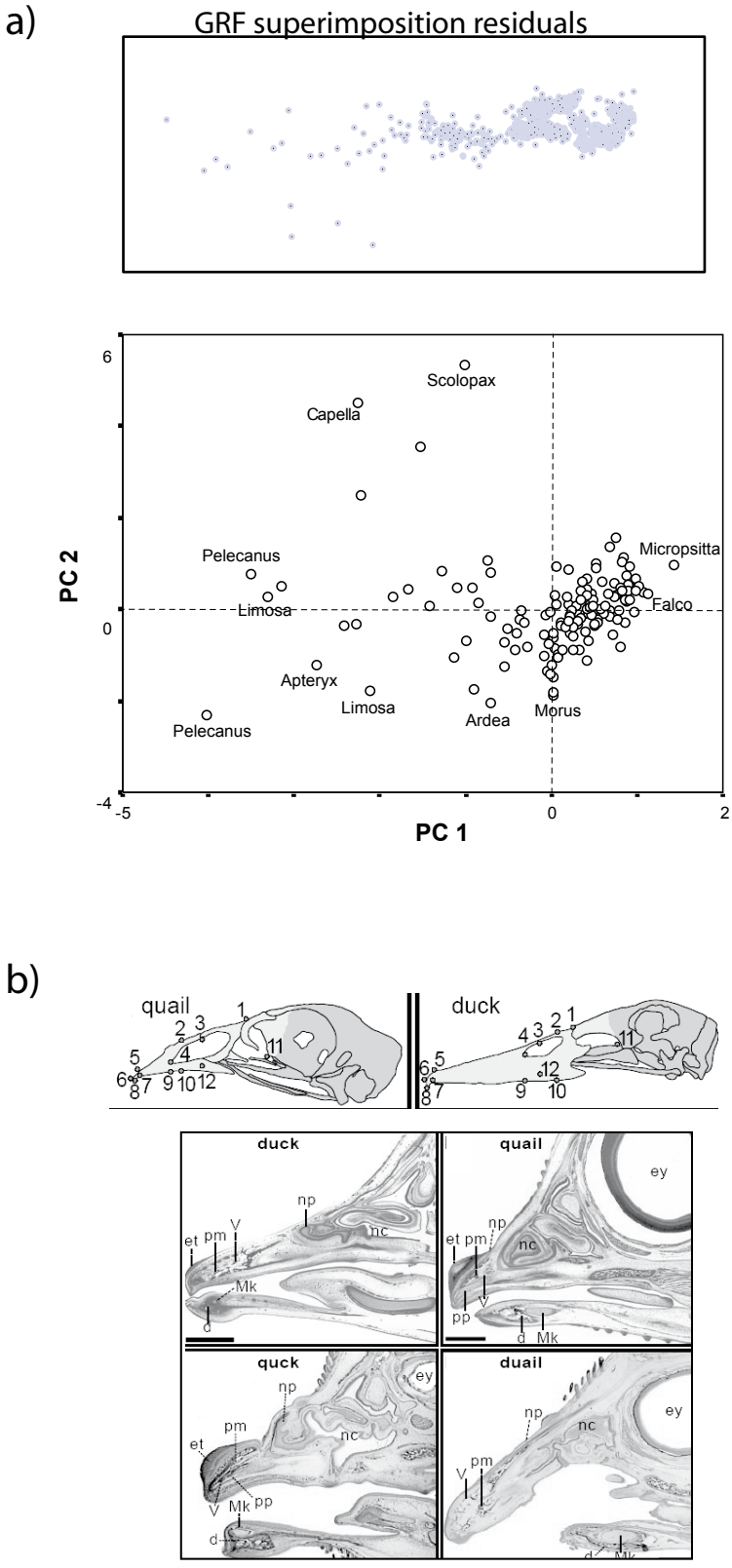

Figure 10. GRF superimposition (same as Fig. 3b), above, and PCA on the covariance matrix of the residuals. Results are nearly-equivalent to those of the RW with the rostrum. X-axis is rostral proportion, and Y-axis are craniofacial configurations. Regrettably, it is not possible to see the meaning of shape change associated to each axis. b) Schenider and Helms (1993) original picture quail-duck craniofacial experiment of grafting (see text). Figure above shows the landmarks used by the authors to speak about shape differences (applying RFTRA). Below are photographs of slices of the original 'chimeras' (the beak of the duck embryo resembled that of the quail and vice versa, the quailed resembled that of the duck).

distribution of longirostrals with respect to the coordinates of the consensus (the mean) on each of the scatter-plots (the first relative warps analyses performed; Fig. 7a, the consensus is at coordinates *x*-0,*y*-0 of the scatter-plot).

The problem the rostrum poses to morphometrics procedures is on the Procrustes superimposition, when minimizing the distance between homologous landmarks using the generalized least squares procedure (GLS; Gower, 1975). What occurs is similar to the example of the nasal opening of the dolphin above stated; the displacement of the beak with respect to the remainder landmarks is so large in certain instances that it inflates the squared distances between configurations, and the GLS spreads such large local differences across all the landmarks in order to produce smaller differences (Slice, 2005). Ralf Chapman's metaphor of the fibber Pinocchio incarnates in some derived Neoaves theropod dinosaurs such as hummingbirds or Pelicans.

The effect could be foreseen when plotting the residuals after Procrustes superimposition (Fig. 3a, b, and c) and became markedly conspicuous on the shape variation encountered by the first relative warp analysis (Fig. 6a). Techniques such as generalized resistant fit (GRF) are suitable for capturing this type of localized variation (Benson et al., 1982; Siegel and Benson, 1982). In effect, resistant fit, and its generalization (Rohlf and Slice, 1990) were techniques suited to overcome these potential problems. Unfortunately, GRF methods are based on linear distances and the use of medians between them, a procedure for superimposition which does not fit into Kendall's theory of shape. This makes multivariate statistical procedures somewhat challenging because it is not possible to ground what is happening behind the analyses (Dryden and Mardia, 1999; Zelditch et al., 2004). Judging from the results, it would perhaps be timely to perform an exploration of its axiomatic underpinnings.

While it may be heretic statistically, we used the matrix of the residuals of the GRF on a PCA, just for the sake of exploration (Fig. 10). Interestingly, the graph shows a very similar pattern to the RW analysis based on Procrustes superimposition (compare distribution with Fig. 7a, b; axis have the same meaning). The graph is equivalent to plotting the first axis of the relative warps analysis including the rostrum against the first axis excluding it.

There is also an obvious alternative source of error that may be underlying the problem of rostral variation, which is not a matter of pure morphological localized variation, but of the resolution of the landmarks used when aiming to capture rostral variability. One particularity of the bony ensemble of the avian skull is that most bones coalesce leaving no imprint or suture upon which to localize and digitize the landmarks. If the anterior margin

of the maxilla (its suture with the premaxilla) could be captured, variation could perhaps appear less localized. This problem occurs when studying adult skulls, and thus, analysing variation could perhaps be more suitably mapped in embryonic (see e.g. Schneider and Helms, 2003, but see their landmarks; Fig. 10b), and post-hatchling studies as long as bones remain unfused.

Another alternative to study the problem could also be the use of outlines based on the superimposition of semilandmarks (see. e.g. Bookstein et al., 2003). However, its use is still under consideration because results may be dependant on the algorithm used when superimposing them (i.e. minimizing the chord distance between semilandmarks by bending energy or Procrustes; see review in Pérez et al., 2006).

It is nevertheless noticeable that rostral morphological variation affects dramatically centroid size calculations. Centroid size is very sensitive to the configuration of landmarks and becomes geometrically confused by the distance at which the tip of the rostrum falls from the remainder landmarks of the configuration. However, CS calculated from the configuration of landmarks without the rostrum, (i.e. still with some rest of elements from the facial skeleton, what we called the cranium), is a very good proxy for cranial size. It is in fact linearly associated to body mass, and therefore and reciprocally, body mass is a rough but feasible approximation to size as an independent variable. This is all demonstrated by the graphs from its relationship with cranial size (Fig. 4b). One interesting outcome associated with this observation is that body mass equates linearly with geometric size (CS) captured in a two dimensional projection of the lateral view of the skull.

Finally, we have found that the allometric association with craniofacial arrangements and their shape change across avian taxa do not relate with size, despite the fact that relative warps analyses would seemed to suggest so. Analysing the configurations of landmarks as wholes is a compromise in geometric morphometrics. Relative warps analyses capture dimensions of shape difference between whole configurations, and order them according to the amounts of explained variance. These dimensions, however, may contain varied portions of shape variance, some of which may pertain to the parts involved, and some to the relationship between them (e.g. variation at the braincase, variation at the facial skeleton, plus the angular relationship between the braincase and the facial skeleton). Some of these portions of shape change within such dimensions may be correlated with size, but others may not, but relative warps will show all of them together, and will not discriminate between them. Thus, some portions may be correlated with other variables (e.g. size, as in our case), making the whole

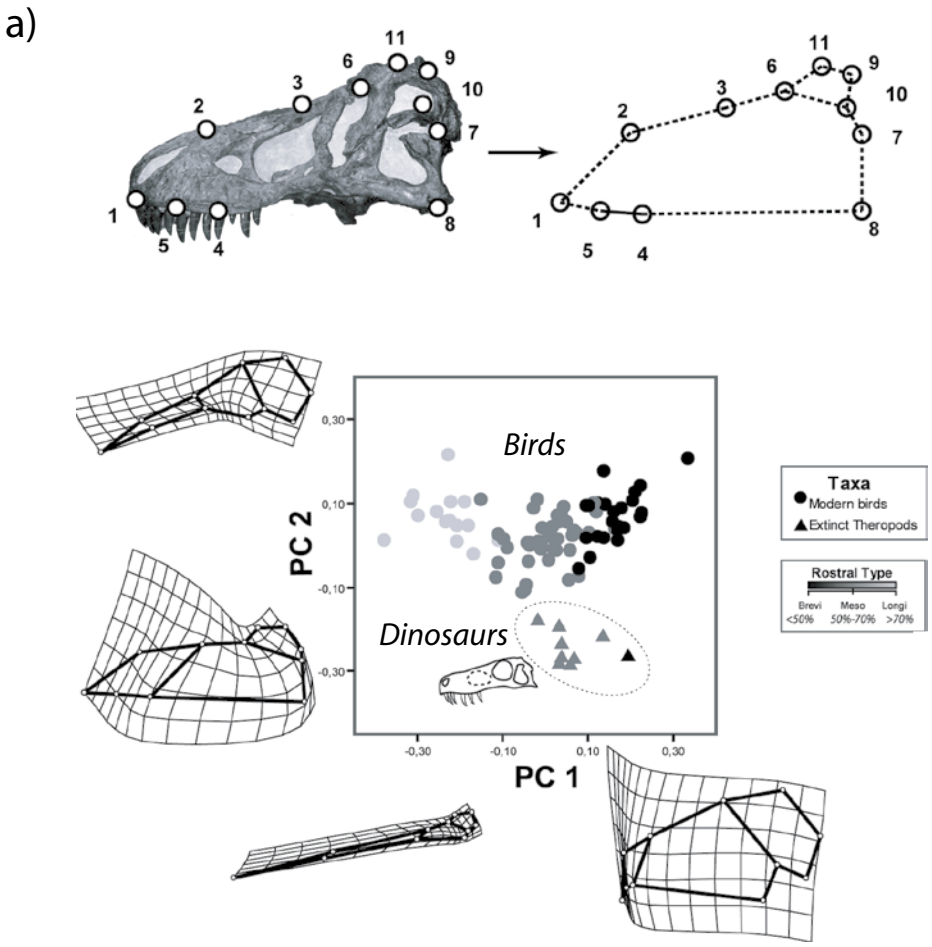

Longirostravis hani

Figure 11. a) Relative Warps analysis of modern avian forms and fossil theropod (avian and non-avian) dinosaurs. Picture above schematizes the landmarks used on the skull of a T. rex in lateral view. Below, the scatter plot of the analysis. Gray-scale denotes rostral proportions among taxa following Marugán-Lobón and Buscalioni, 2003. Fossil theropods lie outside the "moder avians"-region. b) Original reconstruction of *Longirostravis haani*, from the Early Cretaceous of China (Hou et al., 2004).

dimension appear correlated with the variable, in spite of the fact that it is only one fraction of the dimension which is correlated, and not others.

3.2.4.ii Avian skull shape disparity

All the analyses performed lead to the agreement that the major source of skull variance across avian families at a macroevolutionary scale is the facial skeleton, and despite some limitations of capturing rostral shape variation with just a few landmarks, analyses corroborate that most of disparity is particularly concentrated on the rostrum (the beak, when associated with the ramphoteca). Interestingly, birds with particularly long rostra (longirostrals) seem to be less frequent than other types, such as brevi or mesorostrals.

Likewise, other major aspect of avian skull disparity is the different arrangements that can take place between the braincase and the facial skeleton (Marugán-Lobón and Buscalioni, 2004). While these have been commonly evaluated in terms of angles between such parts of the skull, we have found that landmark based geometric morphometrics are a suitable way for capturing and visualizing them in the lateral view of the skull.

However, these different configurations span between two marked extremes, one Klynorhynchal, and other Airorhynchal, and not Orthocranial (Fig. 1. This could only be shown when the rostrum was not included in the analyses. This envisioning suggests that craniofacial organization in birds may likely be modelled as a continuum of morphological changes, whereby angular relationships between the the braincase and the facial skeleton (in a general sense) are simply a matter of a rotation upon each other.

3.2.4.iii Macroevolution

The origins of a rostral shape decoupling (antero-caudal proportion) from the remainder elements of facial skeleton and the rise of different cranial arrangements are of paleobiological interest because they are possibly autapomorphic traits of birds emerged within the clade theropoda, yet extremes are possibly particular to Neoaves birds .

We have elsewhere suggested that mesorostrality was possibly a plesiomorphic trait, not only for Theropod dinosaurs, but shared all archosaurian reptiles, given that numerically, most basal forms in each of the clades shared this trait. In addition, classic literature has often claimed that orthocraniality, the alignment of the facial skeleton and the braincase in one unique plane, is a primitive morphological state because it is typically “reptilian” (Duijm, 1951; Hofer, 1952). In effect, most basal forms (Paleognaths and Galloanseres) explore regions of morphospace that are more orthocranial than any other type (i.e. klyno-

and airo-rhynchal), a craniofacial condition that is shared only by Neoaves birds.

In figure 11a there is a scatter-plot showing how theropod skull disparity, including birds, spans across morphospace (from, Marugán-Lobón and Buscalioni, 2004) in a roughly equivalent relative warps analysis than the ones performed herein (i.e. the difference is in some of the landmarks used). The analysis included several fossil forms of the clade, avian and non-avian theropods (see also figure caption). Fossil forms in the scatter-plot are either mesorostral or slightly brevirostrals (see also Marugán-Lobón and Buscalioni, 2003; Chapter, 1 in this part of the thesis), and other fossil outgroups to modern forms such as Hesperornithiformes (e.g. *Hesperornis*) are also mesorostrals (Fig. 12). Avians thus span the range of morphospace occupancy with rostral proportion by several magnitudes in contrast

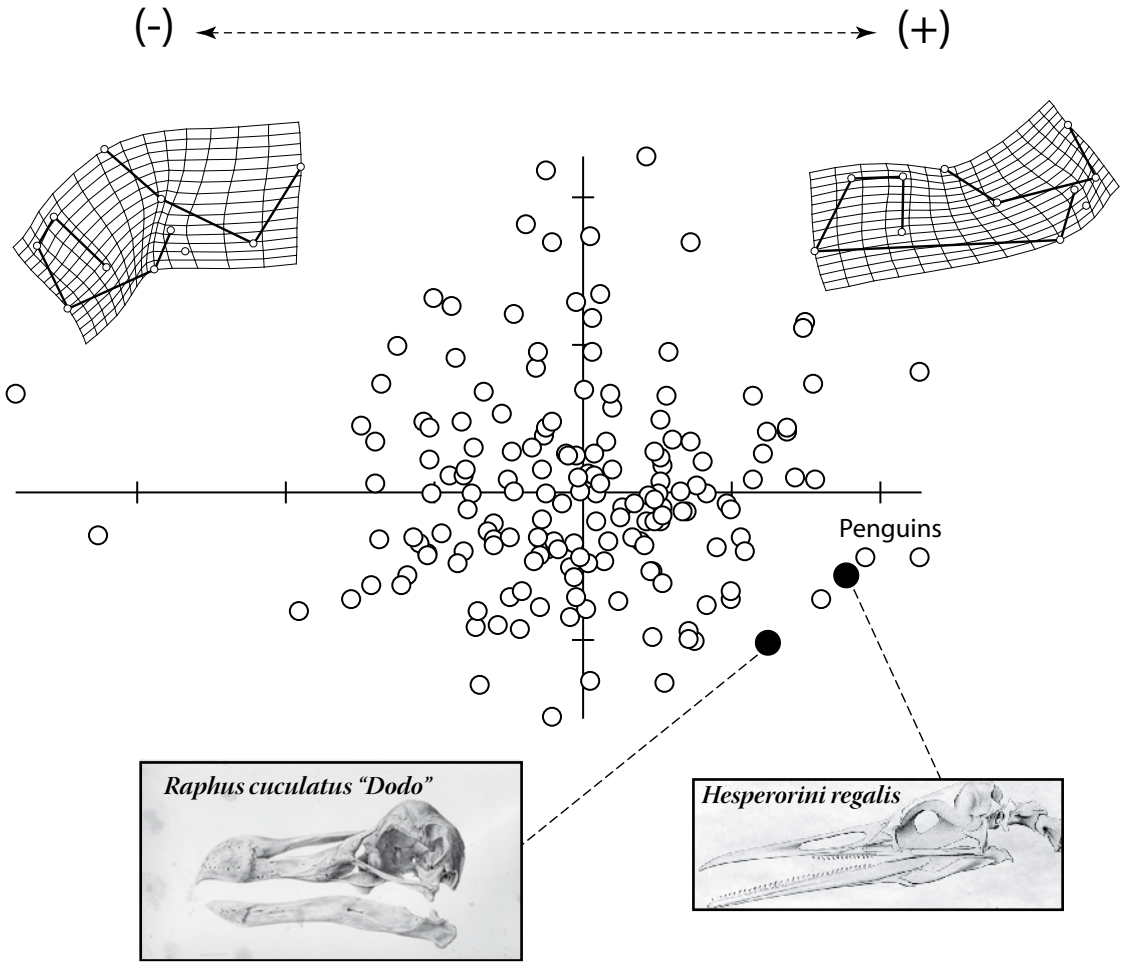

Figure 12. Re-calculation of a relative warps analysis withouth the rostrum, in which all the N=170 individuals of the sample and two fossil birds, *Hesperornis* (reconstructed after Marsh, 1880, and the Dodo, after Strickland and Melville (1848) are incorporated. As expected, (possibly, because they are very large) the two fossil forms are either more orthocranial (possibly, the Dodo), or airorhynchal (Hesperornis). Notice as well that *Hesperornis* lies very close to modern penguins.

to other Theropod dinosaurs.

Longirostrality is a characteristic of birds, yet we don't really know when it emerged. Its rise as a morphological trait may date back to the Early Cretaceous in the form of enantiornithine birds, in forms similar to the recently described *Longirostravis haani* from the Early Cretaceous of China (Hou et al., 2004; Fig. 11a). Unfortunately no enanthiornithine bird allows landmark digitalisations due to the poor preservation of the lateral view of their skull. Thus, we can only speculate from qualitative evidence and wait until more specimens become unearthed.

In figure 11a it is also evident that cranial flexure (klynorhynchy) is typical only for avians, and quite possibly, particular to the clade Neoaves, and the same occurs with airorhynchy (see also Fig. 7a, b, c, d). Again, morphospace boundaries are spanned by morphological particularities of avian skulls. Fossil theropods, in effect, are restrained to regions outside of the bird distribution. However, whether this situation is of extreme Airorhynchy rather than of Orthocraniality remains untestable with fossils. While the situation would imply that fossil theropods are airorhynchal, in the light of our new results, this should be tested with more particular landmarks. Deleting landmarks that outline the rostrum may also convey clearer appreciations, as it occurred when analysing birds, yet the problem with dinosaurs is that it is difficult to obtain more landmarks that suffice to test the hypothesis. This is more complicated if the rostrum is excluded from the analyses (see Fig. 11, landmarks in picture above). Note as well that we have established our hypothesis assuming that we could infer the relative position of the cranial base in birds, something that is impossible in fossil dinosaurs. CT-scans are becoming widespread and will likely aid resolving this crucial issue.

On the other hand, avian cranial morphological organization is also allometrically associated with size, particularly with body mass. Cranial organization seems to relate to size in such a way that larger sizes relate to more extended skull types. This means that it may be possible to approach the underlying basis of phenotypic variation, but also, that certain aspects of evolutionary morphological change may be predictable. For instance, if extended skulls (either orthocranial or airorhynchal) tend to equate with larger sizes we should be able to predict that any large avian skull, or the skull of a close relative, would tend to have this craniofacial condition.

To test this assumption we digitized the same p=11 landmarks of figure 2 (without the rostrum) on the lateral view of two reconstructed skulls of fossil birds, a Dodo and one of *Hesperornis* (Fig. 12). We expected that given their relatively large size (in contrast to other

birds) they would occupy a position in the distribution corresponding to large sizes, that is, of more extended crania. Results in figure 12 shows how these two skulls plot within the relative warps distribution at the expected position. Note that, this is only exploratory and, although not performed, the same should be attained with multivariate regressions.

In principle, this prediction may be also transposable to fossil Theropod dinosaurs who, given their relative larger sizes (e.g. body masses in contrast with other birds), should have, orthocranial skulls, if not airorhynchal. Notice as well, and this is very important, that having an extended skull (*s.l.*) implies that the foramen magnum will always point caudally, and not ventrally (cf. Figs. 7c, d and 9). Allometric explorations with multivariate regressions have suggested that most shape changes related to size associate with the orientation of the foramen magnum via the changes in shape of the supraoccipital, and possibly the cranial base. Allometric shape changes also affect the facial skeleton but only in terms of its configuration (shape), and not its orientation relative to the braincase.

One note about these types of predictions is that, nevertheless, the size of the cranium may be also dissociated from its relationship to body size as a whole. For instance, the sample we used in this study includes very large avian forms such as an ostrich, a rhea and an emu. Both forms locate in a region that does not correspond to their extreme larger body sizes (Fig. 7a, b, c, and d). While interestingly, this may also be associated to the common view that the morphology of these avians is associated to strong heterochronic shifts; Livezey, 1995), it is suggesting, in turn, that the relative size of the whole skull may decouple its growth from somatic size in particular instances. This is a case that herein exemplified with particular birds but may happen in other archosaurs., as might be the case, for instance, of Sauropod dinosaurs, amazingly large organisms whose cranial size does not correspond to what any common allometric relationship would predict. Nevertheless, in reference to relative skull architectural flexures, all these organisms are large, and therefore, should comply with the expectance of having skulls that are extended (at least orthocranial, but may be airorhynchal, but always with the foramen magnum pointing caudally), something that is corroborated by the analyses (Fig. 7).

3.2.4.iv Allometric phenomena

Avian macroevolutionary disparity seems to be allometrically related to size, at least to some extent. However, results show that changes of the facial skeleton that are related to size do not imply changes in orientation, changes that are otherwise related to size and take place

within the braincase. Moreover, longirostrality may have some degree of morphological independence from the remainder parts of the cranium and it is undoubtedly unpredictable allometrically.

In effect, only the elements of the facial skeleton that remain after excluding the beak vary in shape as a function of size, and thus, it is only the rostral part of the facial skeleton (premaxillae and nasals) which decouples its proportional shape in a way that does not match allometric predictions from body mass. Thus, allometric associations of shape change comply with the classic expectation (the relative proportion of the braincase is relatively smaller at larger absolute sizes than the facial skeleton; Von Haller, 1762). However, longirostrality does not coincide with any particular cranial architecture (flexure or extension, and thus, longirostrality is not compromised with any particular type of cranial architectural variant.

Longirostral birds are a special case in which the length of the rostrum has been classically viewed as achieved in post-hatchling stages passing by a more rapid growth rates of the rostrum (i.e. a strong positive allometry) than that which occurs in other non-longirostral species (Rench, 1959). In this view extreme rostral growth has been evaluated as the maintenance of marked growth equivalent to the typical ontogenetic pattern after hatchling (i.e. heterochrony). (Note that, by the same coin, it could also be argued that brevirostrals have "retained" their growth; i.e. negative allometry).

Allometry often associates to developmental processes, despite the fact that it is fundamentally phenomenological. In effect, we can see that evolutionary allometry underlies a pattern of skull homoplasies in avians at a macroevolutionary scale. Thus, allometry in this context is a key trait decoupled from phylogeny in such a way that body size (mass) is linked to skull morphological evolution.

One developmental question that arises at first glance is if longirostral birds, or some of them, hatch with relatively larger rostra than others. In other words, the question is whether embryos of adult longirostral forms distribute in such region within morphospace, in a region of mesorostrals or of brevirostrals. In principle, it appears that classic allometric studies would predict that the "normal" position of hatchling departure would be brevirostral. In Fig. 13 we show an embryo of a kiwi, which may suggest that, otherwise, the onset of its rostral growth may be already at a position within shape space of at least a mesorostrals, if not already a longirostral. While the rostrum would grow from meso- to longirostral (if it wasn't born a longirostral), the primary dissociation towards becoming a longirostral may have been developmental, thus beginning earlier in morphogenesis.

a)

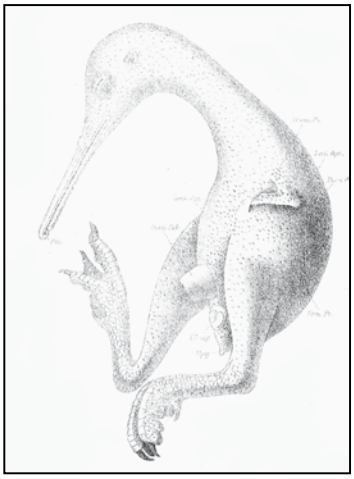

b)

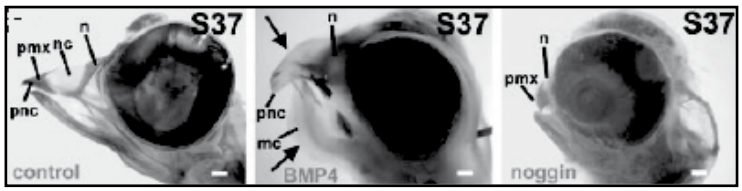

Figure 12. Avian Embryos. a) Original drawing of a Kiwi embryo from Parker (1891). b) Original pictures of Wu et al., (2004) showing how manipulating BMP4 quantities can dramatically modify the proportion of the rostrum in early morphogenesis.

Little is known about the development of craniofacial arrangements. The only information available is the experiments of Lang (1952) in which, regrettably, no measurements were taken, and therefore, all diagnoses were uniquely qualitative. Lang's observations pointed out several aspects of the configuration of the cranial base and the morphology of the craniofacial system. We may highlight that, in her view, all skulls begun as klynorhynchal in early stages. It would be the orthocranial skulls that passed by more dramatic changes in order to attain such arrangement (nothing was stated about airorhynchals).Whether a flexed skull is the effect of a heterochronic retention of an early developmental stage or not may be an important query to promote further studies.

3.2.4. v Some morphogenetic aspects of avian skull integration and rostral variation

The vertebrate skull is often claimed as a tightly integrated structure. This means that while being composed by many different parts, all these constitute a coherently functional whole. The parts of the skull can be subdivided into functional units (see e.g.; Moss, 1975) as the

braincase or the facial skeleton, but also by their skeletogenetic origins (Noden, 1983; Couly et al., 1993; Noden and Trainor, 2005).

Classically, the skull of whatever the vertebrate was conceived as built upon an ordered series of modified vertebrae (i.e. a repetitive series in a pattern of basic element, modules, being vertebrae; viz. *the vertebral theory*). In order to recognize its elementary organization, the skull could thereby be described as "modular", whereby each elementary unit would be each serially placed and "modified" vertebra.

However, the ability to specify a head structure (Huxley, 1858), rather than reiterate another body segment (Goethe and Oken's vertebral theory; fide Huxley *op. cit.*), is now seen as a crucial step that took place in vertebrate evolution. This evolutionary step corresponded to the acquisition of two cell populations: the neural crest and the ectodermic placodes from which the whole facial skeleton emerges (Gans and Northcut, 1983; Northcut and Gans, 1993; reviews in, Chambers and MacGonnell, 2002; Santagatti and Rijli, 2003; Helms et al., 2005).

However, one part of the remainder skull, most of the neurocranium, is of paraxial mesodermic origin (Noden and Trainor, 2005). Thus, the differences in allometric behaviour may root in these compositional differences (Riska, 1986). Cellular embryonic differences among so-well delimited and generically different domains could explain why it would be feasible to expect different systemic responses to growth, since early in development each cell-type population may just be competent to certain particular signals and not to others.

In fact, they convey different parts of the cranium. The facial skeleton can be delimited on the basis of its function (Klaauw, 1945, 1948, 1952; Moss and Vilmann, 1978), and as a functional unit its variation could be partially independent from the braincase, which serves a different function within the system. Interestingly, delimiting the identity of the parts on developmental basis provides an equivalent insight. This latter criterion, however, is as well coherent with a mechanistic hypothesis in which different patterns of variation between parts may be due to different cell population behaviours, hence different morphogenetic machinery (i.e. the identity of its pathways and its reading by some competent cell populations, and not others).

On the other hand, the whole facial skeleton belongs to a skeletogenetic domain that emerges solely from neural crest cell populations, and riddle is why the rostrum, within the facial skeleton does, varies so much and apparently unlinked to the remainder facial skeletal elements. In recent years, a large body of work has begun to reveal in detail how these neural crest cell populations in the facial skeleton are actually generated, what types of

controls are in place to modify neural crest cell migration and, ultimately, the role that this cell population plays in establishing the pattern of the craniofacial skeleton.

Experimental embryology is now beginning to unveil that aside from their neural crest origins, tissue interactions play a crucial role in craniofacial arrangements. One set of interesting grafting experiments have argued about the maintenance of the temporal program of gene expression (i.e. species specific) in neural crest cells after switching their frontonasal cell populations between ducks and quails (Schneider and Helms, 2003; Fig. 10b). These experiments found that grafting altered the tolerance of the chimeras to such an extent that ducks with quail frontonasal neural crest cells had a quail-like beak, and quails carrying duck neural crest cells had a duck like beak. Interestingly, shape differences were advocated in the light of their quantitative comparisons based on pair-wise RFTRA superimpositions (Fig. 10b), which also highlights the potential uses of the technique in embryonic comparisons.

However, it seems to be that it is not all about the pre-programming (and independence) of the fate for neural crest cell populations, but that epithelial tissues are as well important organizers of rostral shape change, and therefore, of integration (despite their still debated origins; ectodermal, neuroectodermal, or endodermal; see e.g. Creuzet et al., 2005; Richman and Lee, 2003). Furthermore, "tinkering" with morphogenetic proteins such as BMP4 at the frontonasal prominence (one of the complex of prominences that coordinate the rise of the facial skeleton) may be enough to modulate the shape of the beak (Wu et al., 2004; see proportional shape changes in the beak of an chicken embryo in, Fig. 13b).

Open questions remains on the issue, as to when did the decoupling of the rostrum from the remainder facial skeleton occurred. Perhaps it took place under a differential production and control of BMP4 morphogen protein in enanthiornithine birds such as *Longirostravis* around the Early Cretaceous. Likewise, it appears crucial to understand not only the moment of emergence in geological time, but the role of one often neglected corneal ramphoteca in morphogenesis.

3.3 Avian skull morphological evolution: exploring endo- and exo-cranial covariation with two block partial least squares

Marugán-Lobón J. & A. D. Buscalioni.

Paper Published in the journal *Zoology*

Available online at www.sciencedirect.com
SCIENCE DIRECT
ELSEVIER
Zoology 109 (2006) 217–230
ZOOLOGY
www.elsevier.de/zool

Avian skull morphological evolution: exploring exo- and endocranial covariation with two-block partial least squares

Jesús Marugán-Lobón*, Ángela D. Buscalioni

Unidad de Paleontología, Dpto. Biología, Universidad Autónoma de Madrid, 28049 Cantoblanco (Madrid), Spain

Received 4 November 2005; received in revised form 27 February 2006; accepted 3 March 2006

Abstract

While rostral variation has been the subject of detailed avian evolutionary research, avian skull organization, characterized by a flexed or extended appearance of the skull, has eventually become neglected by mainstream evolutionary inquiries. This study aims to recapture its significance, evaluating possible functional, phylogenetic and developmental factors that may be underlying it. In order to estimate which, and how, elements of the skull intervene in patterning the skull we tested the statistical interplay between a series of old mid-sagittal angular measurements (mostly endocranial) in combination with newly obtained skull metrics based on landmark superimposition methods (exclusively exocranial shape), by means of the statistic-morphometric technique of two-block partial least squares. As classic literature anticipated, we found that the external appearance of the skull corresponds to the way in which the plane of the caudal cranial base is oriented, in connection with the orientations of the plane of the foramen magnum and of the lateral semicircular canal. The pattern of covariation found between metrics conveys flexed or extended appearances of the skull implicitly within a single and statistically significant dimension of covariation. Marked shape changes with which angles covary concentrate at the supraoccipital bone, the cranial base and the antorbital window, whereas the plane measuring the orientation of the anterior portion of the rostrum does not intervene. Statistical covariance between elements of the caudal cranial base and the occiput inplies that morphological integration underlies avian skull macroevolutionary organization as a by-product of the regional concordance of such correlated elements within the early embryonic chordal domain of mesodermic origin.

Keywords: Birds; Cranium; Morphological integration; Geometric morphometrics; Macroevolution

Introduction

The avian skull is structurally and functionally composed of the rostrum, the orbits and the braincase. Historically, comparative morphologists have described two marked avian skull configurations, extended or flexed, depending on the way in which such structural units are arranged (Marinelli, 1928; Van der Klaauw, 1948). When the skull is viewed laterally, an extended skull type has the rostrum, the orbit and the braincase all aligned consecutively in the same plane. In this condition, the foramen magnum opens caudally (i.e., the plane defined by the foramen magnum is vertical with respect to the horizon), and thus, the medullar axis is also oriented caudally (Fig. 1a). In the flexed condition, the alignment of the rostrum, the orbit and the braincase is decoupled thereby giving the whole skull a "bent" or

*Corresponding author.
E-mail address: jesus.marugan@uam.es (J. Marugán-Lobón).

0944-2006/$ - see front matter © 2006 Elsevier GmbH. All rights reserved.
doi:10.1016/j.zool.2006.03.005

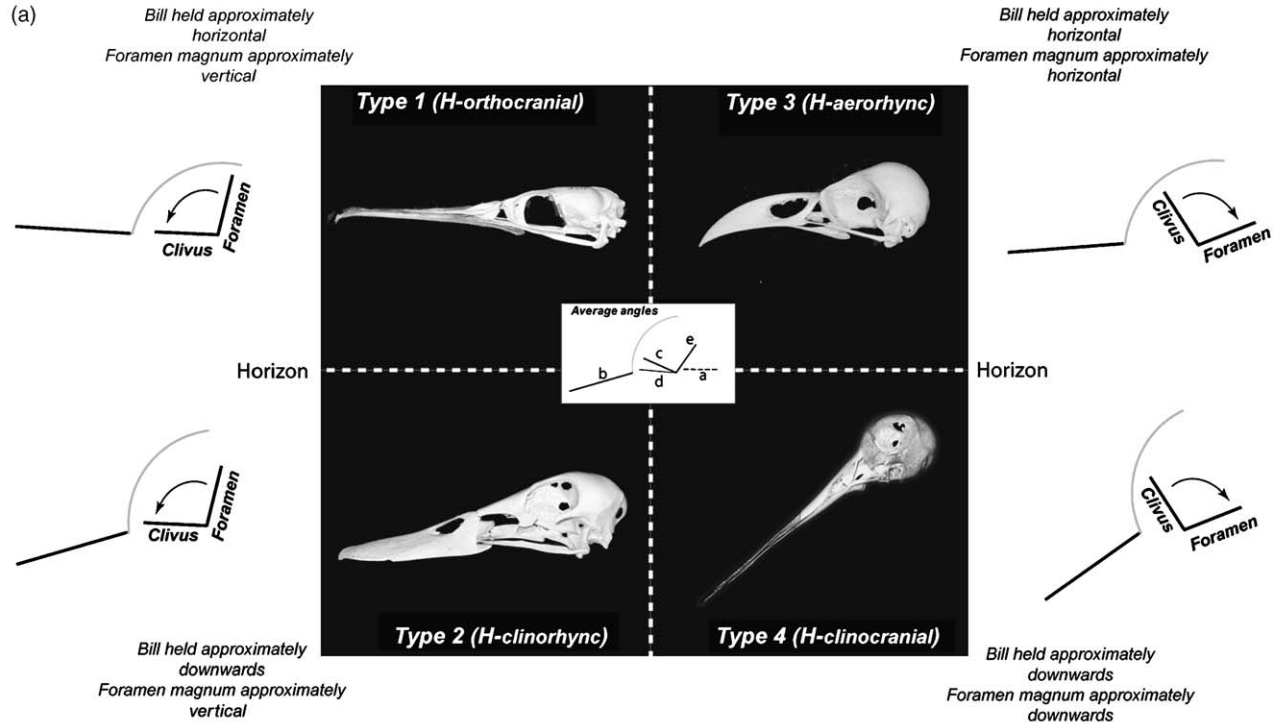

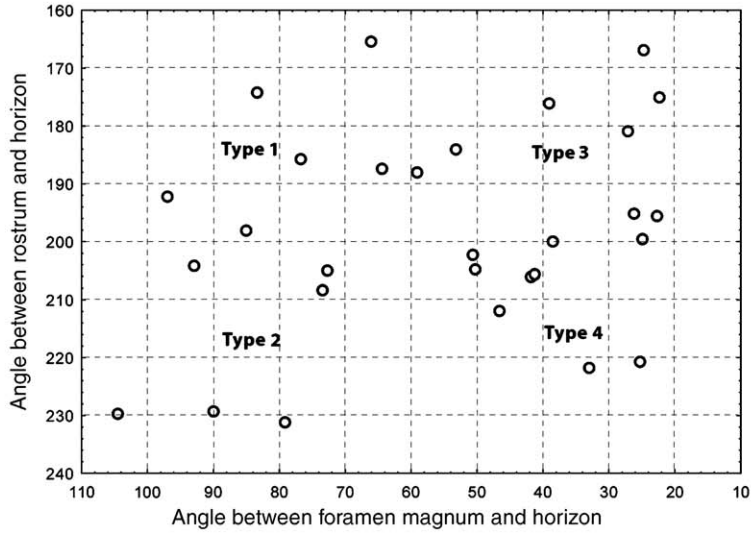

Fig. 1. Evolutionary skull typologies across modern birds (Neognathae). (a) Skull typologies after Duijm (1951): cormorant (Type 1), duck (Type 2), crow (Type 3) and woodcock (Type 4). Types are also labelled according to Hofer (1952) (in brackets), to show the analogies between both studies, even though they were conceptually different. Schematics at the sides show how measurements were depicted in the original paper; schematic in the centre portrays mean angular values of the full data set, with letters corresponding to the measured anatomical parts (see Fig. 2 and text). Horizon was the system reference (white horizontal dashed line), skulls pose in the ''natural'' posture when in alert. Sketches and text on the sides explain the structural meaning and match how measurements were depicted in Duijm (1951) (instead of scalars). (b) Scatter-plot of measured angles corresponding exactly to Duijm (1951, Fig. 5, p. 211). Distribution of points in the quadrants corresponds to types depicted in (a) (in the same order).

flexed appearance (Fig. 1a). In this latter situation the plane of the foramen magnum is declined (i.e., opens ventrally), and therefore, the medullar axis points ventrally. A typical example of an extended skull type would be a cormorant, of a flexed one, either a woodcock or a pigeon.

Comparative studies aiming to understand the evolutionary meaning of this type of structural variation of the avian skull received particular attention in the middle of the 20th century. Several studies attempted to outline what type of structural changes could underlie such phenotypic variants. Although this phenotypic

variation is visible in lateral view (externally), elements of the endocranium, mostly in the mid-sagittal plane, were also found to intervene. A causal explanation of the skull variation could be that the phenotypic organization of the skull would be functionally constrained, for instance, by the need for particular head postures that aided sensory coordination (i.e., vision and hearing). A case example stated that this requirement was fulfilled by holding the head in a posture of alert (Duijm, 1951). Assuming the importance of such a posture of the head and measuring with respect to the horizon, Duijm (1951) found that the position of the clivus (the endocranial midline plane marked by the basioccipital and the sella turcica) showed marked changes in its orientation. In an extended skull, the angle of the clivus was found to be roughly parallel to the horizon whereas in a flexed skull, the clivus would be elevated (dorso-anteriorly elevated at the pre-sphenoid bone, i.e., at the dorsal rim of the sella). Because the relative orientations of the clivus were found to match the orientations of the foramen magnum, both parts were addressed as principal elements involved in the evolutionary organization of the avian skull.

Interestingly, the correlation of changes between the caudal cranial base and the foramen magnum could have been formulated in terms of morphological integration (see, van der Klaauw, 1948), but the concept and its methodological framework was still in an incipient stage of development (Olson and Miller, 1958). Additional to the coincidence in orientation between the caudal cranial base and the foramen magnum at the occiput, Duijm (1951) found that the angle between the rostrum and the orientation of the latter elements was very heterogeneous. These observations led him to differentiate between three different flexed phenotypes against just one extended type (Fig. 1a). Contemporarily, Hofer (1952) approached the same problem, although qualitatively, and arrived at a description of a more complex pattern in which he distinguished between one extended type and four flexed types (Fig. 1a).

More recently, a landmark-based geometric morphometrics survey of avian skull shape variation showed that an important amount of inter-specific morphological differences allowed the polarization of two equivalent morphological extremes, i.e., extended or flexed skull phenotypes (Marugán-Lobón and Buscalioni, 2004). Additionally, avian skull phenotypic differences were found to occur within a single shape cline (i.e., one single dimension of a factor analysis). Finding a coincident morphological account for the avian skull by means of this new morphometric procedure suggested that a reappraisal of the topic would be worthwhile in order to gain further insights on its evolutionary implications. Since shape differences between taxa occurred within a single statistical trend it was also an appealing chance to test if certain elements of the avian skull were morphologically integrated, as early authors were apparently anticipating, and accordingly, to investigate which are the elements involved in skull organization.

This study explores the integration that may underlie the architectural coherence and phenotypic organization of the avian skull at an inter-specific scale. We propose an entirely metric approach by which we explore the possible relationship between endo- and exocranial elements of the skull combining two different sources of skull metrics. For endocranial measurements, we used the "traditional" data set used by Duijm (1951) that accounts for angles in the mid-sagittal plane between skull elements across an inter-specifically broad sample. Angles in this data set describe the orientation of the rostrum, the cranial floor, the clivus, the foramen magnum and the lateral semicircular canal. The use of this source of data solves the methodological difficulty of obtaining first-hand endocranial information, a procedure that is surgically intricate and additionally difficult when working at high taxonomic scales. Also, reprocessing these data bridges a long temporary gap of research on the morphological evolution of the avian skull recovering an incipient hypothesis of morphological integration that was proposed more than half a century ago (Duijm, 1951).

Operatively, we combined the informative contribution of the more traditional metrics (i.e., angles) measured by Duijm (1951) with that of the more recently developed geometric morphometrics (Bookstein, 1991; Adams et al., 2004). For this sake, we replicated a sample with real skulls that matched the genera and number of individuals listed in the original paper ($N = 29$; Duijm, 1951). On the lateral view of the skull, we digitized a series of 12 landmarks known to be suitable for capturing the relative cranial "flexure" or "extension" described for the avian skull (Marugán-Lobón and Buscalioni, 2004). These landmarks do not overlap with the traits that were measured by angles because most angles were measured endocranially and in the mid-sagittal plane, while all landmarks are strictly exocranial.

The method we used to combine the more traditional angular scalars with the new shape-metrics is the statistical-geometric procedure of two-block partial least squares (2BPLS; Rohlf and Corti, 2000; also known as singular warps analysis; Bookstein et al., 2003). Two-block partial least square analysis in geometric morphometrics has been developed as a tool to compare and statistically test covariance between patterns of variation of different sets of variables. These different sets of variables are treated as separate blocks, and comparisons are established between trends of variation pertaining to each block. The use of 2BPLS in geometric morphometrics implies that one block of variables must

correspond to shape variables (i.e., Procrustes coordinates) while the other can either consist of shape variables, or any other type of metric variables (e.g., angles or lengths). In this study, we opted for the second alternative which allows combining shape with traditional (angular) metrics.

As mentioned above, the block of angular scalars represents the angles between specifically assigned and measured cranial parts, between which a particular pattern of morphological association was hypothesized (see Fig. 1 and text above; Duijm, 1951). Our hypothesis of shape variation (i.e., landmark analysis) is that rostral variation (mostly in terms of proportion) should be a dominant aspect of skull shape of a factorial ordination among birds at an inter-specific scale, and that, subsequently, a second factor will account for cranial relative flexed or extended external appearances (and associated shape changes) when explaining the remaining shape variance (see Marugán-Lobón and Buscalioni, 2004). However, the sample used herein has never been analysed using geometric morphometrics statistical procedures. Thus, the principal trends of skull shape variation across individuals of the sample will first be explored using relative warps (RW) analysis (Bookstein, 1991; Rohlf, 1993), in order to test the sustainability of this hypothesis.

While the approach proposed is methodologically unproblematic, it is conceptually elaborate, because it entails (1) a statistical re-evaluation of the angular relationships between cranial parts measured and analysed more than 50 years ago, and (2) an exploration of the principal dimensions of skull shape variance of the equivalent inter-specific sample of birds. By combining both metric data sets with 2BPLS, we expect (3) to find a principal trend of covariation that expresses equivalent morphological accounts as the ones found for each of the metric analyses independently (angular and shape ones). This way we can also ascertain which and how endocranial and exocranial elements might be involved in configuring the phenotypic organization of the avian skull. Findings are discussed in terms of the potential influence that evolutionary morphological integration may have in organizing the avian skull phenotype.

Materials and methods

Sample and skull angles

The studied sample replicates the one used in Duijm's (1951) experiment ($N = 29$ avian skulls; only three individuals were unavailable, but their morphological information was not taxonomically crucial). The sample represents a large extent of cranial diversity and disparity within Neognathae (Galloanseres and Neoaves; Cracraft, 1988; Zusi and Livezey, 2001; Mayr and Clarke, 2003). The specimens represent 18 families (after Sibley and Monroe (1990)): Podicipedidae, Gaviidae, Phalacrocoracidae, Ardeidae, Thereskiornithidae, Ciconiidae, Falconidae, Anatidae, Rallidae, Alcidae, Laridae, Charadriidae, Scolopacidae, Columbidae, Psittacidae, Corvidae, Muscicapidae and Sturnidae; genera, institutions and labels are listed in electronic Appendix 1, see also under supplementary video material at www.elsevier.de/zool.

Angular measurements in the earlier experiment were taken with reference to a "neutral" posture actively attained when the organism was in alert and with respect to the horizon (Duijm, 1951, p. 209). Measurements represent positional angles in the mid-sagittal plane between the ventral edge of the rostrum (therein described as the "fissure of the beak", i.e., in the mid-sagittal ventral edge of the beak), the plane of the clivus within the caudal cranial base (i.e., the midline plane of the basioccipital to the pre-sphenoid, defined from the caudal rim of the foramen magnum to the dorsum sellae at the pre-sphenoid), the cranial floor (the plane defined by the parasphenoid bone), the plane of the foramen magnum, and the plane of the lateral semicircular canal. Because in the original paper angles of planes were provided schematically without their corresponding scalars (see examples in Fig. 1), we scanned them from the figure of the original paper and measured the angles digitally with Scion image (v.4.03; Scion Corporation, 2005). The reliability of our measurements in correspondence to the original source was tested comparing a scatter-plot of our digitized measurements with the one previously published (our plot in Fig. 1 is identical to Fig. 5 in Duijm (1951, p. 211)).

Geometric morphometrics

A series of 12 homologous landmarks (Table 1; Fig. 2) were digitized from digital pictures of the equivalent $N = 29$ avian skulls in lateral view. Digital photographs were obtained following a protocol designed to avoid lens distortion and parallax as described in Marugán-Lobón and Buscalioni (2004). Landmark coordinates (LM) were evenly placed across the whole skull over evolutionary stable (repeatable) structures, and only on externally visible traits. Simultaneously, LM coordinates characterize other cranial parts; e.g., the cranial base (inferred from its outer aspect) is delimited by LM 6, 7 and 12, the rostrum by LM 1, 2 and 3, and the supraoccipital bone by LM 11 and 12 (more are listed in Fig. 2b). Landmark 12 is placed at the foramen magnum, thus partially overlapping on an element whose metric variation is also characterized by an angle. Overlapping could bias the analysis if both

Table 1. Homologous landmarks and their anatomical meaning

Number	Anatomical description
1	Premaxillary symphysis at the tip of the rostrum
2	Joint (in lateral view) of the nasal and lacrimal bones (e.g., craniofacial hinge when possible)
3	Anterior-most edge of antorbital fenestra projected perpendicularly to rim of maxilla
4	Orbitonasal foramen (N. I)
5	Intersection between the palatines at the choana dorsally with mesethmoid
6	Foramen of the olfactory nerve (N. I)
7	Foramen of the optic nerve (N. II)
8	Insertion of quadrate to squamosal bone in braincase
9	Articulation between quadrate and jugal bar
10	External ear (geometric centre of the auditory meatus)
11	Caudal-most junction of parietal and squamosal bone
12	Mid-point of foramen magnum

measurements were capturing the same morphological information (i.e., they would be logically adding a magnitude of correlation between blocks). However, this should not be the case in the present study because the angle of the plane of the foramen magnum captures its relative orientation, while LM 12 at the foramen only captures its geometric localization with respect to the remaining landmarks of the configuration. Only with an additional landmark placed therein (at the foramen), shape analysis could perhaps capture the orientation of the foramen (cf. Fig. 2).

Generalized Procrustes superimposition (GPA; Bookstein, 1991; Adams et al., 2004) is the operational core of landmark-based geometric morphometrics. GPA removes all information of the configurations unrelated to shape, minimizing the distance between homologous

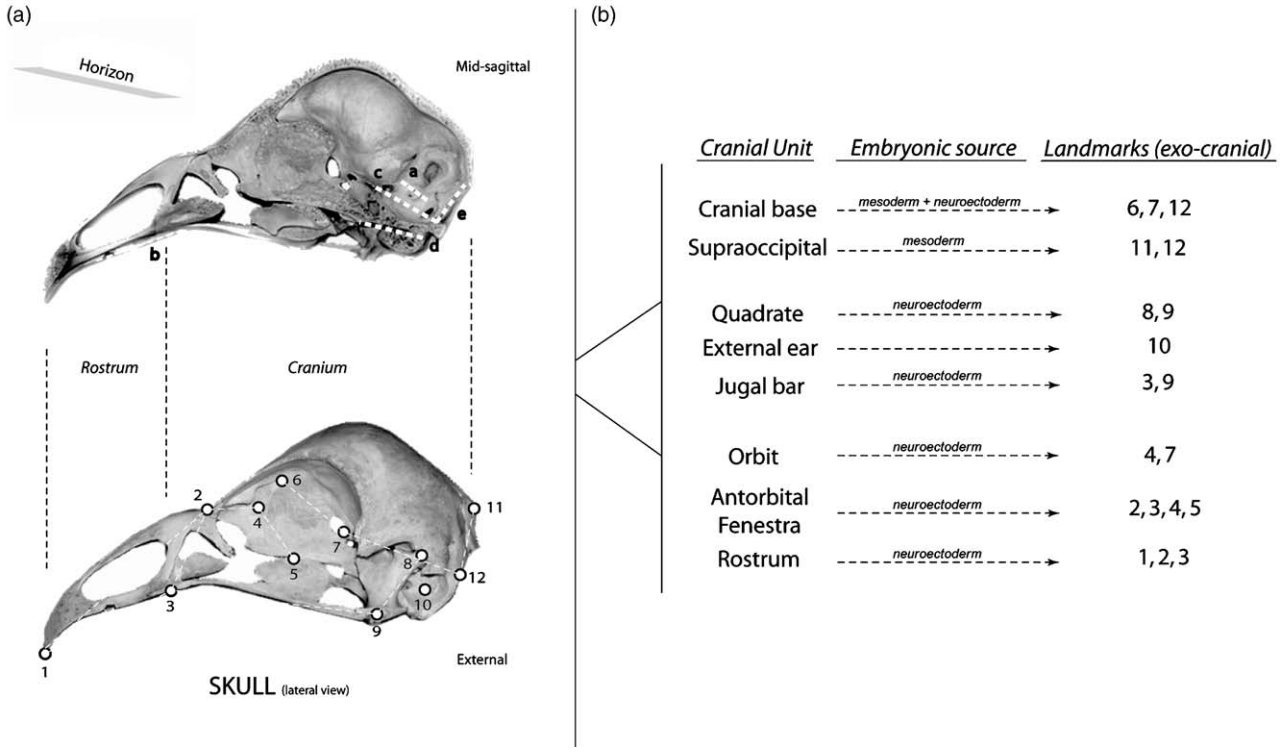

Fig. 2. Sketch of angular measurements and the series of landmarks used. (a) Angular measurements and landmark series on a skull (of a screamer). Above, endocranial (mid-sagittal) view and angular measurements: a = lateral semicircular canal, b = ventral rim of the rostrum, c = clivus (basioccipital bone), d = cranial floor, e = foramen magnum. Plane of the horizon drawn to show how angular measurements were referenced. Below, exocranial view of skull and externally visible landmarks (LM). (b) LM listed in relation to more inclusive skull parts and embryonic precursors of skull parts (after Couly et al. (1993)). Note that some LM may fall either in or close to the mid-sagittal plane (LM 4, 5, 6, 7, 11).

landmarks by translating, rotating and scaling all forms to a common reference (by consensus, the grand mean; Rohlf and Slice, 1990; Bookstein, 1991). What is meant by shape, then, is the geometric information that remains after location, scale and rotational effects are filtered out of form (i.e., Procrustes shape coordinates).

We use the thin plate spline (TPS; Bookstein, 1989, 1991) as a convenient way to visualize shape differences as smooth deformations. TPS is an interpolation function that models a hypothetically thin metal plate with locations marked as in the reference configuration that is then deformed until the locations of the landmarks match those in a determined target configuration. Deformations of the TPS thus show the mismatch between homologous locations from a departure shape (here the consensus) to a target shape. Also, TPS is a convenient tool to secure a suitable set of shape variables for any conventional multivariate statistical analysis, i.e., partial warp (PW) scores plus the uniform component (Bookstein, 1991; Zelditch et al., 2004).

Multivariate statistics – RW and partial least squares

Major trends of shape variation of the sample are explored by means of RW analyses (Bookstein, 1991; Rohlf, 1993). RW is in essence a principal component analysis (PCA) of the PW, and its vectors describing the major trends in shape can be viewed as deformations using the TPS. The choice of metrics for the RW analysis was to uniformly weight the bending energy needed to deform the grid (i.e., $\alpha = 0$, weighting large and small scales between landmarks equally), and also included the uniform component (for further details, see Rohlf (1993)).

Rohlf and Corti (2000) developed the mathematical rationale for 2BPLS, both for shape-to-shape tests and other metric variables to shape tests. Two-block partial least squares is used to explore patterns of covariation between different blocks of variables. The technique is similar to a PCA in that it expresses variation among the observations in terms of a few dimensions that are linear combinations of the original variables. However, it differs in that its dimensions are inter-block generated, its components are ordered according to covariance instead of to explained variance, and the variance–covariance matrix does not need to be squared which is mathematically accomplished by using a single value decomposition (SVD) of the matrix (see also Zelditch et al. (2004)). Each singular dimension of the SVD associates to a pair of singular axes (one per block of variables, each representing a pattern) and measures the covariance explained by pairing the axes. Permutations (999; $P<0.001$) test the statistical significance of the corresponding vector correlations among blocks in the model, as well as the probability that the covariance is restrained to occur within fewer dimensions.

All geometric morphometrics and associated statistical procedures (landmark digitalization, GPA, RW and PLS) were performed using the TPSseries software for morphometrics (TPSdigit v. 1.40, TPSrelw v. 1.41 and TPSpls v.1.12, respectively; Rohlf, 2003–2005 @ http://life.bio.sunysb.edu/morph/). The electronic appendix also includes animated frames of deformations of the TPS for each statistical analysis (RW and PLS) complementary to Figs. 3 and 4.

Results

Descriptive statistics of angular measurements and their correlation matrix are summarized in Table 2. Although the mean angle of the lateral semicircular canal to the horizon is roughly zero as previously suggested (mean = 0.33; Duijm, 1951), its standard deviation is relatively high in contrast to the remaining angular measurements (Table 2). The most significant correlation is found between the orientation of the foramen magnum and the clivus ($r = 0.92$; $P<0.01$); the remaining angles between cranial parts are intercorrelated but with far less significance ($P<0.01$). An exception is the orientation of the rostrum which is not correlated to the angular orientation of any other skull part.

RW analysis of the full landmark data set (the whole skull) shows that the first dimension (RW1) is dominant (67.4% explained variance; Figs. 3a and b). Deformation of the spline concentrates at the rostrum (between LM 1, 2 and 3; see LM in Fig. 2), and associates to a marked variation in antero-caudal proportion. However, changes are not homogeneous, but show a slightly curved deformation of the spline. The scatter-plot between RW1 (strong rostral antero-posterior stretching or compression) and RW2 is very heterogeneous (Fig. 3a).

The second dimension (RW2, 22.65% of explained variance) shows the whole spline curving as well, making the overall appearance of the grid either slightly convex or concave (Fig. 3b), but also homogeneously stretching or compressing dorso-ventrally. This deformation apparently corresponds to rostral shape variation (declination) accompanied by other changes across the remaining landmark configuration (Fig. 3b). When the rostrum is oriented downwards, the spline appears concave and conversely, when the rostrum is tilted upwards, the spline appears convex. Overall, the extreme values of this second dimension correspond in appearance to the two cranial types, flexed and extended, and account for several aspects of skull shape differences aside from rostral orientation (e.g., the

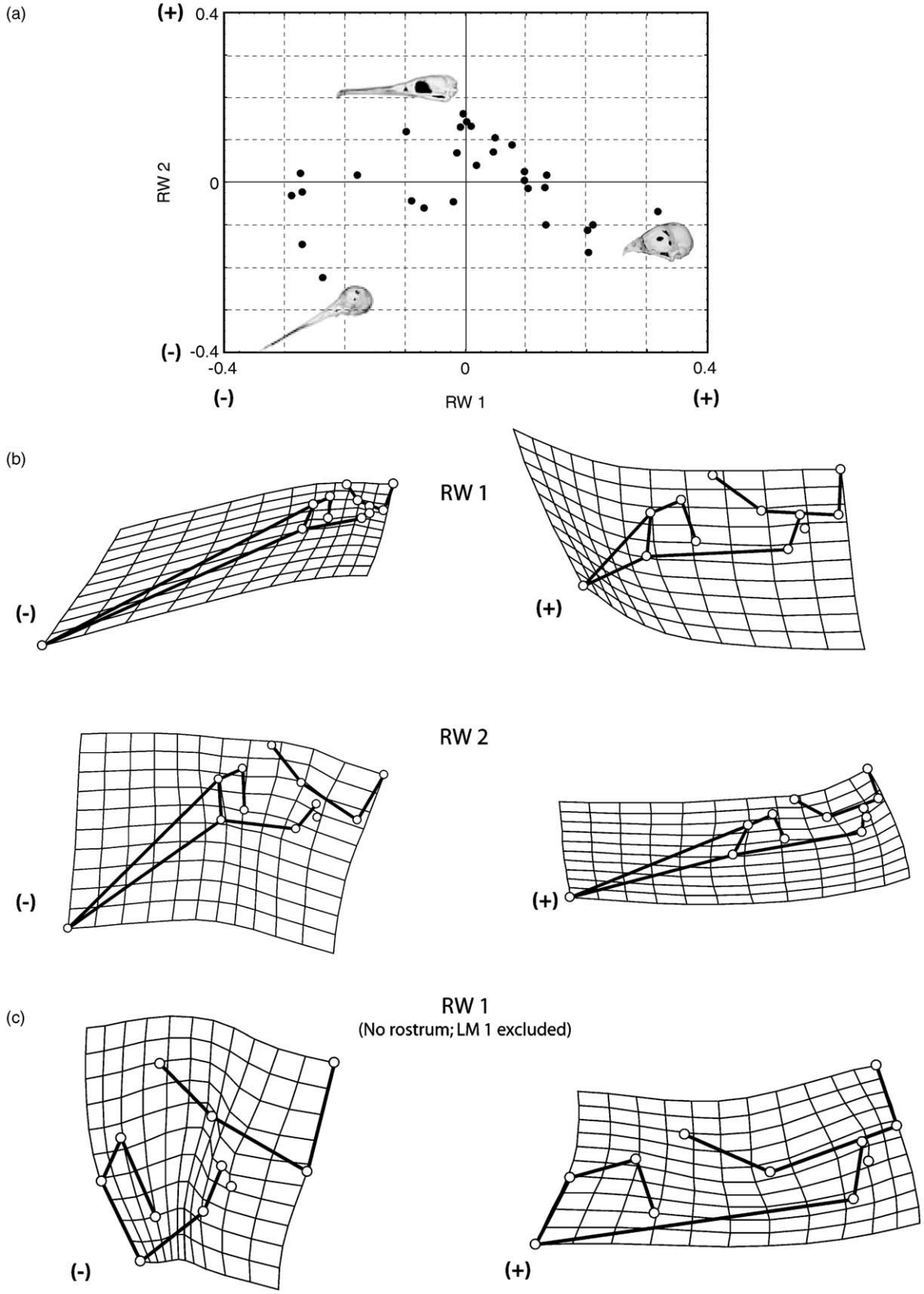

Fig. 3. Relative warps (principal trends) of the full data set, $N = 29$, both including the rostrum and without the rostrum. (a) Scatter-plot of RW1 (x-axis) vs. RW2 (y-axis) with rostrum. Skulls: left, woodcock; centre, cormorant; right, common kestrel. (b) Grids (spline) for RW1 (above) and RW2 (below) shown as deformation of the average in both directions ([−] left and [+] right). (c) Grids (spline) for RW1 without the rostrum shown as deformation of the average in both directions ([−] left and [+] right). Note the shape differences in the antorbital fenestra, jugal bar, quadrate, cranial base and supraoccipital bone (see landmarks in Fig. 2).

antorbital fenestra, the jugal bar, the orbit, and overall, the braincase).

In the extended skull (positive scores; right scheme, second grid below in Fig. 3b), the elevated rostrum coincides with a flexed (convex) cranial base (between LM 6, 7 and 12; flexure is at the foramen of the optic nerve, LM 7), a shorter supraoccipital bone (LM 11 and 12), a dorso-ventrally shorter antorbital fenestra (the

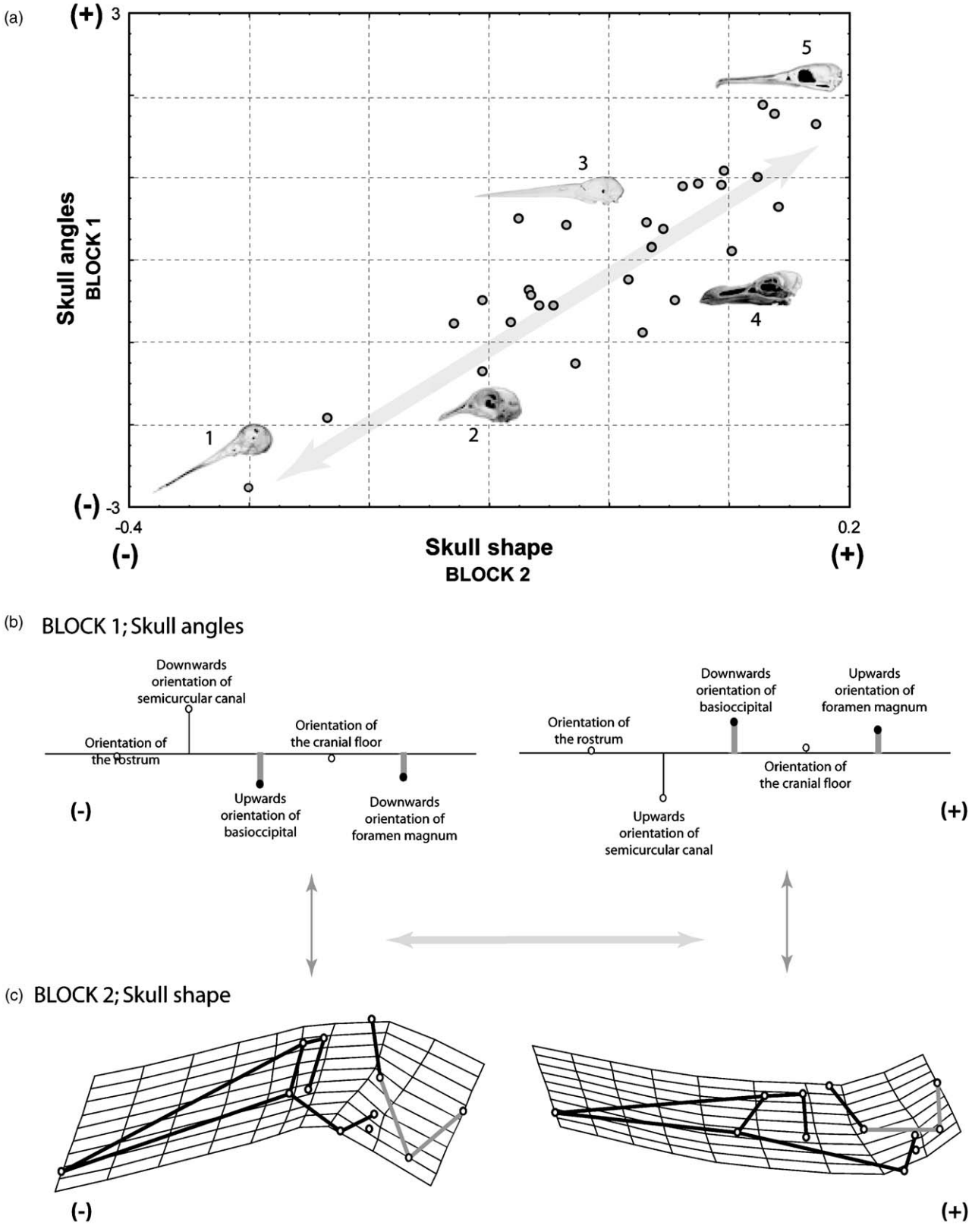

archosaurian preorbital opening in the skull) and a stretched jugal bar. In the opposed extreme (negative scores; left scheme, second grid below in Fig. 3b), the angle of the cranial base is more obtuse (it appears to be more extended), the supraoccipital bone is more dorso-ventrally stretched, the antorbital fenestra stretches dorso-ventrally and the jugal bar is more rostro-caudally compressed. The quadrate bone and the external ear apparently do not vary in shape, but they are both in distinct topographical locations with respect to the braincase on each extreme configuration. The subsequent dimension (RW3) explains 4.06% of variance and associates mostly to the shape of the antorbital fenestra (not shown).

RW analysis was subsequently performed excluding the tip of the rostrum (LM 1). The first dimension of this analysis (RW1; Fig. 3c) accounts for equivalent shape differences in the cranium as the ones observed in the RW2 (i.e., the second dimension of variation when the rostrum was included in the preceding analysis). For instance, compare the variation of the antorbital fenestra (LM 2, 3, 4, 5), together with the variation at the jugal bar (stretching or shortening; LM 3, 9) accompanied by the relative position of the quadrate bone (LM 8, 9) and the external ear. Shape changes are also marked at the braincase, at the cranial base (LM 6, 7, 8) and at the dorso-ventral variation of the supraoccipital bone (LM 11, 12). Thus, this new RW1 without the rostrum explains 55.79% of variance, and although shape accounts are more marked, its extremes without the rostrum are almost equal to those described above for RW2 when incorporating the rostrum (i.e., relative cranial flexure or extension).

To perform the 2BPLS, angles were set as block 1 and shape variables (PWs) as block 2 (see Fig. 4). The analyses yield a pattern (first singular value) with a strikingly high correlation between vectors ($r = 0.87$) explaining a statistically significant and large amount of covariance among blocks (95.78%; $P < 0.01$; Fig. 4a). The second singular value of the 2BPLS shows a much lower correlation between vectors ($r = 0.27$), explaining only 2.14% of covariance, and is not statistically significant ($P < 0.01$; graph not shown).

Within the trend of covariation, shape accounts are almost identical to those expressed by RW2 which incorporated the tip rostrum, as well as to RW1 which did not include the tip rostrum (i.e., the two extremes, extended and flexed, see Fig. 4c and compare with Figs. 3c and d). The only difference is that the whole spline is not dorso-ventrally stretched or compressed, but strongly and homogeneously curved (convex or concave). Likewise, associated shape changes to both extremes are almost identical (i.e., shape changes associated with the cranial base, the supraoccipital bone, the antorbital fenestra and the jugal bar; Figs. 3c,d and 4c).

Only the three angular metrics denoting the orientation of the plane of the lateral semicircular canal, the plane of the clivus and the plane of the foramen magnum covary with shape in the 2BPLS (their bars have a marked magnitude perpendicular to the schematized horizontal, which represents the mean; Fig. 4b). In contrast, rostral and cranial floor orientations do not seem to correlate and therefore, do not intervene in the covariation pattern (their bars have no or only an extremely slight magnitude, because they fall close to, or within, the horizontal line; Fig. 4b). Changes in the orientation of the clivus and the foramen magnum intervene correlating with the same sign (in the scheme, their bars point in the same direction), and almost with the same magnitude, which additionally suggests their direct association (the bar of the foramen is slightly smaller). Conversely, the lateral semicircular canal, which also correlates with the trend of covariation, does it with the opposite sign (i.e., its bar points in an opposite direction to the clivus–foramen magnum correlated composite).

Translated into morphological terms, the upwards tilting of the plane of the clivus is accompanied by a more ventral orientation of the plane of the foramen magnum (both with negative sign of correlation in Fig. 4b left, see also labels at bars within scheme of

Fig. 4. Pattern of covariation after partial least-squares analysis. (a) Pattern of morphological evolution of Neognathae crania showing the scatter-plot of correlation within first singular value ($r = 0.87$; $P < 0.01$; covariance explained = 95.78%), shape variables (x-axis) and angles (y-axis). Skulls: 1, woodcock; 2, pigeon; 3, stork; 4, razorbill; 5, cormorant. (b) Scheme of ordination of the angular variables (block 1, skull angles). This profile plot shows the estimates of the scores for each angle, each sketched as a vertical line. Vertical lines extend from a horizontal line which corresponds to the mean angles (see mean angles in central scheme of Fig. 1a). The pattern of variables is seen as values expressed by being either above or below the horizontal axis. Cranial parts varying are the lateral semicircular canal, the basioccipital bone (clivus) and the foramen magnum, whereas the positions of rostrum and cranial floor do not express height (match the horizon). Basioccipital bone and foramen magnum vary in the same direction, opposed to the semicircular canal. Notice relative magnitude of each variable (foramen is slightly lower). (c) Estimated shapes for the ordination of shape variables (block 2) shown as deformations of the average to extremes with the spline. Compare resemblances in shape with major trends of RW analyses (Figs. 3b–c). Light grey lines indicate the chordal part of the skull (caudal part of the cranial base and the supraoccipital bone, cf. Fig. 2 for LM labelling). Note that the left and right scheme of each block is paired with its equivalent from the other set of variables within the ordination; positive side of angles (lines) are read together with the positive side of shape (TPS), and accordingly, negative side of angles is read together with its correspondent negative side of shape.

Table 2. Correlation matrix of angular scalars between skull parts (measured after Duijm (1951))

	Ear (a)	Rostrum (b)	Clivus (c)	C. floor (d)	F. magnum (e)
Ear (a)	1	0.43	*0.58*	*0.56*	*0.59*
Rostrum (b)	0.43	1	0.14	0.43	0.26
Clivus (c)	*0.58*	0.14	1	*0.5*	*0.92*
C. floor (d)	*0.56*	0.43	*0.5*	1	*0.55*
F. magnum (e)	*0.59*	0.26	*0.92*	*0.55*	1
Mean	0.3393	198.1266	155.9041	175.6976	55.5717
Min.	–19.920	165.3400	106.2200	154.2000	22.3300
Max.	30.530	231.2300	154.2000	210.4700	104.5700
Std. dev.	11.5609	18.1715	22.3300	14.2525	25.6568

Values correspond to Pearson's moment correlation values, those in italics are significant at $P<0.001$. Letters *a* to *e* label the angles and corresponding cranial structures (see also Figs. 1a and 2a).

bars), while at the same time, the lateral semicircular canal tilts downwards (with opposed direction of correlation within the same scheme; Fig. 4b left). This occurs together within the same trend of covariation ($r = 0.87$; $P<0.01$) with the flexed condition and associated shape changes as displayed by the deformation of the grid (Fig. 4b left, the grid below the scheme of bars; shape changes described two paragraphs above). In the opposite direction, a downward tilting of the clivus is accompanied by an anterior, or upward, declination of the foramen magnum (thus pointing caudally), all of which correspond to an extended condition of the spline according to its associated shape changes.

Particularly within the braincase, the extended or flexed appearance of the spline also implies the intervention of the supraoccipital bone in the pattern (LM 11, 12). In the extended type, the supraoccipital bone is more compressed dorso-ventrally, whereas in the flexed type, the supraoccipital bone is more stretched. Thus, the combination of metrics shows that the relative orientation of the plane foramen magnum is structurally affected by the correlated variation of the elements of the clivus (basioccipital and pre-sphenoid bones) and the supraoccipital.

When we refer to the cranial base, it is strictly by inference. Such inference assumes that the optic window (the opening of N. II; LM 7) could serve as a rough external proxy for the boundary between the anterior and posterior cranial bases in birds (i.e., the real boundary is at the sella). However, the location of the basioccipital and pre-sphenoid bones (caudal cranial base, measured as the plane of the clivus) is between LM 7 and 12. From the resultant combination of metrics, we infer that the relatively extended appearance of the entire cranial base (more obtuse angle between the anterior and posterior cranial bases; LM 6, 7, 12, see Fig. 4c) coincides in the flexed cranial type with the upward orientation of the clivus (its angular variation was measured therein by Duijm (1951)). This is correlated with the orientation of the foramen magnum via the dorso-ventral stretching of the supraoccipital (whose contribution is captured by landmarks). Anatomically, this also coincides with the orientation of the laterosphenoid bone (LM 6, 7; synonym of orbitosphenoid bone; Baumel and Witmer, 1993) which is aligned with the caudal cranial base and results in the entire cranial base to look flatter in a flexed skull. Consequently, a flexed cranial base is the result of the more acute angle between the laterosphenoid and basioccipital bone in the mid-sagittal plane, which takes place in an extended skull.

Discussion

Geometric morphometrics are not commonly used in comparative studies at a high taxonomic level (Marcus et al., 2000), and are not commonly applied in avian morphological studies. Two-block partial least squares, on the other hand, is a recently developed technique that may eventually become common in morphological studies, although it currently tends to be used in shape-to-shape comparisons (i.e., comparing blocks of shape residuals). Our study addresses the suitability of geometric morphometrics at a macroevolutionary level. The study also attests that the statistical-geometric technique of 2BPLS offers a unique possibility to combine and supplement new landmark-based proxies and more traditional metrics reciprocally (for its thorough mathematical rationale, algebra and other examples, see Rohlf and Corti (2000)). In this context of intertwining information obtained with different metric methodologies our proxy entailed the combination of shape variation (in a geometric morphometrics sense) with a set of previously published angles measured with respect to a particular reference, viz. the actively attained position of the head when the bird is on alert,

and in such posture, in reference to the horizon (Duijm, 1951).

When dealing with angular metrics, it is necessary to find an independent external reference system in order to capture the topographic variation of every structure (Rabey, 1968). A crucial property of shape analysis is that shape variables are invariant to the effect of orientation. Since all shape analyses render close morphological congruence with the observations made from angular measurements, and because the analysis of covariance between both sets of metrics is highly significant, we can expect that angular relationships among cranial parts remain characteristic of cranial organization regardless of the posture of the head (see, e.g., Fig. 3). The results suggest that functional and developmental factors (e.g., morphological integration, developmental, epigenetic, phylogenetic factors; Olson and Miller, 1958; Smith, 1996; Chernoff and Magwene, 1999) determine the pattern of phenotypic variation encountered.

Early investigations on the phenotypic organization of the avian skull emphasized that evolutionary differences were found in the arrangements of three main functional parts of the skull (the rostrum, the orbit and the braincase; see Marinelli, 1928; Van der Klaauw, 1948). Two extreme types, extended and flexed, were described as extreme configurations dependant upon how the rostrum with the antorbital window, the orbit and the braincase were arranged. Among other features, the most conspicuous was that in the extended type, the foramen magnum points caudally, while in the flexed type, the foramen orients downwards. Further observations confirmed that these configurations were good representatives of inter-specific differences, but also suggested that endocranial parts had an important role in the structural organization of the avian skull. For instance, Duijm (1951) showed that there is a direct relationship between the clivus and the relative position of the foramen magnum, and that this relationship is associated with the morphological features characteristic of either the extended or flexed skull appearances. This assertion was also annotated by Hofer (1952), even though both authors thereafter described different and intricate patterns of skull organization.

Shape analyses showed that rostral shape variation associates primarily with a marked antero-caudal proportion of the premaxilla (between LM 1, 2 and 3), and that this type of variation, and not orientation of the rostrum, dominates the geometric divergence among avian skulls. While this finding corroborates that brevi- to longi-rostral variation characterizes cranial disparity qualitatively and quantitatively across avian taxa (Zusi, 1993; Marugán-Lobón and Buscalioni, 2003; Figs. 3a and b), it also underscores that rostral proportion and rostral orientation may be decoupled (cf. Fig. 3a). Our results show that rostral orientation is better captured by the second RW when the tip of the rostrum (LM 1) was included, or by the covariance pattern between sets of metrics, both of which were measuring an aspect of rostral morphology. The 2BPLS analysis, however, unexpectedly ruled out the intervention of rostral orientation measured by the angle of the plane demarcated by the ventral margin of the rostrum.

This omission of rostral orientation by the 2BPLS analysis in the pattern of covariance might suggest that the angular measurement of the plane of the rostrum was somewhat imprecise. Indeed, this statement of mismeasure was indicated by Duijm (1951, p. 208), for whom measuring rostral orientation was difficult because the rostrum curves homogeneously along its total length, and this curving makes measurements of its true orientation completely arbitrary (and even unrepeatable). Unfortunately, this sort of shape variation of the rostrum could have a close effect on shape analyses if one is attempting to capture rostral shape by placing only a landmark at its tip. This could lead to an underestimatation of its curvature, or worse, it could translate a downward curvature into a downward orientation of the whole structure. However, other landmarks used in this study (i.e., LM 2, 3, 4, 5) delineate the geometry of the antorbital fenestra quite precisely. The antorbital fenestra represents the caudal region of the rostrum, and therefore analyses are capturing a reasonable amount of shape of the rostrum. Variation observed at the antorbital window (Figs. 3b, c and 4c), that is, variation at the caudal part of the rostrum, is captured by the first RW when the tip of the rostrum was excluded. This dimension shows that it varies concomitantly with the observed shape changes of the remaining cranium (note that the shape or arrangements of other elements belonging to the "facial" skeleton, such as the jugal bar or the quadrate, also accompany the trend).

Thus, there is a particular feature of local shape plasticity anterior to the antorbital fenestra (i.e., premaxillary variation, or beak variation per se), that would need to be further explored bearing in mind that it is not only a matter of independent orientation and/or proportion but a consequence of pure shape differences across taxa. While this rostral shape variability would be difficult to capture with real landmarks because it is demarcated by a smooth surface, it could be contoured using semilandmarks, an associated technique of geometric morphometrics properly designed to overcome such problems (review in Adams et al. (2004)).

Since the implication of the cranial floor (the parasphenoid bone) was also ruled out from the pattern of covariance between metrics, only three of the five parts previously measured in the old angular data set remain: the plane of the clivus (basioccipital and presphenoid bones), the plane of the foramen magnum and the plane of the lateral semicircular canal. In angular

terms, only the clivus and the foramen magnum were strongly correlated ($r = 0.92$). This is conspicuously captured in the pattern of covariance between sets of metrics, a pattern in which their correlated association covaries within a single and statistically significant dimension with concise shape changes of the skull (compare Figs. 4b and c). Among such shape changes (displayed by deformations of the TPS; Fig. 4c) covarying with the correlated association between clivus and foramen magnum is the dorso-ventral variation of the supraoccipital bone (captured by LM 11 and 12). Anatomically, the supraoccipital is the bone that forms the dorsal margin of the foramen magnum, and the clivus contains the basioccipital bone, which forms the ventral margin of the foramen. Thus, the orientation of the plane of the foramen magnum is obviously a result of basioccipital and supraoccipital covariation. However, the plane of the clivus includes the whole caudal cranial base, and therefore also contains the presphenoid bone which forms the sella. Variation of this bone must also be involved in the relative orientation of the postcranial base (i.e., orienting the basioccipital), and is likely the only possible candidate causing the slanting of the basioccipital.

In conclusion (Fig. 4a), the general trend suggests that in the extended skull type, the supraoccipital bone is proportionally shorter dorso-ventrally, the plane of the foramen magnum points backwards, the plane of the caudal cranial base is tilted downwards and the whole cranial base is convex (Figs. 4b and c). In contrast, in the flexed skull type, the supraoccipital bone is proportionally larger, the foramen magnum points downwards, the caudal cranial base is inclined upwards and the whole cranial base is flatter. These flexed and extended organizations of the skull are the extremes of a pattern that represents an important aspect of the morphological evolution within Neognathae. However, at this systematic level, the occurrence of either skull type appears to be phylogenetically homoplastic across the avian phylogeny. For example, within the Ciconiformes, the Scolopacidae have flexed skulls while the Phalacrocoracidae have extended skulls. Convergent flexed skulls are found in Passeriformes, Strigiformes and Trochiliformes. We suggest that the correlated changes between elements exclude a phylogenetic factor underlying the pattern. Nevertheless, there is still some debate about a potential use of these correlated traits as discrete phylogenetic characters (discussed for primates, see e.g., Lieberman et al. (2000)).

The combination of different metrics has allowed identifying and delimiting a subset of osteological elements that are involved in the evolutionary phenotypic organization of the avian skull. Additionally, we have observed that this subset of elements varies according to a coordinated scheme. A critical determinant to explain covariation between morphological traits is their developmental origin, as, for instance, if they are derived from the fission of a common developmental precursor, or else, by inductive signalling between different precursors (Klingenberg, 2002). In other words, morphological integration between those elements may be a result of the developmental rules for building them (Chernoff and Magwene, 1999).

The elements within the caudal cranial base (basioccipital and pre-sphenoid bones) and the supraoccipital bone together constitute a domain called by experimental embryologists the ''chordal'' skull (Couly et al., 1993; Le Douarin et al., 1993). The term chordal in the embryo implies that the whole domain (and the prospective bones within it) lies above and along the anterior-most extension of the embryonic notochord (the experimental model on which this was described is the chick embryo). However, apart from grouping elements behind a particular embryonic boundary, the term chordal also implies that all those elements derive from the mesoderm. More particularly, quail-chick markers for mapping the fate of cell populations in the embryo have shown that those of the cranial paraxial mesoderm originate the supraoccipital and the presphenoid bones, whereas the basioccipital is originated by mesodermic cell populations of somitic nature (Couly et al., 1993). In contrast, elements that lie anterior to this boundary (those anterior to the notochord) constitute what is known as the prechordal (or achordal) skull, a domain that comprises bones that originated from cephalic neural crest cells.

Translating the pattern of phenotypic covariation of elements of the avian skull into this embryological terminology suggests that the correlated variation between elements within the chordal domain is due to their common origin from the mesoderm. The pattern also suggests that both prechordal and chordal domains vary concomitantly. Duijm (1951) asserted that in the cases where he found this related variation (i.e., flexed skulls s.l.), it could be a physical epiphenomenon derived from incorporating a large eye within the skull (using as an example the extreme case of the woodcock; Fig. 4a). However, it could also be argued that covariation between the chordal and prechordal domains could be due to inductive signalling between cranial neural crest (prechordal domain) and cranial paraxial mesoderm (chordal domain) cell populations (i.e., a developmental pathway epigenetically signalling between the chordal and prechordal domains). However, finding a direct causality for an interaction between these two domains is more complex and, therefore, other untested models could be equally parsimonious. For instance, our original data is based on adult forms, and mutual correlations determined by growth could be obscuring the particular pattern of integration we have observed from the covariance matrix. Covariation from developmental interactions

should be distinguished from other sources of variation, such as the environmental effects changing more than one developmental pathway simultaneously, thereby making them apparently perform as a single one (Klingenberg, 2002).

Overall, our investigation aimed at insights in the structural interrelationship between cranial elements of the skull in birds. It reveals a pattern of coordinated variation that could be rooted in deep morphogenetic associations. This model of morphological interaction is based on the pattern of statistical covariation between elements of the cranium, an association which is reasonably justified given the straightforward embryological equivalence between some of the correlated elements. Such macroevolutionary model suggests the preservation of a developmental pathway of the avian skull morphogenetic programme throughout evolution. This needs to be explored and tested in depth on an experimental basis, with a comparatively equivalent taxonomic sample that allows mapping the developmental trajectories underlying avian skull disparity.

On the morphological side, forthcoming approximations would need to test in further detail the magnitude of association of the lateral semicircular canal, the cranial floor and other elements not delimited by the metrics used here. It would be equally crucial to explore the functional meaning of the observed evolutionary skull rearrangements. Shape analysis offers a new path to gain insights on the phenotypic organization of the avian skull. Geometric morphometrics are now focused on analysing three-dimensional shape variation (Adams et al., 2004).

Acknowledgements

The authors are grateful to F.J. Rohlf and W. Gharaibeh for valuable advice on geometric morphometrics and statistics, M. Bastir for long and prolific discussions on morphological evolution, J.C. Pavón for reading the early versions of the manuscript, and Matthias Starck and Renate Schilling for their thorough revision of the manuscript in its final stages. A.D. Buscalioni additionally thanks the Konrad Lorenz Institute and its researchers for fruitful debates on phenotypic integration and evolutionary biology. The study belongs to a research programme endorsed by the Ministerio de Educación of Spain (DGCYT-BTE2001-0185-C0201/ and Grant programme FPU), and has been partially aided by the Collection Study grants program of the American Museum of Natural History, and the Jurassic Foundation.

Appendix A. Supplementary materials

Supplementary data associated with this article can be found in the online version at doi:10.1016/j.zool.2006.03.005 and under supplementary video material at www.elsevier.de/zool.

References

Adams, D.C., Slice, D.E., Rohlf, F.J., 2004. Geometric morphometrics: ten years of progress following the ''revolution''. Ital. J. Zool. 71, 5–16.

Baumel, J.J., Witmer, L.M., 1993. Osteologia. In: Baumel, J.J., Evans, H.E., Van den Berge, J.C. (Eds.), Handbook of Avian Anatomy: Nomina Anatomica Avium, second ed. Publications of the Nuttal Ornithological Club 23, pp. 45–132.

Bookstein, F.L., 1989. Principal warps: thin plate splines and the decomposition of deformations. IEEE Trans. Pattern Anal. Mach. Intell. 11, 567–585.

Bookstein, F.L., 1991. Morphometric Tools for Landmark Data. Cambridge University Press, New York.

Bookstein, F.L., Gunz, P., Mitteroecker, P., Prossinger, H., Schaefer, K., Seidler, H., 2003. Cranial integration in *Homo*: singular warps analysis of the midsagittal plane in ontogeny and evolution. J. Hum. Evol. 44, 167–187.

Chernoff, B., Magwene, P.M., 1999. Afterword: morphological integration: forty years later. In: Olson, E.C., Miller, R.L. (Eds.), Morphological Integration. The University of Chicago Press, Chicago.

Couly, G.F., Coltey, P.M., Le Douarin, N.M., 1993. The triple origin of the skull in higher vertebrates: a study in quail-chick chimeras. Development 117, 409–429.

Cracraft, J., 1988. The major clades of birds. In: Benton, M.J. (Ed.), The Phylogeny and Classification of the Tetrapods. Amphibians, Reptiles, Birds, vol. 1. Clarendon Press, Oxford, pp. 339–361.

Duijm, M.J., 1951. On the head posture in birds and its relation to some anatomical features. I–II Proc. Koninklijke Nederlandse Akademie van Wetenschappen, Ser. C. Biol. Med. Sci. 54, 202–271.

Hofer, H., 1952. Der Gestaltwandel des Schädels der Säugetiere und Vögel, mit besonderer Berücksichtigung der Knickungstypen und der Schädelbasis. Verh. Anat. Ges. (Jena) 50, 102–113.

Klingenberg, C.P., 2002. Morphometrics and the role of the phenotype in studies of the evolution of developmental mechanics. Gene 287, 3–10.

Lieberman, D.E., Ross, C.F., Ravosa, M.J., 2000. The primate cranial base: ontogeny, function, and integration. Yearb. Phys. Anthropol. 43, 117–169.

Le Douarin, N.M., Ziller, C., Couly, G.F., 1993. Patterning of neural crest derivatives in the avian embryo: in vivo and in vitro studies. Dev. Biol. 159, 24–49.

Marcus, L.F., Hingst-Zaher, E., Zaher, H., 2000. Application of landmark morphometrics to skull representing the orders of living mammals. Hystrix 11, 27–47.

Marinelli, W., 1928. Über den Schädel der Schnepfe. Paleobiologica 1, 135–160.

Marugán-Lobón, J., Buscalioni, A.D., 2003. Disparity and geometry of the skull in Archosauria (Reptilia: Diapsida). Biol. J. Linn. Soc. 80, 67–88.

Marugán-Lobón, J., Buscalioni, A.D., 2004. Geometric morphometrics in macroevolution: morphological diversity

of the skull in modern avian forms in contrast to some theropod dinosaurs. In: Eleewa, A. (Ed.), Morphometrics in Paleontology and Biology. Springer, Heidelberg, pp. 157–173.

Mayr, G., Clarke, J., 2003. The deep divergences of neornithine birds: a phylogenetic analysis of morphological characters. Cladistics 19, 527–553.

Olson, E.C., Miller, R.L., 1958. Morphological Integration. The University of Chicago Press, Chicago.

Rabey, G., 1968. Morphanalysis. Hatch, Pinner & Co., London.

Rohlf, F.J., 1993. Relative warps analysis and an example of its application to mosquito wings. In: Marcus, L.F., Bello, E., García-Valdecasas, A. (Eds.), Contributions to Morphometrics. Monografías del Museo Nacional de Ciencias Naturales, CSIC, Madrid, pp. 131–158.

Rohlf, F.J., 2005. TPS Series Software for Morphometric Data; TPSdig v.1.34, TPSrelw v. 1.39, TPSpls v.1.14. Department of Ecology and Evolution, SUNY at Stony Brook, NY.

Rohlf, F.J., Corti, M., 2000. The use of two-block partial least-squares to study covariation in shape. Syst. Biol. 49, 740–753.

Rohlf, F.J., Slice, D., 1990. Extension of the Procrustes method for the optimal superimposition of landmarks. Syst. Zool. 39, 40–59.

Scion Corporation, 2005. Scion Image Beta v. 4.03 for Windows 95, 98, ME, NT 2000 and XP. Maryland, USA.

Sibley, C.G., Monroe, B.L., 1990. Distribution and Taxonomy of Birds of the World. Yale University Press, New Haven.

Smith, K.K., 1996. Integration of craniofacial structures during development in mammals. Am. Zool. 26, 70–79.

Van der Klaauw, C.J., 1948. Size and position of the functional components of the skull. A contribution to the knowledge of the architecture of the skull, based on data in the literature. Arch. Need. Zool. 9, 1–558.

Zelditch, M.L., Swiderski, D., Sheets, D., Fink, W., 2004. Geometric Morphometrics for Biologists: A Primer. Elsevier, London.

Zusi, R., 1993. Patterns of diversity in the avian skull. In: Hanken, J., Hall, B. (Eds.), The Skull. Patterns of Structural and Systematic Diversity, vol. 2. The University of Chicago Press, Chicago, pp. 391–437.

Zusi, R.L., Livezey, B.C., 2001. Higher-order phylogenetics of modern aves based on comparative anatomy. Neth. J. Zool. 51, 179–205.

Box 5

The Hess collection at the Museum für Naturkunde

The Hess collection contains approximately 900 avian skulls which were exquisitely hand-sawed mid-sagittaly by Dr. Hesse in the first decade of the Twentieth century. The collection is housed within the Museum für Natürkunde, in the Institute für Systematiche (Ornitologie), under supervision of the current curator in charge, Dr. Sylke Frahner. The meticulousness of Dr. Hess was remarkable yet not only for the patience of being able to saw tones of skulls as small and weak as that of a songbird (ca. 10 mm), but because he was able to prepare the collection in such an elegant way that it displays its magnitude and uniqueness just at a glance (see Figure B5.1). In effect, it has preserved its original aspect across ages.

Therein, each lateral side of each skull was placed aside from its counterpart and needled to the bottom of the wooden and glass cases that guard them. Apart from the delicate way in which skulls were prepared the species richness of the collection is strikingly remarkable. The spectrum of diversity it displays includes from cormorants to woodcocks, galliformes of varied sorts, tones of Anseriformes and Passeriformes, pelicans, albatrosses, and even rare individuals such as small ratites, such as *Rhynchopus*. The only flaw is that while preserving intact its aspect for so many years, names of species have evolved academically, and many labels are thus very outdated (and one must be cautious, because a few may even be wrong).

From what Dr. Frahnert and I have been able to document, the specimens were apparently leftovers from the different worldwide field campaigns of the museum along the end of the Eighteenth century. The aim of dissecting the skulls this way by this mysterious researcher (who disappeared without leaving a trace in the war period), is startling. Such a painstaking preparation of the skulls was to detail the anatomy of the nasal chambers across avian taxa, and not for studying endocranial anatomy. Indeed, between the sawed skulls one can also find series of bird facial skeletons coronally sawed which he used to observe the internal anatomy of the nasal chambers and publish his findings (Hess, 1907).

In spite of the current availability of non-destructive techniques such as MIR, Laser and CTscans, the Hesse collection represents a state-of-the-art legacy for the wealth of vertebrate cranial morphology.

3.4. Braincase shape disparity and evolutionary allometry in modern birds (Neornithes: Archosauria)

4.1. Introduction

The braincase is an inclusive term that refers to the part of the skull which houses and protects the central nervous system (CNS) in amniotes. The relationship between both bone and neural systems is so tight that the phenotypic evolution of the CNS may have an important influence in the structural organization of the braincase. For instance, the structural organization of the cranial base driven by CNS phenotypic evolution is often considered a key structure involved in the evolutionary transformation of the braincase and of the craniofacial system in mammals (Gould, 1977; Enlow and Hans, 1996; Lieberman et al., 2000a, b).

While birds are very encephalised organisms (Jerison, 1973), and many aspects of the phenotypic evolution of the CNS have been thoroughly investigated, very scarce research has been dedicated to their braincase morphological macroevolution. For instance, there is no clear evidence on what types of different arrangements of the cranial base can or cannot be found (Fig. 1), though more importantly; there is no insight whatsoever on whether the role of the cranial base may be as important a feature as it is often alleged for mammals.

Morphologically, most bird taxa have the foramen magnum pointing caudally yet some others, such as hummingbirds or songbirds, have the foramen magnum facing more ventrally in a similar way as it happens in humans. These differences in the orientation of the foramen magnum in birds are caused by the different positions (orientations) of the plane of the clivus (e.g. conveyed by the basioccipital bone; Gaup, 1906; Marinelli, 1928; Duijm, 1951), hence caused by the different orientations in the equivalent to the mammalian caudal cranial base.

The scheme in Figure 1 shows the classic classification of cranial base arrangements in mammals that spans into three different possibilities if viewed mid-sagittaly (Fig. 1; Moss and Vilmann, 1978). All the differing topologies depend on the orientation of the caudal cranial base in such a way that when both parts of the cranial base are in the same plane the configuration may be called *orthobasal* (i.e. the cranial base looks flat). Instead, when the caudal base is oriented more downwards, the configuration may be called *klynobasal* (i.e. the cranial base looks convex), while if it is tilted upwards (or "elevated"), the cranial base will be called *airobasal* (i.e. the cranial base looks concave). Thus, it could be equivalently possible to find that ortho-, klyno-, or airobasal as distinctive features of avian braincase disparity as they are for mammals.

However, the orientation of the foramen magnum in birds (the opening for the pathway of

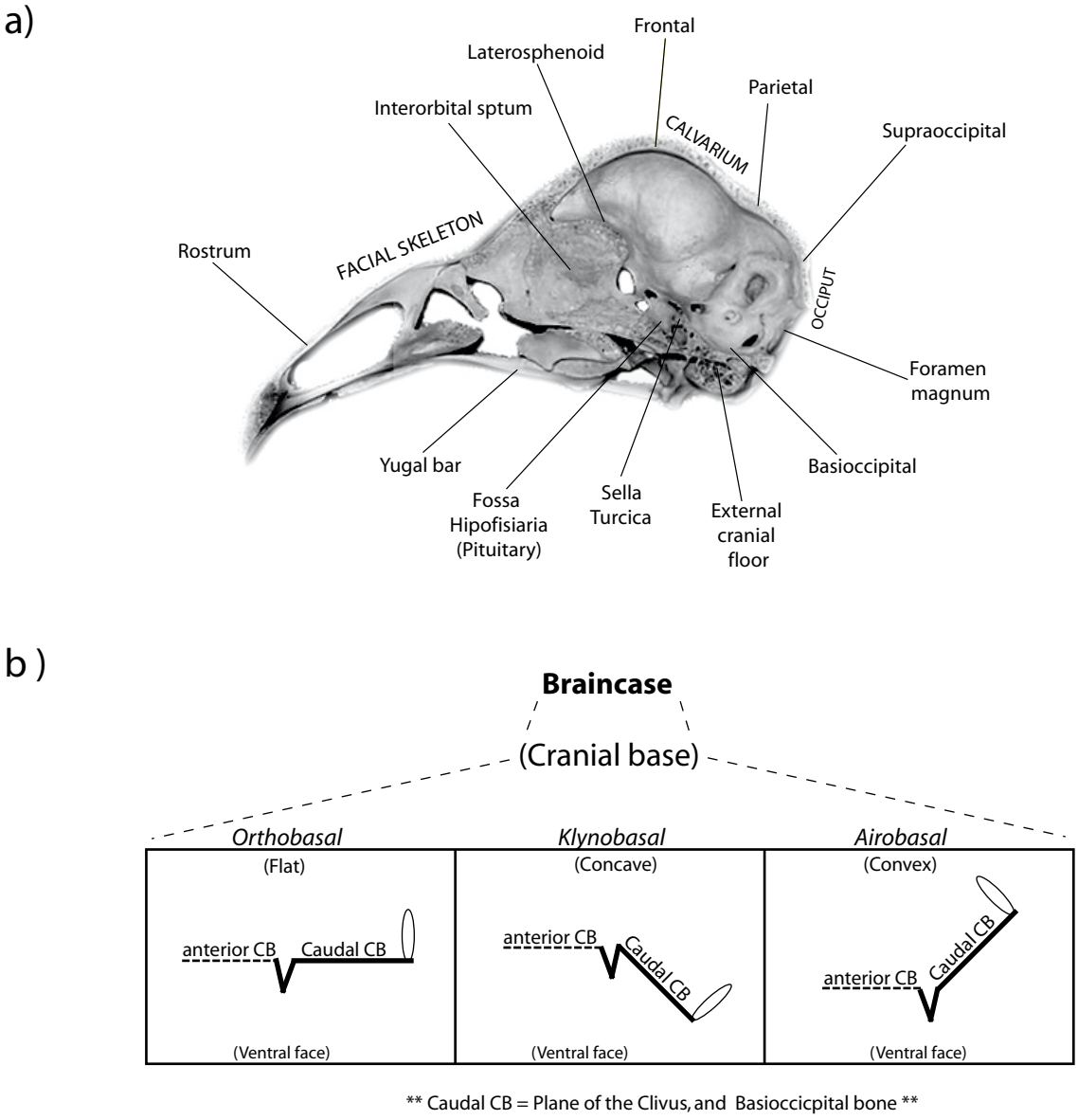

Figure 1. a) General anatomy of the avian braincase and skull in lateral view of *Chauna*. c) Three possible cranial base arrangements proposed by Moss and Vilmann (1978). The ellipse schematizes the relative position of the foramen magnum and its association with the caudal cranial base (which is equivalent to the plane of the Clivus conformed by the basioccipital and the basisphenoid at the Sella; see also Duijm, 1951; Marugán-Lobón and Buscalinoi, 2006).

the medullar axis) does not depend solely on the different orientations of the basioccipital alone as it is shown in the scheme of figure 1, but also on the way in which the basioccipital associates morphologically with the supraoccipital (Marugán-Lobón and Buscalioni, 2006). Overall, it is dependant upon the morphological association between the bones of the occiput, and possibly, yet still to be demonstrated, by changes in the Sella Turcica (i.e. the basisphenoids; Fig. 1).

While the whole occiput has a topographic and chondral identity (it is part of the chondrocranium), recent experimental surveys have also shown that its mesenchyme derives from the dissociation (*sensu*, Raff, 1996) of two embryonic sources of a mesodermic

precursor, the somitic (paraxial) and the cranial paraxial mesoderm (Couly et al., 1993; LeDouarin et al., 1993). These chondral bones in birds are derived from the mesoderm and constitute the so-called *chordal* domain (Fig. 2). The name chordal specifies that this whole mesodermic part can be ventrally located in the braincase, lying over and caudal to the anterior-most extent of the notochord in the early embryo (Fig. 2).

Interestingly, the ventral notochordal-mesodermic boundary of the chordal domain in birds reaches the point of splitting between the caudal and anterior parts of the cranial base. The basioccipital therein (the caudal cranial base) is derived from somitic (paraxial) mesoderm, while the basispenoids at the Sella and the Pituitary Fossa are of cranial paraxial mesoderm. More rostrally, the anterior cranial base (the laterosphenoid bone), belongs to the so-called prechordal part of the skull, the part which lies anterior to the rostral-most tip of the notochord, all of which is of cephalic neural crest origins (Fig. 2).

The avian calvarium (parietals and frontals), on the other hand, may be derived from cranial neural crest for some authors (Couly et al., 1993; LeDouarin et al., 1993; Fig. 1), whereas it may be derived from the mesoderm for others (Evans and Noden, 2006). Thus, while the ventral boundary between the chordal and prechordal domains seems to be clearly defined (see Fig. 2), a more dorso-caudal boundary between the chordal part and the prechordal part remains controversial. The dorso-caudal boundary between the chordal and prechordal parts may rest somewhere separating the occiput (the supraoccipital) and the calvarium (beginning caudally at the parietal), yet if the calvarium is mesodermic, the boundary of the chordal domain would extend as far as to reach most of the braincase (only the lateral walls would be excluded; Evans and Noden, 2006).

These chordal and prechordal parts have a structural and topographical identity, but are also identified by their compositional nature (i.e. the parts emerge from distinguishable embryonic precursors). This definition fits with one notion of modularity whereby each part may be conceived as a module of the system (e.g. the skull, though herein we omit the facial skeleton and refer to the braincase). From this point of view, modules are units of an integrated system, though therein, their variation will be relatively autonomous from the others (Raff, 1996; Bolker, 2001, 2003). Thus, if the chordal and the prechordal parts are considered modules, they should comply with being more internally coherent due to stronger interactions between their own elements (Klingenberg, 2004). Reciprocally, their internal coherence should convey that they are relatively autonomous from each other due to weaker connections between them.

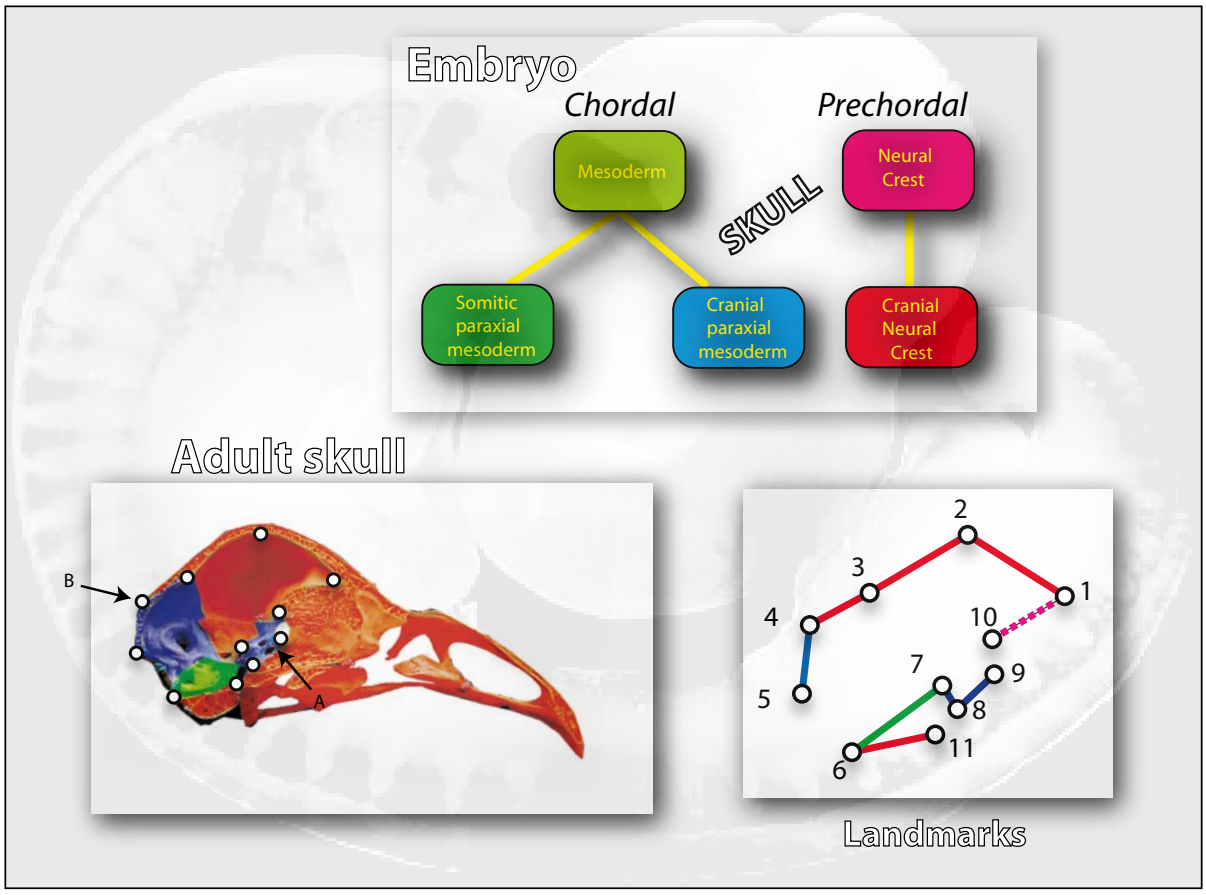

Figure 2. Developmental distinction between cell populations in the embryo and their correspondence with adult bone morphology (based in Couly et al., 1993, and LeDouarin et al., 1993). Below, landmark configuration denoting braincase geometry. The lines between landmarks are coloured following the hypothesis of developmental sources for aiding visualization of modules. The (A) black arrow points the point up to where the nothochord reaches most, which at the same time denotes the boundary that splits the chordal and prechordal parts within the cranial base. The (B) black arrow points at the parieto-supraoccipital boundary between the chordal and prechordal parts. Notice that this boundary may be larger, hence we have coloured the region between landmarks 3 and 4 with both red and blue in order to highlight the differences between experimental findings.

If conceiving the avian braincase as a modular system, disparity (i.e. morphological diversity at a macroevolutionary scale) should likely stem from the boundaries between modules, rather than within modules. That is, major shape differences among avian taxa may possibly locate at the boundaries between the chordal from the prechordal parts of the braincase instead of within them. For instance, the middle of the cranial base splits it into two portions, and is at the same time, a boundary site between the prospective modules. Disparity may be seen in the form of its different arrangements (e.g. as those exemplified in Fig. 1, or perhaps other ones), for it would be the relatively autonomy of the whole chordal part, on the one hand, and the relatively autonomy of the whole prechordal part, on the other, what would convey the different arrangements of the cranial base at their connection boundary.

Equivalently, the expectation would be that avian braincase disparity also roots at the

boundary between the calvarium (parietals and frontals), and the occiput (i.e. at the supraoccipital). Interestingly, this dorso-caudal boundary between the chordal and prechordal parts is still controversial since the calvarium may be mesodermic, hence this may not be the true boundary between the prospective modules. If the challenged null hypothesis is not rejected (i.e. an important amount of difference stems thereof), this boundary should be crucial for avian braincase disparity. Thus, a large-scale evolutionary comparison between bird taxa may eventually shed some light about the location of this controversial boundary.

We have set this comparative framework using standard Procrustes geometric morphometric procedures (GPA; Gower, 1975; Adams et al., 2004; Slice, 2005) digitizing p=11 landmarks on salient, homologous and repeatable features that allow to homogeneously capture the geometry of the avian braincase in the mid-sagittal plane (Fig. 2). The sample comprises N=71 individuals allowing the comparison of the braincase of approximately all major Neornithes clades, each of which is at least represented by one individual (see Appendix 2).

This study is the first approximation to endocranial (mid-sagittal) macroevolutionary differences in birds using geometric morphometrics as a morphological tool. Therefore, it is essential that we begin by exploiting some of its visual capabilities and show the major aspects of braincase shape evolution in birds. For this sake, the working schedule begins by illustrating aspects of braincase morphology comparing particular bird braincases pair-wise (criteria of election being, e.g., relative encephalisation, phylogenetic position, or other special morphological attributes of each taxon). The principal features of braincase shape disparity in the pool sample are thereafter explored and shown using relative warps analyses (Bookstein, 1989; Rohlf, 1993). Once braincase geometric disparity is described, we will map the phylogenetic distribution of well-supported clades (i.e. Paleognathae, Galloanseres and Neoaves; Cracraft and Clarke, 2001; Van Tuinen, 2002).

Evolutionary allometric analyses will then follow, and in them, we will be testing the relationship of braincase shape evolution in birds as a function of size using multivariate regressions. Independent variables of size will be the geometric size of the braincase of each individual of the sample (i.e. centroid size), and body mass of each specimen, the latter data which has been collected from literature matching precisely each of the species included in the sample.

4.2. Materials and Methods

Data was collected on N=71 dried avian skulls sliced in the mid-sagittal plane. Skulls belong

Table 1. Description of homologous landmarks.

Number	*Description*
1	Foramen of olfactory nerve (fossa bulbi; N. I)
2	Mid-point between LM 1 and 3 at ventral edge of frontal bone
3	Ventral edge of endocranial crest separating cerebellar and forebrain cavities
4	External junction between supraoccipital and parietal at occipital crest
5	Dorsal rim of foramen magnum
6	Ventral rim of foramen magnum, anterior to occipital condile
7	Dorsal-most point of Sella Turcica (dorsal tip of basi-postsphenoid)
8	Ventral-most point of fossa hypophisiaria
9	Ventral edge of optic foramen (N. II)
10	Dorsal edge of optic foramen (N. II)
11	Tuba timpanica at rostrum parasphenoidale

to the Hess Collection housed in the Museum für Naturkunde in Berlin (see Appendix 2 for species and institutional labels, BOX 5 describes the collection, which was published as well in Hesse, 1907).

Skulls were digitized in lateral view with an Olympus C-720 digital camera following the protocol summarized in Marugán-Lobón and Buscalioni (2004). Landmarks were digitized on each picture using TPSdigit (v. 1.40; F. J. Rohlf) and are summarized in Table 1 with their anatomical correspondence and depicted in Fig. 2. Anatomical terms follow Couly et al., (1993).

Landmark configurations were superimposed using Procrustes analytical procedures (GPA and the Thin Plate Spline). Adams et al., (2004) overview the techniques, Bookstein, (1991) and Dryden and Mardia (1999) disclose it scholarly, and Zelditch et al, (2004) explain most practice extensively. A first GPA superimposition is performed with Morpheus et al (Slice, 2002) in order to compare, pair-wise, different braincases. The exploration of endocranial shape disparity is thereafter performed using relative warps analyses with TPSrelw (v1.42, F. J. Rohlf).

We used two estimates of size, centroid size (CS; the square root of the sum of the squared distances between the landmarks of each configuration), and body masses collected from literature matching the exact same species of the sample (Dunning, 1993). In order to work at equivalent dimensions between size measurements we transformed body mass to its cube root and then standardized both variables to LogCSc and LogW respectively. Size (endocranial centroid size and body mass) is first mapped onto the axes of the relative warp

scores using a contour plot based on the squared distance matrix interpolation function as implemented in Statistica (v6.0; Statsoft, 2001). Evolutionary allometry is thereafter tested putting all shape variables (partial warps and uniform component) as a function of both measurements of size, using TPSregr (v.1.14; F. J. Rohlf). Unwarped images based on the TPS smoothing function have been obtained using TPSsuper (v1.13, F. J. Rohlf) and are used both to show the average shape of the avian braincase more realistically, and as a complementary visual tool to aid the visualization of the deformation grids as estimates of extreme cases for each statistical analysis.

4.3. Results

4.3.1 Pair-wise comparisons of endocranial shapes

Figure 3 shows that the landmark configuration captures fairly well most the geometry of the avian braincase and the endocranial cranial cavity. This can be seen on the unwarped image in figure 3a, in which at the same time, it is possible to see that bones such as the laterosphenoid or the interorbital septum (Fig. 1a) may not always ossify.

Figure 3b shows some pair-wise comparisons among endocranial cavities of selected birds (notice the close resemblance between parts of the central nervous system and endocranial shape). A songbird (gen. *Parus*) has been elected as a comparative reference (not a superimposition reference) for comparisons because of its proportionally large central nervous system. The braincase of the songbird is spherical, its cranial base is flat and the foramen magnum is ventrally oriented. Figure 3b and c compares the reference (songbird) with a cormorant (gen. *Phalacrocorax*) and a woodcock (gen. *Scolopax*) respectively which were elected because they are classic examples of orthocranial and klynorhynchal craniofacial configurations (definitions refer to the topographical relationship between the facial skeleton and the braincase). Figure 3b shows that the cormorant has an overall proportionally smaller endocranial cavity than the songbird, its foramen magnum is oriented more caudally, and it has a ventrally convex cranial base with a non-spherical vault. In Figure 3c, the woodcock has a relatively smaller forebrain cavity but the cranial base is flat, not convex, and coincides as well with the songbird in presenting a ventrally oriented foramen magnum. Otherwise, both birds differ markedly in the configuration of their supraoccipitals and external cranial floors.

Figures 3 d, e, and f compare the brain shape of the songbird with representative species of

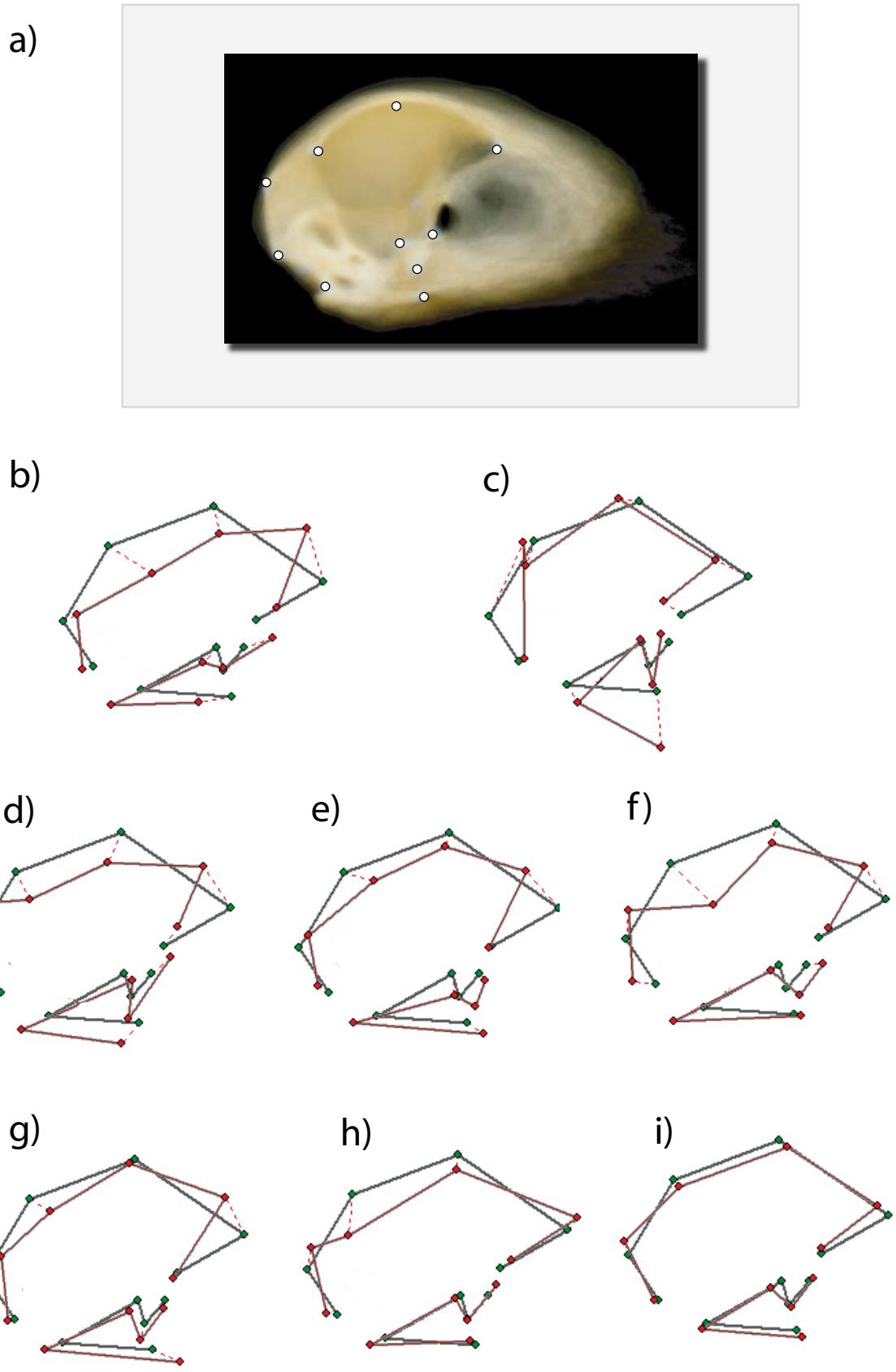

Figure 3. a) Unwarped average (consensus) of the *N*=71 bird braincases. Notice how landmarks capture the geometry of the braincase, plus showing regions such as the laterosphenoid (anterior cranial base), or the interorbital septum, which may not ossify in several birds. b-i) Shows pair-wise comparisons between *Parus* (the selected reference) and selected birds (see text). These latter are b-Cormorant, c-Woodcock, d-Swan, e-quail, f-chicken, g-tinamou, h-parrot, and i-crow. For species please *cf.* Appendix 2.

basal clades in the sample (Paleognaths, and Galloanseres; i.e. Anseriformes and Galliformes). Figure 7.2d compares the songbird with a swan (gen. *Cygnus*), showing that the latter has a proportionally smaller forebrain cavity, a convex cranial base, the whole braincase is less rounded, and the foramen magnum is caudally oriented. The orientation of its supraoccipital and parietal bones is also completely different.

Figure 3e compares a Quail (gen. *Perdix*), a Galliform which has a convex cranial base associated with differences in the proportion of the forebrain cavity, and the orientation of the foramen magnum. Perhaps, the most striking contrast is the one depicted in Fig. 3f in which a chicken (gen. *Gallus*) is compared with the songbird. One most striking difference is the relative proportion of the forebrain cavity, which being markedly smaller in the chicken. This relative small forebrain cavity proportion also coincides in the chicken with a convex cranial base and a marked caudally oriented foramen magnum.

The next comparison shown is between the songbird and a basal Paleognath, a tinamou (gen. *Rhynchopus*), which although has a relatively smaller forebrain cavity, this difference is not so marked (Fig. 3g). The tinamou has a more convex cranial base, yet this does not seem to be associated with the orientation of the foramen magnum. The difference in orientation of the supraoccipital between both birds is quite prominent.

The last comparison is between the songbird and two other very encephalised forms, a parrot (gen. *Amazona*) and a crow (gen. *Corvus*; see Figs. 3h and 3i respectively). Interestingly, the crow and the songbird show almost the same braincase (and endocranial) shapes despite their marked body size differences (the crow is much larger than the songbird). With the parrot, on the other hand, it is not so clear whether the forebrain cavity is a bit smaller, or just shallower, a difference which is more visible around the calvarium. Otherwise, the forebrain cavity of the parrot extends further rostrally than that of the songbird.

Overall, there is a large suit of geometric differences in the avian braincase and the endocranial cavity among bird taxa. The pair-wise comparisons show that establishing a relative proportional size of the whole endocranial cavity is not straightforward since there are many shape differences that relate to the different configurations of the bones. Since the geometry of the endocranial cavity outlines the shape of the brain it is obvious that there are several brain shapes among different avian taxa (in fact, all the reading of the paragraphs above can be translated to the shape of the central nervous system), and variation will depend on differential variation among its parts. All birds compared show that their cranial bases

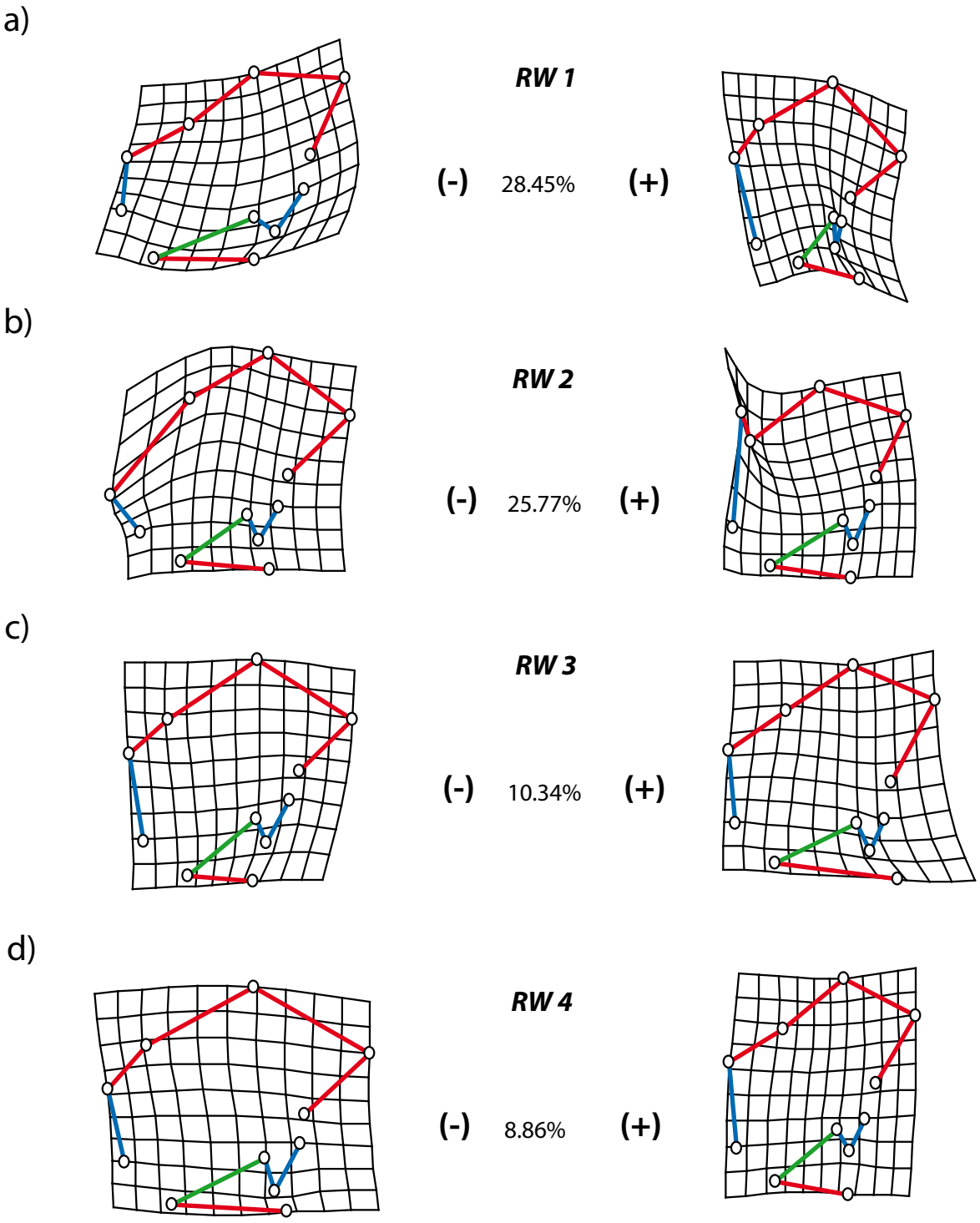

Figure 4. Letters a-d show, orderly, the meaning of the first four relative warps on the basis of grid deformations based on the TPS. Percentages are the explained variance by each relative warp. Positive symbols are positive scores in each axis and, reciprocally, negative symbols are negative axis' scores. Colour coding follows the hypothesis of developmental identity of each braincase module (Fig. 2).

can be flat or convex but never concave. Thus, for the moment, birds apparently have orthobasal or airobasal cranial bases but do not achieve klynobasal configurations (*cf.* Fig. 1).

4.3.2 Shape analysis on the braincase

Relative warps analysis (Fig. 4a, b c, d and Fig. 5) decomposes 100% of endocranial shape variance into 26 eigenvectors at α =0. Among them almost two thirds of variance is contained within the first three ones (respectively labelled, RW1, RW2 and RW3, cumulative variance=60.56%). However, variance is quite evenly distributed between the first two dimensions. RW 1 is accumulates most shape variance (29%) although RW 2 explains a close 22%. RW 3 drops down to 10%, RW 4 explains 8.12%, and subsequent dimensions do not exceed 4%.

The same analysis was performed without the uniform component (homogeneous change in all landmarks) in order to test its possible effect. Interestingly, results without the uniform component differ slightly which thereby suggests that the uniform component may be an aspect of variation in cranial morphological change among birds. Given this possible influence of the uniform component we have not performed analyses at other scales of the bending energy matrix (i.e. α=1, or α=-1).

The first relative warp (RW1) separates two markedly different extremes (positive and negative scores of the firs axis, in the figure right and left, respectively) and accounts for a series of combined shape changes in elements across the entire braincase and the endocranial cavity (Fig 4a). All shape changes in this dimension result in an apparent uniform curving of the grid between the two polarized extremes of the first RW. If referenced ventrally, positive extreme scores correspond to a concave deformation of the whole grid while negative values correspond to a convex deformation. These deformations of the grid transcribes in that one extreme appears to be concavely bent or flexed (positive scores) while the opposed seems to be bent convexly.

More pronounced deformations within the grid correspond to the cranial base (LM 1, 6, 7, 8, 9, 10), yet shape differences are considerably concentrated in its caudal portion (between LM 6, 7, 8 and 9). Likewise, all these changes in the cranial base make it appear either shorter (positive scores) or longer (negative scores), and coincide with changes at the region of the calvarium, particularly in the region of junction between the parietal and the supraoccipital bones.

The whole caudal cranial base appears to cause the relative lengthening of the cranial base being proportionally shorter (more antero-caudally compressed) for positive scores and proportionally larger for negative ones. Such differences results both in relation to

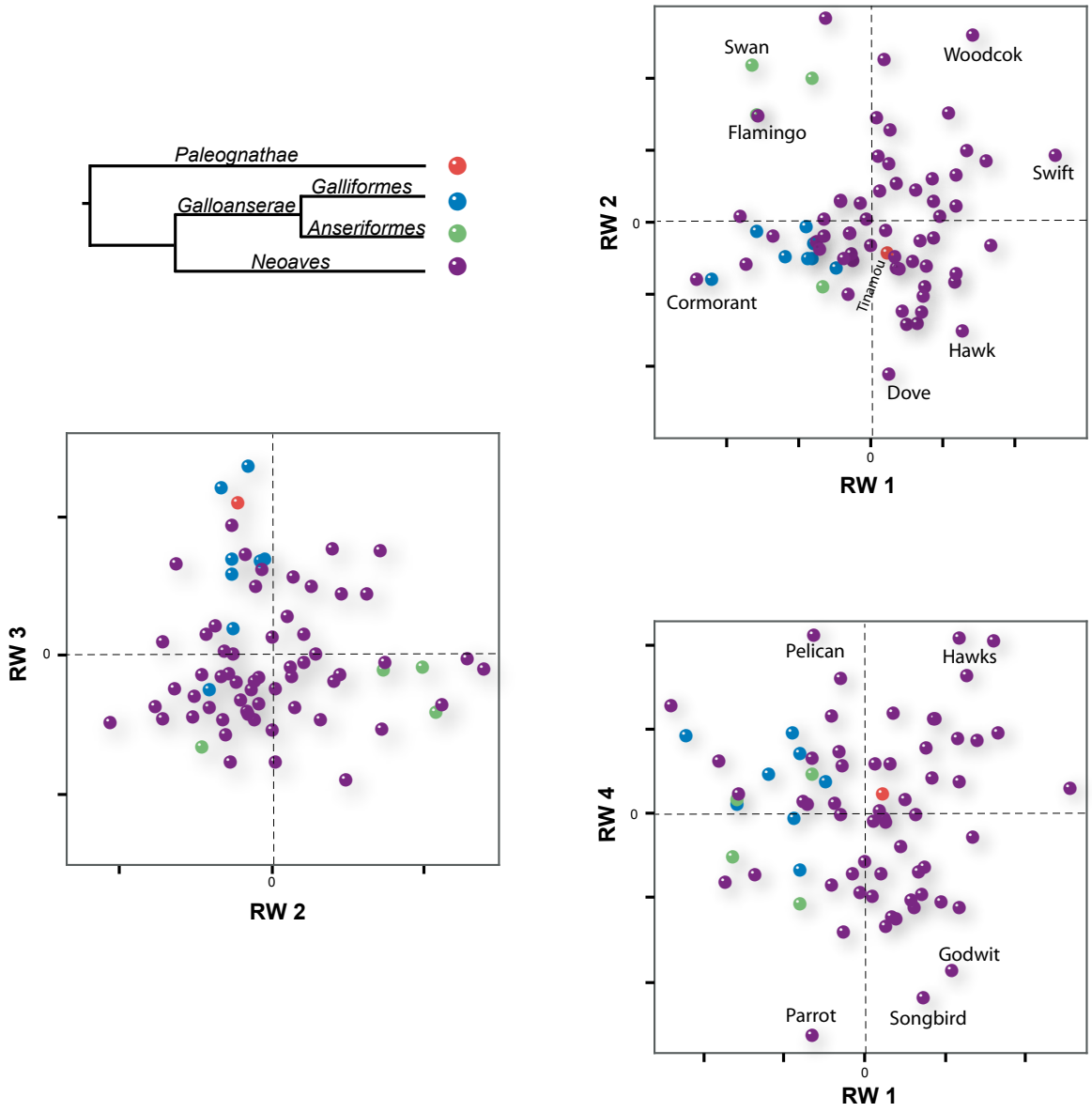

Figure 5. Scatter-plots of relative warps analyses. Colour coding follows stable phylogenetic hypothesis of Neornithes (see e.g. VanTuinen, 2002).

changes in the basioccipital bone (LM 6 and 7) but also with the way in which the Sella and Pituitary Fossa are configured (the basisphenoids; LM 7, 8, 9). The pituitary fossa can be shallower and broader (at negative scores) or narrower and deeper (at positive scores). The reduction or enlargement of the basioccipital (in green, LM 6 and 7) is more noticeable if viewed in comparison with its displacement relative to the external cranial floor (*Lamina Parasphenoidalis*; LM 6, 11). Otherwise, the laterosphenoid bone which bounds the anterior cranial base (LM 1 and 10) seems not to suffer any pronounced change at all. Thus, whether the cranial base is more convex (airobasal, negative scores) or more flat (orthobasal, at opposed scores) appears to be uniquely rendered by elements of the chordal domain (basi and supraoccipital, and basi-pre and post-sphenoids), though is viewed by the orientations between this caudal part in reference with the laterosphenoid. This confirms previous

observations since the plane of the clivus organizes the configuration of the cranial base, yet there are proportional changes as well that are now newly captured.

Thus, the cranial base can be either flat (orthobasal) or convex (airobasal), but apparently, never concave (i.e. klynobasal). A more flat cranial base (orthobasal) apparently associates in this dimension with a more spherical calvarium in positive scores (right side of the plot) than in negative ones, and therefore, the calvarium becomes less domelike with an orthobasal cranial base. Likewise, all such coordinated changes, particularly those taking place in the supraoccipital and the caudal cranial base, submit a re-orientation of the foramen magnum (LM 5 and 6), the latter being more ventrally oriented in positive scores (rounded vaults with a more flat cranial base), or more caudally oriented in the opposed situation.

In RW 2 (Fig. 4b) most deformations of the spline are concentrated at the boundary between the supraoccipital bone (LM 4 and 5) and the parietal (at LM 4 and 3). Corresponding to positive scores, the supraoccipital is markedly reduced dorso-ventrally and becomes somewhat sloped, an orientation that contrasts with a marked expansion of the parietal. In the opposite extreme, negative scores account for an equivalent magnitude of change, herein coinciding with the supraoccipital strongly ventro-dorsally enlarged and more vertical instead of inclined. What this marked changes appear to yield is that, in some instances (some taxa), there is a large topographic distance between the dorsal-most extent of the cerebellar cavity with respect to the external boundary of the supraoccipital with the parietal.

Shape changes associated to RW 3 (Fig. 4c) are mostly related to the cranial floor, while the largest differences encountered in RW 4 (Fig. 4d) associate with an apparently homogeneous expansion or contraction of the region that of the cavity that houses the forebrain (frontal, parietal ad laterosphenoid bones; LM 1, 2, 3). In positive scores (right side of the plot) the region of the forebrain appears to be proportionally smaller than at positive scores in which, conversely, this region is considerably enlarged.

4.3.3 Shape-space distribution

The scatter-plots of the relative warps are depicted separately in Figure 5, and show that all Galloanseres confine within areas that account for cranial base convexity (i.e. airobasality; first RW, negative scores; Fig. 4a), yet some derived Neoaves also converge therein (e.g. a night heron, a grebe, and a cormorant). However, there is one Paleognath in the sample (*Rhynchotus*) which is closer to the consensus though at side for positive scores. Extremes for

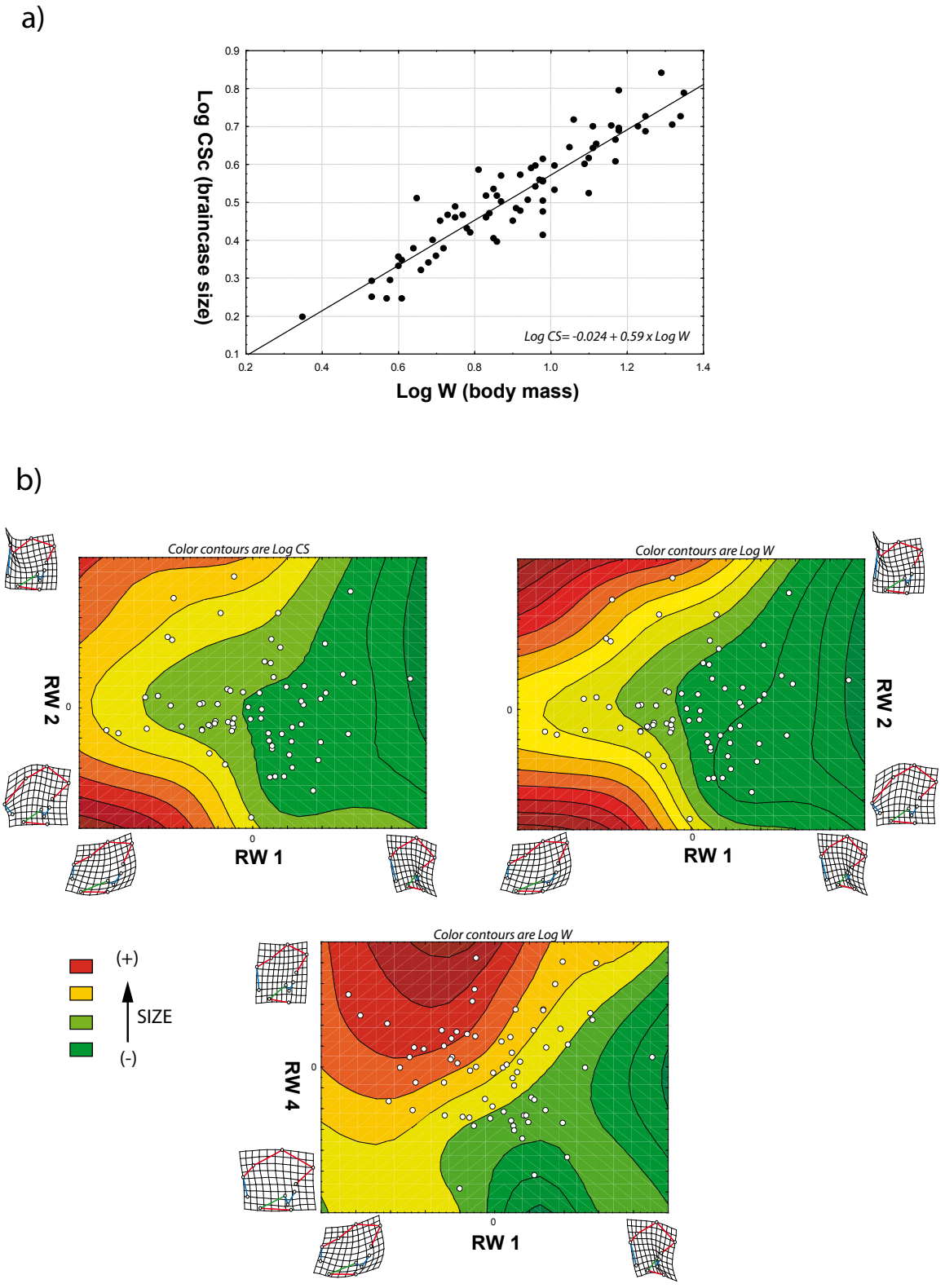

Figure 6. a) Bivariate regression between logW (predictor, x-variable), and logCS (y-axis). Linear regression equation is, *Log CS= -0.024 + 0.59 x Log W*. b) shows the association between relative warps (portion of shape space) and its relation with size with contour plots based on the distance squared smoothing algorithm. Colour grading goes from green (smaller size values), to orange (larger), red to brown being the increasing scalar values for size. Which size variables were used is explained above its corresponding graphic.

positive scores (flat, or orthobasal cranial base, more rounded braincases) are the swift

(*Apus*), followed in less magnitude by the woodcock.

For the second eigenvalue, positive extremes are the pelican and anseres (i.e. have relatively smaller parietal bones, and therefore, large supraoccipitals), and opposed, a hawk (*Buteo*) and a pigeon (*Goura*). In general terms Neoaves occupy a larger extent of shape space. As decomposed by this first relative warps, their braincase shape disparity as a clade is larger, at least in the sense of exploring regions of extreme positive values for RW 1 (see Fig. 4a).

Both the second and third RWs do not show clear distinction among taxa. Interestingly, the plot between RW 1 against RW 4 suggests that the relative size of the forebrain cavity can differentiate for some birds (e.g. a parrot, a songbird, and a godwit) yet these are not extremes for RW 1 (cranial base flexure or relative roundness of the vault). This suggests that these two traits may no be correlated (*cf.* scatter-plot below in Fig. 5b).

4.3.4 Size variables

We have two variables estimating size, one serving as an estimate for braincase scaling (centroid size) and one of body mass. Both variables are linearly related by the equation $LogCS = -0.024 + 0.59 \times LogW$ ($R^2 = 0.8535$; Fig. 6a). The common slope for the pool sample is 0.59 which is very similar to the one found in other studies that have compared brain and body mass allometry among adult birds elsewhere (k=0.55; Bennet and Harvey, 1985a, b). This result is therefore showing that brain size is allometrically related to body mass negatively (slope<1), and centroid size thus serves as a suitable estimation of braincase size, and perhaps also as an estimation of brain size. Note as well that centroid size is capturing endocranial size in two dimensions, which may be what makes the slope differ from other studies, yet at the same time suggests that most size variation among avian brains accrues within the mid-sagittal plane instead of the coronal plane.

4.3.5 Shape distribution and size

The relative warps with a statistically significant correlation with both logCS and logW are RW 1 and RW 4 (r=-0.53, and r=0.44 respectively; please notice the polarity of the axes and the symbol of the r coefficients). We thus depict these two dimensions of the relative warps analysis with size plotted as a function of their distribution scores using the distance weighted least squares smoothing equation (see Figure 6b).

Both relative warps 1 and 4 are statistically correlated with either size variables. The contour plot shows that size relates to RW1 in such a way such that more rounded braincases (and

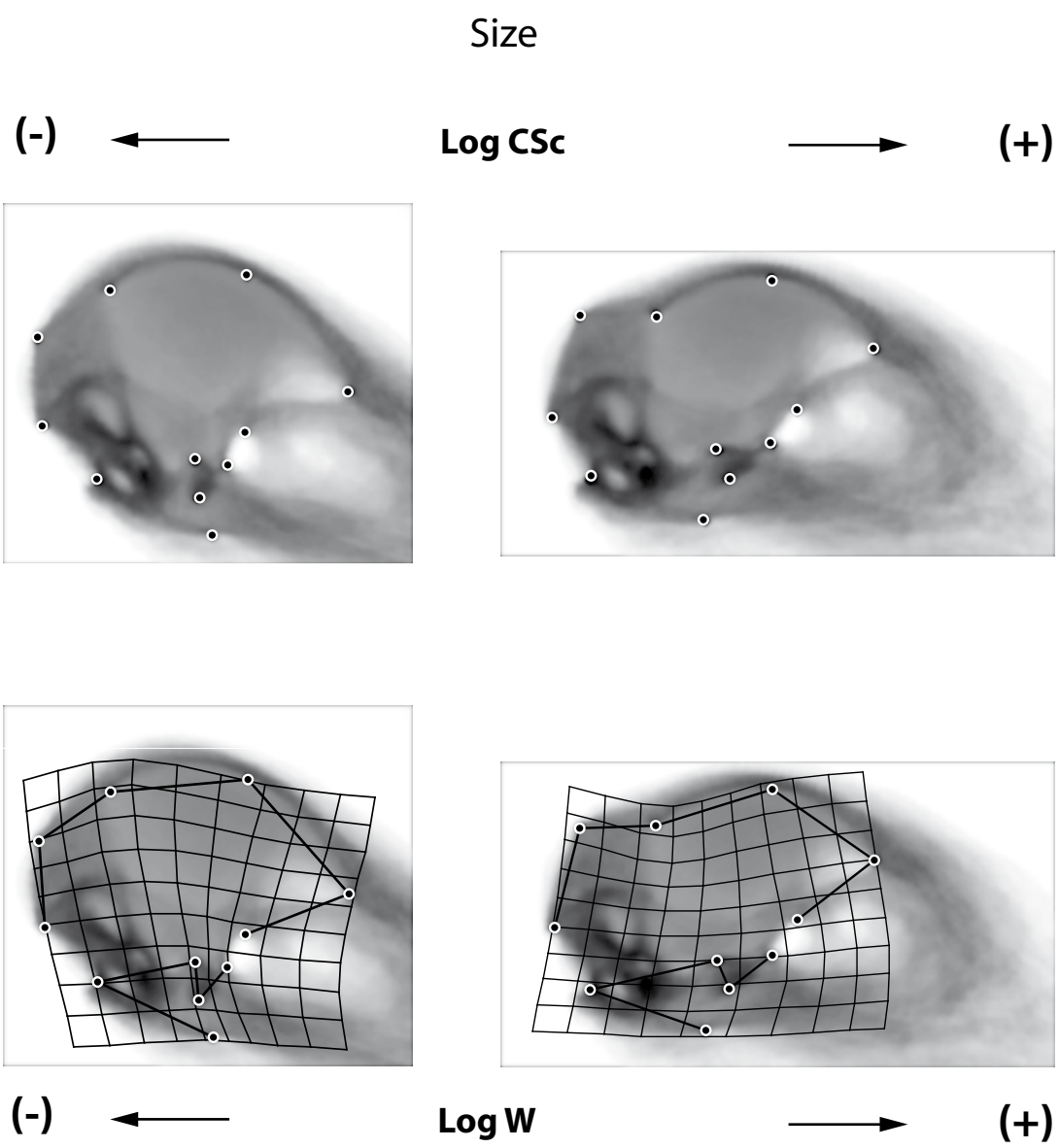

Figure 7. Multivariate allometric shape changes with size. Shape changes are equivalent regardless the size variable used (above, logCS, below, logW). Differences in shape are denoted using the unwarping visual technique and grid deformations superimposed.

shape changes associated at the cranial base) tend to be smaller organisms whereas relatively less rounded (more extended) braincases (with convex cranial bases) tend to be larger. RW 4 corresponds to relative size of the forebrain cavity, and according to its relationship with RW 1 and size, all birds at the region of larger forebrains (not only the parrot or the songbirds all close to the area) tend to be smaller (note that some of them are also Passeriformes).

4.3.6 Braincase shape allometry

Evolutionary allometry accounts for deformations of the grid that are equivalent regardless if we regress shape to LogCS or LogW (Fig. 7; results are shown with the grid and unwarped

images to estimates of small and large extreme sizes). Shape differences as a function of size deform the grid in a similar fashion as did the scores of RW 1. However, differences are that allometric shape change relate only slightly with the different configurations of the cranial base (ortho- or airobasal arrangements). Rather, shape changes associated with size account mostly for the pronounced antero-caudal lengthening of the basioccipital bone and the basisphenoids (the pituitary fossa), which extends to the relative length of the whole cranial base. Likewise, size does not affect the marked differences in the supraoccipital that were observed in RW 1. However, the relative compression or stretching of the basioccipital, Sella and Pituitary Fossa affect the orientation of the foramen magnum and the domelike appearance of the calvarium concomitantly. The whole endocranium may be slightly larger for smaller sizes and smaller for larger sizes, yet this may not be so clearly ascertained.

4.4. Discussion

As in any other vertebrate, the evolution of the avian braincase phenotype is complex and is characterized by pronounced proportional, topographic and architectural differences among its parts. One of the first (and few) quantitative approximations to avian braincase morphology asserted that it was the plane of the clivus (the basioccipital bone) that changed its orientation, and that this was tightly connected with the orientation of the foramen magnum (Duijm, 1951). Lang (1952), on the other hand, compared the development of three different bird taxa (a pigeon, a chicken and a parrot), paying most attention to the arrangements of the cranial base. She affirmed that the caudal and anterior parts of the cranial base in birds (what she called post- and pre-sellar parts respectively) did not change in a coordinated way, and therefore, that both parts should be considered independent from each other.

Moss and Vilmann (1978) emphasized schematically the changes in the plane of the clivus as the causal agent for the differences in the arrangements of the cranial base in mammals (Fig. 1b). Interestingly, we have found that there are differences in the configuration of the cranial base in birds, and that these coincide with only two of the three possibilities that mammals span, the ortho- (flat) and the airobasal (convex) cranial bases. Most of the shape changes that convey these different arrangements in birds are concentrated caudal to the basisphenoids (i.e. caudal to the Sella and the Pituitary Fossa), and not only the basioccipital. These differences become more conspicuous when put in contrast with the external cranial floor (the Lamina Parasphenoidalis), a structure that allows visualizing the changes in

orientation of the plane of the clivus (e.g. Fig. 4a).

Results show that the pronounced changes in orientation of the foramen magnum in birds depend upon coordinated changes between parts that represent the equivalent to the caudal cranial base in mammals (the basioccipital and basisphenoids), yet this occurs in connection with the shape of the supraoccipital bone and in the configuration of the *Sella Turcica* and the *Fossa Hipophysiaria* (i.e. the basisphenoids).

These whole set of associated changes underlie the appearance of the whole cranial base, and the net covariation among all these bones was expected given that they all share a mesodermic identity (Marugán-Lobón and Buscalioni, 2006). If all bones of the occiput are phenomenologically connected, share an equivalent identity, and are also structurally located in a particular area, it may be possible to call this whole part a structural module. This braincase module, however, may not be the occiput alone, but the whole chordal part of the skull *per se*, which in birds contains all bones of mesodermic origin (cranial paraxial, and somitic) lying along the extension of the embryonic notochord up to its most-anterior tip (thus also the basisphenoids; Couly et al., 1993; LeDouarin et al., 1993). Its counterpart, the prechordal one, is the region that lies anterior to this boundary (hence contains part of the anterior cranial base) and is derived from cephalic neural crest mesenchyme.

The null hypothesis we were challenging herein was that braincase macroevolutionary disparity patterns could be the vehicle for asserting whether both the chordal and prechordal domains are divisible modules. For demonstrating the modular identity of the braincase we proposed that braincase shape disparity should stem from the boundaries between each prospective module when comparing the shape of distantly related avian taxa of the monophyletic clade Neornithes. The rationale to ground the hypothesis was that each module should be more coherent internally due to stronger interactions of its elements (Klingenberg, 2004), and reciprocally, that the interactions between modules should be weaker, therefore the ones from which larger macroevolutionary differences should depend upon (Fig. 2).

In effect, analyses show that most avian braincase shape disparity stems from the boundaries between, and not from variation within, each prospective module (i.e. the chordal and prechordal parts). On the one hand, an important amount of avian braincase disparity lies at the boundary between the chordal and prechordal parts in an area of the cranial base that is the site where both prospective modules connect (Fig 4a), a boundary that has been identified with clear-cut skeletogenetic precision (Fig. 2). Thus, the different arrangements

of the cranial base could possibly depend upon being a boundary between the chordal (mesodermic) and prechordal (neural crest) modules, whereby its morphological variation is the outcome of different organizations attained by each module.

On the other hand, another equivalently important aspect of avian braincase shape disparity locates in the territory between the parietal and supraoccipital junction (it explains almost the same amount of shape variance as the first one; Fig. 4b). This area is very important since it is the classic frontier between the occiput and the calvarium, hence the caudal frontier between the neurocranium and the dermatocranium. More importantly, nonetheless, it is also another boundary between the chordal and prechordal domains (cf. Fig 2), even though this is currently more a point of experimental controversy than an undoubted assertion.

The null hypothesis cannot be rejected, nonetheless, since it was assumed that most variation would possibly concentrate therein if this was the dorso-caudal boundary between the chordal and prechordal parts of the braincase (Couly et al., 1993; LeDouarin et al., 1993; Fig. 2). Thus, morphometric comparisons between adult birds favour the argument that the macroevolutionary morphological organization of the avian braincase relies upon its modular nature. Namely, most macroevolutionary disparity of the avian braincase roots at the intersection between the chordal and prechordal domains that build up its integrity.

However, we are comparing phylogenetically distant avian clades, and it could be possible to find changes in the cellular identity of certain bones, such as for instance, the parietal, as it does indeed happen in mammals (e.g. neural-crest-mesoderm boundaries differ, e.g. between rats and humans; Santagati and Rijli, 2003), or else, that the whole calvarium is mesodermic (Evans and Noden, 2006; Noden and Trainor, 2005). Likewise, it could also be argued that the landmark at the boundary in the region of controversy (parieto-supraoccipital junction; LM 3) may not have been placed at a true homologous coordinate.

On the one hand, cell populations of the neural crest may opportunistically assume the role of mesodermic cells in making chondral bone by just arriving earlier to the area of construction (Schneider, 1999). It may also be true that the whole calvarium, of membrane bone, is mesodermic (Evans and Noden, op. cit.). These two possibilities would affect our reasoned hypothesis in the sense that while the boundary exists, the discreteness of the module may not only depend on its cellular nature, but on its whole morphogenetic dynamics. Thus, it may otherwise be more properly called a morphogenetic field (Gilbert et al., 1996; Gass and Bolker, 2003), rather than just a module, for this term more properly

alludes to the dynamic sense of a skeletogenetic module.

This boundary of controversy between the supraoccipital and the parietal represents a transition between chondral and membrane bone, and the region of closure of the braincase that, interestingly, occurs very late in development with a lag-time between taxa depending on whether they are altricial or precocial birds (i.e. this terms refer to a life-history trait related with the way in which birds hatch; in a very relaxed sense means that they do it more or less "developed"; please see Starck, 1993; Starck and Ricklefs, 1999). We cannot know anything about the developmental nature of the boundary from adults, but its marked evolutionary change may entail that the region would be a point of time-dependant signalling thresholds within the morphogenetic field where cell populations, regardless their identity, may change their behaviour to produce chondral or dermal bone once the signal has been assimilated.

On the other hand, an alternative possibility that may explain such a pronounced macroevolutionary difference between bones in the parieto-supraoccipital area is that while the boundaries between the parietal and the supraoccipital may be fixed, the bones may be identified non-homologously across all the species involved (Hanken and Gross, 2005). Jiang et al., (2002), and Evans and Noden (2006) have recently argued in favour of this second possibility, suggesting that the avian frontal may in fact represent the fusion of the frontal and parietal bones (so-called the parieto-frontal). This interpretation also implies that the parietal bone in birds might have been misinterpreted as such, being more properly assigned as homologous to the intra-parietal that is present in other reptiles (e.g. in crocodiles, though therein is called the inter-parietal, see Klembara, 2004).

Thus, this would add a new bone to the chordal part. Some neornithes birds (it is difficult to say which specifically besides the chicken, which was used in the experiments) could therefore have the inter-parietal bone and the parietal fused to the frontal, while others may have lost it, and others may be even be in intermediate situations. We cannot argue against this possibility since all the bones within the avian braincase coalesce, and it is nearly impossible to differentiate any bone nor a boundary therein (i.e. sutures are invisible). While in principle this should not be a pronounced source of error, it does not dismiss the possibility of non-homology of the landmark if there is an additional bone therein, moreover, if this only occurs in certain taxa.

These two boundaries between the hypothesized modules at the cranial base may be keys for gaining crucial insights about cranial morphological macroevolution in birds. However,

the morphological organization of the avian braincase must also be associated with the phenotypic evolution of the central nervous system, either influenced by (Moss and Vilmann., 1978), or just coordinated with it. Most classic studies in birds often advocate that it would not only be the brain but the whole CNS (i.e. including their large eyes) which would exert a strong influence in the surrounding bone system by growing (Gaup, 1906; Duijm, 1951; Lang, 1952).

The phenotypic evolution of the CNS in terms of its relative size (scale) is allometrically associated with body size (mass) evolution (Jerison, 1973). Our results have underscored that evolutionary allometry can be observed among bird taxa, both in the sense of endocranial size to body mass (as other studies have already, and nearly-equivalently, pointed out; Portmann, 1947a, b; Bennett and Harvey, 1989a, b; Starck and Ricklefs, 1998; Iwaniuk and Nelson, 2002; Fig. 6a), and braincase shape differences to cranial size and body mass.

Larger birds (or, more properly, "heavier" birds) tend to have proportionally smaller endocranial cavities with ratio (slope) of either 0.59 or very close values (see references above, and Fig. 6a). Since the whole cavity closely resembles the size of the CNS it houses within we could express our findings about endocranial relative size as facts for the neural CNS itself. However, the shape changes between the chordal-prechordal boundaries do not seem to be fully related with size allometrically (braincase size or body mass) despite the first relative warp axis appeared to be correlated with size (Fig. 6b).

For instance, multivariate regressions hint that cranial base configurations are only slightly associated with size (body mass) increases or decreases (Fig. 7). On the contrary, it is only the relative proportion of the caudal part of the chordal domain what would be truly predictable as a function of size (i.e. mostly the basioccipital bone; contrast Fig 4a and 6b, with Fig. 7), proportional changes which may, in turn, affect the total proportional length of the whole cranial base (considered to be delimited between the foramen olfactorium down to the occipital condile; LM 1, 6, 7, 8, 9, 10; Fig. 2), and not its configuration. This allometric shape trend also relates size with changes in the relative proportional breadth of the forebrain cavity, and overall, with the relative vaulting of the braincase. Thus, smaller birds tend to have domelike calvaria which may be associated with the relative growth of the CNS via the liability of dermal bones to re-conform under mechanical stress caused by neural tissue growth in development (Lieberman et al., 2000a, b; Hallgríssom et al., 2007). This trend may associate with slight changes in the cranial base, perhaps by affecting the relative size of the forebrain cavity (likely, forebrain size), and reorienting the anterior cranial base. Notice, that

a reorientation of this pat or the cranial base may be easy since it does not ossify in many birds (see Fig. 2a).

An evolutionary attainment of a smaller size than the average (e.g. a clade "dwarfism") may associate to relatively larger CNS sizes, with changes between the elements of the chordal module that account for a proportionally shorter cranial base, a more spherical endocranial cavity, a ventrally oriented foramen magnum, and an enlarged forebrain cavity. These shall coincide though with the acquisition of orthobasal, or perhaps very slightly klynobasal, configurations of the cranial base (if using the classic terminology; compare cranial base configurations with the positive extreme in Fig. 4a, and small sizes in Fig. 6), a cranial base configuration which is nonetheless developmentally acquired (i.e. is not size-predictable). This may also explain why only smaller ("lighter") birds seem to attain a ventrally oriented foramen magnum (see, Marugán-Lobón and Buscalioni, 2006, this part of the volume). Any larger (heavier) bird, regardless its cranial base configuration (flat –orthobasal, or convex –airobasal), will presumably show a foramen magnum facing caudally.

These traits altogether may be of great importance for disciplines interested in biological processes and their evolution (e.g. evolutionary morphology, paleobiology, and developmental biology). For instance, they altogether stress that there are marked phenotypic differences in the braincase between birds, and by direct inference, in the morphological organization of the CNS. Some differences may be developmental (morphogenetic) and independent of size, while others may be not. This highlights the need for maintaining a research focus on the evolutionary meaning of size, on the mechanistic basis of its evolutionary shifts, and how it may relate, modulate and/or constraint the morphogenesis of both the braincase and the CNS (e.g. by inference from the endocranial cavity, the CNS may be said to be more rostro-caudally shorter in its base, more rounded and more compact in smaller birds than in larger ones). Additionally, the chordal domain may be homologous to a modified vertebra (Couly et al., 1993). Given its connected shape changes with body mass this whole module of the skull may be more integrated with other post-cranial elements (i.e. vertebrae), than with the facial skeleton which is of neural crest origins, an aspect of skull architecture that elicits consequences on head posture, vestibulo-occular control and, by extension, on patterns of locomotion and behaviour.

Prior to concluding, we should also stress that most allometric estimations of CNS size to body mass available in literature are based on volumetric comparisons of the CNS (or the volume of the endocranial cavity) to body mass, yet have found equivalent ratios to the

ones we have addressed herein (i.e. slopes of 0.59). This implies that the coronal (width) of the CNS is also taken into consideration, and that it might be an important aspect of its phenotypic variation (see e.g. Dabelow, 1931; Dullemeijer, 1961; Lieberman et al., 2000a, b; Hallgríssom et al., 2007). Our study is dimensionally-biased since the inferred size of the CNS is the geometric size (centroid size) of the endocranial cavity captured only from its mid-sagittal view projected to a 2D plane. Hereafter, it would be crucial to test whether most coronal size increase of the CNS in evolution is nearly equivalent to the antero-caudal expansion of the CNS in the mid-sagittal plane, as results apparently suggest, or rather, if results are biased in certain birds.

3.5. Avian braincase and central nervous system shape evolution and their association with ontogenetic strategies.

5.1 Introduction

Phenotypic differences of the braincase are inter-specifically ubiquitous among birds, for instance, in the way in which the foramen magnum is oriented (more ventrally or more caudally), in the angular relationships between different portions of the cranial base (e.g. being either convexly flexed or flat, so-called *airobasal* and *orthobasal* respectively), or in the more or less domelike appearance of the cranial system (for further readings see; Duijm, 1951; Hofer, 1952; Moss and Vilmann, 1978; Marugán-Lobón and Buscalioni, 2006; Chapter 4-Part 3 of the thesis, and Fig. 1).

The braincase holds and protects the central nervous system (CNS), and this fits so tightly within the endocranial cavity that it leaves an almost perfect imprint of its outline (Jerison, 1973; Fig. 1a). These fine carvings manifest that the development of both neural and bone systems are possibly epigenetically synergic (Moss 1997a, b, c, d; Richtsmeier et al., 2006), and therefore, phenotypic differences of the braincase among bird taxa may be intimately connected with the phenotypic evolution of the central nervous system (CNS).

One developmental facet of CNS phenotypic evolution in birds is that evolutionary shifts in its relative size relative to body mass are coupled with different developmental strategies, the latter which have evolved in what is so-called the precocial-altricial spectrum (Starck, 1993). This spectrum is characterized by the remarkable differences displayed by avian hatchlings in terms of their external appearance, activity and behaviour. One extreme type of these different life-history developmental strategies is called *altricial*, and is characterised by hatchlings which appear to have been born "less developed", they are careless (e.g. naked and with their eyes still closed), and remain in the nest for a longer period of time after born under prolonged parental care. The spectrum spans along a continuum of more developed features towards up to the opposed extreme (e.g. more mobility, opening of the eyes, or more feathers in the body; Table 1), the so-called the precocial type, in which hatchlings are almost fully developed, hence being capable of wandering and feeding autonomously.

Most morphometric studies recursively record that the altricial strategy may likely promote neural development and increases in relative brain size (Portmann, 1947a, b; Starck and Ricklefs, 1998; Iwaniuk and Nelson, 2003). However, other phenotypic changes have occurred in the course of avian CNS evolution, since it is markedly visible that endocranial cavities resembling the outline of the CNS differ markedly among bird taxa (see e.g., Fig. 3 in Chapter 4, and Fig. 1 herein).

These aspects of CNS and braincase morphological evolution have seldom been

a)

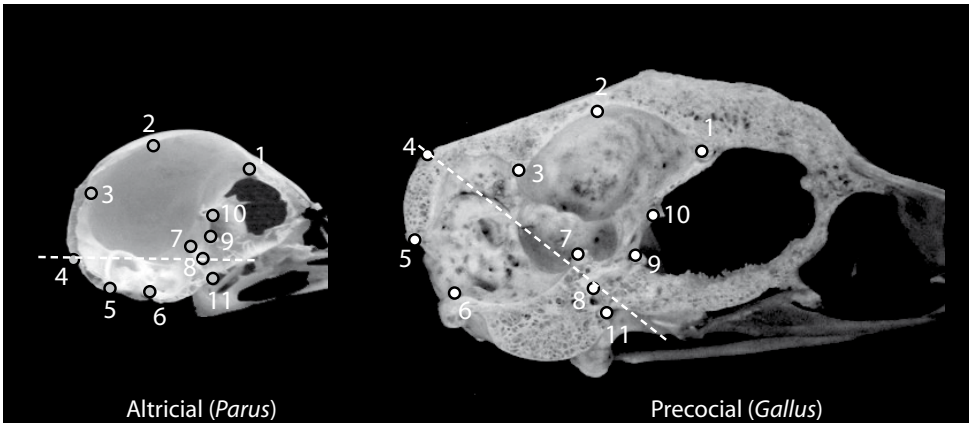

b)

Braincase parts		Landmarks
Cranial base	----------	1, 6, 7, 8, 9, 10
Supraoccipital	----------	4, 3
Calvarium	----------	1, 2, 3
Pituitary fossa	----------	7, 8, 9
Foramen magnum	----------	5, 6
Caudal cranial base (Plane of the Clivus)	----------	7, 8

c)

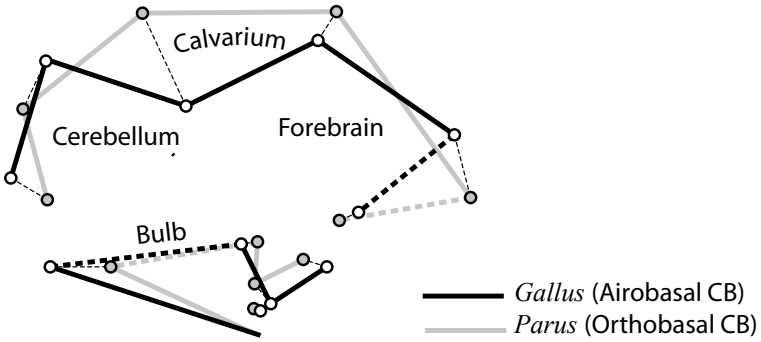

Figure 1. a) Mid-sagittal view of the braincase of *Parus* (songbird, left) and *Gallus* (chicken, right) with landmarks superimposed. Pictures are not to scale but aim tow show that there are differences in size between taxa. b) Anatomical parts outlined by landmarks (see also Table 2). C) GPA superimposed endocranial configurations of landmarks between the specimens above two show morphological differences of both the braincase and the CNS.

explored, and given the fact that they exist, the question we address in this study is if phenotypic differences of the CNS among bird taxa, other than relative size, may also associate with the evolution of avian developmental strategies. Obviously, this question draws out straightforward that the organization of the braincase could also be associated with the evolution of developmental strategies since it reflects the shape of CNS. In fact, rough morphological differences of the CNS may be interpreted from the shape differences of endocranial carvings and counterpart cavities within the braincase (see, Brochu, 2000).

We have opted for this latter proposal as a null hypothesis of braincase and CNS phenotypic evolution in birds to be challenged quantitatively using landmark-based Procrustes geometric morphometrics and its associated multivariate statistics (Bookstein, 1991; Rohlf and Marcus, 1993; Adams et al., 2004). The technique is a refined metric methodology that allows visualizing geometric shape change, while at the same time, aids challenging hypotheses of shape difference and about the covariation of shape with different independent variables (e.g. shape allometry) on the basis of common multivariate statistics. In effect, we have stressed out several important aspects about avian braincase shape disparity on the basis of geometric morphometric procedures which are important because they go by hand with the proposed null hypothesis.

For instance, the ubiquity of cranial base differences among bird taxa is in fact underlined by evolutionary changes within two structural modules, the so-called chordal and prechordal parts which can be delineated by their early developmental identity (Couly et al., 1993). The *chordal* module, which is mesodermic in origins, and the *prechordal* module, which derives from the cephalic neural crest, split at the middle of cranial base (Fig 1), they both change internally, and therefore their variation is visible at their boundary in the cranial base. Additionally, an area of large taxonomic difference between birds is at another boundary between these modules, at the junction between the occipital (chordal) and the parietal (prechordal; Fig, 1, and see Chapter, 4).

Considering the braincase as divided into two modules (*sensu* Wagner, 1996) implies that each module will be partially independent from the other (i.e. the shape changes of each will be more integrated within than between them; see e.g. Klingenberg, 2004). Since each module has a particular location, each is topographically associated with different parts of the CNS; the chordal part surrounds the caudal parts of the CNS (e.g. the medulla, cerebellum) while the prechordal part may be more related with the forebrain (cf. Fig. 1). It might be possible that the whole CNS is also modular in an equivalent way (Iwaniuk and Nelson, 2004).

Interestingly, the different cranial base configurations observable among birds derived from the evolutionary shape changes of the chordal and prechordal parts are likely size-independent (i.e. they are only slightly allometrically predictable). In birds, the evolutionary allometric changes of the braincase that are otherwise predictable from size are the proportion of the basioccipital (which lies in the chordal part and corresponds, anatomically, to the caudal cranial base), and the relative size of the forebrain cavity (prechordal bones such as the frontal and parietal). Proportional changes of the basioccipital make the whole cranial base appear proportionally shorter (for smaller sizes), or larger (for larger sizes), and the relative enlargement (for small sizes) or shrinking (for larger sizes) of the forebrain cavity apparently effects a slight flexure of the cranial base, possibly tilting its anterior part (i.e. the laterosphenoid). Moreover, this whole allometric trend associates with a more or less domelike appearance of the whole braincase (e.g. smaller taxa are the ones that, in principle, tend to have more spherical braincases, with the foramen pointing ventrally and flat –orthobasal to klynobasal, cranial bases; see Fig 1). In turn, these whole set of allometric shape differences could be equivalently translated to the morphology of the CNS and, therefore, extend the hypothesis we are dealing with, to asking whether they will or will not be associated with the evolution of ontogenetic strategies. In other words, the question stresses whether altricials and precocials will show different braincases (endocranial cavities) and CNSs, and if they will show equivalent or different evolutionary allometry trends (i.e. equivalently predictable shape changes associated with size).

Developmental type	*CVA category*	*n*
Superprecocial	*	*
Precocial 1	2	12
Precocial 2	3	9
Precocial 3	4	7
Semiprecocial	5	4
Semialtricial	6	15
Altricial 1	7	7
Altricial 2	8	17
	Total N=	71

Table 1. Precocial and Altricial categories (after Starck, 1993; p. 278; see for other traits). The asterisk (*) denotes absence.

We have explored shape differences of the braincase in the mid-sagittal plane since it contains most relevant features of its phenotypic organization in vertebrates (Moss and Vilmann, 1978). More importantly, this plane allows capturing an ample outlook of the CNS's outline. The sample we have challenged the hypothesis with consists of *N*=71 mid-sagittaly

photographed braincases of birds belonging to a wide array of avian families (see Appendix 2) which, at the same time, allow representing seven out of the eight developmental groups in which the altricial-precocial spectrum can be typified (five types of precocials and three of altricials attending to salient features of their hatchlings; Table 1, see also Starck, 1993).

We have searched for cranial shape differences using Canonical Variates Analysis (CVA), and tests for Separate Slopes using the developmental types as statistical categories. CVA is used for determining if there is a particular predictable braincase shape that corresponds to any particular developmental type (e.g. if there are differences in braincase shape organizations that associate with a particular developmental mode). That is, it embodies the question at the core of the null hypothesis; whether there are, or there are not, morphological differences in the braincase (endocranial cavity) and the CNS predictable by the different developmental types.

Multivariate tests for Separate Slopes, on the other hand, are used to fit endocranial shape variation as a function of size, and then challenge the proposal inherent to the null hypothesis for which developmental modes (altricials and precocials) should have different allometric slopes. If the hypothesis is rejected, developmental types would not follow different allometric shape changes in their braincases, and might only (though perhaps not) differ in their intercepts (i.e. differ in the onset of their trajectories; see e.g.; Gould, 1966).

One important remark we shall stress about this study is that the truly valid results for all the analyses correspond to the possible association between the typified series of ontogenetic strategies and their relationship with braincase phenotypic evolutionary changes, (i.e. neural soft-tissue is completely absent, and the only evidence comes from the bone). However, we can assume that bone arrangements will reflect a reasonable amount of shape variation of the CNS (see; Brochu, 2000), such as for instance, of the forebrain, the cerebellum or the bulb, from the differences in shape of the corresponding cavities carved in the bone by these parts of the CNS. Thus, there can be a parallel reading about the concomitant phenotypic evolutionary changes of both systems (neural and bone tissues respectively).

The evolution of ontogenetic strategies is equivalent to speaking about the evolution of development. If the null hypothesis of the study is not rejected, that is, if particular ontogenetic strategies match with particular braincase architectures, developmental evolution in birds could be read as being associated with both the phenotypic evolution of the braincase and the CNS.

5.2. Materials and Methods

Data was collected on *N*=71 dried avian skulls sliced in the mid-sagittal plane. Skulls belong to the *Hess* Collection housed in the Museum für Naturkunde in Berlin (see Appendix 2 for species and institutional labels, Box 5 describes the collection, but see also; Hesse, 1907). Skulls were digitized in lateral view with an Olympus C-720 digital camera following the protocol summarized in Marugán-Lobón and Buscalioni (2004). Landmarks were digitized on each picture using TPSdigit (v. 1.40; F. J. Rohlf) and are summarized in Table 2 with their anatomical correspondence (their depiction is in Figure 1).

Number	*Description*
1	Foramen of olfactory nerve (fossa bulbi; N. I)
2	Mid-point between LM 1 and 3 at ventral edge of frontal bone
3	Ventral edge of endocranial crest separating cerebellar and forebrain cavities
4	External junction between supraoccipital and parietal at occipital crest
5	Dorsal rim of foramen magnum
6	Ventral rim of foramen magnum, anterior to occipital condile
7	Dorsal-most point of Sella Turcica (dorsal tip of basi-postsphenoid)
8	Ventral-most point of fossa hypophisiaria
9	Ventral edge of optic foramen (N. II)
10	Dorsal edge of optic foramen (N. II)
11	Tuba timpanica at rostrum parasphenoidale

Table 1. Landmarks and their anatomical description

Each species of the sample was characterized by a categorical variable (2 to 7; category 1 is skipped because Superprecocials, -Megapodes, are not present) representing a developmental mode following Starck (1993, p. 281; see also Table 1). Landmark configurations were superimposed using Procrustes analytical procedures (based on Least squares superimposition criteria; Gower, 1975), and visualizations are based on deformation grids calculated with the Thin Plate Spline interpolation function (i.e. data are the partial warp scores plus the uniform component; Bookstein, 1991).

A MANOVA is first used to test if there are statistically significant shape differences between altricials and precocials. Canonical variates analysis (CVA) are thereafter performed to search for functions that discriminate between the categorical variables (containing seven developmental modes; Table 1) and shape differences from within the weighted matrix (partial warp scores and uniform component) of the pool sample. The analysis was set to

use the within-group covariance of the weight matrix of the whole sample and tests for the probability of match were calculated on the basis of group size since this each differed among the eight developmental categories (cf. Table 2). CVA analysis was performed using the SPSS for Windows statistical package (v. 10.06.2; SPSS Inc.).

Each suit of scores for the significant functions of the CVA has been set as an independent variable and regressed to the partial warp scores of the pool sample using a multivariate regression with TPSregr (v1.31; F. J. Rohlf) in order to visualize their shape meaning with deformation grids. In addition to visualizations with grid deformations results are also depicted using the unwarped image of the consensus based on the TPS interpolation function (Rohlf, 2002). This consensus image is transformed to the extremes of the CVA axes resembling the shape of a bird. Image unwarping was performed using the TPSsuper software (v1.14; F. J. Rohlf).

Cranial size is calculated as the centroid size (CS) of the braincase of each bird of the sample (CS is the squared root of sum of the squared distances between landmarks of each configuration). Body masses were also collected from literature (Dunning, 1993), because properly, allometry is a test for proportions against body size (Huxley, 1932). Each of the weights (mass in *g*) matches the exact genus and species for the individuals of the sample. Mass was transformed to its cube root for a better match with the dimensionality of CS, and thereafter, both size variables (CS and body mass) are treated as their logarithms (*logCS* and *logW*). Due to small sample sizes for each particular developmental type, bivariate regressions (logCS *vs.* logW) and multivariate Separate Slopes tests (shape *vs.* logCS and logW) were only performed between altricials and precocials (i.e. two categories) using TPSregr (see above).

5.3. Results

5.3.1 Bivariate size differences

For the pool sample, logCS and logW (braincase size and body mass respectively) are linearly correlated following the equation LogCS= -0.024 + 0.59xLogW (Fig. 2, left). However, slopes change between developmental groups (precocials and altricials (Fig. 2a, right). While precocials show an equivalent slope to the one of the pool, altricials raise it slightly from 0.59 to 0.64. This bivariate prediction agrees with other sources comparing mass measurements of brain and body size yet slope values differ slightly (mostly in the values of the second decimal). However, birds typically considered encephalised such as songbirds (e.g. *Parus* or

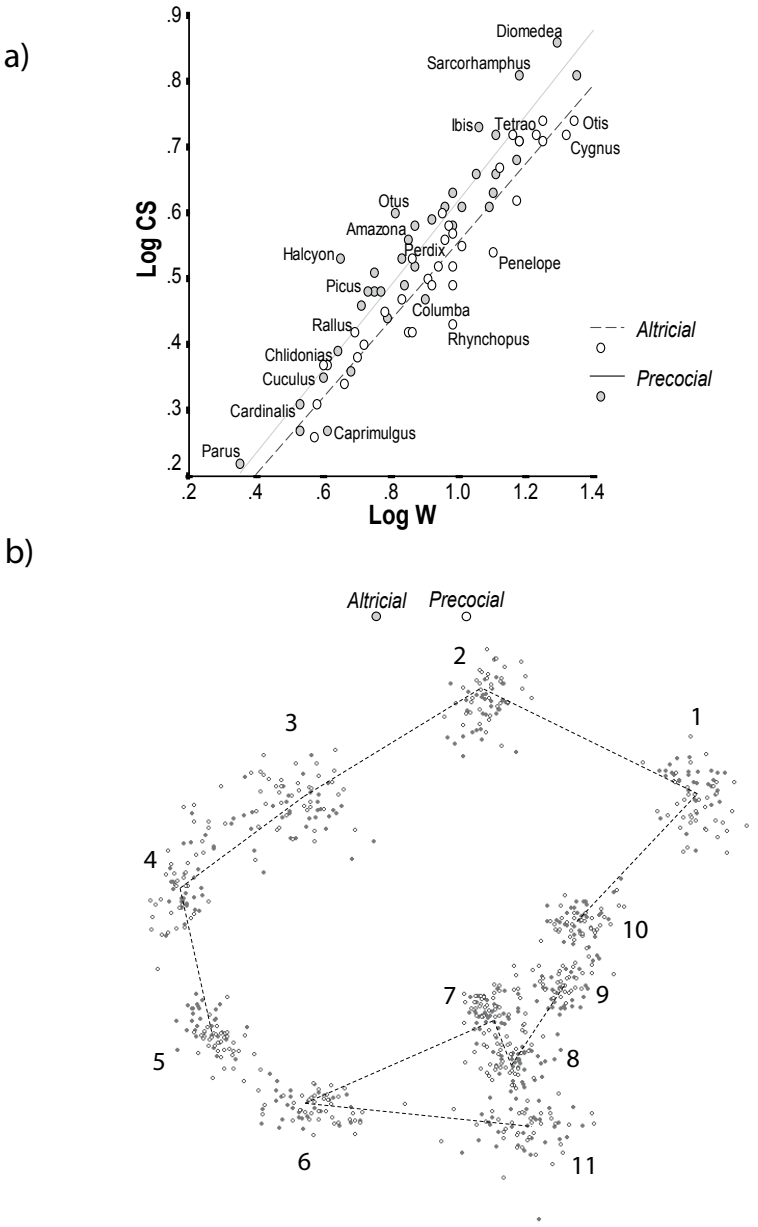

Figure 2. a) Bivariate regressions between logW (body mass) and logCS (braincase size) between altricials and precocials. b) GPA superimposition residuals emphasizing altricials and precocials and upon which the MANOVA is based (see also Fig. 5).

Cardinalis) and parrots (*Amazona*) do not deviate markedly from the predicted allometric regression for altricials. The largest positive residuals from the altricial regression line correspond to *Halcyon*, *Sarcorhamphus*, *Perdix*, or *Diomedea*, whereas the smallest is *Caprimulgus*. Precocials which deviate most positively from their allometric prediction are *Rallus*, *Chlidonias*, *Nyroca* and *Tetrao*, whereas negatively are *Rhynchotus*, *Penelope* and *Pavo*.

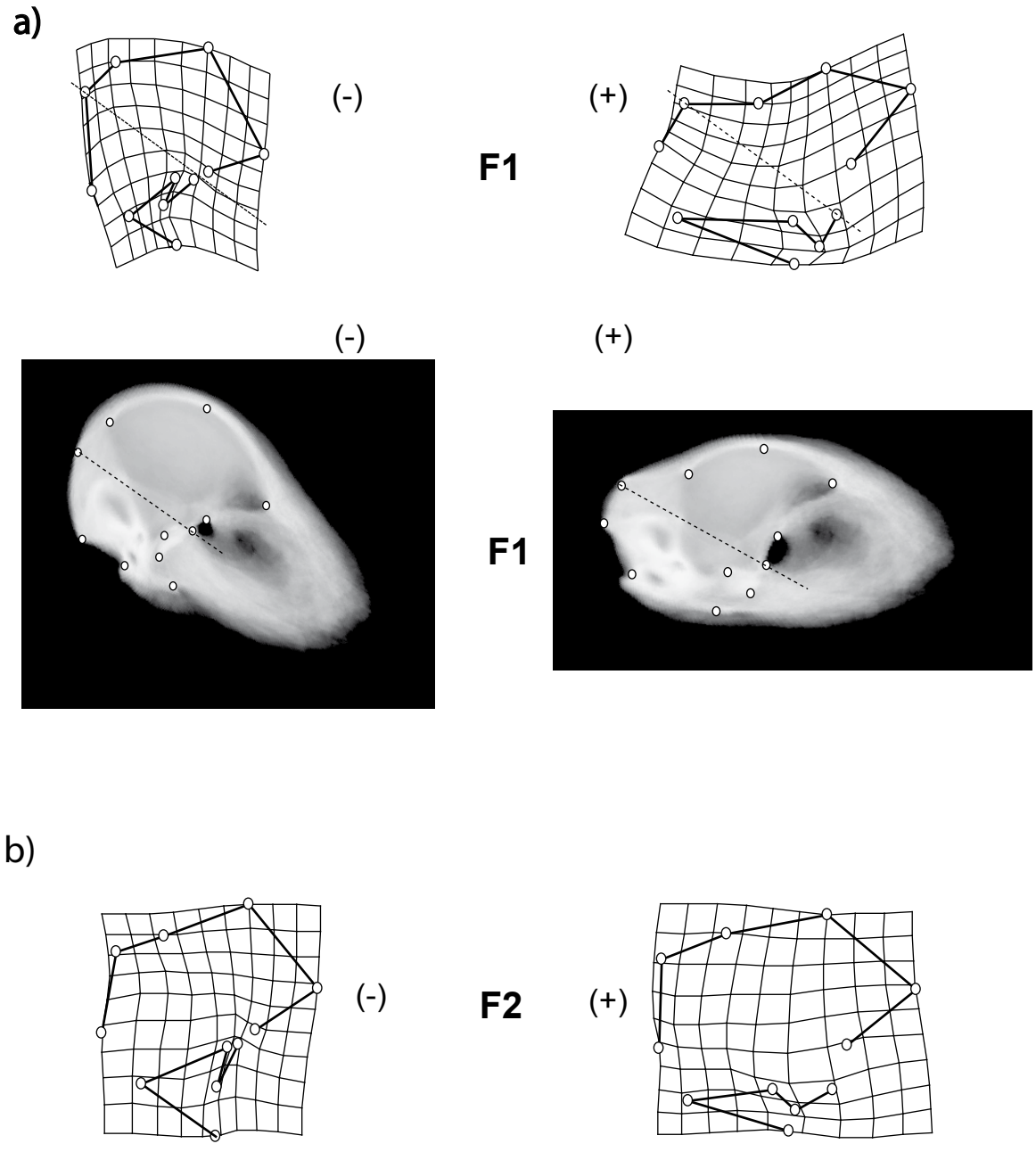

Figure 3. CVA functions (F1 and F2) with their meaning in terms of shape differences between extreme scores with deformation grids and unwarped average (the latter only for function 1 because F2 does not differentiate between altricials and precocials). a) Grid deformations for F1, and b) grid deformations for F2. Dashed line splits the braincase in two halves, one the chordal and the other the prechordal.

5.3.2 Multivariate shape differences

MANOVA analyses on the partial warps scores (including the uniform component) show that there are statistically significant differences in the shape of the braincase between altricials and precocials (Wilks λ=0.342575; Chi-squared= 4.1870; Effect df 22; Error df 48; $P<0.01$; Fig.2b, and 3 when comparing differences for the categorical variable). The CVA for the seven developmental categories renders two statistically significant functions and Figures 3 and 4 summarize their phenotypic meaning.

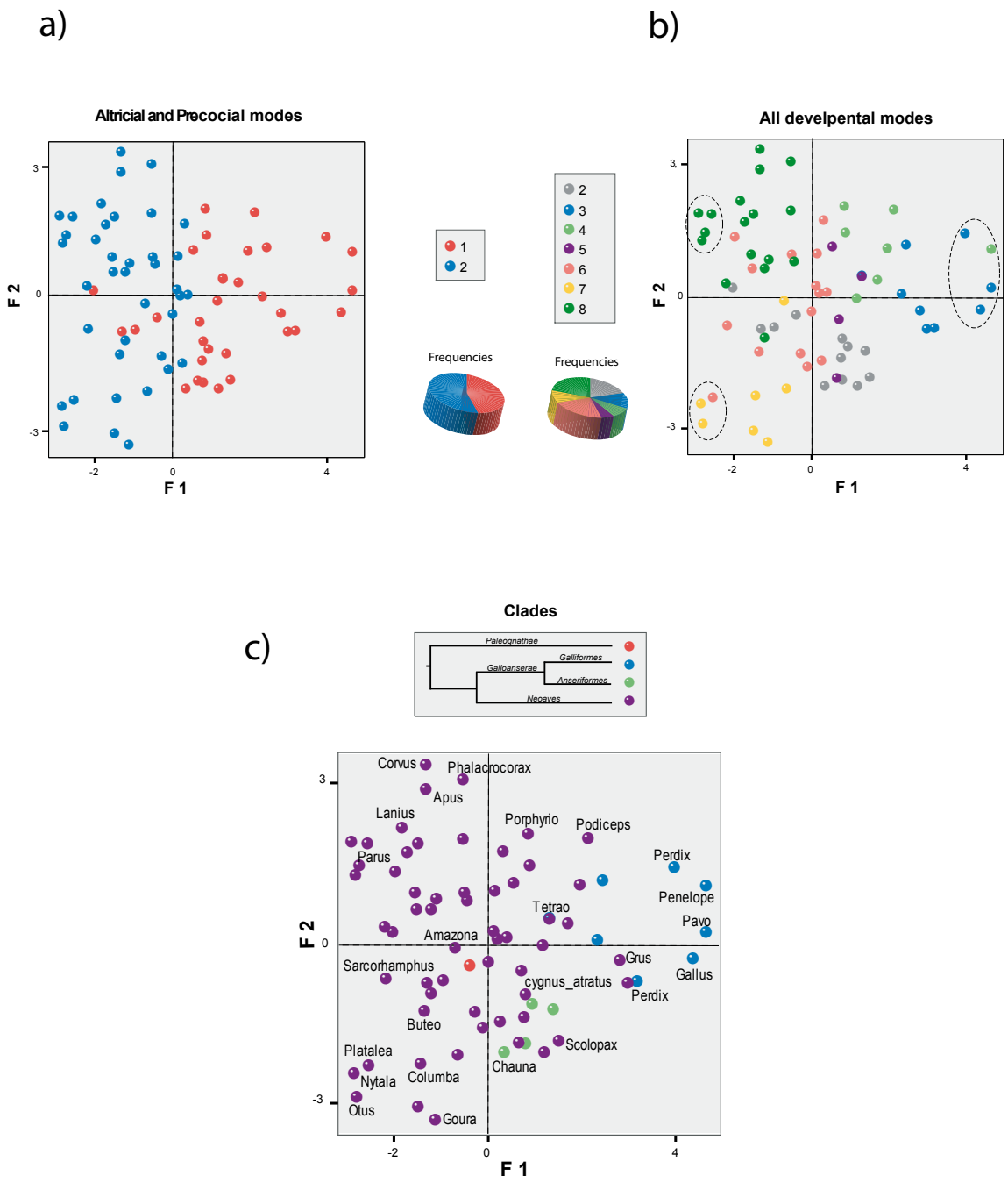

Figure 4. CVA scatter-plots. The CVA was calculated for seven groups (see Table 1). a) CVA scores for F1 and F2 with colour codes representing precocials (1, red) and altricials (2, blue). b) Same scatter-plot but with the real categories of the analysis (all seven categories of developmental types). c) Same CVA scatter-plot but showing the distribution of major nodes of Neornithes phylogeny. 3D pies between show frequencies of individuals for each plotted developmental category.

The first function (F1) of this CVA segregates fairly well between altricials and precocials explaining a total of 42.7% of variance (Wilks λ=0.018, Chi-squared 221.892, df 132, P<0.01; Fig. 3a, b, and Fig. 4a, b). Braincase and endocranial cavity shape differences that associate with this function are complex since they affect most of the whole braincase. There is a clear distinction between the extremes estimated by the function in the way in which the cranial base and the orientation of the foramen magnum are arranged. However, the function

associates these architectural differences in the cranial base with a considerable relative size of the forebrain cavity as well as with pronounced differences in the supraoccipital bone and basispenoids at the Sella and the Pituitary fossa.

The reading of the axis is reciprocal between both extremes (Fig. 3a and b) hence for brevity we will only describe the altricial side. The precocial side of the function can be read equivalently but opposed (i.e. large would be small, compressed stretched, and so on; please, contrast descriptions visually in Fig 3). Thus, F1 predicts that the forebrain cavity is larger in altricial extremes (they locate in negative scores, where it appears that the forebrain is more expanded in birds such as *Parus*, a songbird, *Dendrocopus*, a woodpecker, or *Otus*, a small owl), which associates with a more flat cranial base (orthobasal cranial base), being distinctively antero-caudally shorter due to the reduction of its caudal portion (the basioccipital), and the orientation of the foramen magnum is more ventrally oriented, the supraoccipital is markedly dorso-ventrally stretched, and the pituitary fossa (basisphenoids) is very compressed. It is the relationship between the caudal cranial base and the cranial floor which may be more related with changes in the configuration of the cranial base. The cerebellar cavity becomes less outlined and the calvarium is domelike.

The second function (F2) is also statistically significant (Wilks λ=0.071, Chi-squared 146.825, df 105; P<0.01), explains 24% of variance (66.7% accumulated) yet it is only capable of discriminating braincase shapes within developmental types and not between them (see shape differences associated in Figure 3b). None of the remainder functions are statistically significant, and only the first one (F1) is capable of differentiating among developmental modes, thus differences in the braincase are present yet are subtle between groups. This may explain why the cross validation drops down from 85.9% to a low 46.5%.

The scatter-plot between functions F1 and F2 (Fig. 4a and b) shows that the first function discriminates fairly well between major developmental modes, although there is some overlapping between the categories. However, plotting all seven developmental modes at once (upon which the analyses were based), it is clear that within each general category (altricial or precocial) there is a great deal of overlapping (Fig. 4b). The scatter-plot between F1 and F2 also shows that altricial clusters are not as well outlined as the precocial ones (they are more scattered). Particularly, true altricials and altricials type 1 are better clustered, but semialtricials extend across a large portion of the scatter-plot (though in their corresponding side of altriciality). Among the true altricial Passers such as *Parus*, and *Cardinalis* cluster together though overlap with *Dendrocopos* (Piciformes), and other relatives such as *Corvus* or

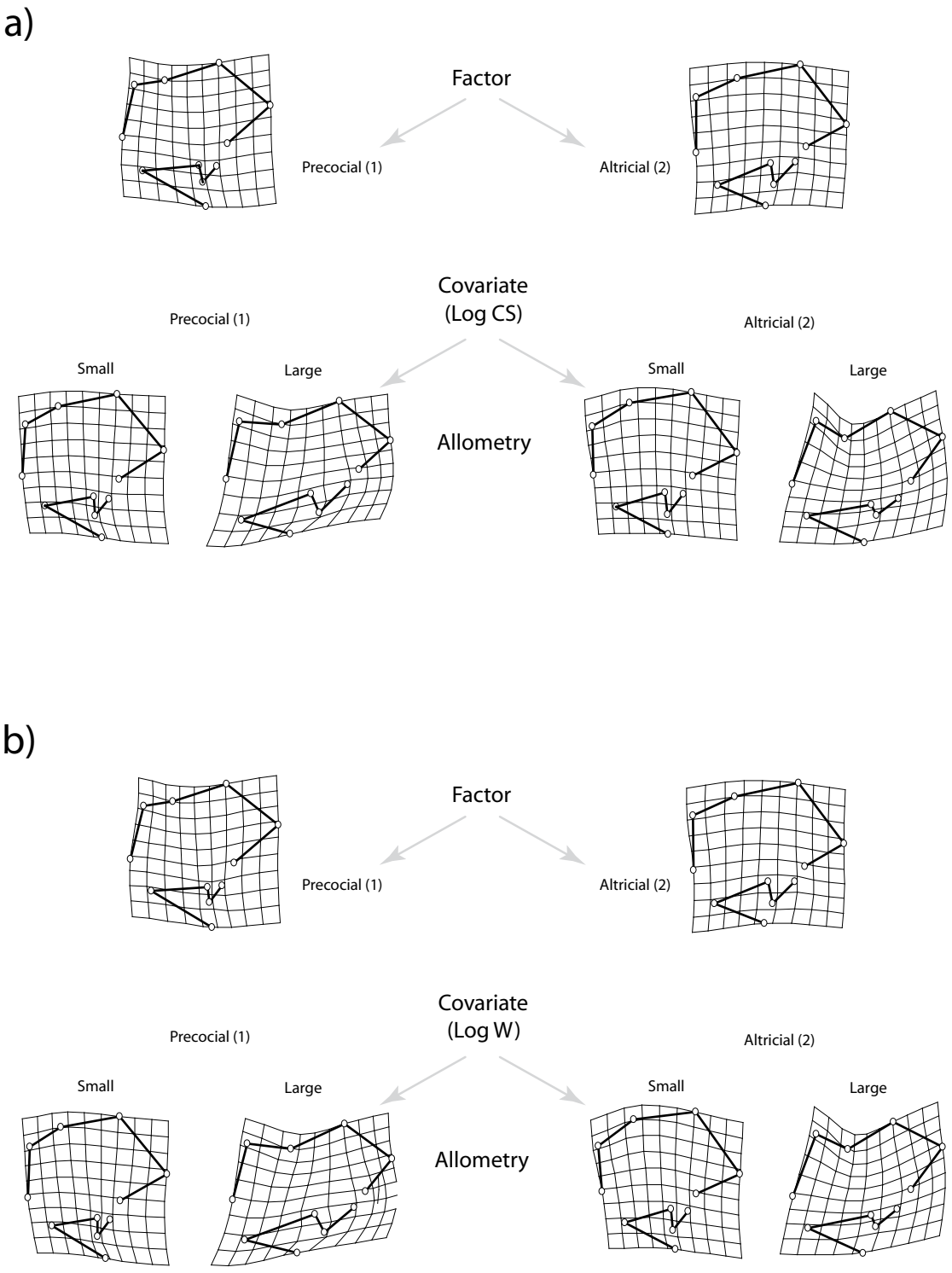

Figure 5. Results of Separates Slopes model shown with deformation grids for extreme size values (largest to always to the right and smallest to the left). Factor is the categorical variable (always set to split between altricials and precocials), equivalent to MANOVA results. a) Model tested for LogCS as a covariate, shape differences are not pronounced (changes in larger altricials is equivalent but slightly more marked). b) Model tested for LogW as a covariate, shape differences are equivalent between developmental modes and to what LogCS predicts. The hypothesis of separate slopes is rejected (they are parallel, only different in the intercept, see text).

Lanius are not extremes. All these are specimens stand for larger forebrain cavities (i.e. a larger telencephalon), flat (orthobasal) and shorter cranial bases (caused by a shorter caudal part), and more domelike calvaria. However, this braincase arrangement is notwithstanding shared with *Nytala* and *Otus* (Two Strigiformes) who are altricials type 1 and *Platalea* (a semialtricial).

Overall, precocials group better than altricials though semiprecocials are not so well clustered. Interestingly, Precocials type 1 cluster closely together but forms such as *Rhynchops (Tinamiformes), Vanellus* and *Limosa (Charadridae)*, and *Haematopus (Scolopacidae)* are outliers which fall out of the general precocial grouping sharing areas of convergent endocranial shapes with altricial birds. Precocial types 2 and 3, on the other hand, cluster quite well among them, though some may also converge with other precocial types. For instance, *Perdix*, *Gallus* and *Pavo*, are Galliformes (Phasianidae) of precocial type 2, and *Penelope* (a Galliform as well) clusters with them even though it is a precocial type 3.

Extreme altricial configurations are not all expressed true altricials, but there is a mix of type 1, 2, and semialtricials. At the same time, precocial extremes are not all true precocials, but have different types of precociality. There seems to be a preferential configuration among basal precocials forms within Neognathae, which is found in Galloanseres (e.g. chicken or ducks) and coincides with airobasal cranial bases and all shape differences that split this configuration from the others (e.g. less spherical braincase, etc.), despite this configuration is also attained by some derived Neoaves taxa (e.g. *Fulica*). Galloanseres with different developmental (precocial) types share equivalent braincase shapes (e.g. *Gallus* and *Penelope*). On the contrary, all extreme shapes of altricials have braincase configurations that belong solely to Neoaves within what was classically so-called the Neognathae birds (which should correspond with Galloanseres and Neoaves).

5.3.3 Evolutionary shape allometry between developmental modes

Two Separate Slopes analyses are performed, one testing the covariation with cranial centroid size (logCS) and the other with body mass (logW) with the whole set of braincase shape variables. As the MANOVA showed before, there are differences between the means of each group (altricial or precocial), yet analyses show now that cranial shape variation as a function of size (allometry) accounts for equivalent shape changes regardless the measurement of size used (logCS or logW; Fig. 5).

More importantly, however, any of these shape changes that covary with size and the altricial and precocial categories are almost visually identical (perhaps changes that covary with logW are slightly more pronounced). In effect, allometric shape changes for logCS between developmental types are not different (i.e. not statistically significant) and thus the hypothesis of separate slopes is rejected (Wilks λ=0.6344, Chi-squared 1.065, df1 18 df2 50.0; *P*=0.0965, *P*>0.01). The same occurs with logW, for which the hypothesis of separate slopes is rejected more clearly (Wilks λ=0.7227, Chi-squared 1.065, df1 18 df2 50.0; *P*=0.4114, *P*>0.01).

Since the hypothesis of different slopes between developmental modes is rejected, we proceeded to test for the homogeneity of the intercept values. The tests shows that intercepts for both logCS and logW are statistically different (respectively, for log CS, Wilks λ=0.3470, Chi-squared 5.330, df1 18 df2 51; P<<0.01, and for log W, Wilks λ=0.3651, Chi-squared 4.926, df1 18 df2 51.0; P<<0.01). Thus, the statistics suggest that precocials and altricials show equivalent evolutionary allometric tendencies, but may differ in their onsets.

Shape changes that covary with size do not differ between developmental modes and are therefore equivalent to the ones previously reported (see Chapter 4). Size does not affect cranial base architecture (ortho- or airobasality, although perhaps slightly in altricials), yet it does relate with the proportional length of the whole cranial base via changes in the proportion of its caudal part (the basioccipital); it is proportionally shorter for smaller sizes and longer for larger sizes. Allometric trends allocate changes in the relative orientation of the foramen magnum, yet relate more markedly with the relative roundness of the whole braincase. In larger birds the tendency is for a less roundness of the braincase (the calvarium is less domelike), which is visible in that the cerebellar and the forebrain cavities are separate and clearly distinguishable. Smaller birds, on the contrary, associate with more rounded braincases in which the forebrain and cerebellar cavities are less patent, and their cranial bases will be shorter due to the relate shrinkage of the caudal cranial base.

5.4 Discussion

Several studies have recursively recorded that the evolution of ontogenetic strategies associates with brain phenotypic evolution (Portmann, 1947a, b; Starck and Ricklefs, 1998; Bennet and Harvey, 1985a, b; Iwaniuk and Nelson, 2003). In particular, it is the acquisition of an altricial strategy what seems to precede the evolutionary phenomenon of relatively enlarged central nervous systems (CNS). We were therefore testing the null hypothesis that

altriciality could also associate with other aspects of CNS phenotypic evolution such as its morphological organization.

Our results agree with previous studies in that altricial birds tend to have proportionally larger CNSs (Fig 2a) though suggest, complementarily, that the evolution of ontogenetic strategies also possibly relates with the particular phenotypic organizations of the avian braincase (Fig. 2a and 3a), and by inference, with different organizations of the CNS.

Most avian braincase disparity stems from the boundaries between the chordal (mesodermic) and prechordal (cranial neural crest) modules into which it can be structurally subdivided (Chapter 4 and Fig. 1). These boundaries are at the cranial base and at the junction between the parietal and the supraoccipital bones. The disparity of the braincase in Neornithes emerges as a phenomenon in which the cranial base varies in its configuration between ortho- and airobasality, or in which the parietal and supraoccipital bones change in their

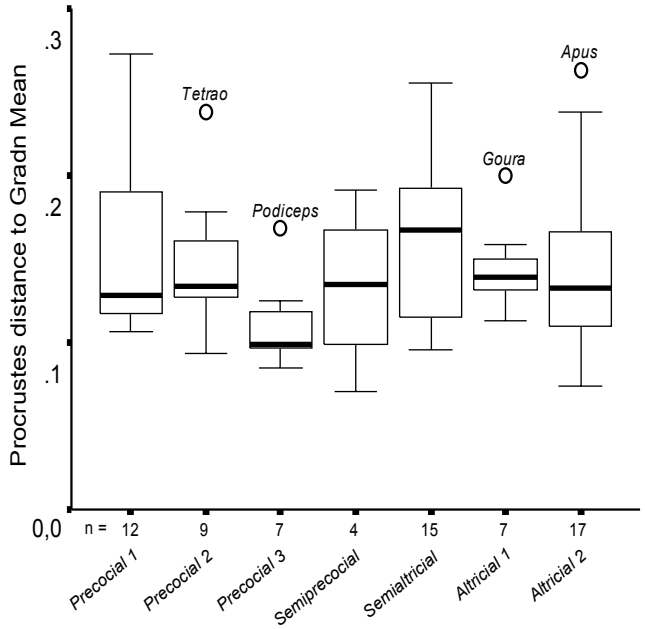

Figure 6. Box and whiskers for Procrustes distances between each individual to the consensus (the Grand Mean) grouped by developmental types (seven categories, see Table 1). Black line is he Median. Range of distance could be different if there weren't any outlier (not the case). For instance, Precocial 2 or 3 would span less distances in shape space, though likewise would occur with altricial 1 birds.

relative proportions and orientations (cf. Fig. 4, in Chapter 4).

Interestingly, disparity (i.e. Procrustes distance from each individual pertaining to each category to the Grand Mean, -the consensus, within shape space) is not markedly different in average between altricials and precocials (Fig. 6). Hence, altriciality may not favor the occupancy of larger distances or ranges of variation in shape space, but only the occupancy of different regions in it, which otherwise entail different morphological organizations of the braincase. Effectively, the only function of the CVA capable of discriminating between developmental types predicted that differences between altricials and precocials would stem

from shape changes in the chordal domain (Fig. 3a; e.g. basisphenoids, basioccipital, and supraoccipital bones), in such a way that most architectural differences associate with changes in the cranial base and bones at the occiput, in coordination with the relative enlargement of the forebrain though. On the contrary, however, differences between developmental types do not depend on changes in the parietal-supraoccipital boundary for differentiating between developmental types.

If endocranial shape differences are treated as a whole and are translated into differences in the outline of the central nervous system, we may also postulate that the association between developmental strategies is also related with CNS shape evolution. Particularly, altricial birds such as songbirds, some woodpeckers, some owls, or spoonbills will possibly be the only birds having shorter, ventrally flat, and more compact and spherical CNSs, in which the medullar axis will face more ventrally than caudally.

It is noteworthy that these altricial birds are all Neoaves (Van Tuinen, 2002), and the morphological organization of their braincases and the shape of their CNSs contrasts with that of more basal and precocial Galloanseres (e.g. the chicken; Fig. 5c), in which the forebrain is rather proportionally small, the base of the CNSs more convex (airobasal), and the medullar axis always points caudally. Altriciality is a derived developmental condition possibly of Neoaves birds (Starck, 1993), which would possibly suggest that the particularly spherical braincase and CNS organization (i.e. with concomitant shape changes associated) arose sometime in such node, not before, and in association with altriciality. However, any other configuration may be highly convergent, since there is an equivalent degree of overlapping of clades as well as there is a re-attainment of precociality in more derived birds (cf. Fig. 5). Thus, the scenario is as complex as the evolution of ontogenetic strategies is on its own.

Studies in mammals predict that a spherical endocranial cavity (and CNS) associates with proportionally large CNS relative to body mass (e.g. in humans; see Lieberman, 2000a). Altricial birds such as songbirds (*Parus*, *Cardinalis*; Fig. 5c) are quite cephalised in terms of their relative CNS size to body mass (Starck and Ricklefs, 1998) and show this spherical organization. Our results agree in that their forebrains and perhaps the cerebellum (both extrapolated from the relative extents of their cavities; cf. Fig 1, and see Fig. 3a and 4a, b), are quite enlarged relative to their ventral bases (i.e. their cranial bases are proportionally shorter relative to the calvarium; Fig. 3). However, the bivariate comparisons between logCS and logW show that these birds do not deviate markedly from their altricial average CNS to

body mass ratios, a stance that does not allow as asserting whehter this relative size of the CNS underlies the acquisition of a spherical configuration and shape changes associated (cf Fig. 2a). Moreover, parrots are also very cephalised organisms (Jarvis et al., 2005; Iwaniuk and Nelson, 2003), are altricial and they were present in the sample (*Amazona*), but did not concord with this extreme architectural situation for their braincase and CNS shapes, nor were clear outliers for the bivariate comparison of the size of their endocranium with respect to body mass (Fig. 2a).

One solid argument for explaining this situation is that the estimation of size for the endocranium may be underestimated since CS only captures its extent in the mid-sagittal plane. It is therefore possible that this particular organization of altricial braincases is associated with the expansion of the CNS laterally (i.e. their braincases are wider). We lack this data in our matrix, and therefore this question cannot be resolved. The absence of data on the lateral expansion of the endocranial cavity (hence, of the CNS) may be biasing the outcomes which may lead to resolve why some taxa have this peculiar CNS (and braincase) configuration. We shall leave this question open until further explorations investigate the morphological organization of the braincase in its full dimensionality (e.g. in three dimensions).

We have elsewhere shown that allometric associations of size to shape differences in the braincase make capturing differences among bird taxa more difficult to discern (see Chapter 4). Tests for different slopes have stressed, nevertheless, that regardless the developmental strategy (i.e. precocial or altricial) all shape changes occurring as a function of size are shared by all avians. These allometric associations are possibly contained within the discriminant function, and should be those predicted by multivariate regressions (e.g. see them comparing Fig. 3 with Fig. 5).

We lack neural soft-tissue, and therefore must commit to mainly interpret braincase differences. Traits related with size are those such as the vaulting of the calvarium, or the relative length of the cranial base via the relative proportion of the caudal cranial base. Perhaps, a slight change in the configuration of the cranial base may also be related with relative size, yet this may more properly be underlined by the relative enlargement of the forebrain cavity (the forebrain itself) which is, indeed, associated with size (notice as well that the anterior cranial base, the laterosphenoid bone, may not be ossified in many birds). Shape differences between developmental types captured by the first function of the CVA such as the pronounced cranial base ortho- or airobasality, caused by changes in the

supraoccipital or changes at the basisphenoid at the Sella and their structural relationship with the external cranial floor (elements of the chordal domain; Fig. 3) are possibly not fully related with size.

One question pending rests upon the finding that there are marked differences shifts in the allometric intercepts between altricial s and precocials. Avian embryonic development is direct, and it is constrained to a constancy of time patterns and a high similarity of structural development (Starck, 1993). Thus, all birds apparently follow the same developmental stage-schedule regardless their developmental strategy.

There are nonetheless three possibilities of shifts in the ontogenetic schedule (Starck and Ricklefs, 1998). The first is the classic view (Portmann, 1962) in which altricials and precocials progress through the same developmental stages but that altricial chicks hatch relatively earlier in the common trajectory. This possibility is not congruent with a shift in the intercepts. The second choice alludes to shifts in the slopes, whereby altricials and precocials would have different relationships between maturity and size throughout developmental period. This possibility is not congruent either with the outcomes of the general lineal models tested (Separate Slopes).

However, one the third possibility implying shape changes, like the latter, whereby developmental types would diverge in the relative duration of some developmental stage, being either more prolonged or retarded. This last option is what seems to occur between developmental types (Starck, 1993), and importantly, is the one that may relate with shifts in the intercept (see also; Gould, 1966, 1971, 1977).

Out of the 42 tabulated stages in Hamburger and Hamilton's (1951) developmental schedule the first 33 seem to be surprisingly constant (Starck, op. cit.). Thereof, differentiation begins (at 34) until stage 42, yet stage 39 is a moment when most conspicuous divergences clearly arise (Starck, 1993). Stage 39 is crucial because it is a moment of embryonic growth and tissue differentiation towards functional differentiation (i.e. its performing shape). Altricials, or at least some of them, may tend to show a more brief stage 39 whereas in some precocials this stage becomes extremely prolonged (e.g. ducks). A more brief stage translates in that neonates will be more immature at hatchling (in some altricials and in varied degrees though), which may be what is statistically seized by shifts on the intercept.

Additionally, braincase and CNS morphological differences and their integration must take place throughout development, yet literature on this issue is very scarce. Lang (1952) has been among the only ones to explore the events of morphological change in the early genesis

of the cranium of a parrot, a pigeon and a chicken. In her observations the author highlighted that changes in the configuration of the cranial base take place in a precise morphogenetic sequence, from more flat (orthobasal) to more convex (airobasal), despite she made no allusion to other elements of the chordal domain (e.g. of the occiput). In her view, all bird embryos start with more flat (orthobasal) cranial bases, and changes therein are apparently quite substantial towards airobasality ('dramatic' in her own words). Seemingly, these occur in very early stages of development, and in association with the CNS (i.e. the large eyes). Unfortunately, the author did not provide a concise definition of time. Observing the original drawings provided it is quite likely that stages were at least around 33 to 39, or later, since there is already much tissue differentiation.

While allometric phenomena tell us very little about shape differences in the braincase between altricials and precocials, statistics verify that differences possibly associate with shifts in the intercept, hence there is an open possibility (in the light of the results the developmental information available) in which to propose that differences in braincase organization in association with the evolution of developmental strategies might stem from time-shifts in stages of tissue growth and differentiation (e.g. 39 or above).

Under this hypothesis, the cranial base may follow the schedule proposed by Lang (1952), and the shorter the time of the 39 developmental stage, the less convex (i.e. the more orthobasal) the cranial base may remain as a phenotypic outcome in the hatchling and, later, in the adult. Furthermore, the cranial base is an area which may grow little after hatchling (Hallgríssom et al., 2007). The CVA suggests that some birds, despite being precocials, might have delayed any of these late developmental stages too (e.g. *Rhynchotus*, *Vanellus*, or *Limosa*), yet it would only be altricials (of different types though), which delay it most.

Despite the rationale is congruent with the available data sources, all inferences are based upon phenomenological outcomes since we are dealing with phenotypic variation across adult stages at a macroevolutionary scale. It would thus be critical to plan a study considering a closely-equivalent taxonomic scale while analyzing pre- and post-hatchling growth-shape trajectories for unraveling the likelihood of the hypothesis. Furthermore, shape changes are detectable morphometrically, yet it would be timely to begin working with refined developmental techniques with which it is becoming possible to understand the epigenetic basis of morphological change as a matter of the evolution of morphogenetic pathways.

It is reasonably possible that neurogenetic and skeletogenetic pathways are inter-linked. Recent morphometric explorations have shown that the evolution of the avian CNS may

be modular (Iwaniuk et al., 2004), just as it seems to be the case for the braincase (Chapter 4). A large body of research in developmental biology is embarked in understanding the mechanics of neural and bone development. The question pending is whether CNS modular patterns of evolutionary change agree with the modular organization of the braincase (i.e. the division into chordal and prechordal parts). That is, whether the modular organization of CNS modules correspond with the recently so-called "cerebrotypes" (Iwaniuk and Hurd, 2005), and if these are related with the organization of braincase modules developmentally. Furthermore, it would be appealing to test if these associations have some functional meaning. For instance, some hypotheses have stated that the spherical shape of the CNS in humans might be advantageous since it possibly aids minimizing distances between neural centers (see discussion in; Ross et al., 2004). The spherical morphological organization in some altricial birds is a fact, yet it is not so clear whether this may be a functional advantage, or rather, if it is just the result of inherent developmental or structural constraints.

3.6 Morphological integration between the avian central nervous system and the braincase

6.1 Introduction

This study is the last of a series in the thesis in which our general scope has been to gain some insights on the phenotypic evolution of the braincase in birds at a macroevolutionary scale. The present investigation has been specifically designed for exploring whether there is a particular pattern of morphological integration between the central nervous system (CNS) and the architectural organization of the braincase.

In principle, braincase and CNS phenotypic evolution are intimately linked (Van der Klaauw, 1948; Moss and Young, 1960; Dullemeijer, 1974), and the wide array of different phenotypic organizations of both systems is the result of complex epigenetic phenomena that take place in early ontogeny (see Moss 1997d, and Hallgríssom et al., 2007). Our bases are not developmental but comparative among adult birds, hence we are only exploring for inter-specific morphological differences. However, these differences are ultimately the by-product of the evolution developmental programs and their epigenetic pathways (Wadington, 1975; Wilkins, 2001). Thus capturing patterns of morphological organization comparatively at a macroevolutionary scale might serve as keys for pointing to the existence of such hidden factors.

Processes of phenotypic evolution and patterns of morphological integration, (i.e. patterns of associated variation between parts; Klingenberg, 2004) are usually elucidated using morphometric procedures (Olson and Miller, 1958; Roth and Mercer, 2000; Klingenberg, 2002). In effect, the morphometric characterization of CNS phenotypic evolution dates back as early as to the studies of Cuvier (*fide* Portmann, 1968) and has been a very fruitful area of research ever since. The parameters used are either masses or volumes, and the biological principle applied is allometric, whereby the term encephalisation denotes an index which compares the mass ratios between the CNS and the body (i.e. CNS scaling).

The classic rationale is that the only neurological character for which a correlation with behavioural capacity (in different animals) is supported by evidence is the total mass of tissue, the index of cephalisation, which seems to represent the amount of brain tissue in excess of that required for transmitting impulses to and from integrative centres (Lashley, 1949). Jerison (1973) extended our contemporary view in which brain size is seen as a natural biological parameter that can be statistically used to estimate other anatomical features of the brain, and that the mass of a neural tissue controlling a particular function is appropriate to the amount of information processing involved in performing its function (i.e. the so-called principle of *proper mass*).

Other approaches have focused on the processes which might underlie this allometric evolution of the CNS, formulating it as a function of the different developmental strategies that birds display at high taxonomic scales (the altricial-precocial spectrum; see e.g. Portmann, 1947a, b; Bennett and Harvey, 1985a, b; Starck and Ricklefs, 1998; Iwaniuk and Nelson, 2003). Overall, conclusions are that the precocial strategy may possibly be basal in birds and that the altricial strategy apparently relates with the acquisition of proportionally larger CNSs.

Investigations on the integration of the avian CNS have forecasted more complex statistical models in which some parts of the CNS appear to evolve more associated than others (i.e. some parts may be more integrated), whereas others may change more autonomously from the rest of the system. Among the phenotypically related parts for which relative sizes change concomitantly would be the mesencephalon and optic lobes, and the myelencepahlon with the cerebellum, whereas in the telencephalon of particular taxonomic cases (e.g. parrots) seems to show patterns of evolutionary change that are relatively autonomous from the rest of the system. The explanation for their integration has been their adjacency and close neural connectivity, and these patterns were advocated as evidences for a "mosaic" evolution of the CNS (Iwaniuk et al., 2004). If there is integration but some parts are more relatively autonomous from the rest, this notion of "mosaic" evolution seems more plausibly a hypothesis of modular evolution (see e.g. Klingenberg, 2004, and Chapter 5).

Studying the outline of the CNS from its imprint in the endocranial cavity on the basis of geometric morphometric procedures we were able to show its phenotypic organization (its outer shape) and how it varies among avian taxa. On these same bases we have also suggested that developmental strategies (i.e. the altricial-precocial spectrum) may not only be associated with the evolution of its phenotypic size-shifts, but also with its architectural configurations. For instance, the altricial strategy in particular cases might relate with more spherical CNSs in with a more ventrally oriented medullar axis and in which the ventral side is rather plane, such as in the case of songbirds.

However, in such studies we lacked CNS soft-tissue data; hence we could only forecast aspects of the organization of the bone surrounding the CNS (the braincase). For instance, we suggested that its phenotypic organization was possibly modular (Marugán-Lobón and Buscalioni, 2006, Chapter 4, and Chapter 5 in this volume).

This latter observation entails that despite the braincase is morphologically integrated and none of its parts may be completely autonomous from each other, some of elements of

delineable parts may counter jointly to evolutionary change (e.g. the bones of the mesodermic chordal part such as those of the occiput, and the basisphenoids), whilst others may possibly be more autonomous in their evolutionary variation, thereby acting more like to modular units (e.g. the chordal vs. the prechordal parts with different origins; i.e. the prechordal is of neural crest).

The question left pending was whether the neural counterparts of the CNS to the chordal and prechordal bone complexes (i.e. the parts of the CNS housed in each region of the braincase such as the brainstem or the forebrain) behaved likewise. In effect, it is reasonable to expect that given the tight relationship between both systems, if one part of the braincase may be considered a module, its neural counterpart (housed therein) will behave concomitantly. In effect, parts of the CNS which associate with the chordal part of the braincase (e.g. mesencephalon, myelencephalon, optic lobes or cerebellum) are apparently more integrated between them than with parts that relate with the prechordal domain (e.g. the forebrain; see Iwaniuk et al., 2004). If this is the case, do integrated phenotypic changes of the CNS result in particular organizations of the braincase?

We will be exploring this query using General Procrustes procedures (GPA) and its associated multivariate statistics, and challenge the hypothesis that the organizations of the CNS and braincase are morphologically integrated. The analyses will be based on the statistical-geometric technique of Two-block Partial Least Squares, which enables testing for the statistical covariation between two separate and distinct sets of quantitative variables (Rohlf and Corti, 2000), in our case-study, one for the CNS and one for the braincase.

In order to perform the analyses separate data-sets for the CNS and the braincase are needed, and it would be preferable to rely on a landmark configuration that captures salient features of the geometry of the central nervous system, and test this set of shape variables against its equivalent ones for the braincase. However, obtaining landmark data from the avian brain is difficult and a costly endeavour, moreover if dealing with a high taxonomic sample. The nature of this metric experiment is preliminary, and consequently, we have preferred to perform the study relying on data from literature (see; Marugán-Lobón and Buscalioni, 2006, Chapter 2 in the Third Part of the volume).

We selected one data-set consisting on series of indexes that denote the proportional weight of each major part of the brain to body weight (indexes of encephalisation) because they were directly measured from neural tissue (Portmann, 1947a, b; see also Bennett and Harvey, 1985a, b), and because we could match them with one of our previously studied

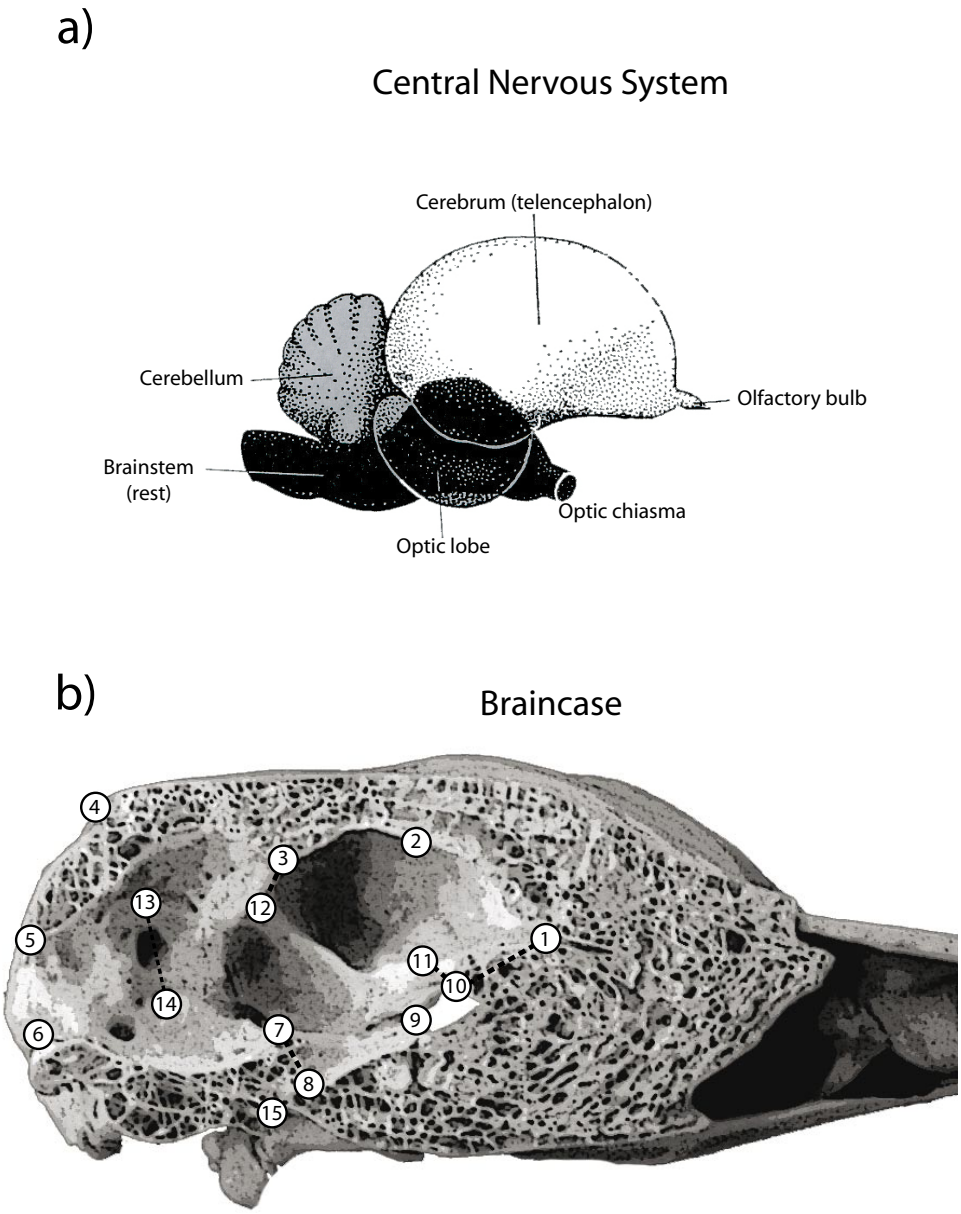

Figure 1. a) General scheme of the avian central nervous system with major parts labelled (after Portman, 1947a). b) Digitally treated picture of the braincase of a chicken with landmark configuration used in the analysis.

samples. In these classic papers by Portmann the measured CNSs are from different taxa (the sample was inter-specific), and the parts of the CNS that were measured represent the relative weight of the optic lobes, the cerebellum and the forebrain (telencephalon), and the so-called brainstem "rest", which is a part smaller than the brainstem that comprises the diencephalon, tegmentum and medullary bulb (Fig. 9.1a). The brainstem rest is commonly accepted by neurologists because it is a part that can be dissected more easily.

In the 2BPLS statistic-geometric model the ratios of the parts of the CNS to body mass measured by Portmann will represent one block of quantitative variables, thus representing CNS phenotypic variation among birds. For the other, a series of p=15 landmarks were

digitized onto the mid-sagittal plane of the braincase in a different collection of specimens, matching though the same species displayed in Portmann's data. The shape variables obtained after GPA will represent the block of data denoting avian braincase shape evolutionary changes (Fig. 9.1b).

The technique is intended to search for and show whether, and in what amount, these two sets of independent measurements may covary statistically between them. The 2BPLS is a multivariate technique and will treat the ratios of parts of the CNS analytically all at once, as it will do with the shape variables. Which ratios or landmarks are more or less correlated within each block will be detected by the analyses (e.g. which of the CNS are more or less correlated within their block, as well as which landmarks are more or less correlated within their block). However, the analysis will try to find which of these intra-block correlation vectors may covary most between blocks, and order them in declining amounts of explained covariance (i.e. from larger to lower), just equivalently as a common PCA does with explained variance. This statistical ordering of covariance is what will be translated as patterns of associated morphological variation between the parts of the braincase and the CNS.

The hypotheses may be straightforward if only asking whether there is or there is not a pattern of covariation between both systems. However, the model becomes more complex since it covers several underlying assumptions. The null hypothesis thus carries with it that there will be a particular pattern of covariation between brain parts such as those proposed by Iwaniuk et al. (2004), whereby the telencephalon should be more autonomous that the rest of the CNS, at least in particular taxonomic instances (and these cases should likewise be altricial). This associates as well with our hypothesis of modularity of the braincase in which the chordal and prechordal parts of the braincase are possibly relatively autonomous in their evolutionary shape changes.

Particularly, we are interested in testing whether test show if the measured parts of the CNS (the brainstem rest, the cerebellum and optic lobes) relate to shape changes in the chordal domain, whereas the forebrain relates more to changes in its bone counter-cavity, which belongs to the prechordal part of the braincase. It is also noteworthy that the analysis will provide, for the first time, a visualization of the shape changes in the braincase (of the endocranial cavity, hence of the outline of the CNS), that associate with the familiar brain sizes and proportions so extended through literature.

We aim to shed a glimpse on if, and how, morphological integration may associate to and/or condition avian phenotypic macroevolution. One eventual motto of this piece of work is to

try to foresee if in the light of the results there is enough evidence upon which to conceptually set forth a functional hypothesis that intertwines the morphological organization of the CNS with its counter organization of the braincase.

6.2 Materials and Methods

We selected *N*=37 specimens from Portmann's (1947a, b) data which we could match with our available individuals from the Hess Collection (see Appendix 2 and BOX 5). Portmann was among the first ones to realize that no constant relationship could be found between brain weight and body weight among birds (*contra* Dubois, 1897, *fide* Portman, 1968). In view of these allometric differences among taxa he used the brainstem "rest" as standard. This structure is rather smaller than the common brainstem, and stands form the diencephalon, tegmentum and medullary bulb (shown in black in Fig. 9.1a). However, its values are non-constant (can vary between 1 and 2.7 in birds of the same weight; see also Pearson, 1972). Galliformes were found to be the order having the lowest values, and from them Portmann (op. cit.) set as a basic unit of comparison (brainstem rest weight called the "basal cipher") in a gallinaceous bird of a given body weight (a given body weight that better approximated the weight of the species that were going to be compared each time). The weight of each brain part was measured after dissecting them. Portmann also facilitated a measurement of body weight in order to test the allometry of the brain. We collected as series of more modern body masses from literature (Dunning, 1993) and regressed them to Portmann's data in order to gain an overall idea of the accuracy of the measurements since no source of measuring error was provided (graph not shown). While brain variables were standardized to the brainstem rest, we re-standardized them in order to assure they were all in the same equivalent units when performing the analysis (see Rohlf and Corti, 2000).

The second block of variables consists of shape data (Partial Warp scores and the uniform component), which does not need to be standardized since this procedure is already performed in their calculations. Landmarks are p=15 and their anatomical meaning is listed in Table 1. Additional coordinates to the ones previously used are LM 14 and 15, capturing the inner ear (dorso-ventral extent of the semicircular canals), and LM 12 and 13 which approximate the extent along the crest that defines the boundary between the anterior and middle fossae (where the forebrain and optic lobes rest respectively). These are now included because they can be digitized in all specimens, and may be more informative in combination with metric data on brain ratios. We also followed the colour coding of Chapter 4 to denote

Number	*Description*
1	Foramen of olfactory nerve (fossa bulbi; N. I)
2	Mid-point between LM 1 and 3 at ventral edge of frontal bone
3	Ventral edge of endocranial crest separating cerebellar and forebrain cavities
4	External junction between supraoccipital and parietal at occipital crest
5	Dorsal rim of foramen magnum
6	Ventral rim of foramen magnum, anterior to occipital condile
7	Dorsal-most point of Sella Turcica (dorsal tip of basi-postsphenoid)
8	Ventral-most point of fossa hypophisiaria
9	Ventral edge of optic foramen (N. II)
10	Dorsal edge of optic foramen (N. II)
11	Point of convergence of laterosphenoid, fossa cranii rostralis and fossa cranii media
12	Point of contact between fossa tecti mesencephali, fossa cerebri and fossa cerebelli
13	Dorsal-most point of dorsal semicurcular canal
14	Fossa acustica interna
15	Fossa timpanica t rostrum parasphenoidale

Table 1. Landmarks and their anatomical description

the different locations of the chordal and prechordal parts of the braincase; see Fig. 2).

Two-block Partial Least squares procedures are detailed in Rohlf and Corti (2000). Tests of significance are set by 999 permutations, all of which was performed using TPSpls (v1.14; Rohlf, 2005). For a detailed reading of the way of interpreting the graphs please refer to Chapter 2 (Marugán-Lobón and Buscalioni, 2006) in this same part of the volume.

6.3 Results

In the 2BPLS block 1 was set for the weight ratios to body mass of the brainstem rest, the optic lobules, the cerebellum and the forebrain and their variation is depicted in bar graphs in this same order (see Fig. 2a), and shape variation associated with their variation is denoted by the second block using deformation grids based on the TPS.

The first singular value captures an amount of covariance of 0.7344 which is high considering that it represents a 73.4473% of the total explained covariance. However, the count and percent of squared singular value iterations is quite high (46% at 999 permutations) implying that it is improbable that all covariation is contended within this unique dimension. The correlation between the pair of vectors of this first singular value is r=0.6278 and is not perfectly statistically significant but very close (count percent=1.10% at 999 iterations). The second dimension captures a covariance of 0.2055 (20.5539%, both first and second singular values accumulate a total of 94%), and the count and percent of squared singular value iterations is again relatively high (34%), meaning that the remainder covariance is still contended within subsequent dimensions. The correlation between pairs of vectors of the second singular value is r=0.6532 and is statistically significant (P<0.01; count percent after 999 iterations is 0.50%).

We proceed to describe the first two singular values because most covariance is accumulated

between them, yet bearing in mind that there is still covariance contained within subsequent dimensions. In the first dimension of covariation all CNS ratios correlate with the block of shape variables with the same sign (all bars change in the same direction from the horizontal line, which represents the mean), yet correlate with the function in different magnitudes. The variable that correlates most is the weight ratio of the optic lobules which is followed by the cerebral trunk, then the cerebellum and afterwards the forebrain. These relative correlation magnitudes within the block of ratios mean that for positive scores all ratios are larger than in negative scores, where conversely, they are smaller. Thus, for positive scores, the CNS is overall proportionally larger, whereas for negative scores, it is proportionally smaller. When the CNS is larger (positive scores) the parts that are larger in a large CNS within this singular value are the brainstem rest, the cerebellum and the optic lobes (these latter being the proportionally largest), and the forebrain is relatively smaller, whereas conversely, when the whole CNS is smaller the parts of the brainstem are relatively smaller than the forebrain.

A proportionally larger CNS covaries with a concave and homogeneous bending of the grid (referenced ventrally to cranial shape) which translates in that the shape of the braincase is more spherical, shows a more flat cranial base (orthocranial) and a pronounced ventral orientation of the foramen magnum (see landmarks in Fig. 9.1 and top of Fig. 9.2 for reference). The caudal cranial base (basioccipital bone and bones of at the Sella Turcica and the pituitary fossa) is proportionally smaller in contrast to the remainder parts of the endocranial cavity, and the forebrain cavity seems slightly larger. In effect, it appears that most shape changes are associate to bones of the chordal domain (in blue and green in the figure).

The reading for negative scores is reciprocal, thus a proportionally smaller CNS coincides with a convex bending of the whole grid, the braincase is not spherical, the cranial base is clearly convex (i.e. airobasal) and the foramen magnum is oriented caudally. The caudal cranial base including the pituitary fossa is much larger in contrast to the remainder elements of the cranium and is more horizontally oriented, while the forebrain cavity is slightly smaller

Some altricial birds are extreme cases for positive scores in the distribution of points for the scores between the vectors of the first singular value; a passeriform (*Pica*), three Falconiformes (*Buteo*, *Falco* and *Accipiter*), which are followed by a crow (*Corvus*, Paseriformes), an owl (*Asio*, Strigiformes) and a parrot (*Amazona*, Psittaciformes). Some precocials are the extreme cases for negative scores; a swan (*Cygnus*, Anseriformes), a flamingo (*Phoenicopterus*, Ciconiformes), a grebe (*Podiceps*), and several Galliformes such as *Tetrao*, *Pavo*, *Perdix*,

a)

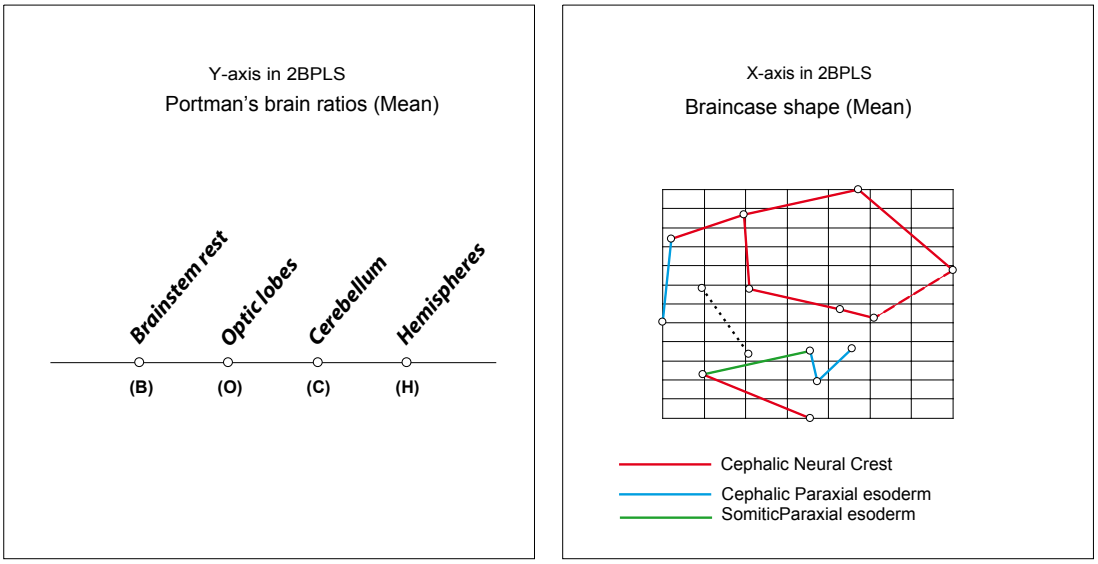

b)

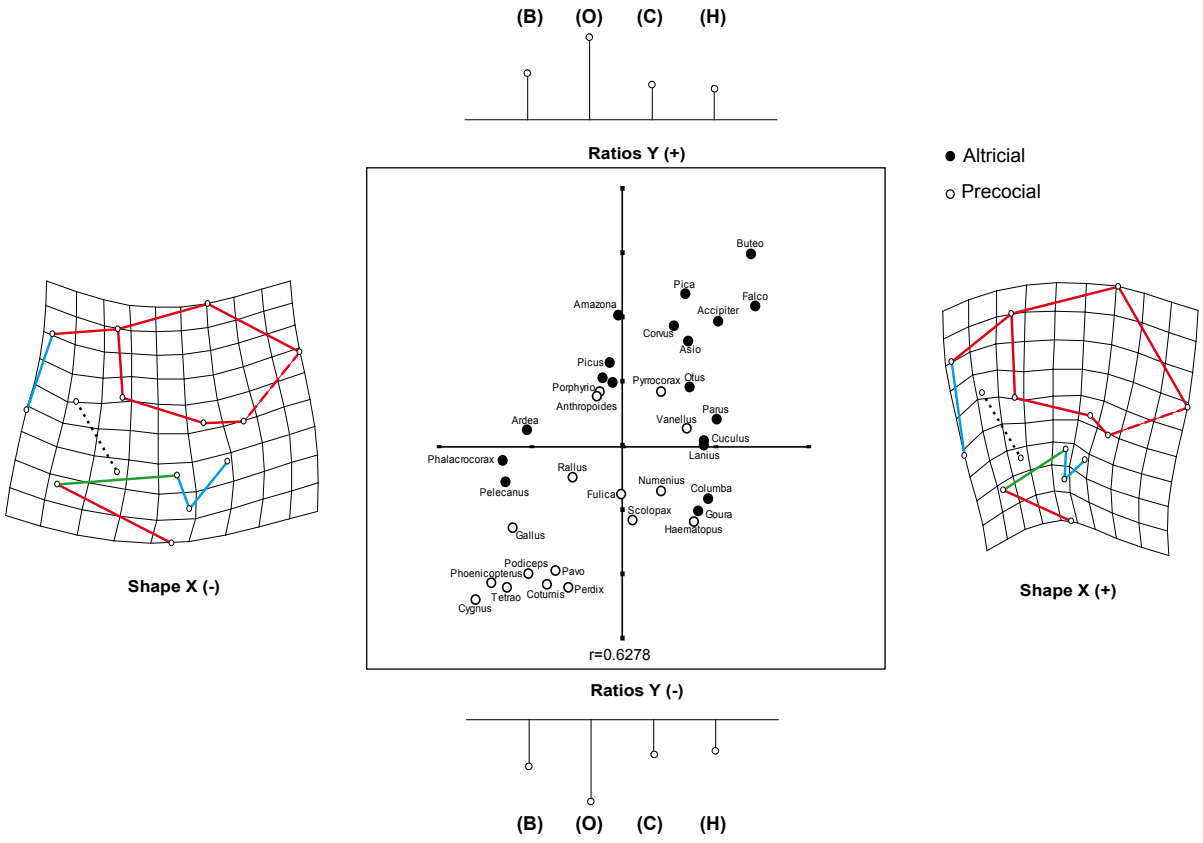

Coturnis and *Gallus*. However, most of the scatter is populated indifferently by birds of any developmental type.

In the second singular value, the vector of ratios shows that most of them correlate with the same sign in the tendency except from the optic lobules which correlate with opposite sign (the bar points to the opposite side of the horizontal bar). The dominant variable (larger correlation) is the ratio of the forebrain which is closely followed in magnitude by

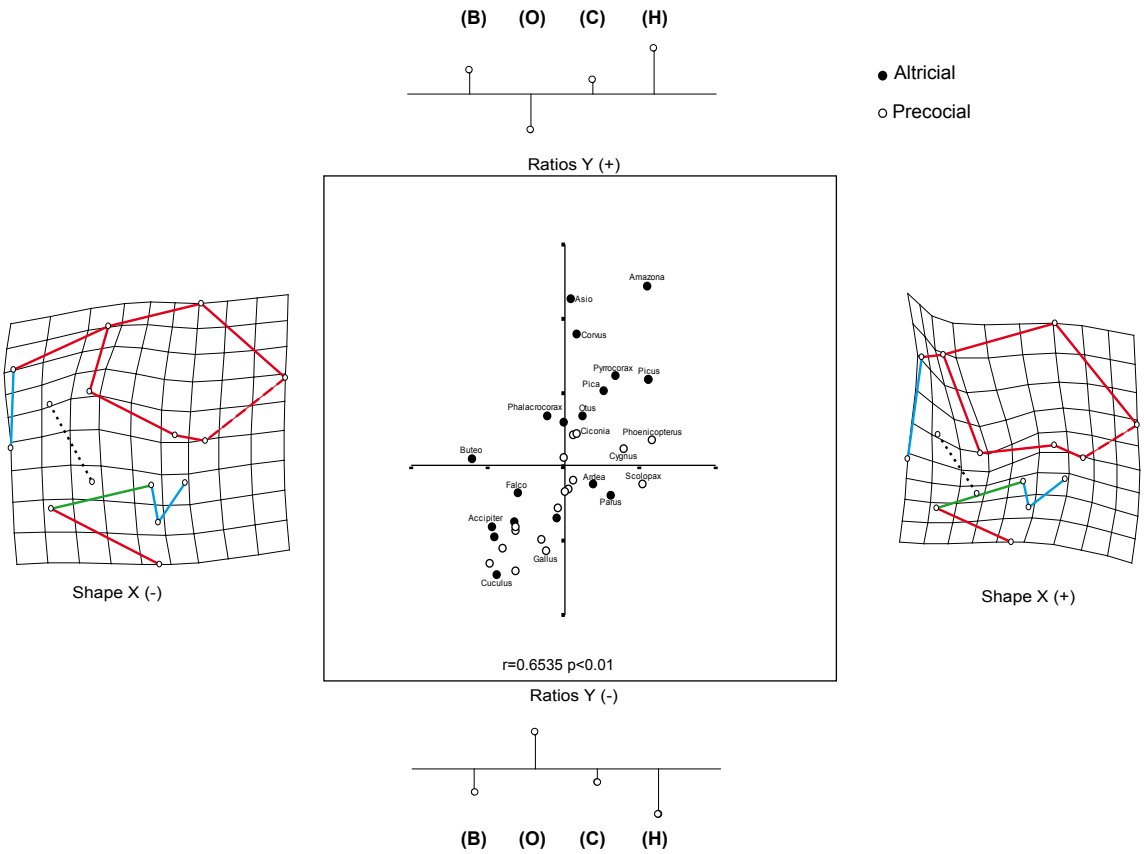

Figure 2. a) Mean values for Portman rations (left) with labels in bar scheme, and average landmark configuration (right). Colour labels follow the distintion of bone origins after Couly et al., (1993). b) First singular value (statistical relationship between paired vectors, one of each block). X-axis is braincase shape with deformation grid, and Y-axis is CNS ratios with bars. c) Second singular value ordered equally as before. See text for correlation values and statistical significance.

the optic lobes but with different sign. Thus, when the forebrain is proportionally larger (positive scores), the brainstem rest and the cerebellum are also relatively larger (yet in lower magnitude), and the optic lobes proportionally smaller. Conversely, when the forebrain is proportionally smaller (negative scores) the cerebral trunk and the cerebellum are smaller and the optic lobes are relatively larger.

In this second dimension proportions of CNS parts correlate with localized deformations around the parietal bone (the region of the cerebellar cavity) and at the forebrain cavity, the latter which seems overall larger in positive scores and smaller in negative ones. The relative expansion of the forebrain cavity is easily seen, and associates to the deformation of the spline in the region of the middle fossa, which seems to displace more ventrally when forebrain cavity becomes larger. When the forebrain cavity is markedly smaller the middle fossa enlarges and the boundary between them displaces dorsally. It is also noteworthy that while the configuration of the cranial base may change it is only slightly, and does not

associate with any change in the orientation of the foramen magnum. It could also be said that the braincase is either more (negative scores) or less (positive) spherical, yet only by the extension seen on the area of the parietal bone, and not on the overall configuration of the braincase.

Extremes for positive scores are again some altricial birds, particularly the parrot, the owl, the passerines crow and cuckoo (*Picus*, Cuculiformes), a cormorant and a stork, yet not others such as *Buteo*, *Falco* and *Accipiter*, as in the first dimension of covariation. Behind this boundary there is a great degree of taxonomic and developmental type overlapping, thus precocials are not extremes for smaller forebrain sizes.

In summary, results stress that it is the proportional size of the whole CNS which is associated with more pronounced changes in the architecture of the braincase. However, in birds with larger CNSs it seems to be the relative larger size the optic lobes, brainstem rest and the cerebellum and not the relative size of the forebrain which associate more with changes in the configuration of the relative orientation of the foramen magnum, all of which affect the configuration of the bones in the chordal part of the braincase. This latter remark stresses that it is the occipital bones and the sphenoids at the Sella and the Pituitary Fossa which are the implicitly associated to the orientation of the foramen magnum and the spherical appearance of the braincase.

6.4 Discussion

Portmann's life-work was influenced by the classic works of Cuvier, and later of Dubois and Lapique (see Portman, 1968). His studies (and later with his collaborators) were at the vanguard of neurological and brain research in the middle of the Twentieth century, and the main body of his research aimed to stress how had the functional organization of the CNS evolved, and how ontogenetic evolution (the precocial-altricial spectrum) could wield its phenotypic evolution.

Among his major contributions, Portmann stressed that the CNS does not evolve changing solely as a whole but, conversely, that some of its parts may evolve proportionally dissociated. Mass was a measurement thought to be directly associated to neural "complexity" for him, thereby assigning parameters which were amenable for comparing and addressing for structural and functional differences between avian taxa. This rationale is still remains in the wealth of contemporary neurological research (see e.g. Jerison, 1973; Pearson, 1972; Iwaniuk and Nelson, 2003; Iwaniuk and Hurd, 2005). As well, the hint that overall larger

CNSs takes place in particular altricial species lead Portmann to formulate that the altricial strategy must precede the acquisition of more developed CNSs, and particularly, of larger brains with larger forebrains (see also; Bennet and Harvey, 1985a, b; Starck and Ricklefs, 1999; Iwaniuk and Nelson, 2003).

Overall, our multivariate statistics corroborate these previously reported findings while rendering, at the same time, some new observations in regard to the challenged hypothesis of CNS and braincase morphological integration. On the one hand, the 2BPLS reveals that there are considerable differences between overall proportional sizes of the CNS between bird taxa, and that these are pronounced between certain altricials and precocial birds. Likewise, the analysis underscores that parts of the caudal CNS are possibly more integrated between them than with the relative size of the forebrain, the latter whose proportional size might sometimes be dissociated from the rest, at least in certain birds. At the same time, the optic lobes and the forebrain may be coordinated despite following different directions of change (i.e. when one is proportionally larger, the other is smaller and *vice versa*).

For instance, the cormorant (*Phalacrocorax*) is closer to negative scores in Fig. 2b (first singular value) whereas it rises its values towards positive ones for the second singular value (Fig. 2c). Thus, this bird has an intermediate CNS proportional size with proportionally smaller caudal parts, yet it has a proportionally enlarged forebrain (and smaller optic lobes, which is congruent with the first dimension). Interestingly, something equivalent occurs for instance with the parrot, a bird with lower score values in the first dimension, but the largest for the second (there are other birds in which this occurs such as some Falconiformes; *cf.* Figs., 2b and c). Passers remain having high values for both singular values hence possibly having the largest CNSs.

Our particular endeavour was notwithstanding to test whether there is any particular association between the phenotypic differences of the CNS (in terms of relative size of its parts) and the architectural arrangements of the braincase. In effect, the proportional changes of the CNS we have just talked about in the lines above associate with particular braincase architectural arrangements. This occurs in such a way that larger CNSs fit within more spherical (and perhaps more compact) braincases, in which the foramen magnum points more ventrally and the cranial base being more flat (orthobasal, sensu Moss and Vilmann, 1978). Thus, the null hypothesis cannot be rejected, which suggests that there is a particular pattern of morphological integration between the CNS and the braincase. However, there are many dimensions into which this pattern of integration spreads.

This phenotypic association between the CNS and the braincase within which it is housed might have been predictable in the sense that proportionally larger CNSs would relate with relatively shorter cranial bases (Gould, 1977). Apparently, this has been observed in primates (see e.g. Lieberman et al., 2000a, b), yet in this organisms it seems to affect as well the topology of the cranial base (for instance, becoming more klynobasal, as in the case of humans; please see Chapter 4 for the terminology), via the enlargement of the forebrain. While in birds the sphericity of the avian braincase associates with larger CNSs, and relates with extension of the cranial base and with its topology, this does not associate with the expansion of forebrain. Instead, the relative spherical appearance of the braincase and its associated shape changes is specially related with the proportional size of the caudal parts of large CNSs. One case example can be the parrots, birds which are often considered very encephalised birds (Jarvis et al., 2005), they have proportionally large forebrains (Iwaniuk and Nelson, 2002, 2003) yet they do not show spherical braincases.

Birds showing this particular spherical braincase phenotypic trait must apparently have large CNSs with their caudal parts relatively enlarged, such as falcons, and they might also have large forebrains, such as it is the case of songbirds. Interestingly these caudal parts of the CNS are physically surrounded by bones of the chordal (mesodermic) part of the braincase. Bones of the chordal part (i.e. occiput and basisphenoids, see colour labelling in Fig. 2c and d) and their association with the phenotypic evolution of the caudal CNS might therefore represent a key module for phenotypic organization of the braincase in avian macroevolution.

In effect, the bones of the chordal domain have elsewhere been termed the “old cranium” (de Beer, 1937) are apparently linked to the morphological evolution of the so-called “old brain” (the caudal parts of the CNS) which has classically been seen as an extension of the medulla (Lang, 1952). Indeed, their mesodermic nature suggests that they might even be much modified homologues of axial vertebrae (Couly et al., 1993), and at the same time, they are closely related with elements of the body, such as neck muscles (Hacker and Guthrie, 1998)

The phylogenetic acquisition of altriciality and the consequence of having relatively larger CNSs in birds apparently arose at the node Neoaves. In the light of our findings the hypothesis can be extended to the rising of the particular organizations of the chordal domain which within the braincase associates with larger CNSs sizes with enlarged caudal parts that, at the same time, yields more spherical, with flat -orthobasal cranial bases with proportionally

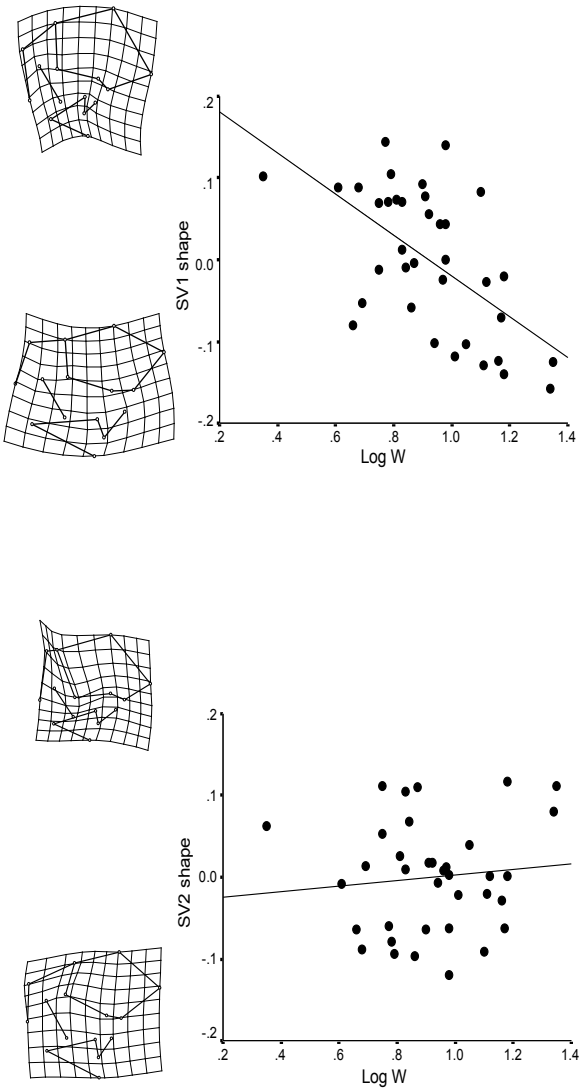

Figure 3. Bivariate regressions between each singular value with log body mass.

smaller caudal parts, and a more ventrally oriented foramen magnum. Thus, while the phylogeny of Neoaves is still unresolved we can trace the evolutionary trajectory from the basal Paleognathae or from any dinosaurian ancestry up to the emergence of the trait at the node Neoaves, and therefore suggest it may represent a type B novelty (Wilkins, 2001; p. 59).

This type B novelty relates braincase shape evolution with an evolved ontogenetic strategy, altriciality, which may have favoured a neural phenotypic evolution, yet particularly larger optic lobes, a larger brainstem rests (diencephalon and medullar bulb), and larger cerebella. Possibly, this might relate with smaller sizes in most instances (Fig. 3).

Importantly, most of these traits features associate with flight performance; in the CNS, the optic tectum (optic lobules) accounts for much motion processing, and the cerebellar and vestibular systems deal with the complexities of movement in three dimensions (Blough, 2001). The cerebellum is involved in the timing, coordination, and modulation of the motor system with incoming visual, vestibular, auditory, and somatosensory information. Additionally, birds rely most heavily on vision to function in their environment to fly. The avian collothalamic visual pathway exhibits high proportions of motion and directional responses that involve the mesencephalic, diencephalic, and telencephalic levels (brainstem). Finally, large body sizes and weights have a tremendous impact on flight demands and impose an important constraint (Norber, 1985).

While most birds fly (flightlesness is a secondary evolutionary loss; Zusi, 1993), most Neoaves birds with spherical braincases (and CNSs) are markedly manoeuvrable flyers, capable of

agile acrobatics or even the so-specialised hovered flight (e.g. from our sample most passers, falcons and owls, but a hummingbird would be also a good example despite it is missing in the sample). Size may underlie this possibility of manoeuvring, and so would forelimb shape (wing). If CNS shape associates with this trend and relates to a particular braincase phenotype, it is plausible that braincase shape relates somehow to this more manoeuvrable airborne activity.

A more spherical braincase has been advocated as to favour neural-network connections since by the geometric properties of the sphere, it minimizes the distances between neural centres (see Ross et al., 2004 cites therein, and how they discuss this assertion). If this holds true, because it is still doubted, it could also aid more agile collothalamic responses if associated with large eyes. All these birds have large eyes that displace positively from the common allometric regression to body mass (Brooke et al., 1999). Might then a more ventrally oriented foramen magnum have a biomechanical association with respect to head movements in acrobatics?

Several studies have pointed out how vestibular control may associate to head postures and visual control in vertebrate locomotion (Erichsen et al.,1989). The orientation of the head thus depends on the orientation of the occipital bones which make up the foramen magnum and the platform upon which most links to neck muscles controlling head movement rest. These connections between the bones of the occiput and neck muscles are developmentally assured since they are all derived from the same mesenchyme sources (the cranial paraxial mesoderm; Hacker and Guthrie, 1998).

Larger birds tend to have less spherical braincases and a more caudally oriented foramen magnum and, conversely to spherical phenotypes, coincide more with cruiser fliers and not so acrobatic ones. While size might be a reasonable rationale for explaining a lack of complex self-rotations (more weight places difficulties upon wings for acrobatics), cruisers do not appear to move their heads in flight (e.g. ducks, swans, flamingos, cormorants, grebes to name but a few). Conversely, birds with a more ventrally oriented foramen magnum flight performance is tightly linked to their lifestyles and do both acrobatics and pronounced head movements in flight for aiming or sight-seeing (e.g. most passers, hawks and owls).

However, this whole set of evidences might not be but mere speculation until further morpho-functional research is conducted. Morphological integration is a complex phenomenon of hierarchically intertwined and multifactor aspects of morphological evolution, and we have aimed to gather all its possible facts in one unique matrix. It has allowed us to argue that

integration may have a role in channelling patterns of skull phenotypic evolution in birds that extend from developmental to functional rationales. We would be flattened if at least the questions posed in this work serve as a pathway for other investigations in birds bridging its treatment multi-disciplinary points of view.

3.7 Conclusions

This study has explored the achosaurian skull as a system from which to approach two macroevolutionary phenomena; disparity and its morphological integration. The scope has been developed quantitatively on the basis of two different methodologies, Theoretical Morphology and Geometric Morphometrics, capturing morphological attributes of the skull in terms of its geometry.

The aim was to test whether we would be capable of distinguishing between parts of the skull (parts delineable after particular criteria, e.g. functional or developmental), upon which disparity could lean on. Likewise, we aimed testing the possible role morphological integration in biasing these disparity patterns. All our obtained results have been summarized in six chapters within this last *Third Part* of the thesis.

In ***Chapter 1*** we have shown that the geometry of the archosaurian skull achieves its lineage identity being constrained in terms of the geometric proportionality among its parts (the rostrum, the orbit and the braincase). Particularly, the occupation of a theoretical morphospace of skull proportions was found to be only partial, and all taxa of the lineage overlap in a tight cluster within one corner of the morphospace (occupying less than a 20% of the total available). Most the dispersion of this cluster over morphospace stemmed from proportional variation of the facial skeleton, yet particularly from the rostrum. At the same time, the cluster had an ellipsoid shape within one corner of morphospace because the proportions of the orbit (housing the eye) and the braincase (housing the CNS) follow a marked geometric rule in which none can be more than twice the proportion of the other in any archosaur. The cluster was so much delineated that we were even capable of formulating it with a straightforward linear regression, and predict whether the skull of a terrestrial vertebrate would or would not be an archosaur in this proportional terms. The interpretation we advocated was that a basal development constraint possibly underlies skull patterning in all archosaurian taxa. The conservativeness of such a conserved skull structural plan contrasts with the great diversity of the Archosaurian clade.

In ***Chapter 2*** we have shown that geometric morphometrics and its suite of multivariate statistics are appropriate for gaining important morphological insights at macroevolutionary scales. However, we have also stressed that particular problems might arise if shape differences are localized, as may be the case of the avian beak. While analyses might not be so much biased, visualizations may get hampered in these particular instances, despite the fact that projections from Shape Space to Tangent Space remain feasible. In effect, other techniques such as GRF are suited for avoiding these difficulties. Thus, we stressed that it would be interesting if skilled mathematicians got deeper into the roots of its axiomatic rationales in order to allow performing statistics more confidently.

The study in this chapter has corroborated that the most variable part of the avian skull upon which shape disparity rests is the facial skeleton. Particularly, the rostrum was found to be

strikingly plastic and somewhat elusive for landmark digitalisations. Furthermore, analyses show that it might be a quite autonomous part of the facial skeleton in terms of its proportional variation; as was previously found, its antero-caudal proportional lengthening but also in some other aspects of its shape variation, such as its orientation with respect to the rest of the cranium. Other aspects of the disparity of the avian skull were the pronounced changes in the orientation of the foramen magnum, and possibly, in the configuration of the cranial base, all of which we were able to label following the classic morphological terminology for craniates. Additionally, body mass was introduced as a way of testing for shape change as a function of size (evolutionary allometry tested complementarily to centroid size estimates), and interesting insights have been gained on its statistical association with avian skull disparity. For instance, the association between craniofacial arrangements might associate with size in such a way that othocranial, or airorhynchal tend to be large organisms, whereas smaller sizes relate with klynorhynchal birds. This prediction was shown to be useful for paleobiological inferences.

In order to explain the nature of these pronounced skull architectural differences we introduced the notion of modularity of the skull on the basis of the embryonic identity of its bones. However, the embryonic distinction between modules was not addressed following the classic definitions of chondral or dermal bone, but from the cellular nature of the mesenchyme from which each bone arises early in ontogeny. Within the framework of the hypothesis of a modular organization of the skull, we brought out a proposal from which to stress the basis upon which avian cranial disparity might rest; for instance "flexure" (ortho-cranial, klyno and Airorhynchal) arrangements of the skull take place between what may possibly be labelled as two different developmental modules. These are the chordal and prechordal parts, which are differentiable not by the type of bone (chondral or dermal), but from the identity of the cell populations involved in their skeletogenesis (e.g. the chordal domain is mesodermic, and the prechordal is of cephalic neural crest).

We have considered, from this point on, that this logic aided getting closer to the notion of morphogenetic field used by developmental biologists from a structural and comparative stand-point. Disparity and morphological integration are phenomena whose mechanistics are deeply intertwined with development and its evolution. The hypothesis is a stand point from which to pose questions to developmental biologists, whose commitment is for unearthing the deepest mechanics of organismic macroevolution. In this Evo-Devo context we reciprocally assume that our role as paleobiologists and morphologists is both to show these researchers shapes through time, while also possible associated phenomena.

For instance, we began discussing how one might expect differences in shape between the chordal and the prechordal parts that integrate the skull system, which we discuss further in later chapters. In Chapter 2 we ventured into discussing how developmental biologists

are beginning to unearth the molecular underpinnings of the striking variation of the rostrum that we found on comparative basis and at higher taxonomic scales. Longirostrality is often considered a typical avian trait, and indeed, it is strongly homoplastic, whereas notwithstanding, distribution over the empirical morphospace has shown that it is not the norm. The rostrum might be a sub-module within the prechordal module which derives from the complex folding of separate facial prominences whereby it might follow different signalling pathways from different surrounding tissues such as the ectoderm. Thus, the paleobiological question would be to ask for the moment in which longirostrality begin. Now we could formulate the query as when did the developmental pathways diverge leading the dissociation of this submodule towards longirostrality in certain taxa? The fossil record is providing evince where the key might be in some basal avian clades such as Enantiornithes birds. Unfortunately, the skull of these birds is still often badly preserved in these specimens, hence impeding the digitalisation of landmarks.

In ***Chapter 3*** we tested the statistical interplay between two different sets of metrics, angles taken from literature and containing both exo- and endocranial information, and landmark-shape variables from the external view of the skull in lateral view. The statistical significant association between related variables (and corresponding skull parts) found with the Two-block Partial Least Squares technique, allowed us to propose that changes in the arrangements conferring different appearances to the avian skull appear also to be related with the correlation between elements of the mesodermic cranial domain (i.e. bones of the occiput, and the basisphenoids at the Sella and Pituitary fossa). At the same time, we stressed that classic terminology is based upon standard references which might have somehow biased older quantitative approximations (e.g. some planes, such as the Visual and the Frankfort ones, or a common posture set forth by the position of the semicircular canals). Procrustes superimposition compares variation against an average which is dependant upon the sample, and therefore, it is a reference suitable for showing shape changes in the absence of an explicitly functional rationale. This entails that perhaps, classic terminology may not be properly applied since it is all based upon these reference frameworks despite we used it for explanatory convenience. More importantly, it entails that a functional posture might otherwise be a by-product of evolutionary architectural reorganizations, reflect constraints, and furthermore, not be the cause of morphological change.

In ***Chapter 4*** we carried out what was possibly the first study dealing with the disparity and the morphological organization of the avian braincase using geometric morphometric procedures, and even though by inference, about the phenotypic organization of the central nervous system in birds. Under an equivalent scope to the one carried out in Chapter 2, we were able to portray what these marked differences are in both the phenotypic organizations of the braincase and the CNS. Departing from the observed patterns in Chapter 3, we also

came to hypothesize that the changes in the elements of the chordal domain are possible keys for understanding the disparity in the organization of the avian braincase. This entails the integrated variation of bones such as the basioccipital and the basisphenoids (making up what is so-called the plane of the clivus) and the supraoccipital, all of which, changing concomitantly, convey different arrangements (and appearances) to the cranial base. Interestingly, these re-arrangements seem to occur within modules, and variation is een at a boundary between the chordal (mesodermic) and prechordal (cranial neural crest) within, or very close to, the Pituitary Fossa, in such a way as if this area was mirroring changes of the modules acting as a developmental "hinge" (the area is, in fact, the end-point reached by the embryonic notochord).

However, we additionally found that an almost equivalent amount of disparity among avian taxa stems from another boundary between these two modules between the parietals and supraoccipital. In effect, while the hypothesis of distinguishing between modules would work, this boundary is still a focus of controversy between developmental biologists, and a counter hypothesis exists. It could be that there is an additional bone therein, the post-parietal, hence the landmark could be non-homologous in certain, but still unknown, instances (i.e. it has only been experimentally advocated for the chicken). Likewise, this region is a transition between chondral and dermal bone, and a region of late closure of the calvarium after hatchling. Both facts might be, otherwise, additional factors involved in such a striking amount of variation of the braincase among birds.

Evolutionary allometry was found to be associated with these patterns of avian braincase shape organization via changes in the cranial base as a function of size, especially in its proportional length. On the contrary, however, these shape changes concurring with size changes did not seem to intervene, at least markedly, on the major changes on the architecture of the avian braincase (e.g. cranial base angular topology).

Using the same data, in ***Chapter 5*** we explored whether different developmental strategies, the altricial-precocial spectrum typified after the phenotypic appearance of the hatchlings, correlates with particular braincase shape configurations among birds (and inferred from the endocranium, with differences in the outline of the CNS). Results were not definite clear, yet showed that altriciality possibly relates with the acquisition of certain braincase (and CNSs) configurations, particularly those in which altricial birds have particularly spherical (and compact) braincases wherein the foramen magnum is oriented ventrally (as in humans) and the cranial base is flat (orthobasal). A marked tendency found for precocials was that they tend to have the opposite configuration (i.e. for convex –airobasal cranial bases, a more caudally oriented foramen magnum). Phylogenetic distribution, however, was found to be quite convergent, just as it appears to be the case for developmental strategies, as well as the range of disparity (as quantified from the mean). The only exception would therefore be

that spherical braincases (and shape changes associated with it) represent a settlement in a different region within morphospace, which seems to be proper of clades within Neoaves.

Interestingly, multivariate tests for Separate Slopes yielded that the only gross allometric difference between altricials and precocials stems from shifts on the intercept (thus, the slopes of their evolutionary allometric trajectories are equivalent). We hypothesized that this shifts might underlie the organizational changes of the bone that we capture in the braincase between developmental groups (perhaps also of the CNS), and possibly in later rather than earlier ontogenetic stages, when most tissue and organ differentiation becomes being ubiquitous.

These latter results suggested an association between the CNS and the braincase. Thus, in a final stage of the whole investigation we explored whether a pattern of morphological integration between the CNS and the braincase could be hypothesized. For this and using data from literature about the phenotypic variation of the CNS (weight ratios) and landmark-based shape endocranial data at a macroevolutionary scale, ***Chapter 6*** combined the information using Two-block Partial Least Squares. Outcomes resulted in an interesting pattern associating the relative larger sizes of the CNS with the relative spherical organization of the braincase (and its shape changes associated).This trend was surprisingly dominated not only by the proportional size of the CNS but by the relative proportion of elements of the CNS other than the forebrain (e.g. optic lobes, cerebellum and brainstem rest). These parts of the system are integrated among them, and at the same time, are physically associated with the chordal (mesodermic) module of the braincase.

However, analyses showed that covariation between changes in the parts of both systems extend to subsequent dimensions, whereby an important one (following the first) was relative forebrain enlargement in a reciprocal connection with the relative size of the optic lobes. This dimension of covariation did not render any organization of the braincase equivalent to the first dimension (i.e. spherical organization and shape changes associated). With these observations in hand the hypothesis of modularity of the braincase might be extended to the CNS, as previous researchers have recently argued (Iwaniuk et al., 2004), whereby the forebrain might be relatively autonomous from the remainder parts of the CNS. However, it is noteworthy that a further enlargement of the forebrain might need to lean on the relative enlargement of the whole CNS, for any of the extreme avian cases with larger forebrains are commonly at high values for overall CNS size (and, therefore, of relatively larger caudal parts).

In a more complex integrative framework, we found that all the parts of the CNS associated with more pronounced spherical shape changes in the braincase are, in a way, related with locomotion, since they are compromised with e.g., visual acuity, vestibulo-occular integration, and equilibrium. For us, it was interesting to suggest that the organization of a

more spherical braincase (in association with a more spherical and compact CNS) might be a type B novelty arising in Neoaves (of course, related with altriciality), and could perhaps be biomechanically associated with flight functional demands.

For instance, the position of the organization of the occiput (and its bones) plus the configuration of the caudal cranial base (all of which are chordal -mesodermic bones) associate with neck muscles derived from the exact same mesenchyme source (paraxial mesoderm). The whole spherical configuration also seems to be related in most cases, with smaller birds in terms of their absolute sizes. Thus the rationale was to proposed relation of braincase shape with the shape of the CNS and head movement, particularly in complex or special flight acrobatics, in birds for which airborne activity is one large part of their life-styles (e.g. foraging or prey sight-seeing).

3.8 Future research

In an early stage of the work schedule we opted for focusing on higher taxonomic ranks of birds and use them as a model for the archosaurian lineage. This was a decision taken after several experimental explorations with fossil data which we collected in several international institutions (experiments were principally carried out with dinosaurs and pterosaurs). In effect, we encountered difficulties in defining a definite landmark configuration capable of capturing most relevant aspects of the skull among both fossil and extant taxa (see one first approximation in Marugán-Lobón and Buscalioni, 2004). Alternatively, we found that birds are plenty in museum collections which led us to assume that it was important to test all the hypotheses we had and fulfil the objectives of the project with a reasonable sample size and with more informative data. This, regrettably, had as a collateral effect the absence of fossil archosaur material.

Thus, one prompt following step we aim to carry out implies new data collection from fossils, though now aided by the increasingly amounts of CT-scan data that, fortunately, is becoming available. One positive point though is that by the hand of these new imaging techniques we will surely be able to re-evaluate and not only extend the scope to fossil material, but also to embark into gaining new insights from three dimensional analyses.

Just as this thesis sees the light a new phylogenetic hypothesis for birds, possibly the largest to-date is being proposed (Livezey and Zusy, 2007). Unfortunately, it was too late for us to optimize our set of hypotheses over this new phylogeny, and shall also leave this as a research project for the near future.

Finally, we have aimed bridging one gap between morphological and macroevolutionary studies and developmental rationales. While queries have been placed as matters to be explored mechanistically under the basis of developmental biology, we shall stress that it would be crucial to enter in this terrain personally. This future research program should have as a starting point an ontogenetic-comparative framework with samples of as many as possible distinct avian taxa for capturing shape change to portray quantitatively its developmental trajectories.

Bibliografía citada/Literature cited

Adams, D. C., Slice, D. E., Rohlf, F. J. 2004. Geometric morphometrics: ten years of progress following the "revolution". Ital. J. Zool. 71, 5-16.

Alberch, P. 1980. Ontogenesis and morphological diversification. Am. Zool. 80, 653-667.

Alberch, P. 1982. Developmental constraints in evolutionary processes. In: Evolution and Development. Bonner, J. T. (ed). Dahlem Konferenzem, Springer-Verlag, Berlin, pp. 313-332.

Alberch, P. 1989. The logic of monsters: evidence for internal constraint in development and evolution. Geobios, mémoire spécial 12, 21-57.

Alberch, P. 1991. Del gen al fenotipo: sistemas dinámicos y evolución morfológica. Revista Española de Paleontología, no. extr., 13-19.

Aldridge, K., Kane, J. L., Marsh, J., Panchal, S. A., Boyd, P., Yan, D., Govier, W., Richtsmeier, J. T. 2005. Brain morphology in non-syndromic unicoronal craniosynostosis. Anat. Rec. A, Discov. Mol. Cell. Evol. Biol. 285, 690-698.

Arthur, W. 2000. The origin of animal body plans. A study in Evolutionary Developmental Biology. Cambridge University Press, U.S.A.

Atchley, W. R., Hall, B. K. 1991. A model for development and evolution of complex morphological structures. Biol. Rev. Camb. Philos. Soc 66, 101-157.

Bateson, W. 1894. Materials for the study of variation: treated with special regard to discontinuity in the origin of species. McMilland and Co., London.

Baumel, J. J., Witmer, L. M. 1993. Osteologia. In: Baumel, J. J., Evans, H. E., Van den Berge, J. C. (eds.), Handbook of Avian Anatomy: Nomina Anatomica Avium, 2nd Ed. Publications of the Nuttal Ornithological Club 23, pp. 45-132.

de Beer, G. R. 1937. The Development of the Vertebrate Skull. Clarendon Press, Oxford.

Bennett, P. M., Harvey, P. H. 1985a. Relative brain size and ecology in birds. J. Zool. Lond. (A) 207, 151-169.

Bennett, P. M., Harvey, P. H. 1985b. Relative brain size, development and metabolism in birds and mammals. J. Zool. Lond. (A) 207, 327-363.

Benson, R. H., Chapman, R. E., Siegel, A. F. 1982. On the Measurement of Morphology and its Change Paleobiology 8(4), 328-339.

Benton, M. 2001. Biodiversity through time. In: Briggs, D. E. G., Crowther, P. R. (eds.). Paleobiology II, Secular changes in diversity Paleobiology II. Blackwell Publishing, Boston, pp. 211-220.

Blough, P. M. 2001. Cognitive strategies and foraging in pigeons. In: Avian visual cognition, Cook, R. G. (ed.). Online; www.pigeon.psy.tufts.edu/avc/pblough/

Bonner, J. T. 1980. Introducción. In: Sobre el Crecimiento y la forma, D'Arcy W. Thompson. Editorial Herman Blume, Madrid.

Bolker, J. A. 2001. Modularity in development and why it matters to evo-devo. American Zoologist 40, 770-776.

Bolker, J. A. 2003. From genotype to phenotype: looking into the black box. In: On Growth, Form and Computers, S. Kumar, Bentley, P. (eds.) Elsevier, pp. 82-91.

Bookstein, F. L. 1989. Principal warps: thin plate splines and the decomposition of

deformations. IEEE Transactions on Pattern Analysis and Machine Intelligence 11, 567-585.

Bookstein, F. L. 1991. Morphometric tools for landmark data: geometry and biology. Cambridge Univ. Press: New York.

Bookstein, F. L. 1996a. Biometrics, biomathematics and the morphometric synthesis. Bulletin of Mathematical Biology 58, 313-365.

Bookstein, F. L. 1996b. Combining the tools of geometric morphometrics. In: Advances in morphometrics. Marcus, L. F., Corti M., Loy, A., Naylor, G., Slice, D. (eds.). Plenum Press, New York, pp. 131-151.

Bookstein, F. L. 1998. A hundred years of morphometrics. Acta Zoologica Academiae Scientiarum Hungaricae 44, 7-59.

Bookstein, F. L., Chernoff, B., Elder, R., Humphries, J., Smith, G., Strauss, R. 1985. Morphometrics in evolutionary biology. The Academy of Natural Sciences of Philadelphia, Michigan.

Bookstein, F. L., Gunz, P., Mitteroecker, P., Prossinger, H., Schaefer, K., Seidler, H., 2003. Cranial integration in Homo: singular warps analysis of the midsagittal plane in ontogeny and evolution. J. Hum. Evol. 44, 167-187.

Brochu, C. A., 2000. A digitally-rendered endocast for *Tyrannosaurus rex*. Journal of Vertebrate Paleontology 20, 1-6.

Brochu, C. A. 2001. Progress and future directions in archosaur phylogenetics. Journal of Paleontology 75, 1185-1201.

Brooke, M. de L., Hanley, S., Laughlin, S. B. 1999. The Scaling of eye size with Body mass in birds. Proceedings: Biological Sciences 266(1417), 405-412.

Buscalioni, A. D. 1999. Animales Fantásticos. Ediciones Libertarias, Madrid.

Buscalioni, A. D., Delgado-Buscalioni, R., de la Iglesia, A., Dejoan, A. 2005. Modularity at the edge between art and science In: Modularity. Understanding the Development and Evolution of Natural Complex Systems. Rasskin-Gutman, D., Callebaut, W. (eds.). Michigan Technological Institute, MIT Press, Chicago.

Callebaut, W., Rasskin-Gutman, D. (eds.). 2005. Modularity. Understanding the Development and Evolution of Natural Complex Systems, MIT Press, Chicago.

Carroll, S. B., Grenier, J. K., Weatherbee, S. D. 2004. From DNA to Diversity: Molecular Genetics and the Evolution of Animal Design. Blackwell Science, Boston.

Chambers, D., MacGonnell, I. M. 2002. Neural crest: Facing the fact of head development. Trends in Ecolology 18(8), 381-384.

Chapman, R. E. 1990. Shape analysis in the study of dinosaur morphology. In: Dinosaur Systematics: Perspectives and Approaches. Carpenter, K., Currie, P. J. (eds). Cambridge University Press, Cambridge, pp. 21-42.

Chapman, R. E., Rasskin-Gutman, D. 2001. Quantifying morphology. In: Palaeobiology II. Briggs, D. E. G., Crowther, P. R. (eds.). Blackwell Science, London, pp. 489-492.

Chernoff, B., Magwene, P. 1999. Afterword. In: Morphological Integration, Olson E. C., Miller, R. L. The University of Chicago Press, Chicaco, U.S.A.

Cheverud, J., Wagner, G., Dow, M. 1989. Methods for the comparative analysis of variation patterns. Systematic Zoology 38, 201-213.

Chiappe, L. M. 1995. The first 85 million years of avian evolution. Nature 378, 349-355.

Clarke, J. A., Norell, M. A. 2002. The Morphology and Phylogenetic Position of Apsaravis ukhaana from the Late Cretaceous of Mongolia. American Museum Novitates 3387.

Couly, G. F., Coltey, P. M., Le Douarin, N. M. 1993. The triple origin of the skull in higher vertebrates: a study in quail-chick chimeras. Development 117, 409-429.

Cracraft, J. 2001. Avian evolution, Gondwana biogeography and the Cretaceous-Tertiary mass extinction event. Proceedings of the Royal Society of London B 268, 459-469.

Cracraft, J., Clarke, J.A. 2001. The basal clades of modern birds. In: New perspectives on the origin and early evolution of birds: proceedings of the international symposium in honor of John H. Ostrom. Peabody Mus. Nat. Hist., Yale Univ., New HAven, pp. 143-156.

Cracraft, J., Eldredge, N. 1979. Phylogenetic Analysis and Palaeontology. Columbia University Press, New York.

Creuzet S., Couly G., Le Douarin, N. M. 2005. Patterning the neural crest derivatives during development of the vertebrate head: insights from avian studies. J. Anat. 204, 447-459.

Dabelow A. 1931. Über Korrelationenin der phylogenetischen Entwicklung der Schädelform. II. Die Beziehungen zwischen Gehirn und Schädelbasisform bei den Mammaliern. Gegenbaurs Morphol Jahrb 67, 84-133.

De Renzi, M., Moya, A., Pertó, J. 1999. Evolution, development and compleity in Pere Alberch (1954-1998). Journal of Evolutionary Biology 12, 624-626.

Dressino, V., Lamas S. G. 2003. Teoría craneana funcional de Cornelius Jakob van der Klaauw: una teoría sobre adaptación morfológica. Episteme 16, 99-110.

Dryden, I. L., Mardia, K. V. 1999. Statistical shape analysis. Wiley: New York. 347 pp.

Dubbeldam, J. L. 1968. On the shape and the structure of the braincastem in some species of birds. Unpublished DPhil Thesis, Rijksuniversiteit Leiden.

Duchon, J. 1976. Interpolation des fonctions de deux variables suivant le principe de la flexion des plaques minces. RAIRO Analyse Numérique 10, 5-12.

Dubois, E. Sur le rapport du poids de l'encephale avec la grandeur corps chez les mammiféres. Bull. Soc. Anthrop. 8(4).

Duijm, M. J., 1951. On the head posture in birds and its relation to some anatomical features. I-II Proc. Koninklijke Nederlandse Akademie van Wetenschappen, Ser. C, Biological and Medical Sciences 54, 202-271.

Dullemeijer, P. J. 1961. Shape and size of the brain parts as architectural factors in the skull of birds. Acta Morphol. Néerl. Scand. 4, 96.

Dullemeijer, P. J. 1974. Concepts and approaches in animal morphology. Van Gorcum & Co., B. V., Assen, The Netherlands.

Dunning, J. B. 1993. CRC Handbook on avian body masses. CRC Press, Boca Ratón, U.S.A.

Eble G. J. 2000. Theoretical morphology: the concepts and its applications. Paleobiology 26(3), 520-528.

Eble, G. J. 2004. The macroevolution of phenotypic integration. In: Pligliucci M., and Preston, K. Phenotypic integration. Studying the ecology and evolution of complex phenotypes. Oxford University Press, U.S.A, pp. 253-273.

Eldredge, N., Gould, S. J. 1972. Punctuated Equilibria: An Alternative to Phyletic Gradualism. In: Models in Paleobiology. Schopf, T. J. M. (ed.). Freeman, Cooper and Co., San Francisco, pp. 82-115.

Enlow, D. H. 1968. The Human Face: An Account of the postnatal growth and development of the craniofacial skeleton. Harpers & Row, New York.

Enlow, D. H., Hans, M. G.1996. Essentials of Facial Growth., W.B. Saunders Co., Philadelphia, U.S.A.

Erichsen, J. T., Hodos, W., Evinger, C., Bessette, B. B., Phillips, S. J. 1989. Head orientation in pigeons: postural, locomotor and visual determinants. Brain Behav. Evol. 33, 268-278.

Evans, D. J. R., Noden, D. M. 2006. Spatial relations between avian craniofacial neural crest and paraxial mesoderm cells. Developmental Dynamics 235(5), 1310-1325.

Felsenstein, J. 2002. Quantitative characters, phylogenies, and morphometrics.. In: Morphology, Shape, and Phylogenetics, N. MacLeod (ed.). Systematics Association Special Volume Series, 64. Taylor and Francis, London, pp. 27-44.

Foote, M. 1997. Sampling, taxonomic description, and our evolving knowledge of morphological diversity. Paleobiology 23, 181-206.

Galton, F. 1907. Classification of portraits. Nature 76(1981), 617-618.

Gans, C., Northcut, R. G. 1983. Neural crest and the origin of vertebrates: a new head. Science 220, 268-274.

Gass, G., Bolker, J. A. 2003. Modularity. In: Keywords and Concepts in Evolutionary Developmental Biology. B. K. Hall and W. M. Olson, (eds.). Harvard University Press, pp. 260-267.

Gaup, E. 1906. Die entwicklung des kopfskelttes in hertwig. In: Hertwig O (ed) Handbuch der Vergleicherden und Experimentellen Entwickelungstehre vol. III, pp 573-855.

Gauthier, J., Padian, K. 1985. Phylogenetic, functional, and aerodynamic analyses of the origin of birds and their flight. In: The Beginnings of Birds. Hecht, M. K., Ostrom, J. H., Viohl, G., Wellnhofer P. (eds.). Freunde des Jura-Museum, Eichstatt, pp. 185-197.

Gayon, J. 2000. History of the concept of allometry. Amer. Zool. 40, 748-758.

Gilbert, S. F., Opitz, J., Raff, R. A. 1996. Resynthesizing evolutionary and developmental biology. Developmental Biology 173, 357-372.

Goodall, G. 1991. Procrustes methods in the statistical analysis of shape. J. R. Statistical Soc. (B) 53, 285-339.

Gould, S. J. 1966. Allometry and size in ontogeny and phylogeny. Biol. Rev. Camb. Philos. Soc. 41, 587-640.
Gould, S. J. 1971. Geometric similarity in allometric growth: A contribution to the problem of scaling in the evolution of size. Am. Nat. 105, 113-136.
Gould, S. J. 1977. Ontogeny and Phylogeny. Harvard University Press, Cambridge, Massachusetts.
Gould S. J. 1981. The mismeasure of man. W.W. Norton and Co., New York.
Gould, S. J. 1983. The hardening of the Modern Synthesis. In: Dimensions of Darwinism. Marjorie Grene, (ed.), Cambridge UK: Cambridge University Press, pp. 71-93.
Gould, S. J. 1999. La vida maravillosa. Editorial Crítica, Barcelona.
Gould, S. J. 1990. Speciation and sorting as the source of evolutionary trends, or 'things are seldom what they seem'. In: Evolutionary Trends, McNamara K. J. (ed.). University of Arizona Press, Tucson, U.S.A.
Gould, S. J. 2002. The structure of evolutionary theory. The Belknap Press, Cambridge, U.S.A.
Gower, J. C. 1975. Generalized Procrustes analysis. Psychometrika 40, 33-51.
Gower, J. C., Dijksterhuis, G. B. 2004. Procrustes Problems. Oxford University Press, U.S.A.
Gunz, P. 2005. Statistical and Geometric reconstruction of Hominid Crania. Reconstructing Australopithecine Ontogeny. Unpublished DPhil Thesis, Wien Universität.
Hacker, A., Guthrie, S. 1998. A distinct developmental programme for the cranial paraxial mesoderm in the chick embryo. Development 125, 3461-3472.
Haller, A. von. 1762. Elementa physiologiae corporis humani. IV, Lausanne.
Hallgrímsson, B., Lieberman, D. E., Liu, W., Ford-Hutchinson, F. A., Jirik, F. R. 2007. Epigenetic interactions and the structure of phenotypic variation in the cranium. Evolution & Development 9(1), 76-91.
Hamburger, H., Hamilton, H. L. 1951. A series of normal stages in the development of the chick embryo. J. Morph. 88, 49-98.
Hanken, J., Gross, J. B. 2005. Evolution of cranial development and the role of neural crest: insights from amphibians. Journal of Anatomy 207, 437-446.
Hanken, J., Hall, B. K., (eds). 1993. The Skull, Vol. 3: Functional and Evolutionary Mechanisms. University of Chicago Press, Chicago.
Hesse, E. 1907. Über der inneren knöcheren Bau des Volgelsechnabels. Journal für Ornithologie 55(2), 185-248.
Helms, J. A., Cordero, D., Tapadia, M. D. 2005. New insights into craniofacial morphogenesis. Development 132(5), 851-61.
Henning, W. 1968. Elementos de una sistemática filogenética, Buenos Aires, Editorial Universitaria de Buenos Aires, EUDEBA.
Hickman, C. S., 1993. Theoretical design space: a new program for the analysis of structural diversity. Neues Jahrbuch für Geologie und Paläontologie Abhandlungen 190, 183-190.

Hofer, H. 1952. Der Gestaltwandel des Schädels der Säugetiere und Vögel, mit besonderer Berücksichtigung der Knickungstypen und der Schädelbasis. Verhandlungen der Anatomischen Gesellschaft (Jena) 50, 102-113.

Holtz, T. R., Jr. 2000. A new phylogeny of the carnivorous dinosaurs. Gaia 15, 5-62.

Hou, L., Chiappe, L. M., Zhang, F., Chuong, C. 2004. New Early Cretaceous fossil from China documents - a novel trophic specialization for Mesozoic birds. Naturwissenschaften 91, 22-25.

Huxley, T. H. 1858. On the theory of the vertebrate skull. In: The Croonian Lectures, Proceedings of the Royal Society, Scientific Memoirs I.

Huxley, J. S. 1932. Problems of relative growth. Methuen and Co., Ltd., London, 276 pp.

Iwaniuk, A. N., Dean, K. M., Nelson, J. E. 2004. A mosaic pattern characterizes the evolution of the avian brain. Proceedings of the Royal Society of London, Series B 271, S148-S151.

Iwaniuk, A. N., Hurd, P. L. 2005. The evolution of cerebrotypes in birds. Brain, Behavior and Evolution 65, 215-230.

Iwaniuk, A. N., Nelson, J. E. 2002. Can endocranial volume be used as an estimate of brain size in birds?. Canadian Journal of Zoology 80, 16-23.

Iwaniuk, A. N., Nelson, J. E. 2003. Developmental differences are correlated with relative brain size in birds: A comparative analysis. Canadian Journal of Zoology 81, 1913-1928.

Jarvis, E.D., Güntürkün, O., Bruce, L., Csillag, A., Karten, H., Kuenzel, W., Medina, L., Paxinos, G., Perkel, D. J., Shimizu, T., Striedter, G., Wild, J. M., Ball, G. F., Dugas-Ford, J., Durand, S. E., Hough, G. E., Husband, S., Kubikova, L., Lee, D. W., Mello, C. V., Powers, A., Siang, C., Smulders, T. V., Wada, K., White, S. A., Yamamoto, K., Yu, J., Reiner, A. Butler, A. B. 2005. Avian brains and a new understanding of vertebrate evolution. The Avian Brain Nomenclature Consortium. Nature Rev. Neurosc. 6, 151-159.

Jerison, H. J. 1973. Evolution of the Brain and Intelligence. Academic Press, New York.

Jiang, X., Iseki, S., Maxson, R. E, Sucov, H. M., Morriss-Kay, G. M. 2002. Tissue origins and interactions in the mammalian skull vault. Dev. Biol. 241, 106-116.

Kardong, K. V. 1995. Vertebrates. Comparative Anatomy, Function, Evolution. Wm. C. Brown Publishers, Iowa, 777 pp.

Kauffmann, S. A. 1993. The Origins of Order: Self-Organization and Selection in Evolution. Oxford University Press, U.S.A.

Kellner, A. W. A. 2003. Pterosaur phylogeny and comments on the evolutionary history of the group. In: Evolution and Palaeobiology of Pterosaurs. Buffetaut, E., Mazin, J.-M. (eds), Geological Society, London, Special Publications 217), pp. 1105-139.

Kendall, D. G. 1977. The diffusion of shape. Advances in Applied Probability. 9, 428-430.

Klaauw, C. J. van der. 1945. Cerebral skull and facial skull. A contribution to the

knowledge of skull-structure. Archives Néerlandaises de Zoologie 7, 16-37.
Klaauw, C. J. van der. 1948. Size and position of the functional components of the skull. A contribution to the knowledge of the architecture of the skull, based on data in the literature. Archives Néerlandaises de Zoologie 9, 1-176.
Klaauw, C. J. van der. 1951. Size and position of the functional components of the skull. A contribution to the knowledge of the architecture of the skull, based on data in the literature. Archives Néerlandaises de Zoologie 8, 177-368.
Klaauw, C. J. van der. 1952. Size and position of the functional components of the skull. A contribution to the knowledge of the architecture of the skull, based on data in the literature. Archives Néerlandaises de Zoologie 8, 369-559.
Klembara, J. 2004. Postparietal and prehatching ontogeny of the supraoccipital in Alligator mississippiensis (Archosauria, Crocodylia). Journal of Morphology 249(2), 147-153.
Klingenberg, C. P. 2002. Morphometrics and the role of the phenotype in studies of the evolution of developmental mechanisms. Gene 287, 3-10.
Klingenberg C. P. 1996. Multivariate allometry. In: Advances in morphometrics. Marcus L. F. (ed.). Plenum Press, New York, pp. 23-49.
Klingenberg, C. P. 2004. Integration, modules and development: Molecules to morphology to evolution. In: Pligliucci M., and Preston, K. Phenotypic integration. Studying the ecology and evolution of complex phenotypes. Oxford University Press, U.S.A, pp. 213-230.
Klingenberg, C. P., Mebus, K., Auffray, J. C. 2003. Developmental integration in a complex morphological structure: how distinct are the modules in the mouse mandible? Evolution & Development 5, 522-531.
Lasng C. T. 1952. Über die Ontogenie der knickungsverhältnisse bein Vogelshädel. Verhandl. Anat. Ges. 50, Vers. In Marburg, 127-136.
Lande, R. 1979. Quantitative genetic analysis of multivariate evolution, applied to brain: Body size allometry. Evolution 33, 402-416
Lashley, K. S. 1949. Persistent problems in the evolution of mind. Quart. Rev. Biol. 24, 28-42.
Le Douarin, N. M. 1986. Investigations on the Neural Crest. Methodological Aspects and Recent Advances. Annals of the New York Academy of Sciences 486 (1), 66-86.
Le Douarin, N. M., Ziller, C., Couly, G. F. 1993. Patterning of neural crest derivatives in the avian embryo: in vivo and in vitro studies. Dev. Biol. 159, 24-49.
Lele, S., Richtsmeier J. T. 2001. An invariant approach to statistical analysis of shapes. Chapman & Hall, New York.
Lewontin, R. C. 1974. The genetic basis for evolutionary change. Columbia University Press, New York.
Lieberman D. E., Mowbray, K. M., Pearson, O. M. 2000a. Basicranial influences on overall cranial shape. Journal of Human Evolution 38, 291-315.
Lieberman D. E., Ross C. R., Ravosa M. J. 2000b. The primate cranial base: ontogeny, function and integration. Yearbook of Physical Anthropology 43, 117-169.

Livezey, B. C. 1995. Heterochrony and the evolution of avian flightlessness. In: Evolutionary Change and Heterochrony . McNamara K. J. (ed.). Wiley, London, pp. 169-193.

López Piñero, J. M. 1992. La anatomía comparada antes y después del darwinismo. Col. Historia de la Ciencia, Akal, Madrid.

Livezey, B. C., Zusi, R. L. 2000. Higher-Order phylogenetics of modern aves based on comparative anatomy. Netherlands Journal of Zoology 51(12), 179-205.

Livezey, B. C., Zusi, R. L. 2007. Higher-Order phylogeny of modern birds (Theropoda, Aves: Neornithes) based on comparative anatomy. II. Analysis and discussion. Biol. J. Linn. Soc. 149(1), 1-139.

Magwene, P. M. 2001. New tools for studying integration and modularity. Evolution 55, 1734-1745.

Marcus, L. F. 1990. Traditional morphometrics. In: Proceedings of the Michigan morphometrics workshop. Rohlf, F. J., and Bookstein F. L. (eds.). Special Publication Number 2. University of Michigan Museum of Zoology, Ann Arbor, pp. 77-122.

Marcus, L. F., Corti, M., Loy, A., Naylor, G. J. P., Slice, D. E. 1996. Advances in Morphometrics. Plenum Press, New York.

Marcus, L. F., Hingst-Zaher, E., Zaher, H. 2000. Application of landmark morphometrics to skulls representing the orders of living mammals. Hystrix 11(1), 27-47.

Marinelli, W. 1928. Über den Schädel der Schnepfe. Paleobiologica 1, 135-160.

Marugán-Lobón, J. Buscalioni, A. D. 2003. Disparity of the Skull in Archosauria (Reptilia: Diapsida). Biological Journal of the Linnean Society 80, 67-88-

Marugán-Lobón, J., Buscalioni, A. D. 2004. Geometric morphometrics in macroevolution: morphological diversity of the skull in modern avian forms in contrast to some theropod dinosaurs. In: Morphometrics in Paleontology and Biology. Eleewa, A. (ed.). Springer Verlag, Heidelberg, pp. 157-173.

Marugán-Lobón, J., Buscalioni, A. D. 2006. Avian skull morphological evolution: exploring exo- and endocranial covariation with Two-block Partial Least Squares. Zoology 109, 217-230.

Marugán-Lobón J, Bastir M. 2004. Common Patterns of Morphological Variation in the Skull of Vertebrates: Invariant Processes?. Journal of Morphology 260, 310.

Marsh, O. C. 1880. Odontornithes: A monograph on the extinct toothed birds of North America. U.S. Geological Expl. 40th Parallel (King) 7.

Maynard-Smith, J., Burian, R., Kauffman, S., Alberch, P., Campbell, J., Goodwin, B. Lauder, R., Raup, D. M., Wolpert, L. 1985. Developmental constraints and evolution: A perspective from the Mountain Lake Conference on development and evolution. Quaterly Reviews of Biology, 60, 265-287.

Mayr, E. 2000. What evolution is. Basic Books, New York.

McGhee G. R. Jr. 1999. Theoretical morphology. The concept and its applications. Perspectives in paleobiology and Earth history. Columbia University Press, New York.

McLain, D. H. 1974. Drawing contours from arbitrary data points. The Computer Journal, 17, 318-324.

Mitteroecker, P., Gunz, P., Bernhard, M., Shaefer, K., Bookstein, F. L. 2004. Comparison of cranial ontogenetic trajectories among great apes and humans. J. Hum. Evol. 46(6), 679-98.

Moss, M. L. 1962. The functional matrix. In: Vistas in orthodontics. Kraus B., Riedel R. (eds). Philadelphia: Lea & Febiger, pp. 85-98.

Moss, M. L. 1975. The effect of rhombencephalic hypoplasia on posterior cranial base elongation in rats. Arch. Oral. Biol. 20, 489-492.

Moss, M. L. 1997a. The functional matrix hypothesis revisited. 1. The role of mechanotransduction. Am. J. Orthod. Dentofac. Orthop. 112, 8-11.

Moss, M. L. 1997b. The functional matrix hypothesis revisited 2. The role of an osseous connected cellular network. Am. J. Orthod. Dentofac. Orthop. 112, 221-226.

Moss, M. L. 1997c. The functional matrix hypothesis revisited 3. The genomic thesis. Am. J. Orthod. Dentofac. Orthop. 112, 338-342.

Moss, M. L. 1997d. The functional matrix hypothesis revisited 4. The epigenetic antithesis and the resolving synthesis. Am. J Orthod. Dentofac. Orthop. 112, 410-417.

Moss, M. L., Salentijn, L. 1969. The capsular matrix. Am. J. Orthod. 56, 474-490.

Moss-Salentjin, L. 1997. Melvin L. Moss and the Functional Matrix. J. Dent. Res. 76(1212), 1814-1817.

Moss, M. L., Vilmann, H. 1978. Studies on orthocephalization of the rat head. Gegenbaurs morph. Jahrb. 124(4), 559-579.

Moss, M. L., Young, R. 1960. A functional approach to craniology. Am. J. Phys. Anthropol. 18, 281-292.

Nagel, E. 1961. La estructura de la ciencia. Paidós Ibérica S.A., Barcelona.

Needham, J. 1936. Order and Life. Yale University Press, New Haven.

Needham, J. 1950. Biochemistry and Morphogenesis. Cambridge University Press, Cambridge.

Nicola, P. A., Monteiro, L. R., Pessôa, L. M., von Zuben, F. J., Rohlf, F. J. Furtado dos reis, S. 2003. Congruence of hierarchical, localized variation in cranial shape and molecular phylogenetic structure in spiny rats, genus Trinomys (Rodentia: Echimyidae). Biological Journal of the Linnean Society 80 (3), 385-396.

Noden, D. M. 1983. The embryonic origins of avian cephalic and cervical muscles and associated connective tissues. Am. J. Anat. 168, 257-276.

Noden, D. M., Trainor, P. A. 2005. Relations and interactions between cranial mesoderm and neural crest populations. J. Anat. 207, 574-601.

Norber, U. M. 1985. Flying, Gliding, and Soaring. In: Functional Vertebrate Morphology. Hildebrand, M., Bramble, D.M., Liem, K. F, Wake D. W. (eds.). Belknap Press (Harvard University Press), Cambridge, MA.

Northcutt, R. G., Gans, C. 1983. The genesis of neural crest and epidermal placodes: a reinterpretation of vertebrate origins. Quart. Rev. Biol. 58, 1-28.

O'Higgins, P., Jones, N. 1999. Facial growth in *Cercocebus torquatus*: an application

of three-dimensional geometric morphometric techniques to the study of morphological variation. J. Anat. 193, 251-272.
Olson E. C, Miller, R. L. 1958. Morphological integration. University of Chicago Press, Chicago.
Oppenheimer, J. M. 1966. The growth and development of developmental biology. In: Major Problems in Developmental Biology. Locke, M. (ed.). Academic Press, New York, pp. 1-27.
Osborn, H. F. 1905. *Tyrannosaurus* and other Cretaceous carnivorous dinosaurs. Bulletin of the American Museum of Natural History 35, 733-771.
Oster, G. F., Alberch, P. 1982. Evolution and bifurcation of developmental programs. Evolution 36, 444-459.
Oster G. F., Shubin, N., Murray, J. D., Alberch, P. 1988. Evolution, 42(5), 862-884.
Padian, K., Chiappe, L. M. 1998. The origin and early evolution of birds. Biological Reviews 73, 1-42.
Padian, K., J. Huchinson, R., Holtz, T. R. 1999. Phylogenetic definitions and nomenclature of the major taxonomic categories of the carnivorous Dinosauria (Theropoda). Journal of Vertebrate Paleontology 19, 69-80.
Parker, T. J. 1891. Observations on the anatomy and development of Apteryx. Phil. Trans. Roy. Soc. B 182, 25-131.
Pearson, R. 1972. The avian brain. Academic Press, New York.
Pérez, S. I., Bernal, V., González, P. 2006. Differences between sliding semi-landmark methods in geometric morphometrics, with an application to human craniofacial and dental variation. Journal of Anatomy 208(6), 769-784.
Pirlot, P. 1976. Morfología evolutiva de los cordados. Omega, Barcelona.
Pligliucci, M., Preston, K. 2004. Phenotypic integration. Studying the ecology and evolution of complex phenotypes. Oxford University Press, U.S.A.
Portmann, A. 1947a. Études sur la cérébralisation chez les oiseaux 1. Alauda 14, 2-20.
Portmann, A. 1947b. Études sur la cérébralisation chez les oiseaux 2. Alauda 15, 1-15.
Portmann, A. 1962. Cerebralisation und Ontogenese. Medizin. Grundlagemforsch 4, 1-62.
Portman, A. 1968. Nuevos caminos de la biología. Ediciones Iberoamericanas, Madrid.
Rabey, G. 1968. Morphanalysis. Hatch, Pinner & Co., London.
Raff, R. A. 1996. The shape of life. Genes, development and the evolution of animal form. University of Chicago Press, Chicago.
Rasskin-Gutman D. 1995. Modelos geométricos y Topológicos en Morfología. Exploración del morfoespacio afín. Aplicaciones en paleobiología. Unpublished DPhil Thesis, Universidad Autónoma de Madrid.
Rasskin-Gutman D., Ipsizúa-Belmonte, J. C. 2004. Theoretical morphology of developmental asymmetries. Bioessays 26, 405-412.
Rasskin-Gutman, D., Wegner, Callebaut. (eds.). Modularity. MIT Press, Chicago.
Raup, D. M. 1962. Computer as aid in describing form in gastropod shells. Science, 138, 150-152.

Raup, D. M. 1969. Modeling and simulation of morphology by computer. In: Proceedings of the North American Paleontology Convention, pp. 71-83.

Raup, D. M., Michelson, A. 1965. Theoretical morphology of the coiled shell. Science, 147, 1294-1295.

Raup, D. M., Stanley, S. M. 1978. Principles of paleontology. Freeman & Co., San Francisco.

Reif, W. E., Weishampel, D. B. 1991. Theoretical morphology, an annotated bibliography 1965-1990. Cour. Forsch.-Inst. Senckenberg 142, 1-140.

Rensch, B. 1959. Evolution above the species levels. Columbia University Press, New York.

Richman, J. M., Lee, S. H. 2003. About face: signals and genes controlling jaw patterning and identity in vertebrates. BioEssays, 25, 554-568.

Richtsmeier J. T., Aldridge K., DeLeon, V. B., Panchal, P. K., Kane, A., Marsh, J. L., Yan, J., Cole, T. M. III. 2006. Phenotypic Integration of Neurocranium and Brain. Journal of Experimental Zoology (Mol. Dev. Evol.) 306(B), 1-19.

Riedl, R. 1978. Order in Living Systems: A Systems Analysis of Evolution. New York: Wiley.

Riska, B. 1986. Some models for development, growth, and morphometric correlation. Evolution 40, 1303-1311.

Roth, V. L., Mercer, J. M. 2000. Morphometrics in development and evolution. Amer. Zool. 40, 801-810.

Rohlf, F. J. 1990. Rotational fit (Procrustes) methods. In: Proceedings of the Michigan Morphometrics Workshop. Rohlf, F. J., Bookstein F. L (eds.). Univ. of Michigan, Museum of Zoology (Special Publication no. 2), pp. 227-236.

Rohlf, F. J. 1993. Relative warps analysis and an example of its application to mosquito wings. In: Contributions to Morphometrics. Marcus L. F., Bello, E., García-Valdecasas, A. (eds.), Monografías del Museo Nacional de Ciencias Naturales, CSIC, Madrid, pp. 131-158.

Rohlf, F. J. 1995. Statistical analysis of shape using partial-warp scores. In: Proceedings in Current Issues in Statistical Shape Analysis. Mardia, K. V. and Gill, C. A. (eds.). Leeds Univ. Press. pp. 154-158.

Rohlf F. J. 1996. Morphometric spaces, shape components and the effects of linear transformations. In: Advances in Morphometrics. Marcus L. F., M. Corti, A. Loy, G. J. P. Naylor, D. E. Slice. Plenum Press. New York, pp. 117-129.

Rohlf, F. J. 1999. Shape statistics: Procrustes superimpositions and tangent spaces. Journal of Classification, 16, 197-223.

Rohlf, F. J. 2000. Statistical power comparisons among alternative morphometric methods. American Journal of Physical Anthropology 111, 463-478.

Rohlf, F. J. 2002. Geometric morphometrics in phylogeny. In: Forey, P. and N. Macleod (eds.) Morphology, shape and phylogenetics. Francis & Taylor: London, pp. 175.

Rohlf, F. J., Bookstein, F. L. 2003. Computing the uniform component of shape variation. Systematic Biology 52, 66-69.

Rohlf, F. J., Corti, M. 2000. The use of two-block partial least-squares to study covariation in shape. Syst. Biol. 49, 740-753.

Rohlf, F. J., Marcus, L. F. 1993. A revolution in morphometrics. Trends in Ecology and Evolution 8, 339-339.

Rohlf, F. J., Slice, D. E. 1990. Extensions of the Procrustes method for the optimal superimposition of landmarks. Systematic Zoology 39, 40-59.

Romer, A. S. 1966. Vertebrate Paleontogoloy. The Univeristy of Chicago Press, Chicago.

Romer, A. S., Parsons, T. 1986. The vertebrate body. University of Chicago Press, Chicago.

Ross, C. F., Henneberg, M., Richard, S., Ravosa, M. J. 2004. Curvilinear and geometric modeling of basicranial flexion in a phylogenetic context: Is it adaptive? Is it constrained? J. Hum. Evol. 46, 185-213.

Russel, E. S. 1916. Form and Function. Murray Eds., London.

Santagatti, F., Rijli, F. M., 2003. Cranial neural crest and the building of the vertebrate head. Nature Reviews Neuroscience 4, 806-818.

Sanz, J. L. Chiappe,L. M., Buscalioni, A. D. 1995. The osteology of Concornis lacustris (Aves: Enantiornithes) from the Lower Cretaceous of Spain and a reexamination of its phylogenetic significance. American Museum Novitates 3133, 1-23.

Schneider, R. A. 1999. Neural Crest Can Form Cartilages Normally Derived from Mesoderm during Development of the Avian Head Skeleton. Developmental Biology 208, 441-455.

Schneider, R. A., Helms, J. A., 2003. The Cellular and Molecular Origins of Beak Morphology. Science 24 January 299(5606), 565-568.

Seilacher, A. 1970. Arbeitkonszept zur Konstructions-Morphologie. Ethaia 3, 393-396.

Seilacher, A. 1991. Self-organizing mechanisms in morphogenesis and evolution. In.Constructional Morphology and Evolution. Schmidt-Kittler, N. Vogel, K. Springer-Verlag, Berlin, pp. 251-273.

Sewall-Wright, G. 1932. The roles of mutation, inbreeding, crossbreeding, and selection in evolution. Proceedings of the Sixth International Congress on Genetics 355-366.

Sheets, H. D. 2001. IMPseries- Coordgen. Dept. of Physics, Canisius College, Buffalo, NY, U.S.A; http://www.canisius.edu/~sheets/morphsoft.html.

Sibley, C. G., Ahlquist, J. E., 1990. Phylogeny and classification of birds: a study in molecular evolution. Yale University Press, New Haven.

Siegel, A. F., Benson, R. H. 1982. A robust comparison of biological shapes. Biometrics 38, 341-350.

Simon, H. A. 1969. The architecture of complexity. In: The Sciences of the Artificial MIT Press, Cambridge, pp. 192-229.

Simpson, G. G. 1944. Tempo and Mode in Evolution. Columbia University Press, New York.

Simpson, G. G. 1953. Life of the past: an introduction to paleontology. Yale University

Press, New Haven.
Slice, D. E. 2002. Morpheus et al. Department of Biomedical Engeneering, West Forest University School of Medicine,Winston-Salem, U.S.A; http://life.bio.sunysb.edu/morph/morpheus.
Slice, D. E. 2005. Modern morphometrics. In: Modern Morphometrics in Physical Anthropology. Slice, D. E (ed). Kluwer Academic Publishers, New York, pp. 1-45.
Small, C. G. 1996. The statistical theory of shape. Springer, New York.
Solé, R., Goodwin, B. 2002. Signs of life. How complexity pervades biology. Basic Books, New York.
Spemann, H. 1938. Embryonic Development and Induction. Yale University Press, New Haven.
Stanley, S. M. 1979. Macroevolution: Pattern and Process. W. H. Freeman, Co., San Francisco.
Starck, J. M. 1993. Evolution of avian ontogenies. In: Current ornithology. Power, D. M. (ed)., Vol. 10. Plenum Press, New York, pp 275-366.
Starck, J. M., Ricklefs, R. E. 1998. Avian Growth and Development. Evolution within the Altricial-Precocial Spectrum Oxford University Press, New York.
Statsoft, Inc. 2001. Statistica v. 6.0. Tulsa, OK, U.S.A.
Stone, J. R., Hall, B. K. 2004. Latent homologues for the neural crest as an evolutionary novelty. Evol. & Devel. 6, 123-129.
Thomas, R. D. K., Shearman, R. M., Stewart, G. W. 2000. Evolutionary Exploitation of Design Options by the First Animals with Hard Skeletons. Science 288, 1239-1242.
Thompson, D. W. 1942. On growth and form. The complete revised version. Dover, New York.
Turing, A. 1952. The Chemical Basis of Morphogenesis, Phil. Trans. R. Soc. London B 237, pp 37-72.
Turner, A., Pol, D., Norell, M. 2006. Resolving dromaeosaurid phylogeny. New information and additions to the tree. Journal of Vertebrate Paleontology, 26(3), 133A.
Unwin, D. M. 2003. On the phylogeny and evolutionary history of pterosaurs. In: Evolution and Palaeobiology of Pterosaurs. Buffetaut, E., Mazin, J. M. (eds), Geological Society, London, Special Publications 217, pp. 139-191.
Van Tuinen, M. 2002. Relationships of Birds: Molecules versus Morphology, Electronic Encyclopedia of Life Sciences, Nature publishing group (online).
Waddington, C. H. 1963. La naturaleza de la vida. Editorial Norte y Sur, Madrid.
Waddington, C. H. 1975. The evolution of an evolutionist. Cornell University Press, Ithaca, New York.
Wagner, G. P. 1996. Homologues, Natural Kinds and the Evolution of Modularity Amer. Zool. 36, 36-43.
Wagner, A. 2006. Robustness and Evolvability in Living Systems. Princeton University Press.

Walker, C. A. 1981. A new subclass of birds from the Cretaceous of South America. Nature, 292, 51-53.

Weiss, P. 1939. Principles of Development. Holt, New York.

Witmer, L. M. 1995. Homology of facial structures in extant Archosaurs (Birds and Crocodilians), with special reference to paranasal pneumacity and nasal conchae. Journal of Morphology 225, 269-327.

Witmer, L. M. 1997. The evolution of the antorbital cavity of archosaurs: a study in soft-tissue reconstruction in the fossil record with an analysis of the function of pneumacity. Journal of Vertebrate Paleontology 17 (Suppl. 1), 1-73.

Wills, M. A. 1998. Cambrian and Recent disparity: the picture from priapulids Paleobiology 24, 177-199.

Wilkins, A. 2001. The evolution of developmental pathways. Sinauer Associates Inc., Sunderland.

Winther, R. G. 2001. Varieties of modules: Kinds, levels, origins, and behaviours. J. Exp. Zool. 291, 116-129.

Wu, P., Jiang T., Suksaweang, S., Widelitz, R., Chuong, W. 2004. Molecular Shaping of the Beak. Science 305 (5689), 1465-1466.

Zelditch, M. L., Swiderski, D., Sheets, D., Fink, W. 2004. Geometric Morphometrics for Biologists: A Primer. Elsevier, London.

Zhang, F., Zhou, Z. 2000. A primitive enantiornithine bird and the origin of feathers. Science 290, 1955-1959.

Zusi R. L. 1993. Patterns of diversity in the reptilian skull. In: Hanken J., Hall, B. (eds). The skull, patterns of structural and systematic diversity, Vol. 2. The University of Chicago Press, Chicago.

APPENDIX 1

APPENDIX 1. List of species, Institutional label, Classification, Node and Body Mass

Species	Label	Order	Family	Clade	Body mass (g)
Chauna chavaria	ZMB 580	Anseriformes	Anhimidae	Galloanseres	4800
Marmaronetta angustrirostris	MNCN 18723	Anseriformes	Anatidae	Galloanseres	477
Anas platyrhynchos	MAUV (exp)	Anseriformes	Anatidae	Galloanseres	1082
Anser caerulescens	MAUV (exp)	Anseriformes	Anatidae	Galloanseres	2630
Aythya fuligula	ZMB 606	Anseriformes	Anatidae	Galloanseres	694
Cygnus olor	ZMB 986	Anseriformes	Anatidae	Neoaves	10735
Cygnus atratus	ZMB 932	Anseriformes	Anatidae	Neoaves	5650
Apus apus	ZMB 650	Apodiformes	Apodidae	Neoaves	37,6
Selasphorus sasin	AMNH 26236	Apodiformes	Trochilidae	Neoaves	2,85
Bucorvus abissinicus	AMNH 1770	Bucertiformes	Bucorvidae	Neoaves	3841
Pygoscelis antartica	AMNH 26161	Ciconiiformes	Sphenicidae	Neoaves	4150
Pygoscelis antartica	MNCN 25519	Ciconiiformes	Sphenicidae	Neoaves	4150
Spheniscus demersus	MAUV (exp)	Ciconiiformes	Sphenicidae	Neoaves	3310
Gavia immer	AMNH 24131	Ciconiiformes	Gaviidae	Neoaves	4134
Aechmophorus ocidentalis	AMNH 18667	Ciconiiformes	Podicipedidae	Neoaves	1477
Podiceps cristatus	ZMB 803	Ciconiiformes	Podicipedidae	Neoaves	673,5
Calonextris diomedea	MNCN 18656	Ciconiiformes	Procellaridae	Neoaves	535
Fulmarus glaicialis	MNCN 18653	Ciconiiformes	Procellaridae	Neoaves	544
Diomedea exulans	ZMB 4	Ciconiiformes	Procellaridae	Neoaves	3751
Oceanodroma furcata	AMNH 18492	Ciconiiformes	Procellaridae	Neoaves	40,5
Puffinus puffinus	AMNH 17600	Ciconiiformes	Procellaridae	Neoaves	453
Phaethon lepturus	AMNH 24187	Ciconiiformes	Phaetonthidae	Neoaves	334
Pelecanus onocrotalus	AMNH	Ciconiiformes	Pelecanidae	Neoaves	11000
Palacrocorax aristotelis	MNCN 18672	Ciconiiformes	Phalacrocoracidae	Neoaves	1940
Morus bassanus	MNCN	Ciconiiformes	Sulidae	Neoaves	3499,5

Fregata magnificens	AMNH 4338	Ciconiiformes	Fregatidae	Neoaves	1474
Ciconia ciconia	ZMB 253	Ciconiiformes	Ciconiidae	Neoaves	3473
Ardea cinerea	ZMB 396	Ciconiiformes	Ardeidae	Neoaves	1443
Scopus umbretta	AMNH 4003	Ciconiiformes	Scopidae	Neoaves	422,5
Egretta garcetta	MNCN 18681	Ciconiiformes	Ardeidae	Neoaves	500
Thereskiornis aethiopicus	ZMB 988	Ciconiiformes	Thereskiornithidae	Neoaves	1498
Platalea leucorodia	ZMB 313	Ciconiiformes	Thereskiornithidae	Neoaves	1521
Nycticorax nycticorax	ZMB 5	Ciconiiformes	Ardeidae	Neoaves	883
Leptoptilos dubius	AMNH 4023	Ciconiiformes	Ciconiidae	Neoaves	4767
Phoenicopterus ruber	ZMB 809	Ciconiiformes	Phoenicopteridae	Neoaves	3035
Buteo buteo	ZMB 149	Ciconiiformes	Accipitridae	Neoaves	875
Falco tinnunculus	ZMB 365	Ciconiiformes	Falconidae	Neoaves	201,5
Pernis apivorus	ZMB 657	Ciconiiformes	Accipitridae	Neoaves	758
Gampsonyx	AMNH 4198	Ciconiiformes	Accipitridae	Neoaves	92,5
Pandion haliaetus	AMNH 26217	Ciconiiformes	Accipitridae	Neoaves	1485
Rostramus sociabilis	AMNH 21185	Ciconiiformes	Accipitridae	Neoaves	421
Sagittarius serpentarius	AMNH 9165	Ciconiiformes	Sagittaridae	Neoaves	3607
Sarcoramphus papa	ZMB 987	Ciconiiformes	Ciconiidae	Neoaves	3400
Accipiter nisus	ZMB 1	Ciconiiformes	Accipitridae	Neoaves	1024,5
Aegypius monachus	MNCN 26231	Ciconiiformes	Accipitridae	Neoaves	9625
Aquila crisaetos	MNCN 19124	Ciconiiformes	Accipitridae	Neoaves	4195
Gyps fulvus	MNCN 25838	Ciconiiformes	Accipitridae	Neoaves	7436
Neophron perpterus	ZMB 656	Ciconiiformes	Accipitridae	Neoaves	2120
Vultur gryphus	AMNH 26157	Ciconiiformes	Ciconiidae	Neoaves	11300
Recurvirostra avosseta	MAUV (exp)	Ciconiiformes	Charadridae	Neoaves	306
Recurvirostra_avosetta	MNCN 18847	Ciconiiformes	Charadridae	Neoaves	306

Burhinus oedichnemus	MNCN 23802	Ciconiiformes	Burhinidae	Neoaves	459
Larus argentatus	MNCN 18878	Ciconiiformes	Laridae	Neoaves	1135
Larus ridibundus	MNCN 19995	Ciconiiformes	Laridae	Neoaves	284
Limos fedoa	AMNH 15601	Ciconiiformes	Scolopacidae	Neoaves	342,5
Limosa limosa	MNCN 18823	Ciconiiformes	Scolopacidae	Neoaves	291
Sterna hirundo	MAUV (exp)	Ciconiiformes	Laridae	Neoaves	120
Phalaropus minor	AMNH 11573	Ciconiiformes	Scolopacidae	Neoaves	33,8
Vanellus vanellus	ZMB 887	Ciconiiformes	Charadridae	Neoaves	218,5
Scolopax rusticola	ZMB 160	Ciconiiformes	Scolopacidae	Neoaves	197,5
Gallinago gallinago	MAUV (exp)	Ciconiiformes	Scolopacidae	Neoaves	122
Tringa totanus	ZMB 826	Ciconiiformes	Scolopacidae	Neoaves	129
Fratercula arctica	MNCN 18865	Ciconiiformes	Laridae	Neoaves	381
Actophilornis africana	AMNH 12151	Ciconiiformes	Jacanidae	Neoaves	57
Cursorius temioninki	AMNH 545	Ciconiiformes	Glareolidae	Neoaves	69
Haematopus ostralegus	ZMB 968	Ciconiiformes	Charadridae	Neoaves	526
Chionis alba	AMNH 8849	Ciconiiformes	Chionididae	Neoaves	400
Rynchops niger	AMNH 27252	Ciconiiformes	Laridae	Neoaves	301,5
Stercorarius	AMNH 27194	Ciconiiformes	Laridae	Neoaves	510
Thinocorus rumicevorus	AMNH 669	Ciconiiformes	Thinocoridae	Neoaves	79,5
Uria aalge	AMNH 20109	Ciconiiformes	Laridae	Neoaves	992,5
Capella galligano	AMNH 26378	Ciconiiformes	Scolopacidae	Neoaves	122
Charadrius melodia	AMNH 9977	Ciconiiformes	Charadriidae	Neoaves	97
Pterocles quadricinqtus	AMNH 2867	Ciconiiformes	Pteroclediidae	Neoaves	308
Chlidonias niger	ZMB 307	Ciconiiformes	Laridae	Neoaves	65
Larus_dominic_camus	ZMB 774	Ciconiiformes	Laridae	Neoaves	900
Cyanocorax chrysopus	ZMB 686	Ciconiiformes	Ciconiidae	Neoaves	157

Numenius arquata	ZMB 45	Ciconiiformes	Scolopacidae	Neoaves	766
Milvus vus	ZMB 727	Ciconiiformes	Accipitridae	Neoaves	1080
Neophron perpterus	ZMB 656	Ciconiiformes	Accipitridae	Neoaves	2120
Tringa totanus	ZMB 826	Ciconiiformes	Scolopacidae	Neoaves	52
Colius macrorus	AMNH 24231	Coliiformes	Coliidae	Neoaves	51,1
Columba palumbus	ZMB 248	Columbiformes	Columbidae	Neoaves	354,5
Columba palumbus	ZMB 248	Columbiformes	Columbidae	Neoaves	490
Goura cristata	ZMB 879	Columbiformes	Columbidae	Neoaves	2000
Alcedo cristata	AMNH 16898	Coraciformes	Alcedinidae	Neoaves	40
Todus angustrirostris	AMNH 25419	Coraciformes	Todadidae	Neoaves	6,85
Halcyon	ZMB 777	Coraciformes	Alcedinidae	Neoaves	92
Megaceryle torquata	AMNH 4654	Coraciiformes	Alcedinidae	Neoaves	317
Merops ornatus	AMNH 7601	Coraciiformes	Meropidae	Neoaves	36,55
Leptosomus rafer	AMNH 448	Coraciiformes	Leptosomidae	Neoaves	220
Baryphthengus ruticapillus	AMNH 6669	Coraciiformes	Momotidae	Neoaves	163
Coracias garrulus	AMNH 1471	Coraciiformes	Coracidae	Neoaves	146
Alectura lathami	AMNH 1388	Craciformes	Megapodiidae	Neoaves	2330
Penelope purpurens	ZMB 196	Craciformes	Cracidae	Neoaves	2060
Crax mitu	AMNH 1559	Craciformes	Cracidae	Neoaves	3816
Opisthocomus hoatzin	AMNH 8992	Cuculiformes	Opistocomidae	Neoaves	855
Centropus phasianicus	AMNH 19786	Cuculiformes	Cuculidae	Neoaves	366
Geococcyx californianus	AMNH 16575	Cuculiformes	Cuculidae	Neoaves	289,5
Cuculus canorus	ZMB 242	Cuculiformes	Cuculidae	Neoaves	113
Galbulatombacia	AMNH 7086	Galbuliformes	Galbulidae	Neoaves	23,8
Monasa atra	AMNH 5163	Galbuliformes	Bucconidae	Neoaves	92,8
Perdix perdix	ZMB 310	Galliformes	Phasianidae	Galloanseres	390

Coturnis coturnis	ZMB 308	Galliformes	Phasianidae	Galloanseres	97
Gallus domesticus	ZMB 77	Galliformes	Phasianidae	Galloanseres	1094
Lagopus lagopus	ZMB 172	Galliformes	Phasianidae	Galloanseres	559
Pavo cristatus	ZMB 902	Galliformes	Phasianidae	Galloanseres	3288
Aramus	AMNH 4334	Gruiformes	Aramidae	Neoaves	1080
Otis tarda	ZMB 329	Gruiformes	Otidae	Neoaves	5200
Chunga burmisteri	AMNH 4250	Gruiformes	Cariamidae	Neoaves	1298
Eurypyga helias	AMNH 4293	Gruiformes	Eurypygidae	Neoaves	222
Grus grus	ZMB 557	Gruiformes	Gruidae	Neoaves	5500
Balearica_pavonina	MAUV (exp)	Gruiformes	Gruidae	Neoaves	3590
Porphyrio porphyrio	ZMB 229	Gruiformes	Rallidae	Neoaves	786,5
Rhynochetos jubatus	ZMB 719	Gruiformes	Rhynochetidae	Neoaves	860
Rallus aquiaticus	ZMB 894	Gruiformes	Rallidae	Neoaves	120
Gallinula cloropus	MAUV (exp)	Gruiformes	Rallidae	Neoaves	302,5
Psophia leucoptera	AMNH 3824	Gruiformes	Psophiidae	Neoaves	1000
Anthropoides virgo	ZMB 853	Gruiformes	Gruidae	Neoaves	2308
Fulica atra	ZMB 489	Gruiformes	Rallidae	Neoaves	853
Porphyrio porphyrio	ZMB 229	Gruiformes	Ralidae	Neoaves	140
Musophaga	MAUV (exp)	Musophagiformes	Musophagidae	Neoaves	360
Lathrotriccus euleri	AMNH 23861	Passeriformes	Tyrannidae	Neoaves	12
Cerhia sp.	MNCN 23049	Passeriformes	Certhiidae	Neoaves	9,75
Lanius exultor	ZMB 674	Passeriformes	Laniidae	Neoaves	57
Turdus sp	MNCN 19156	Passeriformes	Muscicapidae	Neoaves	77,9
Corvus corone	ZMB 148	Passeriformes	Corvidae	Neoaves	1199
Cracticus torquatus	AMNH 9646	Passeriformes	Corvidae	Neoaves	142
Dinemellia dinemelli	AMNH 23005	Passeriformes	Passeridae	Neoaves	63,9

Sturnus unicolor	MAUV (exp)	Passeriformes	Sturnidae	Neoaves	102,8
Pyroderus sculattus	ZMB 990	Passeriformes	Cotingidae	Neoaves	357
Bombycilla garrulax	ZMB 792	Passeriformes	Bombycillidae	Neoaves	56
Cardinalis virginianus	ZMB 898	Passeriformes	Embericidae	Neoaves	40
Pica pica	ZMB 623	Passeriformes	Vireonidae	Neoaves	178
Parussp	ZMB 762	Passeriformes	Paridae	Neoaves	11
Pyrrhocorax pyrrhocorax	ZMB 697	Passeriformes	Corvidae	Neoaves	400
Aulacorhynchus prasina	AMNH 2157	Piciformes	Rhamphastidae	Neoaves	178,5
Celeus flavescens	AMNH 4212	Piciformes	Picidae	Neoaves	132,1
Picus viridis	ZMB 505	Piciformes	Picidae	Neoaves	176
Semnornis rhamphastinus	AMNH 5658	Piciformes	Rhamphastidae	Neoaves	77,4
Dendrocopus major	ZMB 52	Piciformes	Picidae	Neoaves	82
Ramphastos discolor	ZMB 2	Piciformes	Rhamphastidae	Neoaves	324
Anodorhynchus hyacinthinus	AMNH 2777	Psittaciformes	Psittacidae	Neoaves	1500
Lorius lory	AMNH 3454	Psittaciformes	Psittacidae	Neoaves	240
Micropsitta finschi	AMNH 23407	Psittaciformes	Psittacidae	Neoaves	12,9
Amazona automnalis	ZMB 778	Psittaciformes	Psittacidae	Neoaves	416
Asio clamator	MAUV (exp)	Strigiformes	Strigidae	Neoaves	153,5
Asio flammeus	ZMB 334	Strigiformes	Strigidae	Neoaves	262
Bubo bubo	MNCN 20384	Strigiformes	Strigidae	Neoaves	2686
Strix aluco	MNCN 23238	Strigiformes	Strigidae	Neoaves	340
Athene noctua	MNCN 19235	Strigiformes	Strigidae	Neoaves	164
Tyto alba	MNCN 19205	Strigiformes	Tytonidae	Neoaves	400
Steatornis_caripensis	AMNH 3167	Strigiformes	Steatornithidae	Neoaves	414
Caprimulgus europaeus	ZMB 83	Strigiformes	Caprimulgidae	Neoaves	43,2
Podargus strigoides	AMNH 10442	Strigiformes	Podargidae	Neoaves	245

Mycteria leucocephala	ZMB 940	Strigiformes	Strigidae	Neoaves	3180
Aegolius funereas	ZMB 877	Strigiformes	Strigidae	Neoaves	134
Asio otus	ZMB 768	Strigiformes	Strigidae	Neoaves	262
Strutio camellus	AMNH 4261	Strutioniformes	Struthionidae	Paleognathae	8300
Apteryx australis	AMNH 5372	Strutioniformes	Apterygidae	Paleognathae	2090
Rhea americana	MAUV (exp)	Strutioniformes	Rheidae	Paleognathae	23000
Casuarius casuarius	AMNH 3870	Strutioniformes	Casuariidae	Paleognathae	44000
Dromaius novaehollandiae	MAUV (exp)	Strutioniformes	Dromaiidae	Paleognathae	31160
Crypturellus undulatus	AMNH 2751	Tinamiformes	Tinamidae	Paleognathae	900
Orthoprocta ornata	AMNH 6499	Tinamiformes	Tinamidae	Paleognathae	458
Rhynchotus rufences	ZMB 740	Tinamiformes	Tinamidae	Paleognathae	900
Trogon violaceus	AMNH 19422	Trogoniformes	Trogonidae	Neoaves	96,25
Pharomachrus mocino	AMNH 5869	Trogoniformes	Trogonidae	Neoaves	206
Turnix velox	AMNH 9658	Turniciformes	Turnicidae	Neoaves	41
Phoeniculus sp	AMNH 4232	Upupiformes	Phoenculidae	Neoaves	55,5
Upupa epops	AMNH 8768	Upupiformes	Upupidae	Neoaves	61,4

APPENDIX 2

Taxon	*ZMB No.*	*Clade*	*Taxon*	*ZMBNo.*	*Clade*	*Taxon*	*ZMB No.*	*Clade*
Rhynchotus rufences	740	Paleognathae	*Ardea cinerea*	396	Neoaves	*Cardinalis virginianus*	898	Neoaves
Tetrao urogallus	24	Galloanseres	*Ciconia ciconia*	253	Neoaves	*Chlidonias niger*	307	Neoaves
Cygnus odor	986	Galloanseres	*Buteo buteo*	149	Neoaves	*Mycteria leucocephala*	940	Neoaves
Cygnus atratus	932	Galloanseres	*Asio otus*	768	Neoaves			
Perdix perdix	310	Galloanseres	*Falco tinnunculus*	365	Neoaves			
Coturnis coturnis	308	Galloanseres	*Aegolius funereas*	877	Neoaves			
Lagopus lagopus	172	Galloanseres	*Neophron perpterus*	656	Neoaves			
Penelope purpurens	196	Galloanseres	*Asio flammeus*	334	Neoaves			
Pavo cristatus	902	Galloanseres	*Accipiter nisus*	1	Neoaves			
Phasianus colchicus	500	Galloanseres	*Rhynochetus jubatus*	719	Neoaves			
Gallus domesticus	77	Galloanseres	*Goura cristata*	879	Neoaves			
Otis tarda	329	Neoaves	*Columba palumbus*	248	Neoaves			
Grus grus	557	Neoaves	*Cacatua mollucrensis*	53	Neoaves			
Chauna torcuata	580	Neoaves	*Amazona automnalis*	778	Neoaves			
Aythya fuligula	606	Neoaves	*Conutus melanocephalus*	838	Neoaves			
Anthropoides virgo	853	Neoaves	*Corvus corone*	148	Neoaves			
Sarcorhamphus papa	987	Neoaves	*Scolopax rusticola*	160	Neoaves			
Thereskiornis aethiopicus	988	Neoaves	*Porphyrio porphyrio*	229	Neoaves			
Pyroderus sculattus	990	Neoaves	*Fulica atra*	489	Neoaves			
Cyanocorax chrysopus	686	Neoaves	*Rallus aquaticus*	894	Neoaves			
Ramphastus discolor	2	Neoaves	*Numenius arquata*	45	Neoaves			
Halcyon giganteus	777	Neoaves	*Haematopus ostralegus*	968	Neoaves			
Picus viridis	505	Neoaves	*Limosa lapponica*	974	Neoaves			
Cuculus canorus	242	Neoaves	*Vanellus vanellus*	887	Neoaves			
Lanius exultor	674	Neoaves	*Parus sp.*	762	Neoaves			
Larus camus	774	Neoaves	*Apus apus*	650	Neoaves			
Dendrocopus major	52	Neoaves	*Porphyrio porphyrio*	646	Neoaves			
Podiceps cristatus	803	Neoaves	*Tringa totanus*	826	Neoaves			
Phoenicopterus ruber	809	Neoaves	*Tringa hippolemus*	281	Neoaves			
Platalea leucorodia	313	Neoaves	*Milvus milvus*	727	Neoaves			
Pelecanus onocrotalus	763	Neoaves	*Pernis apivorus*	657	Neoaves			
Phalacrocorax carbo	570	Neoaves	*Pica pica*	623	Neoaves			
Diomedea exulans	4	Neoaves	*Pyrrhocorax pyrrhocorax*	697	Neoaves			
Nycticorax nycticorax	5	Neoaves	*Bombycilla garrulax*	792	Neoaves			

APPENDIX 2

Specimens of the Hess Collection Chapters: 4, 5 & 6 (Part III)